Elucidating the Function of ARTD1 in Macrophages *In Vivo*

Dissertation

zur

Erlangung der naturwissenschaftlichen Doktorwürde
(Dr. sc. nat.)

vorgelegt der

Mathematisch-naturwissenschaftlichen Fakultät

der

Universität Zürich

von

Friedrich Alexander Kunze

aus
Deutschland

Promotionskommission

Prof. Dr. Dr. Michael O. Hottiger
(Vorsitz und Leitung der Dissertation)
Prof. Dr. Burkhard Becher
Prof. Dr. Jean Pieters
Prof. Dr. Sabine Werner

Zürich, 2018

SUMMARY

The fundamental principle of immunity is self and non-self discrimination. To do so, innate immune cells express pattern recognition receptors (PRRs) that recognize foreign pathogen associated molecular patterns (PAMPs) and endogenous danger associated molecular patterns (DAMPs). ARTD1, the major nuclear enzyme catalyzing the post-translational modification ADP-ribosylation, has been reported to enhance PRR-induced proinflammatory gene expression as a transcriptional co-factor of NF-κB in cultured cells. The cell type specific ARTD1 contributions *in vivo* as well as the contribution of other ADP-ribosylating enzymes during inflammation are currently under investigation.

The main aim of this study was to comprehensively determine the function of ARTD1 specifically in macrophages *in vivo*. In addition, we investigated in which cell type ADP-ribosylation inhibitors affect LPS-induced proinflammatory signaling. Finally, we analyzed all ARTD family members and their function during LPS-proinflammatory signaling in fibroblasts.

RNA sequencing of LPS/IFN-γ stimulated bone marrow derived macrophages (BMDM) identified *Il12b* expression to be significantly reduced in *Artd1* knock-out BMDMs as compared to wild-type controls. To confirm the relevance of reduced *Il12b* levels during Th1 immune responses *in vivo*, we generated a myeloid cell specific *Artd1* knock-out strain ($Artd1^{\Delta Myel}$) and tested three inflammatory models: i) a systemic LPS-induced inflammation, ii) a local gastric *Helicobacter pylori* infection and iii) a subcutaneous MC-38 tumor xenograft model. In all three tested models, we observed using $Artd1^{\Delta Myel}$ mice reduced lymphocyte activation due to decreased IFN-γ expression. We observed a decreased NK cell activation during sepsis and decreased CD4 and CD8 T cell activation during *Helicobacter pylori* infection as well as the MC-38 tumor xenograft model. Moreover, co-treatment of wild-type mice with LPS and ADP-ribosylation inhibitors (i.e. PARPi) reduced the serum levels of the quantified cytokines (e.g. IFN-γ or TNF-α), and co-treatment of splenocytes from the same mice revealed the same effect. Interestingly, the activation of NK cells, the major IFN-γ producer during sepsis with IL-18, was inhibited by PARPi. Furthermore, a siRNA screen targeting every individual ARTD family member revealed ARTD11 to selectively enhance *Cxcl10* and *Cxcl2* gene expression in fibroblasts but not in macrophages during LPS-signaling.

Together these data provide strong evidence that ARTD1 controls the Th1 immune response in macrophages via the IL-12/18-IFN-γ axis. Moreover, we identified IL-18 simulated NK cells to be sensitive to PARPi treatment and ARTD11 as a potential interesting ARTD family member to influence proinflammatory gene expression in fibroblasts. Thus, ADP-ribosylation catalyzing enzymes differently promote proinflammatory cytokine expression in several cell types, strongly suggesting clinical significance. Future investigations of ADP-ribosylation functions *in vivo* require an ARTD family and cell type specific approach.

ZUSAMMENFASSUNG

Das Grundprinzip der Immunität ist Selbst- und Nicht-Selbstdiskriminierung. Dazu exprimieren angeborene Immunzellen Mustererkennungsrezeptoren (PRRs), die fremde pathogenassoziierte molekulare Muster und endogene gefahrassoziierte molekulare Muster erkennen. ARTD1, das wichtigste nukleare Enzym, das die posttranslationale Modifikation ADP-Ribosylierung katalysiert, steigert die PRR-induzierte proinflammatorische Genexpression als transkriptioneller Co-Faktor von NF-κB in kultivierten Zellen. Die zelltypspezifischen ARTD1-Beiträge *in vivo* sowie der Beitrag anderer ADP-ribosylierender Enzyme während Entzündungen werden derzeit untersucht.

Das Hauptziel dieser Studie war die umfassende Bestimmung der Funktion von ARTD1 speziell in Makrophagen *in vivo*. Darüber hinaus haben wir untersucht, in welchen Zelltypen ADP-Ribosylierungsinhibitoren die LPS-induzierte proinflammatorische Signalübertragung beeinflussen. Schließlich analysierten wir alle ARTD-Familienmitglieder und ihre Funktion während der LPS-proinflammatorischen Signalübertragung in Fibroblasten.

Die RNA-Sequenzierung von LPS/IFN-γ stimulierten Knochenmark-Makrophagen (BMDM) ergab, dass die *Il12b*-Expression in *Artd1*-defizienten BMDMs im Vergleich zu Wildtyp-Kontrollen signifikant reduziert war. Um die Relevanz reduzierter *Il12b*-Spiegel während der Th1-Immunreaktionen *in vivo* zu bestätigen, haben wir einen myeloischen zellspezifischen *Artd1*-Knock-out-Stamm ($Artd1^{\Delta Myel}$) generiert und drei Entzündungsmodelle getestet: i) eine systemische LPS-induzierte Entzündung, ii) eine lokale gastrische *Helicobacter pylori*-Infektion und iii) ein subkutanes MC-38-Tumormodell. In allen drei getesteten Modellen beobachteten wir in $Artd1^{\Delta Myel}$ Mäusen eine reduzierte Lymphozytenaktivierung basierend auf einer verminderten IFN-γ-Expression. Wir beobachteten eine verminderte NK-Zellaktivierung während der Sepsis und eine verminderte CD4- und CD8-T-Zellaktivierung während der *Helicobacter pylori*-Infektion sowie während des MC-38-Tumormodells. Außerdem reduzierte die Co-Behandlung von Wildtyp-Mäusen mit LPS- und ADP-Ribosylierungsinhibitoren (z.B. PARPi) die Serumspiegel einiger quantifizierter Zytokine (z.B. IFN-γ oder TNF-α), und die Co-Behandlung von Milzzellen derselben Mäuse zeigte den gleichen Effekt. Interessanterweise wurde die Stimulation von NK-Zellen, den wichtigsten Produzenten von IFN-γ nach LPS-Stimulation, mit IL18 durch PARPi gehemmt. Zudem identifizierten wir mittels einer siRNA-Screen aller ARTD-Familienmitglieder, dass ARTD11 die LPS-induzierte *Cxcl10* und *Cxcl2* Genexpression in Fibroblasten, aber nicht in Makrophagen, selektiv steigerte.

Zusammengenommen liefern diese Daten starke Hinweise darauf, dass ARTD1 in Makrophagen die Th1-Immunantwort über die IL-12/18-IFN-γ-Achse steuert. Darüber hinaus identifizierten wir IL-18 simulierte NK-Zellen als empfindlich für die PARPi-Behandlung und ARTD11 als potenziell interessantes ARTD-Familienmitglied, um die proinflammatorische Genexpression in Fibroblasten zu beeinflussen. So fördern ADP-Ribosylierung katalysierende Enzyme unterschiedlich die proinflammatorische Zytokinexpression in verschiedenen Zelltypen, was auf eine starke klinische Bedeutung hindeutet. Zukünftige Untersuchungen von ADP-Ribosylierungsfunktionen *in vivo* erfordern eine ARTD-Familien und einen zelltypspezifischen Ansatz.

TABLE OF CONTENTS

INTRODUCTION

1. ADP-ribosylation

ADP-ribosylation is an evolutionary conserved post translational modification (PTM) that is present in many prokaryotic and all eukaryotic cells, except for yeast[1]. The PTM is catalyzed by ADP-ribosyltransferases (ARTs) that covalently attach ADP-ribose (ADPr) to amino acid residues of target proteins using nicotinamide adenine dinucleotide (NAD^+) as substrate. Bacterial toxins such as *diphteriae*[2], *cholerae*[3], *pertussis*[4] or *clostridia* toxins[5] mono-ADP-ribosylate host proteins to inhibit their function and promote bacterial pathogenesis[6]. Beside prokaryotic ARTs, various eukaryotic proteins have been described to catalyze, hence "write" ADP-ribosylation[7]. Based on structural homologies to bacterial toxins the writers have been classified into two groups: Intracellular diphtheria toxin-like ARTs (ARTDs, formerly known as PARPs[8]) and the ectopic cholera toxin-like ARTs (ARTCs[9]). Additionally, Sirtuins (specifically SIRT4[10] and SIRT6[11]) are also considered to possess ADP-ribosylating activity. While all of the known ARTs attach a single ADPr molecule to a protein, which is called mono-ADP-ribosylation or MARylation, only few ARTs can further modify the initial ADPr with additional ADP-ribose molecules generating linear or branched chains which is called poly-ADP-ribosylation or PARylation[12].

Genome wide sequence analysis identified 18 intracellular eukaryotic ARTDs that share a common "PARP signature" motif in their C-terminal ART domain[13] and localize to various intracellular compartments (Figure 1)[14]. While four members (ARTD1, 2, 5, 6) catalyze PARylation, twelve members (ARTD3, 4, 8, 10, 11, 12, 14, 15, 16, 17 and 18) catalyze MARylation. For two of them, ARTD9 and ARTD13, no enzymatic activity has been described so far[15]. Furthermore, numerous proteins possess ADP-ribose interaction domains and are considered as "readers" of ADP-ribosylation[1,16] (Figure 1). Another set of enzymes including the PAR-degrading enzyme poly (ADP-ribose) glycohydrolase (PARG) hydrolase "erase" ADP-ribosylation (Figure 1) on target proteins making ADP-ribosylation a fully reversible PTM[1,7].

Protein ADP-ribosylation can either affect the enzymatic activity of the modified protein or their interaction with nucleic acids and with other proteins[12]. Similar to other post-translational modifications such as acetylation, phosphorylation, ubiquitination, sumoylation or methylation, protein ADP-ribosylation is implicated in a plethora of different cellular processes including genomic stability, transcriptional control, energy metabolism and cell death[17-20].

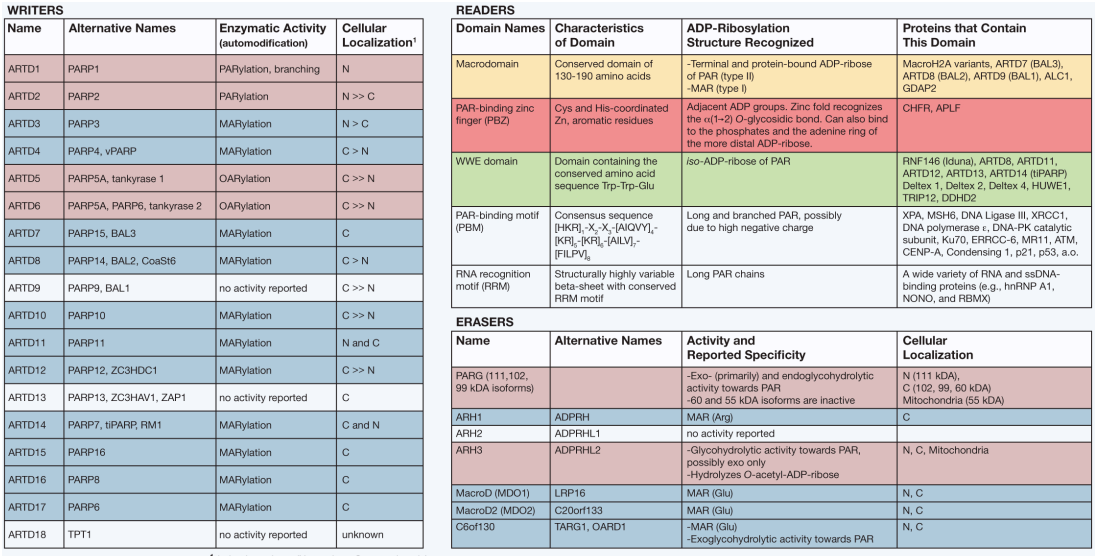

WRITERS

Name	Alternative Names	Enzymatic Activity (automodification)	Cellular Localization[1]
ARTD1	PARP1	PARylation, branching	N
ARTD2	PARP2	PARylation	N >> C
ARTD3	PARP3	MARylation	N > C
ARTD4	PARP4, vPARP	MARylation	C > N
ARTD5	PARP5A, tankyrase 1	OARylation	C >> N
ARTD6	PARP5A, PARP6, tankyrase 2	OARylation	C >> N
ARTD7	PARP15, BAL3	MARylation	C
ARTD8	PARP14, BAL2, CoaSt6	MARylation	C > N
ARTD9	PARP9, BAL1	no activity reported	C >> N
ARTD10	PARP10	MARylation	C >> N
ARTD11	PARP11	MARylation	N and C
ARTD12	PARP12, ZC3HDC1	MARylation	C >> N
ARTD13	PARP13, ZC3HAV1, ZAP1	no activity reported	C
ARTD14	PARP7, tiPARP, RM1	MARylation	C and N
ARTD15	PARP16	MARylation	C
ARTD16	PARP8	MARylation	C
ARTD17	PARP6	MARylation	C
ARTD18	TPT1	no activity reported	unknown

READERS

Domain Names	Characteristics of Domain	ADP-Ribosylation Structure Recognized	Proteins that Contain This Domain
Macrodomain	Conserved domain of 130-190 amino acids	-Terminal and protein-bound ADP-ribose of PAR (type II) -MAR (type I)	MacroH2A variants, ARTD7 (BAL3), ARTD8 (BAL2), ARTD9 (BAL1), ALC1, GDAP2
PAR-binding zinc finger (PBZ)	Cys and His-coordinated Zn, aromatic residues	Adjacent ADP groups. Zinc fold recognizes the α(1→2) *O*-glycosidic bond. Can also bind to the phosphates and the adenine ring of the more distal ADP-ribose.	CHFR, APLF
WWE domain	Domain containing the conserved amino acid sequence Trp-Trp-Glu	*iso*-ADP-ribose of PAR	RNF146 (Iduna), ARTD8, ARTD11, ARTD12, ARTD13, ARTD14 (tiPARP) Deltex 1, Deltex 2, Deltex 4, HUWE1, TRIP12, DDHD2
PAR-binding motif (PBM)	Consensus sequence $[HKR]_1$-X_1-X_1-$[AIQVY]_4$-$[KR]_2$-$[KR]_0$-$[AILV]_2$-$[FILPV]_0$	Long and branched PAR, possibly due to high negative charge	XPA, MSH6, DNA Ligase III, XRCC1, DNA polymerase ε, DNA-PK catalytic subunit, Ku70, ERRCC-6, MR11, ATM, CENP-A, Condensing 1, p21, p53, a.o.
RNA recognition motif (RRM)	Structurally highly variable beta-sheet with conserved RRM motif	Long PAR chains	A wide variety of RNA and ssDNA-binding proteins (e.g., hnRNP A1, NONO, and RBMX)

ERASERS

Name	Alternative Names	Activity and Reported Specificity	Cellular Localization
PARG (111,102, 99 kDA isoforms)		-Exo- (primarily) and endoglycohydrolytic activity towards PAR -60 and 55 kDA isoforms are inactive	N (111 kDA), C (102, 99, 60 kDA) Mitochondria (55 kDA)
ARH1	ADPRH	MAR (Arg)	C
ARH2	ADPRHL1	no activity reported	
ARH3	ADPRHL2	-Glycohydrolytic activity towards PAR, possibly exo only -Hydrolyzes *O*-acetyl-ADP-ribose	N, C, Mitochondria
MacroD (MDO1)	LRP16	MAR (Glu)	N, C
MacroD2 (MDO2)	C20orf133	MAR (Glu)	N, C
C6of130	TARG1, OARD1	-MAR (Glu) -Exoglycohydrolytic activity towards PAR	N, C

Figure 1. Overview of the writers, readers and erasers of ADP-ribosylation. Enzymatic activity and cellular localization (nuclear (N) or cytoplasmic (C)). Adapted from Hottiger (2015)[7].

2. ADP-ribosylation induced cell death and the release of danger associated molecular patterns (DAMPs)

The macroscopic hallmarks of inflammation include swelling, heat, redness, pain and/or loss of function[21]. On the cellular and molecular level, inflammation is a process that is initiated by tissue damage (sterile inflammation) or microbial infections[22] and is regulated in a very complex, cell-type and stimulus dependent manner[23]. Tissue damage or cell death can be initiated in a regulated manner (i.e. apoptosis or necrosis) or by cell injury. While apoptotic cell death does not induce an inflammatory response, the necrotic cell death does so due to the release of DAMPs or alarmins (see below)[24].

The constant exposure of cells to genotoxic sources, such as UV light, reactive oxygen species or alkylating agents induces and requires PARylation to maintain genome integrity[25,26]. It is very well documented that ARTD1, ARTD2 and to a lower extent also ARTD3 recognize and bind to single- and double strand breaks but also abnormal DNA structures, leading to activation and PAR formation[27-32]. PARylation marks the sites of DNA damage and facilitates DNA repair to restore cellular homeostasis[25]. While adequate DNA repair promotes cell survival and lowers the risk of oncogenic transformations, inhibition of PARylation, knock-out or knock-down of ARTD1 sensitizes cells to DNA-damaging agents[33].

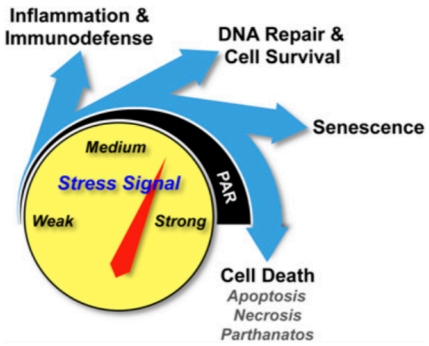

Figure 2. ARTD1 activation is a proxy for cell stress. Genotoxic stress levels correlate with ARTD1 activation. Whereas basal PARylation is beneficial for the host during the DNA damage response, ARTD1 hyperactivation drives cells into necrosis. Figure taken from Luo et al 2012[34]

Increasing genotoxic stress levels correlate with increasing ARTD1 activity, ultimately resulting in ARTD1 hyper-activation (Figure 2). The fact that ARTD1 cleavage was among the first identified caspase "death substrates", suggested a regulatory role during apoptosis[35]. However, pharmacologic inhibition or generation of a knock-in mouse expressing a non-cleavable ARTD1 did neither influence cellular susceptibility nor the processing of the apoptotic program itself, indicating that caspase-mediated cleavage of ARTD1 and subsequent inhibition of its enzymatic activity has another physiological role[36,37]. DNA fragmentation is a hallmark of apoptosis, which would lead to ARTD1 hyper activation and energy expenditure. Thus, ARTD1 cleavage during apoptosis excludes its activation and preserves energy for ATP sensitive steps during apoptosis[36,38].

In contrast to ARTD1's passive role during apoptosis, PARylation actively influences cell fate during necrosis. Hyper-activated ARTD1 (i.e. by DNA damage) may cause regulated necrosis via distinct pathways. Extensive PARylation decreases cellular NAD^+ levels up to 20% in 5-15 mins and is considered as the main NAD^+ catabolizing process in the cell[39-41]. To balance decreased NAD^+ levels the cells activate adenosine triphosphate (ATP)-dependent salvage pathways resulting in ATP depletion and an comprised metabolic state of the cell[42]. Emerging concepts describe ARTD1 as a proxy/sensor for cellular stress levels and PARylation as critical determinant of cell fate[34,36,43]. Depending on the severity and duration of stress, cells exhibit different ways to limit cell and subsequent tissue damage, ranging from senescence via apoptosis to necrosis. Massive genotoxic stress thus triggers severe PARylation-dependent NAD^+ and ATP depletion ending up in cellular energy crisis[44-46]. Yet, other studies challenge the NAD^+ exhaustion model as only reason for cell death. Although after middle cerebral artery occlusion (MCAO)-induced ischemia ARTD1 knock-out mice have reduced infarct sizes compared to wild-type animals, the energy status of the cells were similar[47]. In addition, another study showed that reduced NAD^+ levels do not always correlate with reduced ATP levels during ischemia reperfusion injury[48]. Moreover, PARG-deficient

cells induce parthanatos without NAD^+ exhaustion[49]. Thus, PARylation-induced NAD^+ depletion is not exclusively responsible for cell death[50].

The initial observation that ARTD1 hyper-activation resulted in cell death by the release of the apoptosis-inducing factor (AIF) from the mitochondria[51], lead to the definition of parthanatos as a new necroptosis module[52]. Parthanatos, a name derived from *par* for PAR polymer, and *Thanatos* the personification of death in Greek mythology, is a caspase-independent mode of cell death that combines apoptotic and necrotic features[50,53]. The function of AIF under physiological and pathophysiological roles has been extensively studied[54]. Whereas the main pool of AIF localizes to the mitochondrial intermembrane space and plays essential roles in the mitochondrial respiratory chain and is involved in redox-metabolism[54], a smaller pool of AIF associates to the outer mitochondrial membrane (cytosolic side)[55]. Impaired AIF expression *in vivo* increases oxidative stress in the brain and retina proposing a function as free radical scavenger in mitochondria[56-58]. Experiments in neurons and HeLa cells subjected to genotoxic stress or the ectopic delivery of *in vitro* generated PAR into cells identified the PAR polymer as major contributor of cell death[59,60]. AIF has been identified as a high affinity PAR-binding protein via three critical amino acid residues (Arg^{588}, Lys^{589} and Arg^{592})[61,62]. Mutants maintain their NADH oxidase activity, DNA binding and chromatin cleaving properties, but fail to leave the mitochondria[46]. In line with the aforementioned mechanistic insights, cell death was abolished by either administrating PAR neutralizing antibodies or by overexpressing PARG[59,60]. The accumulation and translocation of complex nuclear PAR molecules into the cytoplasm causes the release of AIF from the mitochondria and the induction of chromatin condensation and DNA fragmentation[63]. The exact mode of DNA cleavage is currently under debate, since murine AIF does not possess recognizable structural DNA-binding motifs, while human AIF does[64,65]. Additionally, it is not known whether AIF possesses an intrinsic endonuclease activity or whether it recruits a proposed parthanatos AIF-associated nuclease (PAAN)[53].

Characteristically, cells dying from parthanatos, like other necrotic cells lose their membrane integrity that releases intracellular material into the extracellular space, of which some components function as DAMPs[24]. The high mobility group box 1 protein (HMGB1) is among the most studied DAMPs and recognized by toll-like receptor 4 (TLR4) and receptor for advanced glycation endproducts (RAGE). Under physiological conditions HMGB1 functions as a DNA binding protein that stabilizes nucleosomes and regulates transcription[66]. In contrast, during necrotic cell death, HMGB1 is released in an PARylation dependent manner, a process also identified during autophagy[67,68]. Hence, ARTD1 does not only regulate cell fate by depleting cellular energy pools (see above), but also specifically induces immune responses via HMGB1. This concept is strengthened by a recent publication, where ARTD1 is activated in macrophages by reactive oxygen species (ROS) and/or MAPK-signaling and

induces HMGB1 release[69]. Mechanistically, HMGB1 PARylation seemed to facilitate its acetylation, an essential prerequisite for the release[69]. The latter model could explain how immune cells actively secrete HMGB1 after the initiation of the TLR signaling.

3. ADP-ribosylation during immune responses initiation

Inflammation is orchestrated by different cell types that integrate diverse stimuli for the generation of a specific immune response to kill invading pathogen and/or to clear and regenerate damaged tissue[1]. A typical immune response can be divided in three phases: A recognition and initiation phase, a second amplification and modulation phase followed by a third effector phase[2]. Whereas the innate immune system senses and initiates inflammation, both innate and adaptive immune systems regulate the second and third phase[3].

Not only immune cells such as the antigen presenting macrophages or dendritic cells but also epithelial, endothelial and fibroblast cells express pathogen recognition receptors (PRRs) that initiate innate immune responses[4]. PRRs recognize a variety, but yet defined set of conserved PAMPs, such as bacterial and fungal cell wall components (i.e. lipopolysaccharides, LPS) or DAMPs (Figure 3). The recognition of DAMPS and PAMPs, often by the same receptors, activates intracellular signaling pathways, which are controlled by different ARTD-family members and result in the expression of proinflammatory cytokines such as IL-12, IL-23, IL-6 and IL-1β[6]. The following chapter focuses mainly on reports that involved inflammatory stimuli and cells, mostly excluding findings from tumor research. For information about tumor cell signaling, readers are advised to consult respective reviews[12,34,43].

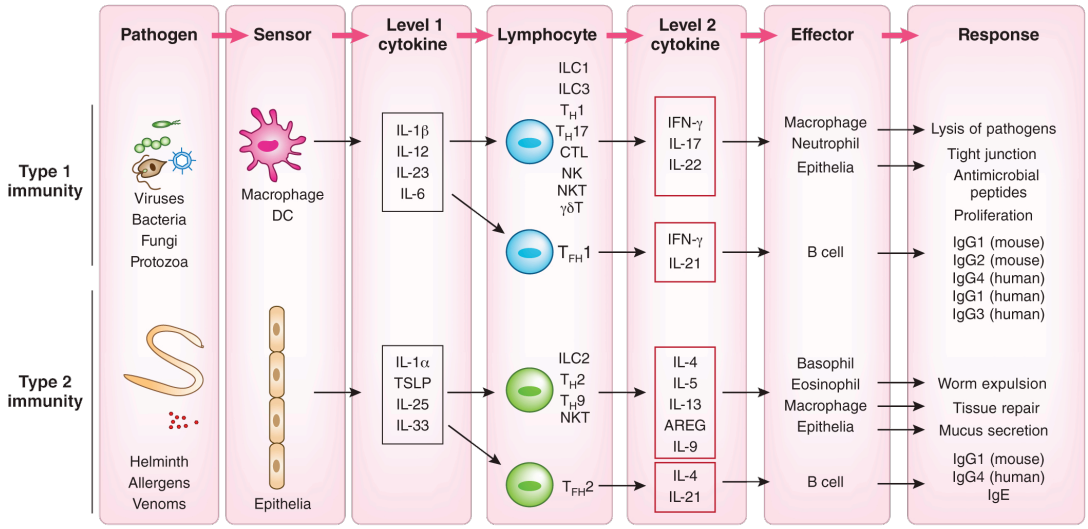

Figure 3. The immune response. Immune responses (Th1 and Th2) are orchestrated by specialized cell types in three distinct phases. Cells of the innate immunity (Sensors) sense PAMPs or DAMPs and initiate the first phase by level 1 cytokines. The activation of lymphocytes characterize the second phase of an immune response and level 2 cytokines determine the third phase: Effector functions and elimination of the pathogen. Figure adapted from Iwasaki et al (2005)[70].

3.1. ARTD1 co-activates NF-κB dependent gene expression

While both the recognition of PAMPS (i.e. LPS) or DAMPs (i.e. HMGB1) by TLRs and the TLR-induced cytoplasmic signaling events in different cell types do not seem to be regulated by ARTs, several reports have described the involvement of ARTD1 during the transcriptional activation of proinflammatory genes by PAMPs. However, nothing is known so far about ARTD1 function during DAMP-mediated inflammatory signaling. In LPS- but also TNF-α stimulated macrophages[71-74], microglia[75,76], fibroblasts[72,75,77,78], endothelial cells[76] and smooth muscle cells[71,73,78], ARTD1 was found to promote the NF-κB dependent expression of proinflammatory cytokines. The transcription factor NF-κB represents the most studied inflammatory transcription factor (TF) so far[7]. The eukaryotic NF-κB family consists of five proteins, p65 (RelA), RelB, c-Rel, p105/p50 (NF-κB) and p100/52 (NF-κB1). Dimerization of the different subunits can result in 15 different combinations, the p50/p65 heterodimer being the most abundant one[8]. In its inactive form the p50/p65 heterodimer is bound by IκB, inhibiting its nuclear translocation[79]. TLR-mediated signaling (Figure 4) induces the canonical NF-κB by activating a signal cascade leading to the phosphorylation of IκB, its subsequent ubiquitination and degradation[80]. In turn, p50/p65 translocate into the nucleus.

Different mechanistic models have been reported how ARTD1 influences NF-κB-dependent gene expression. ARTD1 acts as a transcriptional co-factor for NF-κB and promotes gene expression by functional cooperation with the transcription machinery in response to proinflammatory stimuli[81]. LPS- and TNF-α-induced NF-κB dependent gene expression in macrophages and fibroblasts was enhanced by ARTD1 independently of its enzymatic activities, but by complex formation with the mediator complex, p300/CBP and the p50 and p65 subunit of NF-κB[82,83].

Mutating the ARTD1 cleavage site Asp^{214} renders ARTD1 uncleavable and inhibited its release from chromatin and chromatin decondensation, thereby restraining the expression of cleavage-dependent NF-κB target genes. Interestingly, knock-in mice expressing the non-cleavable ARTD1 (D214N) mutant were highly resistant to endotoxic shock and to intestinal and renal ischemia-reperfusions. This was associated with reduced inflammatory responses in the target tissues and cells due to the compromised production of specific inflammatory mediators[37]. Despite normal binding of NF-κB to DNA, NF-κB-mediated transcriptional activity was impaired in the presence of caspase-resistant ARTD1. LPS stimulation of macrophages activated caspase 7 by caspase 1, induced its translocation to the nucleus, and cleaved ARTD1 at the promoters of a subset of NF-κB target genes (e.g *CSF2, IL6* or *LIF*), thus negatively affecting their gene expression[84]. These findings propose an apoptosis-

independent regulatory role for caspase 7-mediated ARTD1 cleavage in proinflammatory gene expression and provide insight into inflammasome signaling.

In contrast to these reports suggesting that not the enzymatic activity of ARTD1, but only the protein itself is required for NF-κB target gene expression, another group reported that LPS treatment of macrophages induced ARTD1's enzymatic activity and nucleosome remodeling at promoters of proinflammatory genes, directly destabilizing histone-DNA interactions and facilitating NF-κB binding and gene expression[85]. The discrepancies could be explained by methodological differences such as the cell type (RAW.267.4 macrophages and primary BMDM or fibroblasts), the source of LPS (*S. enterica* and *E. coli*) or the serum starvation overnight prior LPS stimulation.

Proinflammatory mediators such as *Il1b*[86], *Il6*[87], *Tnfa*[75,76] and *Cxcl2*[78]; and adhesion molecules such as *Icam1*, *Vcam* or *Eselectin*[87,88] were significantly lower expressed in ARTD1 knock-out cells. In LPS stimulated glial cells, ARTD1 also enhances the DNA binding of the transcription factors SP-1, YY-1, AP-1 and STAT1 independently of its enzymatic activity[88]. Although the exact mechanisms are unknown, *Il6*, *Il1b* and *Tnfa* expression were markedly reduced in ARTD1 knock-out glial cells[88].

These findings are supported by the fact that ARTD1 knock-out mice are resistant to LPS-induced shock[89]. So far, other ARTD family members have not been implicated in the initiation of inflammation. The fact that ARTD1 knock-out mice are resistant to endotoxic shock suggests a dominant role of ARTD1 during inflammatory signaling.

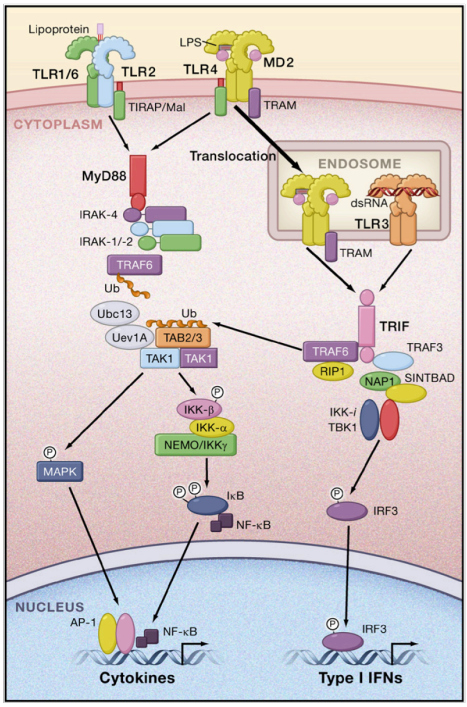

Figure 4. TLR2, TLR3 and TLR4 signaling pathways[90]. Pattern recognition by TLR receptors trigger distinct signaling cascades either via MyD88 and NF-κB or via TRIF and IRF8 to express proinflammatory genes.

3.2. ADP-ribosylation regulates mRNA stability

Although transcription is a highly regulated step during the expression of cytokines, cells evolved posttranscriptional mechanisms to regulate the translational machinery and the conversion of mRNA into protein[91,92]. This is particularly important for immune effector proteins to either re-program gene expression at a global level or modulate the stability and translation of specific immune transcripts[18]. One of the central aspects of the posttranscriptional regulation is mRNA stability. Indeed, ARTD1 was identified to promote mRNA stability of individual transcripts during LPS-induced proinflammatory signaling in an enzymatically dependent manner[93]. ADP-ribosylation of specific RNA-binding proteins modulate RNA processing including splicing, polyadenylation, translation, miRNA biogenesis and rRNA processing[94]. Upon LPS stimulation of macrophages, adenylate-uridylate-rich element-binding protein embryonic lethal abnormal vision-like 1 (Elavl1)/human antigen R (HuR) was described to be PARylated[95]. ARTD1-mediated PARylation of HuR enhanced nucleoplasmatic shuttling and mRNA binding, and promoted mRNA stablility[96]. Comparably, pharmacologic inhibition of ARTD1 reduced mRNA stability of e.g. *Cxcl2* during inflammation[93].

Additionally, LPS-induced expression of *Tf* (tissue factor) is an important link between inflammation and thrombosis. In LPS-treated macrophages, ARTD8 was identified to negatively regulate *Tf* mRNA stability, by forming a complex with the mRNA destabilizing protein tristetraprolin (TTP) and a conserved adenylate-uridylate-rich element in the *Tf* mRNA 3` untranslated region resulting in tissue factor mRNA degradation[93]. Beside ARTD8, no other ARTD family member was described to affect these steps so far.

4. ADP-ribosylation during immune response modulation

The cytokines and chemokines that are expressed during the initiation of an immune response activate and recruit lymphoid cells, including innate lymphoid cells (ILCs) such as NK-cells but also adaptive immune cells like T and B cells. For example, during this second phase of inflammation NK cells produce high levels of IFN-γ to amplify the immune response and promote Th1 immune responses. Additionally, CD4 T cells differentiate into T helper type 1 cells expressing additional IFN-γ with a certain delay, repressing Treg and Th17 immune responses.

4.1. ADP-ribosylation controls T cell activation and survival

Bone marrow-derived lymphoid progenitor cells migrate to the thymus to give rise to T cells, which will subsequently seed to peripheral lymphoid tissues[97]. A critical balance between cell division and cell death must be maintained to ensure T cell homeostasis throughout life[98]. With respect to T cell development, *Artd2*$^{-/-}$ mice were reported to have a to two-fold

reduction in the CD4 CD8 double positive (DP) thymocytes associated with decreased DP cell survival and increased apoptosis[99]. Although ARTD1 and ARTD2 do not influence peripheral T cell homeostasis individually, their double deficiency leads to severe DNA damage, cell death and diminished T cell numbers in peripheral lymphoid tissues[100]. In addition, T-dependent antigen-treated (TNP-KLH) *Cd4*-Cre *Artd2*$^{flox/flox}$ *Artd1*$^{-/-}$ mice exhibited defective antibody responses determined by decreased IgM and IgG1 serum levels 14 days after treatment, suggesting defective T and B cell cooperation[100].

Membrane receptors are crucial initiators of signal transduction in T cells and activate T cells to proliferate and differentiate[101]. Necrotic cells that lost their membrane integrity release NAD^+ into the extracellular space. In presence of extracellular NAD^+, ectopically expressed ARTC2.2 mediates on CD4 and CD8 T cells ADP-ribosylation of the purinergic P2X7 receptor at Arg^{125}, which induces a Ca^{2+} influx, macropore formation, phosphatidylserine exposure, CD62L shedding, and accelerated cell death (Figure 5)[102-104]. Additionally, necrosis-activated ARTC2 modifies LFA-1, CD8, CD27, CD43, CD44 and CD45 on the surface of CD8 cytotoxic T cells, resulting in decreased proliferation and decreased cytotoxicity[105]. Thus, ARTC2.2 acts as a safeguard to prevent undesirable T cell activation during necrosis.

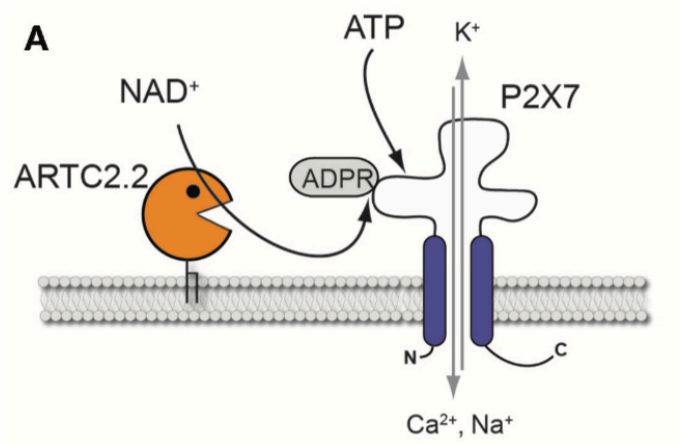

Figure 5. Cellular consequences of P2X7 activation on mouse T cells. ARTC2.2-mdiated ADP-ribosylation of the purinergic P2X7 receptor on mouse T cells leads to its activation and ultimately to cell death. Figure taken from Rissiek et al (2015)[106].

4.2. ADP-ribosylation regulates gene expression in activated T cells

TGF-β and IL-6 promote naïve CD4 T cells differentiation towards proinflammatory Th17 cells that are characterized by the expression of IL-17 and IL-22[107]. In contrast, TGF-β and IL2 drive naïve CD4 T cells differentiation into $CD4^+$ $CD25^+$ regulatory T cells (Treg) that play an important role during immune homeostasis[108,109]. Balancing the differentiation of proinflammatory Th17 as well as regulatory Treg allows establishing a protective and not harmful immune response. In CD4 T cells ARTD1 represses the expression of both subunits

of the TGF-β receptor: Whereas the expression of TGFbRI is repressed by ADP-ribosylation, the expression of TGFbRII is repressed only by the ARTD1 protein[110]. ARTD1 knock-out CD4 T cells expressed increased levels of both TGF-β receptors, which was associated with enhanced Smad2/3 activation and up regulation of FoxP3, the master transcription factor of T helper cell differentiation[110]. Studies confirm ARTD1 function during Treg differentiation, associated with increased numbers of $FoxP3^+$ Treg cells in lymphoid organs of ARTD1 knock-out mice compared to wild-type mice[111,112].

T cell activation is not only driven by cytokines but also by the engagement of the T cell receptor (TCR) with the major histocompatibility complex (MHC)-bound antigens on cells. TCR activation triggers the activation of receptor-associated tyrosine kinases that lead to the activation of phospholipase C-γ (PLC-γ) signaling cascade and intracellular Ca^{2+} release[113]. T cells express three (NFAT1/NFATc2, NFAT2/NFATc1 and NFAT4/NFATc5) of the four Ca^{2+} regulated nuclear factor of activated T cells (NFAT) transcription factors[113]. Under basal conditions NFAT proteins reside highly phosphorylated in the cytoplasm. The calmodulin-dependent phosphatase calcineurin dephosphorylates NFAT proteins, allowing nuclear translocation and DNA binding[114]. During PMA/Ionomycin-induced T cell activation (which mimics the TCR activation), ARTD1 was shown to interact with NFATc1 and NFATc2 in the nucleus and to modify the proteins[115]. In particular for NFATc2 the PARylation site could be determined at its regulatory region spanning amino acids 1–460. Interaction studies suggest that the modification is mediated by direct interactions between ARTD1 and NFATc1 and NFATc2 respectively. NFAT PARylation delays its nuclear export and enhances NFAT-dependent gene expression. Thus, ARTD1 knock-out T cells exhibit markedly reduced *Il2* and *Il4* expression[114].

TCR activation can also be accomplished by specific antibodies (i.e. anti-CD3) *in vitro*. Anti-CD3 or anti-CD3/anti-CD28 mediated T cell activation implicated ARTD1 in T cell polarization. Microarray-mediated transcriptional profiling revealed increased T helper type 1 (Th1) cytokine (*Ifng*) and chemokine (*Cxcl1*, *Ccl4* and *Ccl9*) expression and a reduced *Il4* expression in ARTD1 knock-out pan T cells[116]. So far, nothing is known about ADP-ribosylation and the posttranscriptional control during the amplification and modulation phase of an immune response. Furthermore, ADP-ribosylation has not been connected to NK cell function that amplifies acute phase immune responses.

5. ADP-ribosylation during immune response effector phase

To eliminate pathogens, infected or necrotic cells, the immune system relies on innate and adaptive immune cells. Typically, effector functions of the innate immune system, such as macrophages and neutrophils are quickly recruited, but do not discriminate well between microbial and host targets, so collateral damage to host tissues is unavoidable[22]. Severe

pathogenic infections are usually linked to tissue damage, the release of DAMPs and secondary inflammatory reactions[117]. To do so, macrophages produce high levels of nitric oxide (NO) to lyse the pathogen, neutrophils are recruited to the site of infection to produce antimicrobial oxygen radicals and epithelial/endothelial cells close their tight junctions to prevent the spreading of the pathogen[70].

In contrast, cells of the adaptive immune system, such as cytotoxic CD8 T cells specifically recognize only infected cells by T cell receptor – MHCI interactions[118]. Additionally CD4 Treg cells modulate and manage the immune response without direct cytotoxicity towards infected cells. Another mechanism to clear evading pathogens very specifically are antibody-producing plasma B cells that also establish immunological memory.

5.1. ADP-ribosylation regulates effector cell-specific gene expression

In macrophages, glial cells and fibroblasts, ARTD1 functions as co-factor of NF-κB (see above) to enhance inducible nitric oxide synthase (iNOS) expression[72,88]. Beside its cytotoxic role during pathogen killing, increased NO production leads to increased genotoxic stress for host cells. During severe pathogen infections ARTD1 is believed to increase the genotoxic stress of cells via iNOS-mediated NO production ultimately driving cells into necrosis[117], thereby linking bacterial infections and necrosis. Thus ARTD1 drives tissue injury in a positive feedback loop and serves as a critical immunecheckpoint for the host to prioritize pathogen elimination over cell death[119].

Historically, each myeloid cell type was assigned to a specific type of infection: Macrophages/neutrophils to microbial infections (M1) and eosinophiles/basophiles to helminth infections (M2)[70]. Especially for macrophages the view has drastically changed from a simple LPS/IFNγ-induced M1 or IL4-induced M2 polarization model to a more diverse concept, where the macrophage origin and the specific activation state determine the effector function[120]. A recent publication identified ARTD8 and ARTD9 as opposing regulators during macrophage polarization[121]. Whereas ARTD8 depletion during M(IFN-γ) polarization enhanced STAT1 phosphorylation and gene expression of inflammatory cytokines (i.e. TNF-α and Il-1β), ARTD9 depletion resulted in decreased STAT1 phosphorylation and decreased proinflammatory gene expression[121]. Mechanistically, the authors provided evidence that ARTD8 ADP-ribosylated STAT1 at the C-terminal AA residues Glu^{657} and Glu^{705}, which was abolished in the presence of ARTD9. The expression of ADP-ribosylation deficient mutants of STAT1 enhanced its phosphorylation and the expression of *Nos2, Il1b* and *Ccl2*[121]. Additionally, during M(IL-4) polarization, ARTD8 depletion reduced STAT6 phosphorylation and *Arg1* expression[121]. Thus, ARTD8 suppresses M(IFN-γ) polarization and enhances M(IL-4) polarization.

During IL-1β and TNF-α mediated signal transduction, ARTD10 was identified to play an important role in NF-κB activation[122]. Both cytokines initiate the tumor-necrosis factor receptor-associated factor (TRAF) protein, which function as K63-specific E3 ubiquitin ligases synthetizing K63-pUB chains on TRAF itself. ARTD10 binds to K63-pUb, MARylates NF-κB essential modulator (NEMO) whereby its polyubiqination and subsequent degradation is inhibited. The degradation of NEMO would release IKK-α and IKK-β to phosphorylate IκB allowing nuclear translocation of NF-κB. Thus, ARTD10 dampens NF-kB gene-expression (i.e. IL-8) in HeLa and U2OS cells.

Another important cell type for the elimination of pathogens are neutrophils[123]. Neutrophils are recruited to the site of inflammation by chemotaxis to release high levels of genotoxic radicals. ARTC1 expression is markedly increased in chemotaxin stimulated neutrophils (i.e. by fMLP, IL-8 or the platelet activating factor)[124], which has a profound impact during neutrophil effector function[125]. Activated neutrophils produce antimicrobial and cytotoxic HNPs (human neutrophil peptide), which can activate epithelial cells or recruit T cells[125]. Indeed, ARTC1 modifies HNP-1 *in vitro*, suggesting that modified HNP-1 could inhibit its antimicrobial and cytotoxic activity, while retaining its T cell chemoattractant abilities *in vivo*[126,127].

5.2. ADP-ribosylation influences immunoglobulin class switching in B cells

Antibodies are produced by B cells and are central mediators of immunity, since they neutralize pathogens or pathogen-derived products and recruit cellular immune effectors to eliminate infections[128]. Antibodies are classified according to their constant region into IgM, IgD, IgG, IgA and IgE. By default, naïve B cell express IgM and IgD surface antibodies, but the immunoglobulin class (isotype) can change during the course of an infection depending on the nature of the eliciting antigen or its entry route[129].

Under basal conditions, ARTD1 inhibition or ARTD1 knock-out increased class switching frequency to IgA, IgG1 or IgG2 and decreased the switching frequency of IgG2a by unknown mechanisms[130]. The data supports earlier findings reporting that nicotinamide treatment increases IgA producing B cells[131]. Although this study did not analyze whether ARTD1's catalytic activity is required for the observed phenotype, the authors speculated about ARTD1's function as a co-factor during the DNA double-strand forming class switching process[130].

Immunoglobulin class switch is also induced by cytokines. In IL-4 stimulated B cells ARTD8 was identified as a transcriptional switch during STAT6-dependend gene activation[132]. Mechanistically, in the absence of the class-switch stimulating cytokine IL-4, ARTD8 associates with HDAC2 and HDAC3 to repress *Iε* (IgE) gene expression. IL-4

activates ARTD8 and leads to the dissociation of the HDACs from the promoter, to expression of *Iε* and to IgM to IgE class switching [132].

6. ADP-ribosylation inhibitors (i.e. PARP inhibitors)

Historically, ARTD1 and ARTD2 are known for their role during DNA damage response (DDR), particularly the base excision repair (BER) pathway and double strand break (DSB) repair pathway, although both proteins likely regulate independent, but intrinsically linked aspects of DNA base damage response[12,26,133]. These involvements lead to the development of small-molecule ADP-ribosylation inhibitors (i.e. PARP inhibitors; PARPi).

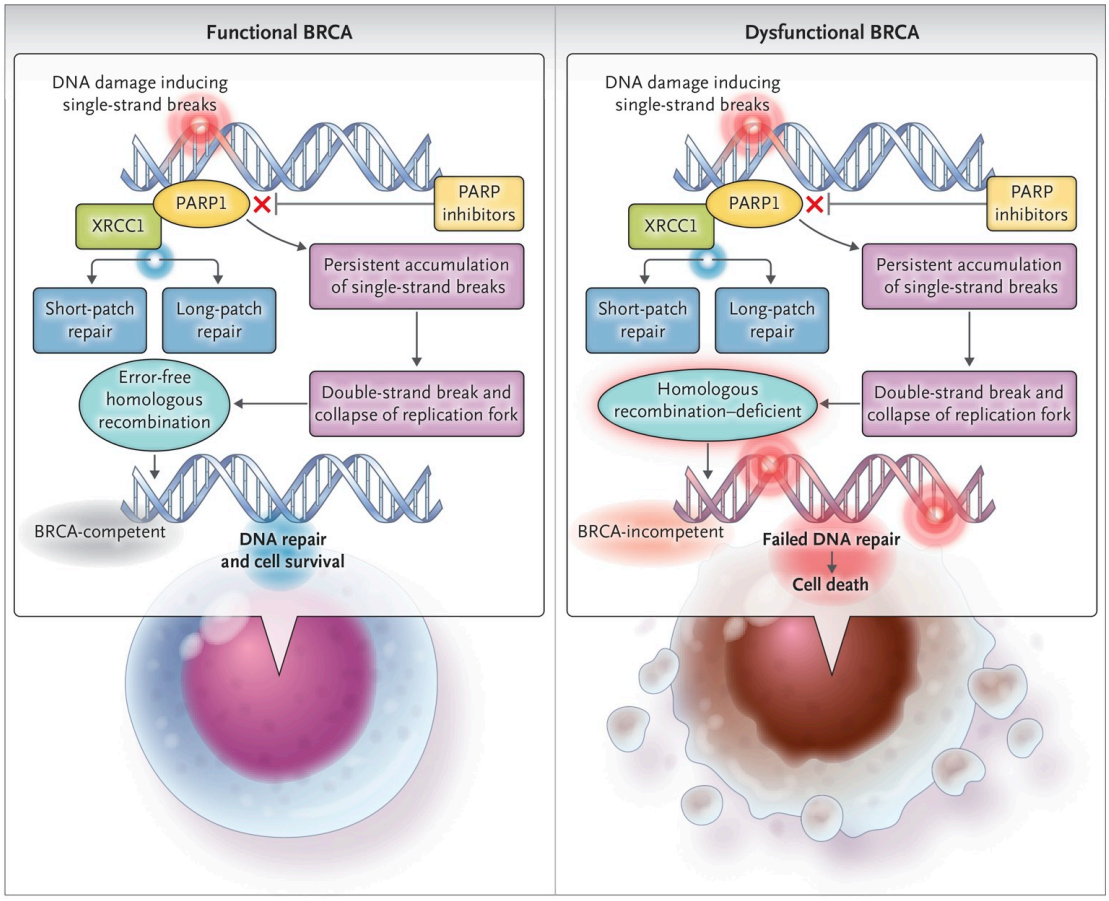

Figure 6. Synthetic lethal interaction between ARTD1 and BRCA1/2. Single strand breaks (SSB) are repaired by the base excision repair (BER) pathway in an ARTD1/PARP1 dependent manner (left panel). PARPi treated cells accumulate SSB eventually leading to double strand breaks and replication fork collapse. BRCA deficient cells cannot initiate homologous-recombination repair pathways, thus leading to cell death (right panel). Figure taken from McLornan et al (2014)[134].

The underlying concept was that the inhibition of the DNA-repair machinery could sensitize tumor cells to conventional DNA-damage-based therapies such as chemo- or radiotherapy (Figure 6)[135].

More than 30 years ago, nicotinamide and nicotinamide derivatives, including 3-aminobenzamide (3-AB) were identified as the first PARP inhibitors[136-138]. Advances in drug design and screening lead to the discovery of several new generations of PARPi compounds,

all of them competing with NAD^{+}[139]. Today, some of these PARPi are clinically approved as anti-cancer agents, including veliparib (Abbvie), rucaparib (Pfizer/Clovis), olaparib (KuDOS/AstraZeneca), niraparib (Merck/Tesaro) and talazoparib (Lead/Biomarin/Medivation/Pfizer)[117,140]. Two cancer treatment strategies with PARPi have been suggested: Either combinatorial therapies of PARPi and chemo- or radiotherapy[141] or PARPi monotherapy[142]. *BRCA*-deficient breast and ovarian cancers seem particularly sensitive to PARPi. The tumor suppressors *BRCA1* and *BRCA2* are essential proteins for the DNA DSB repair machinery to resolve DSBs by homologous recombination (HR)[142]. Defects in HR results in the accumulation of genetic alterations that promote tumorigenesis. In 2005, two independent groups discovered a synthetically lethal interaction between ARTD1, BRCA1 and BRCA2[143,144]. Synthetic lethality describes a genetic interaction in which single-gene defects are compatible with cell viability, but the combination (or synthesis) of gene effects results in cell death[142]. Thus, *BRCA* mutated cells are up to 1000 times more sensitive to PARPi than wild-type cells[144]. Recently, another PARPi mode of action called "PARP trapping" was proposed for a subset of PARPi (especially rucaparib, olaparib, niraparib and talazoparib)[145,146]. Inhibitor-bound ARTD1 is "trapped" to the DNA and interferes with ARTD1 function and/or replication resulting in cell death[147].

Although the potency and specificity of PARPi greatly enhanced during the last decades, ART-specific PARPi are still missing[148]. Interestingly, PARPi have also been reported to dampen different inflammation types, strongly corroborating the notion that ADP-ribosylation also regulates one or several inflammatory processes and that this might also contribute to the anti-tumor activity of PARPi[81,135,149]. At which stage of inflammation and to which extent this effect is cell type specific is currently under investigation.

7. Anti-inflammatory effects of PARPi

Beneficial effects of PARPi have been implicated in numerous inflammatory disease models like neurological diseases, sepsis, chronic inflammatory diseases and reperfusion injuries[36,117,150,151].

7.1. Neurological diseases

Excessive release of the neurotransmitter glutamate results in hyper-activated neurons characterized by massive Ca^{2+} influx. Calcium-mediated activation of various enzymes including endonucleases, proteases and neuronal nitric oxide synthase (nNOS) ensuing in neuronal excitotoxicity[152,153]. NO and superoxide form highly reactive peroxynitrile[154]. Endonuclease- and peroxynitrile-induced DNA breaks activate ARTD1, leading to parthanatos and inflammation. In fact, ROS, reactive nitrogen species (RNS), DNA alkylating agents and glutamate receptor agonists efficiently activate parthanatos in neuronal cells[155-157]. Further *in vivo* studies suggest important therapeutic opportunities of PARPi for the treatment

of neuronal inflammatory diseases such as Parkinson`s disease (PD), stroke and cerebral ischemia[46]. Mouse models identified both ARTD1 hyper-activation and AIF translocation as characteristic features of the diseases, which are significantly lowered or absent in ARTD1 deficient mice or administrating PARPi[158-160].

7.2. Septic shock

Sepsis is defined as a life-threatening organ dysfunction caused by a deregulated host response to infection, eventually leading to septic shock, the more severe form associated with increased mortality[161]. The high bacterial load of typically Gram-negative bacteria ultimately results in hypotension and multiple organ failure including liver, kidney and heart[162]. The bacterial cell wall component LPS induces the expression of important inflammatory mediators, such as TNF-α, IL-1β, IL-2, IL-6, IL-8, adhesion molecules and iNOS which determine the pathologic outcome[163]. So far, two not mutually exclusive models have been proposed to explain the relationship between ARTD1 and LPS-induced septic shock[139]: First, ARTD1 regulates proinflammatory gene expression as a co-factor of NF-κB (discussed above in detail)[139]. Second, excessive production of anti-microbial ROS, RNS or radicals by macrophages and neutrophils, induce DNA-damage of host cells resulting in necrosis and parthanathos[117]. In line, pharmacologic inhibition or knock-out of ARTD1 reduces the inflammatory burden significantly[89,164-166].

7.3. Chronic inflammatory diseases

PARylation not only influences acute phase, but also various chronic inflammatory diseases such as Rheumatoid Arthritis (RA) and diabetes[117]. RA is an autoimmune disease of the peripheral joints. Chronic inflammation leads to the destruction of bones and cartilage, thereby impairing joint function[167]. RA is initiated by an immune response against unknown antigens and followed by monocytes/macrophages, B and T cells infiltration into the affected joint where they produce proinflammatory mediators. Additionally, the expression of matrix-metalloproteases cause bone and cartilage degeneration[167].

PARPi studies discovered reduced incidence and severity of RA in mouse models under PARPi treatment, associated with reduced ROS/RNS levels and reduced neutrophil-infiltration into the joints[168,169]. Additionally, PARPi decreased the expression of proinflammatory cytokines and the Th1-driven immune response[170]. Pharmacologic inhibition or RNAi-mediated knock-down of ARTD1 partially impaired NF-κB and AP-1 binding and activation in synovial fibroblasts[171].

Type I Diabetes is an autoimmune disease against insulin-producing pancreatic β-cells and is most prevalent in children and young adults. Specific destruction of β-cells results in decreased glucose uptake, increased glucagon secretion and hypoglycemia[172]. So far the underlying mechanisms for β-cell destruction are largely not known, but include the

recognition of auto-antigens by T and B cells[173]. Rodent models of type I diabetes that resemble the human pathology use specific β-cells toxins (such as streptozotocin) to deplete β-cells *in vivo*[174-176]. Animal studies identified NO and various other free radicals and oxygen species to be the major cause of β-cell death by DNA damage induced hyperactivation of ARTD1 and the induction of apoptosis and parthanatos[172]. In addition, a study of streptozotocin-induced diabetes linked ARTD1 activation and ATP exhaustion to the inhibition of proinsulin synthesis in β-cells ultimately resulting in cell death[177]. In all of these models the inhibition of ARTD1 had beneficial effect on the severity of the disease[172].

7.4. Myocardial infarction

Organs essentially need constant blood supply for proper functioning. For example, coronary artery diseases can lead to decreased blood supply to the heart tissue and eventually block blood flow resulting in ischemic myocardial tissue[178]. A rapid restoration of blood flow within the infarcted area aims at minimizing irreversible myocardial injury. Despite the benefits of reperfusion, the therapies come with adverse effects such as microvascular injury and extension of myocyte necrosis, which is in part due to oxidative stress[178].

Studies *in vitro* identified ARTD1 over-activation, NAD^+ depletion and the induction of parthanatos in myocytes accounting for myocyte cell death during heart failure[179]. Pharmacologic inhibition of ARTD1 or genetic ablation attenuates myocardial necrosis during myocardial infarction[180]. Moreover, PARPi treatment reduced the expression of inflammatory cytokines and decreased neutrophil infiltration to the infarct area[181].

7.5. Inflammatory bowel disease

Inflammatory bowel disease (IBD) is a chronic disorder of the gastrointestinal tract that is mainly diagnosed as ulcerative colitis or Crohn`s disease[182,183]. Although the exact cause of the disease is unknown, hallmarks of IBD include a diffuse mucosal inflammation with increased expression of proinflammatory mediators and a significantly augmented infiltration of neutrophils[182]. Genetic ablation or pharmacologic inhibition of ARTD1 provides resistance in various hapten-induced colitis rodent models[184-188]. In addition, the PARPi 3-aminobenzamide (3AB) reduced spontaneously developing experimental colitis in *Il-10* knock-out mice via reduction of inflammatory cytokine expression[189]. Although the underlying mechanisms remain largely elusive, a recent study in ARTD1 knock-out mice suggests that a ARTD1-dependent transcriptional reprogramming of the colon tissue in combination with altered colonic microbiota are responsible for the resistance against dextran sulfate sodium **(**DSS)-induced colitis[190].

8. The role of erasers during inflammation

Erasers degrade ADP-ribosylation by cleaving glycosidic bonds to generate mono ADP ribose that eventually serves as a substrate for ATP production[191]. Hence, erasers are the biochemical and physiological counterpart of writers (i.e. ARTs) and involved in the ADP-ribosylation metabolism[192]. The eraser family includes ARH1, ARH2, ARH3, MacroD1, MacroD2, TARG and the founding member PARG[7]. So far, only PARG has been implicated in inflammatory diseases and will thus be discussed here.

Human PARG has five isoforms with distinct cellular localizations: A 111 kDa (nuclear), a 102 kDa (cytoplasm), a 99 kDa (cytoplasm), a 60 kDa (nuclear and cytoplasm) and a 55 kDa (mitochondria) isoform[193-197]. The murine PARG protein exists in two isoforms which differ in their N-terminal region: while wild type PARG ($PARG_{110}$) is a 110 kDA protein composed of an N-terminal regulatory domain and a C-terminal catalytic domain, the PARG mutant isoform ($PARG_{60}$) is a 60 kDa protein that lacks the N-terminal regulatory domain[193,198,199]. Interestingly, full ablation of PARG causes embryonic lethality in mice and *Drosophila*. Mice with a hypomorphic deletion of only the nuclear 110 kDa PARG isoform ($PARG_{110}^{-/-}$), but retaining the 60 kDa isoform are viable and fertile, potentially by compensatory mechanisms of the 60 kDa isoform[198].

Strikingly, either inhibition or genetic ablation of ADP-ribosylation writers (i.e. ARTD1) and erasers (i.e. PARG), protect against many inflammatory diseases. So far, PARG has been implicated in different PAMP and DAMP-associated inflammation models, such as peritonitis, LPS-induced septic shock, Dinitrobenzene sulfonic acid (DNBS)-induced colitis and oxidative-stress induced neuronal cell death[192]. However, without providing underlying molecular mechanisms. During pathogenic infections PARG has opposing functions: While PARG inhibition by GPI 18214 protects mice during zymozan (glucan of cell surface of yeast)-induced peritonitis, by decreased neutrophil infiltration into the lungs and decreased plasma TNF-α and IL-1β levels[200], $PARG_{110}^{-/-}$ are hypersensitive to LPS-induced septic shock[198].

PARG has also been suggested to promote ischemia-reperfusion-induced tissue injuries. For example, PARG inhibition or genetic ablation of PARG in mice and rats decreased neutrophil infiltration, endothelial expression of ICAM-1 and P-Selectin and TNF-α plasma levels during gastrointestinal ischemia[201]. Moreover, PARG inhibition decreased the infarct size in a rat-model of cerebral ischemia reperfusion[202]. In a model of renal ischemia reperfusion, $PARG_{110}^{-/-}$ mice exhibited significantly reduced tissue injury and dysfuntion[203]. Analogously to ARTD1, PARG does also promote IBD. $PARG_{110}^{-/-}$ mice were resistant and PARG inhibitor treated mice were significantly protected in a model of DNBS-induced colon injury[204]. Mutant mice exhibited significantly lower colon TNF-α and IL-1β levels.

Overall the currently available data suggests important functions of PARG during different inflammatory conditions that are worthwhile pursuing in the future. Especially PARGi could open new therapeutic opportunities for treating inflammatory diseases. However, functional analyses to understand the molecular mechanisms of the abovementioned phenotypes are critically needed. Moreover, the role of other erasers during inflammation might be attractive targets for further investigations.

9. ADP-riboslyation as anti-viral defense mechanism

Viruses are non-living biological agents which only replicate in infected host cells, hence "hijack" the cellular machinery to generate new viral particles. Successful virus replication in infected cells is strongly determined by the balance between two competing processes: (i) the ability of cells to sense virus-specific PAMPs and (ii) the ability of viral proteins to interfere with the cellular response to viral infection[205]. In fact, cells rely on ARTD1 family member dependent defense mechanisms during different phases of viral replications.

Interferon stimulated cells are primed for antiviral responses and express various antiviral genes. Recently, Zhang et al identified the ARTD9-deltex E3 ubiquitin ligase 3L (DTX3L) interaction as potent antiviral mediators[206]. During interferon signaling, ARTD9-DTX3L and STAT1 interaction activates the E3 ubiquitin ligase activity towards histone H2B at distinct chromatin loci to facilitate host proinflammatory gene expression. In addition, ARTD9-DTX3L E3 ubiquitin ligase activity also targeted the viral 3C protease degradation by the immunoproteasome[206]. Thus, ARTD9-DTX3L targets host and viral protein to promote viral clearance.

Host antiviral protein expression during infection is crucial for viral elimination. In plants and intervetebrates, the expression of these transcripts is in part regulated post transcriptionally by RNAi[207]. In eukaryotic virus infected cells, ARTD13 reduced RNAi activity and promoted interferon-stimulated gene (ISGs) expression. Mechanistically, the authors observed a correlation between the poly-ADP-ribosylation of the RNA-induced silencing complex (RISC) and ARTD13[207]. Since ARTD13 is enzymatically inactive, we propose that another ARTD family member PARylates RISC in an ARTD13 dependent manner.

After successful entry into a host cells, viral mRNA needs to be expressed by the host transcription machinery. In an elegant search for novel host antiviral factors Gao et al. identified a *Zinc-finger Antiviral Protein*, today known as the catalytically inactive ARTD13 being a viral RNA binding protein[208]. Interaction studies identified two RNA helicases (p72 and DHX30) and exosome components to associate with ARTD13 suggesting that ARTD13 regulates viral RNA unwinding and exosome degradation [209]. So far, ARTD13 inhibits various retroviruses including human immunodeficiency virus 1 (HIV-1), or other RNA

viruses such as Alphaviruses and Filoviruses[209]. Recently, ARTD14/PARP7 has been identified to sense viral RNA as well and initiate viral RNA degradation in an exosome-dependent manner[210]. Thereby ARTD14 inhibits Sindbis Virus replication in host cells.

Viral replication oftentimes occurs in the nucleus of the infected cell. Under basal conditions, tankyrase 1 and tankyrase 2 (ARTD5 and ARTD6) regulate telomere maintenance, WNT-signaling and mitosis[211]. A recent study identified that during herpes simplex virus (HSV) infection, particularly tankyrase 1 is phosphorylated and localized to the nuclear viral replication compartment[212]. HSV did not replicate in tankyrase 1 and 2 depleted cells or pharmacologically inhibited (XAV939) cells, suggesting that tankyrase activity promote HSV replication.

Host ribosomes translate viral transcripts and mediate viral amplification. A recent study identified ARTD12/PARP12 to interfere with viral translation[205]. Mechanistically, the data suggests that the longer isoform of the two ARTD12 isoforms, ARTD12L as well as its catalytic activity are required for complex formation with ribosomal proteins at polysomes to efficiently inhibit venezuelan equine encephalitis virus (VEEV) translation[205]

AIM OF THE THESIS

ADP-ribosylation plays important roles during various PAMP and DAMP-mediated inflammatory conditions. Several *in vitro* studies identified ARTD1 as promoter-specific transcriptional co-activator for NF-κB and critical regulator of proinflammatory gene expression in macrophages. Since inflammatory processes involve very complex multicellular networks, the lack of cell type specific ARTD1 knock-out mice significantly limit functional investigations of ARTD1 *in-vivo*. In addition, PARPi reduced the inflammatory burden of the host, but which cell types are particularly PARPi sensitive and which ARTD family members contribute to PARPi activities during inflammation are currently not clear.

The thesis addressed the following specific aims:

(i) To develop a macrophage-specific ARTD1 knock-out mouse and to investigate the contribution of ARTD1 in macrophages *in vivo* using three different models inducing a Th1 response.

(ii) To investigate in which cell type ADP-ribosylation inhibitors (i.e. Talazoparib or Olaparib) affect LPS-induced proinflammatory signaling.

(iii) To identify additional ARTD family members involved in the LPS-induced inflammatory signaling response in fibroblasts.

RESULTS

1. Overview of manuscript in preparation

1.1. ARTD1 in macrophages controls the IL-12/18-IFN-γ axis in an acute sepsis model, during *Helicobacter pylori* infection and in a MC-38 tumor model

Authors **F. A. Kunze**, M. Bauer, J. Komuczki, M. Lanzinger, K. Gunaserkara, A. Hopp, M. Lehmann, B. Becher, A. Müller and M. O. Hottiger

Contribution Conceived and planned the project, Generated ARTD1$^{\Delta Myel}$, ARTD1$^{del/del}$ mice, RNA-seq of BMDM, qPCR and ELISA analyses of BMDM, NK cells, total spleen tissue and blood serum, assisted in writing the paper

2. Overview of published manuscripts

2.1. ARTD1-induced poly-ADP-ribose formation enhances PPARγ ligand binding and co-factor exchange

Authors M. Lehmann, E. Pirinen, A. Mirsaidi, **F. A. Kunze**, P. J. Richards, J. Auwerx, and M. O. Hottiger

Journal Nucleic Acids Research, vol. 43, no. 1, pp. 129–142, Jan. 2015

Contribution Performed gene expression in adipose tissue (Figure 1)

2.2. ARTD1 regulates osteoclastogenesis and bone homeostasis by dampening NF-κB-dependent transcription of IL-1β

Authors A. Robaszkiewicz, C. Qu, E. Wisnik, T. Ploszaj, A. Mirsaidi, **F. A. Kunze**, P. J. Richards, P. Cinelli, G. Mbalaviele, and M. O. Hottiger

Journal Science Reports, vol. 6, no. 1, p. 21131, Feb. 2016

Contribution Performed gene expression in bone (Figure 5)

ARTD1 in macrophages controls the IL-12/18-IFN-γ axis in an acute sepsis model, during *Helicobacter pylori* infection and in a MC-38 tumor model

Friedrich A. Kunze[1,2], Michael Bauer[3,5], Juliana Komuczki[1,4], Margit Lanzinger[1,4], Kapila Gunasekera[1], Ann-Katrin Hopp[1,2], Mareike Lehmann[1,4], Burkhard Becher[4], Anne Müller[3] and Michael O. Hottiger[1*]

[1]Department of Molecular Mechanisms of Disease, University of Zurich, Winterthurerstrasse 190, CH-8057 Zurich, Switzerland,
[2]Molecular Life Science PhD Program of the Life Science Zurich Graduate School, Winterthurerstrasse 190, CH-8057 Zurich, Switzerland,
[3]Institute of Molecular Cancer Research, University of Zurich, Winterthurerstrasse 190, CH-8057 Zurich, Switzerland,
[4]Institute of Experimental Immunology, University of Zurich, Winterthurerstrasse 190, CH-8057 Zurich, Switzerland,
[5]Molecular Life Science PhD Program of the Life Science Zurich Graduate School, Winterthurerstrasse 190, CH-8057 Zurich, Switzerland,

Short title: ARTD1 in macrophages controls the IL-12/18-IFNγ axis
Key words: ADP-ribosylation, PARP, LPS, IFN gamma, Helicobacter pylori, MC-38,

Corresponding authors:
michael.hottiger@dmmd.uzh.ch

ABSTRACT/Summary

Toll-like receptors (TLR) transcriptional activation of proinflammatory genes in different cell types has been described to involve ARTD1/PARP1 *in vitro*. Also *Artd1* knockout mice were protected against PAMPs induced inflammation model. However, it is not clear to which extent ARTD1 contributes *in vivo* to the T_H1 polarization in a specific cell type. We therefore generated a conditional macrophage-specific *Artd1* knockout strain (i.e. $Artd1^{\Delta Myel}$) which was investigated in three different immunological models: i) acute systemic LPS-induced inflammation, ii) local gastric Helicobacter pylori infection and iii) subcutaneous MC-38 tumor model. We observed that ARTD1 deficiency in bone marrow-derived macrophages regulated a specific set of genes in an enzymatically independent manner and reduced the LPS induced IL-12/IFN-γ signaling in an acute sepsis model *in vivo*. The loss of ARTD1 in macrophages reduced the T_H1 response to *H. pylori* and led to *H. pylori* hyper-colonization of the gastric mucosa. Similarly, $Artd1^{\Delta Myel}$ mice failed to control tumor growth in a subcutaneous MC-38 xenograft model due to reduced T_H1 and CD8 responses. Together, these data provide strong evidence that ARTD1 controls type I immunity by regulating IL-12 and IL-18 expression in macrophages in a manner that is independent of its enzymatic activity.

INTRODUCTION

Inflammation is orchestrated by different cell types that integrate diverse stimuli for the generation of a specific immune response to kill invading pathogen and/or to clear and regenerate damaged tissue[1]. Beside immune cells such as the antigen presenting macrophages or dendritic cells also epithelial, endothelial and fibroblast cells express pathogen recognition receptors (PRRs) that initiate an innate immune response[2]. PRRs recognize a variety, but yet defined set of conserved pathogen associated molecular patterns (PAMPs), such as bacterial and fungal cell wall components (i.e. lipopolysaccharides, LPS) or danger associated molecular patterns (DAMPs)[3]. The recognition of DAMPS and PAMPs, often by the same receptors, activates intracellular signaling pathways, which are controlled by different proteins and result in the expression of pro-inflammatory cytokines such as IL-12, IL-23, IL-6 and IL-1β [4]. IL-12 produced by antigen presenting cells (APCs) in response to certain pathogenic infections activates NK cells and promotes T_H1 differentiation and interferon γ (IFN-γ) production[5].

Septic shock is the most common cause of death in intensive care units and it is usually the result of a systemic Gram-negative bacterial infection resulting in hypotension and failure of several organ systems, in particular the liver, kidney and heart[6]. The bacterial membrane component lipopolysaccharide (LPS), when injected into animals, causes a shock-like state that can even lead to death. The mechanism by which LPS induces endotoxic shock is related to its ability to activate the NF-κB/Rel family of transcription factors, enabling the expression of several critical genes involved in the pathogenesis of septic shock mediated by an excessive T_H1/T_H17-predominant responses[7]. LPS binding to TLR4 induces the activation of several primary response genes such as *Ifnb1* and *Ccl5*[8]. Comparably, *Helicobacter pylori* (*H. pylori*) causes a persistent mucosa-associated but non-invasive infection that is characterized by either regulatory T cell (Treg)- or T_H1/T_H17-predominant responses[9]. In children and neonatally infected mice, the *H. pylori*/host interaction is generally asymptomatic and characterized by a lack of effector T cell responses, predominance of Tregs, and high level colonization[10,11]. Mice infected in adulthood exhibit a striking T cell infiltrate that is dominated by effector T cells and limits the bacterial burden without clearing *H. pylori* completely[10,11]. Rather, the large quantities of IFN-γ produced by *H. pylori*-specific T_H1 cells are believed to be the direct cause of the pre-malignant lesions, i.e. epithelial hyperplasia and intestinal metaplasia that precede the development of gastric cancer[10].

Myeloid cells populate the tumor microenvironment[12]. These myeloid cells are highly heterogeneous with cells of both the monocytic and granulocytic lineages, and have considerable phenotypic plasticity with both positive and negative effects on tumor growth

and metastasis[13,14]. The balance between anti-tumor and pro-tumor functions can depend on the polarization state, the interaction with the tumor microenvironment and/or the tumor type[12,15,16]. Grafting MC38 cells (derived from a mouse colon adenocarcinoma), to a genetically identical inbred, immune competent mouse ('syngraft' or 'isograft') is a way of overcoming the species mismatch between tumor and stroma, which likely affects cell communication and the use of immune-deficient hosts[17]. We recently reported that MC-38 mouse colon cancer cells contain functional hypoxic (HIF-1α) and inflammatory (p65/RelA) signaling pathways[18]. In contrast to cells of the myeloid lineage, HIF-1α levels remained unaffected in MC-38 cells treated with LPS, and hypoxia failed to induce NF-κB. The correspondent regulation of canonical HIF and NF-κB target genes confirmed these results.

Furthermore, we and others have reported that ARTD1 (also known as PARP1) promotes NF-κB dependent expression of pro-inflammatory cytokines such as IL-1β, IL-6, TNF-α and CXCL-2; and adhesion molecules such as ICAM, VCAM or E-Selectin in LPS- but also TNF-α stimulated macrophages and fibroblasts[19-21]. ARTD1 belongs to the family of intracelluar diphtheria toxin-like ADP-ribosyltransferases that covalently attach ADP-ribose (ADPr) to amino acid residues of target proteins using nicotinamide adenine dinucleotide (NAD^+) as substrate. This process is called protein ADP-ribosylation and represents an ancient posttranslational modification (PTM) found in a wide range of biological species[22-24]. Protein ADP-ribosylation can either affect the enzymatic activity of the modified protein or their interaction with nucleic acids and with other proteins[25]. The above findings regarding the transcriptional regulation of ARTD1 in different cells types is further supported by the fact that ARTD1 knock-out mice are resistant to a high dose LPS-induced endotoxin shock model[26], suggesting a dominant role of ARTD1 during inflammatory signaling. Historically, ARTD1 is known for its role during DNA damage response (DDR), particularly the base excision repair (BER) pathway and double strand break (DSB) repair pathway[27]. These involvements let to the development of small-molecule ADP-ribosylation inhibitors (i.e. PARP inhibitors; PARPi). The underlying concept was that the inhibition of the DNA-repair machinery could sensitize tumor cells to conventional DNA-damage-based therapies such as chemo- or radiotherapy[28]. Beside the treatment of cancer patients with PARPi, these compounds have also been reported to dampen different inflammation types, confirming that ADP-ribosylation also regulates one or several inflammatory processes and that this might also contribute to the anti-tumor activity of PARPi[28,29]. Beneficial effects of PARPi have also been implicated in numerous inflammatory disease models[30-32]. For example, we showed that PJ34 could prevent and also cure Helicobacter-associated, T cell–driven immunopathology that precedes gastric cancer development. PJ34 exerts its anti-inflammatory effects in a Helicobacter model by impairing T cell priming and T_H1 polarization in the gut-draining

mesenteric lymph nodes[33]. Our data indicate that PJ34 directly suppresses T cell effector functions by blocking the IFN-γ production of mesenteric lymph node T cells *ex vivo*. However, it is not clear whether ARTD1 or another ARTD family member contributes to these observations and to which extent ARTD1 regulated a specific cell type that contributes to the T_H1 polarization. The presence of ARTD1 in the nucleus of LPS-stimulated macrophages hinted at its possible role in mediating some nuclear effects elicited by LPS, a possibility also suggested by previous reports describing a transcriptional coregulator activity of ARTD1[34-36].

To address the role of ARTD1 in macrophages during different inflammatory responses, we generated a mouse strain with a Cre-mediated deletion of ARTD1 specifically in macrophages. We observed that ARTD1 deficiency in BDMB of regulates a specific set of genes in an enzymatically independent manner and reduces the LPS induced IL-12/IFN-γ signaling in an acute sepsis model *in vivo*. Moreover, *H. pylori* infection in $ARTD1^{\Delta Myel}$ mice induced a reduced IFN-γ expression in gastric CD4 T cells and $ARTD1^{\Delta Myel}$ mice displayed a significantly increased MC-38 tumor growth due to a reduced activation of CD4 and CD8 T cells. Together, we provide strong evidence that ARTD1 controls in macrophages the IL-12/18-IFN-γ axis in an enzymatically independent manner.

RESULTS

ARTD1 regulates IL-12/IL-18 gene expression in BMDM in an enzymatic independent manner

ARTD1 plays important roles in a wide variety of functionally interconnected cell types that control inflammation outcomes, including macrophages, dendritic cells, T or B cells[37], making it difficult to separate the effects of ARTD1 in one cell type from effects in other cell type. Thus, studies with whole-body *Artd1*-null mice in which ARTD1 is absent throughout development have often yielded conflicting results[38]. To avoid these complications while examining the specific role of ARTD1 in inflammation, we developed a mouse line with a conditional ("floxed") exon 4 of *Artd1* (*Artd1*$^{flox/flox}$) (Fig. 1A and S1A, S1B). In order to establish that the floxed allele can be inactivated, we first crossed the *Artd1*$^{flox/flox}$ mice with transgenic mice containing a *CMV-cre* cassette to generate a full body ARTD1 knockout (*Artd1*$^{flox/flox}$*;CMV-cre*), hereafter called *Artd1*$^{del/del}$ (Fig. 1A). The whole body ARTD1 deficient mouse developed normally and was fertile comparably to the corresponding ARTD1 proficient mouse and the classical *Artd1*$^{-/-}$ mouse[39]. Although western blotting showed complete loss of ARTD1 in the organs tested (Fig S1C), ARTD1 loss did not affect organ weight or organ structure (Figure S1D, data not shown).

Since we aimed for an investigation on the role of ARTD1 in macrophages specifically, we generated bone marrow derived macrophages (BMDM) from *Artd1*$^{del/del}$ mice and confirmed the genetic deletion of the *Artd1* gene by qPCR (Fig. S1E).

To assess the functional role of ARTD1 in macrophages, BMDM from *Artd1*$^{del/del}$ mice and *Artd1*$^{flox/flox}$ controls at day 6 of differentiation were treated with LPS/IFN-γ for 4 hrs, RNA was extracted and the RNA was subsequently analyzed by deep sequencing. We compared untreated and LPS/IFN-γ-treated BMDM to directly identify target genes regulated downstream of TLR4/IFN-γ-receptor. The overall gene expression patterns in untreated and LPS/IFN-γ treated *Artd1*$^{flox/flox}$ BMDM were quite distinct (Fig. 1B). Stimulation caused a robust induction of pro-inflammatory response genes (approx. 2500, Fig 1B), including NF-κB-dependent genes (e.g. *Ifnb1, Ccl5 and Cxcl10*), while the expression of many basal expressed genes was reduced (approx. 3000; Fig. S1F). When focusing only on the activated inflammatory response genes, deletion of ARTD1 reduced the induced expression levels of some genes suggesting that ARTD1 would act, as already reported by our group and others, as transcriptional co-activator for these genes (Fig 1C, lower panel). The other half of genes was upon deletion of ARTD1 further enhanced providing evidence that the lack of ARTD1 would also negatively affect gene expression (Fig. 1 C, upper panel). Independent qPCR

analysis of a defined set of genes belonging to both clusters confirmed the quantitative RNA-seq analysis (Fig. 1D). These data suggested that ARTD1 indeed regulated LPS/IFN-γ-induced gene expression in macrophages in different ways, although the expression of pro-inflammatory gene expression is rather positively regulated.

To gain insight into potential pathways driving LPS/IFN-γ-mediated transcriptional regulation and their downstream effects, gene ontology (GO) analyses were performed. Analyzing all LPS/IFN-γ-induced genes (Fig. 1B) revealed macrophage characteristic pro-inflammatory pathways significantly enriched including T cell activation, IFN-γ-production and NK cell activation (Fig 1E, left). Next, to investigate the degree of ARTD1 co-activating and co-repressing gene expression during LPS/IFN-γ signaling, the previously identified GO terms were matched to co-activated genes of ARTD1 (lower expression in ARTD1 deficiency, identified in Fig. 1C lower panel) and co-repressed by ARTD1 (higher expression in ARTD1 deficiency, identified in Fig 1 C upper panel). For all analyzed pathways ARTD1 co-represses significantly more genes than it activates. The data thus suggests that, globally, ARTD1 acts predominantly as a co-activator of pro-inflammatory gene expression rather than as a repressor.

To investigate whether the observed transcriptional regulation of LPS/IFN-γ induced target genes by ARTD1 is dependent on its enzymatic activity, the stimulation experiment was repeated in presence of two ADP-ribosylation inhibitors (i.e. PARPi) (Fig. S1G, S1H). Although treatment of WT BMDM with PARPi affected the expression of a few genes under the tested conditions, the pro-inflammatory genes observed above, where not affected, suggesting that the enzymatic activity of ARTD1 in macrophages is not contributing under the tested conditions to the innate immune response (Fig. S1G, S1H).

To confirm that the observed transcriptional changes are indeed also relevant at the protein level, the expression levels of a distinct set of cytokines was confirmed by ELISA after treatment of BMDM from *Artd1*$^{flox/flox}$ and *Artd1*$^{del/del}$ mice with LPS/IFN-γ for 18 hrs. The quantified levels of IL-12p70, IL-18, IL-6 and TNF-α were all significantly reduced in BMDM from ARTD1 deficient mice compared to WT mice (Fig. 1F) strongly confirming that ARTD1-mediated transcriptional control affects the T_H1-mediating polarization of the innate immune response in macrophages *in vitro*.

Myeloid cell-specific deletion of ARTD1 reduces the LPS induced IL-12/IFN-γ signaling in an acute sepsis model *in vivo*

Given the above reported results on the impact of ARTD1-deficiency in macrophages on their transcriptional reprogramming with respect to their T_H1 polarizing potential, we investigated in more detail the role of ARTD1 in macrophages in three different animal

models that are mediated and regulated by a strong T_H1 response.

Treating mice with a lethal dose of lipopolysaccharide (LPS, 40mg/kg) resulted in the rapid activation of NF-κB in macrophages from wildtype but not from ARTD1-deficient mice[26]. ARTD1-deficient mice proved to be extremely resistant to LPS-induced endotoxic shock. Although a deficient activation was found in isolated macrophages from ARTD1-deficient mice injected with LPS, the contribution of ARTD1 specifically in macrophages *in vivo* was not tested due to the lack of conditional knockout mice. To explore the specific role of ARTD1 in macrophages *in vivo*, we first crossed the *Artd1*$^{flox/flox}$ mice with transgenic mice containing a *LyzM-cre* cassette to generate a conditional ARTD1 knockout in macrophages (*Artd1*$^{flox/flox}$*;LyzM-cre*), hereafter called *Artd1*$^{\Delta Myel}$. Mice lacking ARTD1 only in macrophages developed normally and were fertile comparably to the corresponding ARTD1 proficient mouse (data not shown). The macrophage specific targeting was confirmed by western blotting for ARTD1 in *ex vivo* BMDMs and *in vivo* peritoneal macrophages (Fig. S2A).

To study the initiation of the innate immune response under non-lethal LPS conditions, we performed low dose LPS treatments in *Artd1*$^{\Delta Myel}$ mice and controls. *Artd1*$^{flox/flox}$ and *Artd1*$^{\Delta Myel}$ mice of 6–12 weeks of age were intraperitoneally (i.p.) injected with 4 mg/kg body weight of LPS. Both *Artd1*$^{flox/flox}$ and *Artd1*$^{\Delta Myel}$ mice equally showed a series of responses such as fever and lethargy, but none of the animals died during the 4 h time course of the experiments (data not shown). Furthermore, the activation of the macrophages *in vivo* following the low LPS i.p. injection was determined using serum samples obtained from control or LPS-treated mice. Four hours LPS treatment very strongly induced the serum level of IFN-γ, IL-12p70, IL-18, TNF-α and IL-6 (Fig. 2B). The serum levels of IFN-γ were significantly reduced in *Artd1*$^{\Delta Myel}$ mice, while the other tested cytokines were reduced although under the tested conditions not to a significant extent (Fig. 2B). Analyses for anti-inflammatory cytokines revealed that except for IL-4, the serum levels of IL-10 and IL-13 were unchanged (Fig. S2B), suggesting that the observed differences in proinflammatory cytokine levels were not due to an enhanced anti-inflammatory response under the tested conditions. Together these data confirm the initiation of an innate immune response with the applied low LPS dose and support the *in vitro* data that ARTD1 deficient macrophages fail to express IFN-γ-inducing Il-12 and IL-18.

Since the expression of IFN-γ is strongly induced by IL-12/18[40], we analyzed the transcriptional expression levels of the same cytokines in isolated spleen tissue from LPS treated *Artd1*$^{flox/flox}$ and *Artd1*$^{\Delta Myel}$ mice. LPS induced a strong expression of *Ifng, Il12b, Il18, Tnfa* and *Il6* mRNA which was significantly reduced in spleen tissue from *Artd1*$^{\Delta Myel}$ mice (Fig. 2C) indicating that this inflammatory program is strongly regulated by macrophage-

resident ARTD1.

To assess whether the macrophage-specific ARTD1-deletion affects the cellular composition of the spleen that could be responsible for altered cytokine production, splenocytes from *Artd1*$^{flox/flox}$ and *Artd1*$^{\Delta Myel}$ mice were immunophentoyped by flow cytometry using cell type specific markers. These experiments revealed that only the B and CD4 T cell counts were significantly increased in untreated *Artd1*$^{\Delta Myel}$ compared to the *Artd1*$^{flox/flox}$ control mice, while all the other tested cell types including CD8 T, NK, granulocytes, and most importantly macrophages, monocytes or neutrophils were not altered (Fig. S2C), indicating that the lack of ARTD1 in macrophages did not affect the macrophage development or colonialization of the spleen *in vivo*.

During acute inflammation and the innate immune response IFN-γ is mainly expressed from NK and to a lower extent by T cells[41]. To identify the cell type responsible for the observed IFN-γ levels in the spleen (Fig. 2C) and the serum (Fig. 2B), we performed an intracellular staining for IFN-γ in NK, CD4 and CD8 T cells isolated from the spleen of LPS treated *Artd11*$^{flox/flox}$ and *Artd1*$^{\Delta Myel}$ mice (Fig. 2D). In all three cell types, LPS treatment lead to a detectable IFN-γ level, although the number of NK cell expressing IFN-γ was considerably higher compared to CD4 and CD8 T, suggesting that NK cells from spleen are the main cell type responsible for the observed differences in IFN-γ expression (Fig. 2D). Moreover, in *Artd1*$^{\Delta Myel}$ mice only the numbers of IFN-γ positive NK cells were lowered but not the ones of IFN-γ expressing CD4 and CD8 T cells, suggesting that ARTD1-deficiency in macrophages mainly affects the IFN-γ levels in NK cells. To exclude that NK cells from *Artd1*$^{flox/flox}$ and *Artd1*$^{\Delta Myel}$ mice were differently responsible to IFN-γ-inducing IL-12/18 signaling, isolated NK cells from both cell types were isolate and stimulated for 18 hrs with IL-12p70 (10 ng/ml) and subsequently the IFN-γ expression was measured by ELISA. Stimulation of the NK cells from both mouse strains induced the IFN-γ expression in an IL-12p70 dependent manner and most importantly to the same extent (Fig. 2E), providing strong evidence, that the reduced IFN-γ levels in *Artd1*$^{\Delta Myel}$ mice are indeed due to the reduced production of IL-12/18 cytokines in macrophages and that ARTD1 is an important transcriptional activator for these genes.

ARTD1 expression by macrophages is required for T_H1 responses and bacterial immune control

Immunocompetent adult C57BL6 mice infected with the human gastric pathogen *H. pylori* exhibit a striking T cell infiltration that is dominated by T_H1- and T_H17-polarized CD4 T-cells and limits the bacterial burden[9]. The large quantities of IFN-γ and IL-17 produced by *H. pylori*-specific T_H1 and T_H17 cells are believed to be the direct cause of the pre-malignant

lesions, i.e. epithelial hyperplasia and intestinal metaplasia that precede the development of gastric cancer[42]. To investigate the role of ARTD1 in macrophages for the development of *H. pylori*-specific T_H1 and T_H17 responses we infected *Artd1*$^{flox/flox}$ and *Artd1*$^{\Delta Myel}$ mice with 10^8 CFU of the human patient isolate *H. pylori* PMSSI (Fig. 3A). After 30 days, the mice were sacrificed and colony forming unit (CFU) assays of homogenized stomach tissue displayed successful gastric *H. pylori* colonization (Fig. 3A). In addition, *H. pylori* infected *Artd1*$^{\Delta Myel}$ stomach homogenates exhibited significantly increased CFU when compared to *Artd1*$^{flox/flox}$ counterparts (Fig. 3A). To test the ability of ARTD1 deficient myeloid cells to initiate a T_H1 and T_H17 response we quantified CD4 T cells in the stomach of *Artd1*$^{flox/flox}$ and *Artd11*$^{\Delta Myel}$ mice either given PBS or *H. pylori*. Although a significant *H. pylori* dependent increase of gastric CD4 T cell infiltration was observed 4 weeks post infection, the levels of CD4 T cells were similar between *Artd1*$^{flox/flox}$ and *Artd1*$^{\Delta Myel}$ mice (Fig. 3B). To assess the activation status of the infiltrated CD4 T cells we quantified IFN-γ and IL-17 expression by intracellular flow cytometrical cytokine staining (Fig. 3C). *H. pylori* infection induced a mild IFN-γ expression in gastric CD4 T cells (Fig. 3C), which was slightly decreased in *Artd1*$^{\Delta Myel}$ mice compared to *Artd1*$^{flox/flox}$ mice. Additionally, IL-17 was *H. pylori* dependently induced however not differently in *Artd1*$^{flox/flox}$ and *Artd1*$^{\Delta Myel}$ mice. The data suggests that ARTD1-deficient gastric macrophages recruit equal numbers of CD4 T cells, but fail to activate them in an IFN-γ-T_H1-dependent manner.

Artd1$^{\Delta Myel}$ mice displayed a significantly increased MC-38 tumor growth due to a reduced activation of CD4 and CD8 T cells

Understanding the impact of myeloid cells on cancer development could be essential in distinguishing and possibly manipulating positive and negative myeloid effectors. Myeloid cells recognize tumors and are important initiators of T_H1-mediated tumor elimination but some subpopulations of myeloid cells have also be described to promote tumor growth [43]. To investigate the role of myeloid cell-specific ARTD1 to the contribution to tumor growth we subcutaneously injected $0.5x10^6$ colon adenocarcinoma MC-38 cells into the flanks of *Artd1*$^{flox/flox}$ and *Artd1*$^{\Delta Myel}$ mice. Caliper measurements of the tumor volume demonstrated efficient engraftment of MC-38 cells in both mouse strains. From day 6 on, *Artd1*$^{\Delta Myel}$ mice displayed a significantly increased tumor growth compared to *Artd1*$^{flox/flox}$, which lasted until the end of the study at day 14 (Fig. 4A).

To assess tumor infiltration in *Artd1*$^{flox/flox}$ and *Artd1*$^{\Delta Myel}$ mice we quantified macrophages by flow cytometry after 14 days. Increased tumor volume in *Atd1*$^{\Delta Myel}$ mice was associated with decreased tumor macrophage infiltration (Fig. 4B) and reduced macrophage activation in MC-38 tumors (i.e. TNF-α expression) (Fig. 4B). Myeloid cells recruit and activate CD4 and CD8 T cells to the tumor site where they differentiate into T helper or

cytotoxic T cells, respectively. Whereas the overall CD4 and CD8 T cell infiltration of *Artd1*$^{flox/flox}$ and *Artd1*$^{\Delta Myel}$ mice was similar (Fig 4C) we observed a reduction in their IFN-γ and TNF-α expression (Figure 4D). The combined data suggest that ARTD1-deficient macrophages infiltrate MC-38 tumors less efficiently and fail to produce TNF-a. Although overall CD4 and CD8 T cell recruitment to the tumor microenvironment is similar in *Artd1*$^{flox/flox}$ and *Artd1*$^{\Delta Myel}$ mice, their activation and IFN-γ and TNF-α expression is significantly reduced thus allowing aberrant tumor growth.Together, the above described three models all provide strong insights into the function of ARTD1 in macrophages. In all three models, lack of ARTD1 reduced the T_H1/T_H17 response due to the strongly reduced expression of IL-12/18 and subsequently the expression of IFN-γ either in NK cells (acute systemic LPS model) or in CD4/8 T cells in the local *H. pylori* and MC-38 tumor model.

DISCUSSION

In this study, we investigated the role of ARTD1 in macrophages in three different immunological models: i) an acute systemic LPS-induced inflammation, ii) a local gastric *H. pylori* infection or iii) a subcutaneous MC-38 tumor model *in vivo*. We observed that in BMDM of ARTD1-deficient mice a specific set of pro-inflammatory genes is regulated in an enzymatically independent manner which leads to reduced LPS-induced IL-12/IFN-γ serum levels and to altered inflammatory signaling in an acute sepsis model *in vivo*. Moreover, *H. pylori* infection in $Artd1^{\Delta Myel}$ mice induced only a reduced IFN-γ expression in gastric CD4 T cells, and $Artd1^{\Delta Myel}$ mice displayed a significantly increased MC-38 tumor growth due to a reduced activation of CD4 and CD8 T cells. Together, these data provide strong evidence that ARTD1 controls in macrophages the IL-12/18-IFN-γ axis in an enzymatically independent manner.

To investigate the relevance of ARTD1 in macrophages, we generated conditional knockout animals with an ARTD1-deficiency in macrophages. Analyses of the cell type composition in the spleen of these animals revealed that only the B and CD4 T cell counts were significantly increased in untreated $Artd^{\Delta Myel}$ compared to the $Artd1^{flox/flox}$ control mice, while all the other tested cell types including macrophages were not altered. It is currently not clear why B and CD4 T cells counts were increased, but given that the number of macrophages was not altered, and an increase of particularly CD4 T cells might have rather lead to increased IFN-γ levels upon LPS-stimulation, the observed changes in cell numbers rather unlikely contributed to the changes in cytokine expression.

Different mechanistic models have been reported on how ARTD1 influences NF-κB-dependent gene expression. ARTD1 acts as a transcriptional co-factor for NF-κB and promotes gene expression by functional cooperation with the transcription machinery in response to pro-inflammatory stimuli[44]. LPS- and TNF-α-induced NF-κB dependent gene expression in macrophages and fibroblasts was enhanced by ARTD1 independently of its enzymatic activities, by initiating a mediator complex with p300 and NF-κB. Also in these presented studies, treatment of BMDM with ADP-ribosylation inhibitors (e.g. Olaparib or PJ34) did not affect the expression of LPS/IFN-γ induced gene expression, although some non-inflammation related genes were susceptible to the inhibitors. In contrast to these reports, another report suggested that LPS treatment of macrophages induced ARTD1's enzymatic activity and nucleosome remodeling at promoters of pro-inflammatory genes, which directly destabilized histone-DNA interactions and facilitated NF-κB binding and gene expression[45]. The discrepancies could be explained by methodological differences such as the cell type

(RAW.267.4 macrophages and primary BMDM or fibroblasts), the source of LPS (*S. enterica* and *E.coli*) or the serum starvation overnight prior LPS stimulation.

The LPS-induced expression of IL-12/18 in primary macrophages seemed to be dependent on ARTD1 *in vitro* but also *in vivo*. Whether these two genes are regulated in a similar manner and as indicated above remains to be investigated. The *Il12b* gene is a well-studied example of a gene that requires chromatin remodeling during inflammation-induced gene expression. Studies of the *Il12b* promoter identified binding sites for various transcription factors including NF-κB, C/EBP, AP-1 and NFAT[46-48]. However their binding sites, -30 to -175 bp upstream the transcription start site, are blocked by nucleosomes and require nucleosome remodeling prior transcription[49]. Indeed the SWI-SNF complex, which is responsible for nucleosome positioning[50] is recruited to target genes in LPS-stimulated macrophages[51]. Different models describe the targeting of chromatin remodeling machines to their site of action, i.e. acetylated histones that target and stabilize the SWI-SNF complex at target loci[52]. Very recently another report confirmed that small hairpin RNA–mediated knockdown of the endogenous ARTD1 expression resulted in reduced IL-12p40 mRNA expression and *Il12b* promoter activity[53]. BMDM from ARTD1–deficient mice had also decreased IL-12p40 expression at both mRNA and protein levels.

IL-12 is a cytokine that connects innate and adaptive immune responses either indirectly via NK cell activation or directly by activating CD4 and CD8 T cells[7]. In this study, we observed a reduced NK cell activation during sepsis in $Artd1^{\Delta Myel}$ compared to $Artd1^{flox/flox}$ mice. Our data suggests that ARTD1 deficient macrophages fail to activate NK cells via *IL-12* expression, ultimately leading to decreased IFN-γ serum levels and thus protecting against an acute LPS-induced sepsis. Several lines of evidence suggest that NK cells might be involved in key functions during sepsis[41]. Similar to ARTD1 knock-out mice, antibody mediated NK cell depletion *in vivo* protected against LPS-induced shock and significantly decreases IFN-γ cytokine levels[26,54]. NK cells promote and particularly amplify as very early and main producers of IFN-γ during sepsis the inflammatory response. Today, NK cells represent promising targets for novel approaches in sepsis therapy[41].

Reduced NK cells activation significantly reduces the speed of pathogen clearance during sepsis[41]. Thus, by enhancing *Il12b* expression in macrophages ARTD1 also contributes to a potent immune response to pathogens. This was very obvious in the second disease model we investigated. Previous studies characterized the stomach under basal conditions to be a predominantly myeloid organ with little or no lymphocyte contribution[42]. Myeloid cells centrally function as initiators of immune responses against pathogens. Our study revealed that ARTD1 deficient macrophages recruit equal numbers of CD4 T cells during gastric *H. pylori* infections into the stomach than their wild-type counterparts, but lead to a significantly decreased T_H1 CD4 T cell polarization. The decreased IFN-γ expression explains the

increased *H. pylori* colonization of the stomach. Thus, ARTD1 limits pathogen spreading via IL-12 and the initiation of potent immune responses, but is also involved in the fine balance of maintaining tissue homeostasis while efficiently controlling invading pathogens.

Macrophages play important yet bimodal roles in orchestrating tumor associated immune responses[43]. On the one hand side they are involved in tumor killing and other effector functions, but they can also promote tumor growth by skewing and suppressing T cell responses. Our data suggests ARTD1 to function as the latter one. First, ARTD1 deficient macrophages do not infiltrate the tumor as efficient as ARTD1 proficient do (Figure 4B). In addition, their activation status is significantly reduced displayed by reduced TNF-α expression. The fact that we identified many cell adhesion molecules to be significantly lower expressed in ARTD deficient macrophages (Figure 1C) could explain the impaired recruitment to the site of action. Nevertheless, both ARTD1 pro- and deficient macrophages recruited equally CD4 and CD8 T cells to the MC-38 tumor, xenograft but their activation was significantly decreased, indicating that ARTD1 in macrophages maintains the activation of T_H1 immune responses also during tumor formation, thereby limiting tumor growth.

Taken together we identified ARTD1 in macrophages as critical regulator of pro-inflammatory cytokine expression. In particular, ARTD1 ensures the initiation of several potent immune responses to react against LPS or to eliminate pathogens and tumors *in vivo.*

ACKNOWLEDGMENTS

We would like to thank Tobias Suter (University of Zurich) for the helpful discussions and for providing editorial assistance. We thank Maria Domenica Moccia and Giancarlo Russo from the Functional Genomics Center of the University of Zurich for the RNA Sequencing and data analysis. We also thank Rafaela Santoro (University of Zurich) for providing the CMV-Cre mouse. ADP-ribosylation research in the laboratory of MOH is funded by the Kanton of Zurich and the Swiss National Science Foundation (grant 310030_157019).

AUTHOR CONTRIBUTIONS

F.A.K. generated the mice and performed the sepsis *in vivo* models, RNA-Seq, ELISA, qPCR, Wersternblot analyses. J.K. and M.L performed sepsis ICS and immunophenotyping. M.B performed the *Hp* and MC-38 studies. K.G. analyzed the RNA sequencing. A.H. helped during the sepsis model. M.L. helped in generating the floxed ARTD1 mouse. F.A.K. and M.O.H. prepared the manuscript. M.O.H and A.M. and B.B. directed and supervised all aspects of the study. All authors critically reviewed the manuscript.

COMPETING FINANCIAL INTERESTS

The authors declare no competing financial interests.

References

1. Abplanalp, J. & Hottiger, M. O. Cell fate regulation by chromatin ADP-ribosylation. *Semin. Cell Dev. Biol.* **63,** 114–122 (2017).
2. Antoine, R. & Locht, C. Roles of the disulfide bond and the carboxy-terminal region of the S1 subunit in the assembly and biosynthesis of pertussis toxin. *Infect. Immun.* **58,** 1518–1526 (1990).
3. Aktories, K. *et al.* Botulinum C2 toxin ADP-ribosylates actin. *Nature* **322,** 390–392 (1986).
4. Simon, N. C., Aktories, K. & Barbieri, J. T. Novel bacterial ADP-ribosylating toxins: structure and function. *Nat. Rev. Microbiol.* **12,** 599–611 (2014).
5. Iwasaki, A. & Medzhitov, R. Control of adaptive immunity by the innate immune system. *Nat. Immunol.* **16,** 343–353 (2015).
6. Parrillo, J. E. Pathogenetic mechanisms of septic shock. *N. Engl. J. Med.* **328,** 1471–1477 (1993).
7. Chaudhry, H. *et al.* Role of Cytokines as a Double-edged Sword in Sepsis. *In Vivo* **27,** 669–684 (2013).
8. Ramirez-Carrozzi, V. R. *et al.* Selective and antagonistic functions of SWI/SNF and Mi-2beta nucleosome remodeling complexes during an inflammatory response. *Genes Dev.* **20,** 282–296 (2006).
9. Koch, K. N. & Müller, A. Helicobacter pylori activates the TLR2/NLRP3/caspase-1/IL-18 axis to induce regulatory T-cells, establish persistent infection and promote tolerance to allergens. *Gut Microbes* **6,** 382–387 (2015).
10. Arnold, I. C. *et al.* Tolerance rather than immunity protects from Helicobacter pylori-induced gastric preneoplasia. *Gastroenterology* **140,** 199–209 (2011).
11. Harris, P. R. *et al.* Helicobacter pylori gastritis in children is associated with a regulatory T-cell response. *Gastroenterology* **134,** 491–499 (2008).
12. Gabrilovich, D. I., Ostrand-Rosenberg, S. & Bronte, V. Coordinated regulation of myeloid cells by tumours. *Nat. Rev. Immunol.* **12,** 253–268 (2012).
13. Piccard, H., Muschel, R. J. & Opdenakker, G. On the dual roles and polarized phenotypes of neutrophils in tumor development and progression. *Crit. Rev. Oncol. Hematol.* **82,** 296–309 (2012).
14. Souto, J. C., Vila, L. & Brú, A. Polymorphonuclear neutrophils and cancer: intense and sustained neutrophilia as a treatment against solid tumors. *Med Res Rev* **31,** 311–363 (2011).
15. Fridlender, Z. G. *et al.* Polarization of tumor-associated neutrophil phenotype by TGF-beta: "N1" versus ‘N2’ TAN. *Cancer Cell* **16,** 183–194 (2009).

16. DeNardo, D. G., Andreu, P. & Coussens, L. M. Interactions between lymphocytes and myeloid cells regulate pro- versus anti-tumor immunity. *Cancer Metastasis Rev.* **29,** 309–316 (2010).
17. Voskoglou-Nomikos, T., Pater, J. L. & Seymour, L. Clinical predictive value of the in vitro cell line, human xenograft, and mouse allograft preclinical cancer models. *Clin Cancer Res* **9,** 4227–4239 (2003).
18. Müller-Edenborn, K. *et al.* Hypoxia attenuates the proinflammatory response in colon cancer cells by regulating IκB. *Oncotarget* **6,** 20288–20301 (2015).
19. Hassa, P. O., Haenni, S. S., Elser, M. & Hottiger, M. O. Nuclear ADP-Ribosylation Reactions in Mammalian Cells: Where Are We Today and Where Are We Going? *Microbiology and Molecular Biology Reviews* **70,** 789–829 (2006).
20. Bai, P. & Virág, L. Role of poly(ADP-ribose) polymerases in the regulation of inflammatory processes. *FEBS Letters* **586,** 3771–3777 (2012).
21. Ba, X. & Garg, N. J. Signaling Mechanism of Poly(ADP-Ribose) Polymerase-1 (PARP-1) in Inflammatory Diseases. *The American Journal of Pathology* **178,** 946–955 (2011).
22. Hottiger, M. O., Hassa, P. O., Lüscher, B., Schüler, H. & Koch-Nolte, F. Toward a unified nomenclature for mammalian ADP-ribosyltransferases. *Trends in Biochemical Sciences* **35,** 208–219 (2010).
23. Rack, J. G. M. *et al.* Identification of a Class of Protein ADP-Ribosylating Sirtuins in Microbial Pathogens. *Molecular Cell* **59,** 309–320 (2015).
24. Feijs, K. L. *et al.* ARTD10 substrate identification on protein microarrays: regulation of GSK3β by mono-ADP-ribosylation. *Cell Commun. Signal* **11,** 5 (2013).
25. Gupte, R., Liu, Z. & Kraus, W. L. PARPs and ADP-ribosylation: recent advances linking molecular functions to biological outcomes. *Genes Dev.* **31,** 101–126 (2017).
26. Oliver, F. J. Resistance to endotoxic shock as a consequence of defective NF-kappa B activation in poly (ADP-ribose) polymerase-1 deficient mice. *The EMBO Journal* **18,** 4446–4454 (1999).
27. Ray Chaudhuri, A. & Nussenzweig, A. The multifaceted roles of PARP1 in DNA repair and chromatin remodelling. *Nat Rev Mol Cell Biol* **18,** 610–621 (2017).
28. Lord, C. J. & Ashworth, A. PARP inhibitors: Synthetic lethality in the clinic. *Science* **355,** 1152–1158 (2017).
29. Hottiger, M. O. Poly (ADP-ribose) polymerase inhibitor therapeutic effect: are we just scratching the surface? *Expert opinion on therapeutic targets* (2015).
30. Virág, L. & Szabó, C. The therapeutic potential of poly(ADP-ribose) polymerase inhibitors. *Pharmacol. Rev.* **54,** 375–429 (2002).
31. Jagtap, P. & Szabó, C. Poly(ADP-ribose) polymerase and the therapeutic effects of its

inhibitors. *Nature Reviews Drug Discovery* **4,** 421–440 (2005).

32. Berger, N. A. *et al.* Opportunities for the repurposing of PARP inhibitors for the therapy of non-oncological diseases. *Br. J. Pharmacol.* **175,** 192–222 (2018).
33. Toller, I. M., Altmeyer, M., Kohler, E., Hottiger, M. O. & Müller, A. Inhibition of ADP Ribosylation Prevents and Cures Helicobacter-Induced Gastric Preneoplasia. *Cancer Res* **70,** 5912–5922 (2010).
34. Hassa, P. O. & Hottiger, M. O. A role of poly (ADP-ribose) polymerase in NF-kappaB transcriptional activation. *Biol. Chem.* **380,** 953–959 (1999).
35. Hassa, P. O., Covic, M., Hasan, S., Imhof, R. & Hottiger, M. O. The enzymatic and DNA binding activity of PARP-1 are not required for NF-kappa B coactivator function. *J. Biol. Chem.* **276,** 45588–45597 (2001).
36. Hassa, P. O. *et al.* Acetylation of poly(ADP-ribose) polymerase-1 by p300/CREB-binding protein regulates coactivation of NF-kappaB-dependent transcription. *J. Biol. Chem.* **280,** 40450–40464 (2005).
37. Rosado, M. M., Bennici, E., Novelli, F. & Pioli, C. Beyond DNA repair, the immunological role of PARP-1 and its siblings. *Immunology* **139,** 428–437 (2013).
38. Bürkle, A. & Virág, L. Poly (ADP-ribose): PARadigms and PARadoxes. *Molecular Aspects of Medicine* (2013).
39. Wang, Z. Q. *et al.* Mice lacking ADPRT and poly(ADP-ribosyl)ation develop normally but are susceptible to skin disease. *Genes Dev.* **9,** 509–520 (1995).
40. Ma, X. *et al.* Regulation of IL-10 and IL-12 production and function in macrophages and dendritic cells. *F1000Res* **4,** (2015).
41. Chiche, L. *et al.* The role of natural killer cells in sepsis. *J. Biomed. Biotechnol.* **2011,** 986491–8 (2011).
42. Arnold, I. C. *et al.* NLRP3 Controls the Development of Gastrointestinal CD11b+Dendritic Cells in the Steady State and during Chronic Bacterial Infection. *Cell Rep* **21,** 3860–3872 (2017).
43. Mantovani, A., Marchesi, F., Malesci, A., Laghi, L. & Allavena, P. Tumour-associated macrophages as treatment targets in oncology. *Nat Rev Clin Oncol* **14,** 399–416 (2017).
44. Krishnakumar, R. & Kraus, W. L. The PARP Side of the Nucleus: Molecular Actions, Physiological Outcomes, and Clinical Targets. *Molecular Cell* **39,** 8–24 (2010).
45. Hassa, P. O. & Hottiger, M. O. The functional role of poly(ADP-ribose)polymerase 1 as novel coactivator of NF-kappaB in inflammatory disorders. *Cell. Mol. Life Sci.* **59,** 1534–1553 (2002).
46. Plevy, S. E., Gemberling, J. H., Hsu, S., Dorner, A. J. & Smale, S. T. Multiple control elements mediate activation of the murine and human interleukin 12 p40 promoters:

evidence of functional synergy between C/EBP and Rel proteins. *Mol. Cell. Biol.* **17,** 4572–4588 (1997).

47. Zhu, C., Gagnidze, K., Gemberling, J. H. & Plevy, S. E. Characterization of an activation protein-1-binding site in the murine interleukin-12 p40 promoter. Demonstration of novel functional elements by a reductionist approach. *J. Biol. Chem.* **276,** 18519–18528 (2001).
48. Murphy, T. L., Cleveland, M. G., Kulesza, P., Magram, J. & Murphy, K. M. Regulation of interleukin 12 p40 expression through an NF-kappa B half-site. *Mol. Cell. Biol.* **15,** 5258–5267 (1995).
49. Weinmann, A. S. *et al.* Nucleosome remodeling at the IL-12 p40 promoter is a TLR-dependent, Rel-independent event. *Nat. Immunol.* **2,** 51–57 (2001).
50. Whitehouse, I. *et al.* Nucleosome mobilization catalysed by the yeast SWI/SNF complex. *Nature* **400,** 784–787 (1999).
51. Lai, D. *et al.* Induction of TLR4-target genes entails calcium/calmodulin-dependent regulation of chromatin remodeling. *PNAS* **106,** 1169–1174 (2009).
52. Becker, P. B. & Hörz, W. ATP-dependent nucleosome remodeling. *Annu. Rev. Biochem.* **71,** 247–273 (2002).
53. Zhao, Q., Du, Q., Wei, F., Xie, J. & Ma, X. An Infectious Disease-Associated Il12b Polymorphism Regulates IL-12/23 p40 Transcription Involving Poly(ADP-Ribose) Polymerase 1. *J Immunol* **198,** 2935–2942 (2017).
54. Heremans, H., Dillen, C., van Damme, J. & Billiau, A. Essential role for natural killer cells in the lethal lipopolysaccharide-induced Shwartzman-like reaction in mice. *European Journal of Immunology* **24,** 1155–1160 (1994).
55. Skarnes, W. C. *et al.* A conditional knockout resource for the genome-wide study of mouse gene function. *Nature* **474,** 337–342 (2011).
56. Lim, S. Y., Yuzhalin, A. E., Gordon-Weeks, A. N. & Muschel, R. J. Tumor-infiltrating monocytes/macrophages promote tumor invasion and migration by upregulating S100A8 and S100A9 expression in cancer cells. *Oncogene* **35,** 5735–5745 (2016).
57. Zhang, X., Goncalves, R. & Mosser, D. M. The isolation and characterization of murine macrophages. *Curr Protoc Immunol* **Chapter 14,** Unit 14.1 (2008).
58. Fortier, A. H. & Falk, L. A. Isolation of murine macrophages. *Curr Protoc Immunol* **Chapter 14,** Unit 14.1–14.1.9 (2001).
59. Bolger, A. M., Lohse, M. & Usadel, B. Trimmomatic: a flexible trimmer for Illumina sequence data. *Bioinformatics* **30,** 2114–2120 (2014).
60. Dobin, A. *et al.* STAR: ultrafast universal RNA-seq aligner. *Bioinformatics* **29,** 15–21 (2013).

61. Lawrence, M. *et al.* Software for computing and annotating genomic ranges. *PLoS Comput Biol* **9,** e1003118 (2013).

62. Robinson, M. D., McCarthy, D. J. & Smyth, G. K. edgeR: a Bioconductor package for differential expression analysis of digital gene expression data. *Bioinformatics* **26,** 139–140 (2010).

63. Minotti, R., Andersson, A. & Hottiger, M. O. ARTD1 Suppresses Interleukin 6 Expression by Repressing MLL1-Dependent Histone H3 Trimethylation. *Mol. Cell. Biol.* **35,** 3189–3199 (2015).

64. Abplanalp, J. *et al.* Proteomic analyses identify ARH3 as a serine mono-ADP-ribosylhydrolase. *Nature Communications* **8,** 2055 (2017).

Material and Methods

Animals and Animal Experiments

The conditional *Artd1* allele in ESCs as well as the generation of the *Artd1*$^{flox/flox}$ mice was performed by Polygene as described[55]. Briefly, the vector from EUCOMM (targeting project 45261) was electroporated in C57Bl/6 ES cells and analyzed by PCR. Correctly integrated ES cell clones were injected into blastocysts resulting in chimeric mice. Subsequent mating of the chimeric mice with the Flp-deleter mice resulted in the Flp-mediated deletion of the gene trap cassette and leaving only the loxP flanked exon 4 of *Artd1*. To generate whole-body *Artd1* knock-out mice (*Artd1*$^{del/del}$) the generated *Artd*$^{flox/flox}$ mouse strain was crossed to the CMV-Cre deleter strain (provided by R. Santoro). Myeloid specific *Artd1* knock-out mice (*Artd1*$^{\Delta Myel}$) were generated by crossing *Artd1*$^{foxl/flox}$ mice to *LyzM*-Cre (The Jackson Laboratory, strain 004781) mice. For all experiments 6-12 week old, age and sex matched mice were used. LPS (*Escherichia coli* O111:B4, Sigma-Aldrich) was injected i.p. at a concentration of 4 mg per kg bodyweight.

Helicobacter pylori infections were performed as described[42]. Briefly, Mice were infected orally on 2 consecutive days with 10^8 colony-forming units (CFUs) *H. pylori* PMSS1 and analyzed at 1 and 3 months p.i. unless specified otherwise. The subcutaneous MC38 tumor model was performed as described earlier[56]. Briefly, Colon adenocarcinoma cells (MC-38, $0.5x10^6$ cells in 100 µl phosphate buffered saline) were injected subcutaneously (s.c.) into the flanks and tumor progression was determined by caliper measurements every second day. After two weeks, mice were sacrificed, tumors were weighed and the volume was calculated using the formula $(a^2 \times b)/2$, where a constitutes the shorter and b the longer dimension of the tumor.

All animals were housed in pathogen free conditions at the University of Zurich. All animal experiments were carried out in accordance with the Swiss and EU ethical guidelines and have been approved by the local animal experimentation committee of the Canton Zurich under licenses 207/2015 and 266/2014.

Cell Culture and reagents

Murine bone marrow derived macrophages (BMDM) were generated as previously described[57] and maintained in RPMI1640 supplemented with 10 % fetal calf serum, 5 % penicillin/streptamycin and 20 ng/ml recombinant murine M-CSF (Preprotech). Thioglycollate (Sigma-Aldrich) elicited murine peritoneal macrophages were isolated as described[58]. Cell culture grade LPS (*Escherichia coli* O111:B4) was purchased from Sigma-Aldrich and recombinant murine interferon gamma from Preprotech. The PARP inhibitors

PJ34 and Olaparib were purchased from Selleckchem. MC-38 cells were cultured as described[56].

ELISA

Whole blood serum of mice and cell culture supernatant of BMDM was analyzed by ProcartaPlex Immunoassay (ThermoFisher) according to the protocol and measured on a Bio-Plex instrument (Bio-Rad).

Flow cytometry

Flow cytometrical analyses of spleens, tumors and stomach tissue were performed as described earlier[42]. Briefly, tumors were cut into pieces and digested with 15 mM HEPES, 500 U/ml of type IV collagenase (Sigma-Aldrich) and 0.05 mg ml^{-1} DNase I in RPMI-1640 medium with 10% fetal bovine serum and 100 U ml^{-1}penicillin/streptomycin shaking at 37°C for 60 min. Subsequently, the samples were pushed through a cell strainer (70µm) using a syringe plunger. Single cell suspensions were stained with the respective antibodies and analyzed on LSR Fortessa (BD Bioscience).

RNA sequencing and bioinformatic analysis

For the library preparation the quality of the isolated RNA was determined with a Qubit® (1.0) Fluorometer (Life Technologies) and a Bioanalyzer 2100 (Agilent). Only those samples with a 260 nm/280 nm ratio between 1.8–2.1 and a 28S/18S ratio within 1.5–2 were further processed. The TruSeq RNA Sample Prep Kit v2 (Illumina) was used in the subsequent steps. Briefly, total RNA samples (100-1000 ng) were poly-A enriched and then reverse-transcribed into double-stranded cDNA. The cDNA samples were fragmented, end-repaired and polyadenylated before ligation of TruSeq adapters containing the index for multiplexing. Fragments containing TruSeq adapters on both ends were selectively enriched with PCR. The quality and quantity of the enriched libraries were validated using Qubit® (1.0) Fluorometer and the Caliper GX LabChip® GX (Caliper Life Sciences). The product is a smear with an average fragment size of approximately 260 bp. Library DNA concentrations were normalized to 10 nM in Tris-Cl 10 mM, pH8.5 with 0.1% Tween 20.

Cluster generation and sequencing were performed using the TruSeq PE Cluster Kit HS4000, or the TruSeq SR Cluster Kit HS4000 (Illumina) was used for cluster generation using 2 nM of pooled normalized libraries on the cBOT. Sequencing were performed on the Illumina HiSeq 4000 paired end at 2 x 150 bp or single end 125 bp using the TruSeq SBS Kit HS4000 (Illumina).

Reads were quality-checked with FastQC. Sequencing adapters were removed with Trimmomatic[59]. Subsequently, reads of at least 20 base length, and with an overall average

phred quality score greater than 10 were aligned to the reference genome and transcriptome of *Mus Musculus* (FASTA and GTF files, respectively, downloaded from GRCm38) with STAR v2.5.1[60] with default settings for single end reads.

Distribution of the reads across genomic isoform expression was quantified using the R package GenomicRanges[61] from Bioconductor Version 3.0. Differentially expressed genes were identified using the R package edgeR[62] from Bioconductor Version 3.0. A gene is marked as differentially expressed (DE) if it possesses the following characteristics: (1) at least 10 counts in at least half of the samples in one group; (2) $p <= 0.05$; (3) fold change >= 1.5.

RNA extraction and quantitative real time PCR (qPCR) analysis.

RNA isolation and qPCR were performed as described[63]. Briefly, RNA extraction was performed with the NucleoSpin RNA II kit (Macherey-Nagel). RNA was quantified with a NanoDrop and reverse transcribed using the High-Capacity cDNA Reverse Transcription Kit (Applied Biosystems) according to the supplier's protocol. qPCRs were performed with the SYBR green KAPA SYBR® FAST (Sigma-Aldrich) and a Rotor-Gene Q 2plex HRM system (Qiagen). See Table S1 in the supplemental material for primer sequences. The relative amounts of each mRNA were normalized to the *Rps12*.

Westernblot

Western blotting was performed as described[64]. For western blot analysis, proteins were separated by SDS-PAGE, and bands were visualized using the Odyssey infrared imaging system (LI- COR). Antibodies used for western blotting were anti-PARP-1 (1:1000, Santa Cruz sc-7150) and anti-Tubulin (1:10,000, Sigma, #T6199).

Table 1. Genotyping primer

Gene	Forward primer	Reverse primer
floxed *Artd1*	GCTTCTACTACCTCCCAAGAAA GAGCG	GGCTTTAGTGTGGCAACTTATCCC
Artd1 localization 3`	CACTGAACTGTCTCCTTAGCCA ACTCTGC	GGAACTTCGGAATAGGAACTTCGG TTCC
Artd1 localization 5`	CTAGGATTCTGTGTCTTGACCA TGCACTTG	CGTATAGCATACATTATACGAAGTT ATGTCGAG
Deleted *Artd1*	GCTTCTACTACCTCCCAAGAAA GAGCG	CCTCTGCTGCGTGACTAAGGC

Table 2. qPCR Primer

Gene	Forward Primer	Reverse Primer
Il12b	GAAGTTCAACATCAAGAGCAGTAG	AGGGAGAAGTAGGAATGGGG
Cxcl3	ACCCAGACAGAAGTCATAGCC	ACACATCCAGACACCGTTGG
Cd55	CGGGCAAGGTCTCTTCTACC	CAGTCTCCGCGTACAGTTGG
Il23a	ACCAGCGGGACATATGAATCT	AGACCTTGGCGGATCCTTTG
Itgax	GCAGACACTGAGTGATGCCA	TCGGAGGTCACCTAGTTGGG
Socs1	CCGCCAGATGAGCCCAC	GGTTGCGTGCTACCATCCTA
Il18	ATGCTTTCTGGACTCCTGCC	ATTGTTCCTGGGCCAAGAGG
Il6	CCAATTTCCAATGCTCTCCT	ACCACAGTGAGGAATGTCCA
Tnfa	GTCGTAGCAAACCACCAAGTGG	GAGATAGCAAATCGGCTGACGG
Ifng	CCTTCTTCAGCAACAGCAAGGCGA	TGGACCTGTGGGTTGTTGACCTCA

Figure legends:

Figure 1: ARTD1 regulates IL-12/IL-18 gene expression in BMDM in an enzymatic independent manner

A) Targeting strategy for the generation of the Cre-mediated whole body ARTD1-deficient mouse (adapted from Skarnes, Rosen et al. 2011). Cre-mediated recombination deletes Exon 4 of the *Artd1* gene.

B) RNA-sequencing of total RNA extracted from $Artd1^{flox/flox}$ and $Artd1^{del/del}$ BMDM either left untreated or treated with 10 ng/ml LPS and 2 ng/ml INF-γ for 4 h. All LPS/IFN- γ-induced genes (approx. 2500 genes) (fold-change ≤ 2, $P < 0.05$) were clustered.

C) Up-regulated genes identified in B) were clustered to identify ARTD1 co-activating and co-repressing function.

D) Quantitative Real-time PCR analysis of selective co-activated and co repressed genes in $Artd1^{flox/flox}$ and $Artd1^{del/del}$ BMDM identified in C. Data presented as mean + SD of three biological replicates. *t*-Test: $*P < 0.05$, $**P < 0.01$

E) Gene enrichment analysis of all significantly LPS/IFN- γ-induced genes (left panel, identified in B), ARTD1 co-activated and ARTD1 co repressed genes (middle and right panel, identified in C) in $Artd1^{flox/flox}$ and $Artd1^{del/del}$ BMDMs.

F) ELISA of cell culture supernatants for the quantification of the indicated cytokines produced by $Artd1^{flox/flox}$ and $Artd1^{del/del}$ BMDM, respectively, stimulated with 10 ng/ml LPS and 2 ng/ml INF-γ for 18 h. Data presented as mean concentration + SD of three independent experiments. *t*-Test: $*P < 0.05$, $**P < 0.01$

Figure 2: Myeloid-specific depletion of ARTD1 reduces the LPS-induced IL-12/IFN-γ signaling *in vivo*

A) Targeting strategy for the generation of myeloid specific ARTD1 knock-out mouse (adapted from Skarnes, Rosen et al. 2011). Cre-mediated recombination deletes Exon 4 of the *Artd1* gene.

B) $Artd1^{flox/flox}$ and $Artd1^{\Delta Myel}$ *mice* were intraperitoneally injected with PBS or 4 mg/kg of LPS. After 4 h whole blood serum was collected and the levels of selected cytokines were quantified by Luminex ELISA. Data shown as mean ± SEM of three independent experiments. *t*-Test: $*P < 0.05$

C) $Artd1^{flox/flox}$ and $Artd1^{\Delta Myel}$ *mice* were intraperitoneally injected with PBS or 4 mg/kg of LPS. After 4 h total spleen tissue was isolated and indicated gene expression quantified by qPCR. Data shown as mean ± SEM of three independent experiments. *t*-Test: $*P < 0.05$, $**P < 0.01$

D) Intracellular cytokine staining of splenocytes from *Artd1*$^{flox/flox}$ and *Artd1*$^{\Delta Myel}$ mice intraperitoneally injected with either PBS or 4 mg/kg of LPS. After 4 h, intracellular INF-γ was detected by flow cytometry and positively stained NK-, CD4 T- and CD8 T cells were quantified. Data shown as mean ± SEM of two independent experiments. *t*-Test: **P* < 0.05.

E) ELISA for IFN-γ secreted from MACS-sorted NK cells isolated from of *Artd1*$^{foxl/flox}$ and *Artd1*$^{\Delta Myel}$ mice. NK cells were stimulated with recombinant murine IL-12p70 for 18 hrs and cell culture supernatant was analyzed.

Figure 3: ARTD1 controls Helicobacter-associated T cell–driven immunopathology

A) *H. Pylori* or PBS were orally administrated to *Artd1*$^{flox/flox}$ and *Artd1*$^{\Delta Myel}$ mice. After 4 weeks gastric homogenates were streaked out and the colony forming unit were determined.

B) In the stomach of the same mice as in A, CD4 T cell infiltration was flow cytometrically determined.

C) Intracellular cytokine staining for IFN-γ and IL-17 in gastric CD4 T cells (determined in B)

Figure 4: ARTD1 controls macrophage infiltration and CD4/CD8 T cell activation in tumors

A) Tumor growth of MC-38 cells subcutaneously injected into the flanks of *Artd1*$^{flox/flox}$ and *Artd1*$^{\Delta Myel}$ mice was determined by caliper measurements after 6 and after 14 days.

B) Infiltration and TNF-α expression of macrophages in the tumors grown within *Artd1*$^{flox/flox}$ and *Artd1*$^{\Delta Myel}$ mice were flow cytometrically determined.

C) Infiltration, IFN-γ and TNF-α expression of CD4 T cells in the tumors grown within *Artd1*$^{flox/flox}$ and *Artd1*$^{\Delta Myel}$ mice were flow cytometrically determined.

D) Infiltration, IFN-γ and TNF-α expression of CD8 T cells in the tumors grown within *Artd1*$^{flox/flox}$ and *Artd1*$^{\Delta Myel}$ mice were flow cytometrically determined.

Supplementary Figure 1

A) Successful modification of the *Artd1* locus. To verify the integration of the targeting vector at the *Artd1* locus on chromosome 1, a long range PCR amplifying the 3`and 5`homolgy arm of the *Artd1* gene was performed on genomic DNA from the initial breeding pair. Embryonic stem cell DNA used for the blastocyst injection served as control. Size of the bands are indicated as base pairs (bp).

B) PCR amplification of mouse genomic DNA of $Artd1^{flox/wt}$, $Artd1^{wt/wt}$, and $Artd1^{flox/flox}$ mice. Size of the bands are indicated as base pairs (bp).

C) Westernblot analysis of the indicated organs for ARTD1 expression in $Artd^{wt/wt}$, $Artd1^{del/del}$ and $Artd1^{wt/del}$mice.

D) Necropsy analysis of three $Artd1^{flox/flox}$ and two , $Artd1^{del/del}$ male mice of 8 weeks. Body weights as well as indicated organ weights were determined.

E) Quantitative Real-time PCR analysis of *Artd1* expression in $Artd1^{flox/flox}$ and $Artd1^{del/del}$ BMDM, respectively.

F) RNA-sequencing of total RNA extracted from $Artd1^{flox/flox}$ and $Artd1^{del/del}$ BMDM either left untreated or treated with 10 ng/ml LPS and 2 ng/ml INF-γ for 4 h. All LPS/IFN- γ-repressed genes (approx. 3000 genes) (fold-change ≤ 2, $P < 0.05$) were clustered.

G) RNA-sequencing of PARPi BMDMs

H) ELISA of cell culture supernatant for the quantification of the indicated cytokines from $Artd1^{flox/flox}$ and $Artd1^{del/del}$ BMDMs. Cells were treated either with DMSO or 5 µM PARPi (PJ34/Olaparip) prior to stimulation with 10 ng/ml LPS and 2 ng/ml INF-γ for 18 h. Data presented as mean concentration + SD of three independent experiments.

Supplementary Figure 2

A) Western blot analysis of BMDM and thioglycolate elicited peritoneal macrophages from $Artd1^{flox/flox}$ and $Artd1^{\Delta Myel}$ *mice*. ARTD1 levels were quantified in whole cell lysates. Tubulin was used as loading control.

B) $Artd1^{flox/flox}$ and $Artd1^{\Delta Myel}$ *mice* were intraperitoneally injected with PBS or 4 mg/kg of LPS. After 4 h whole blood serum was collected and the levels of selected cytokines were quantified by luminex ELISA. Data shown as mean ± SEM of three independent experiments. *t*-Test: $*P < 0.05$

C) Immunophenotyping of the spleen from $Artd1^{flox/flox}$ and $Artd1^{\Delta Myel}$ mice. Spleen single cell suspensions were stained with fluorescently labeled antibodies and cell counts were determined by flow cytometry.

Figure 1

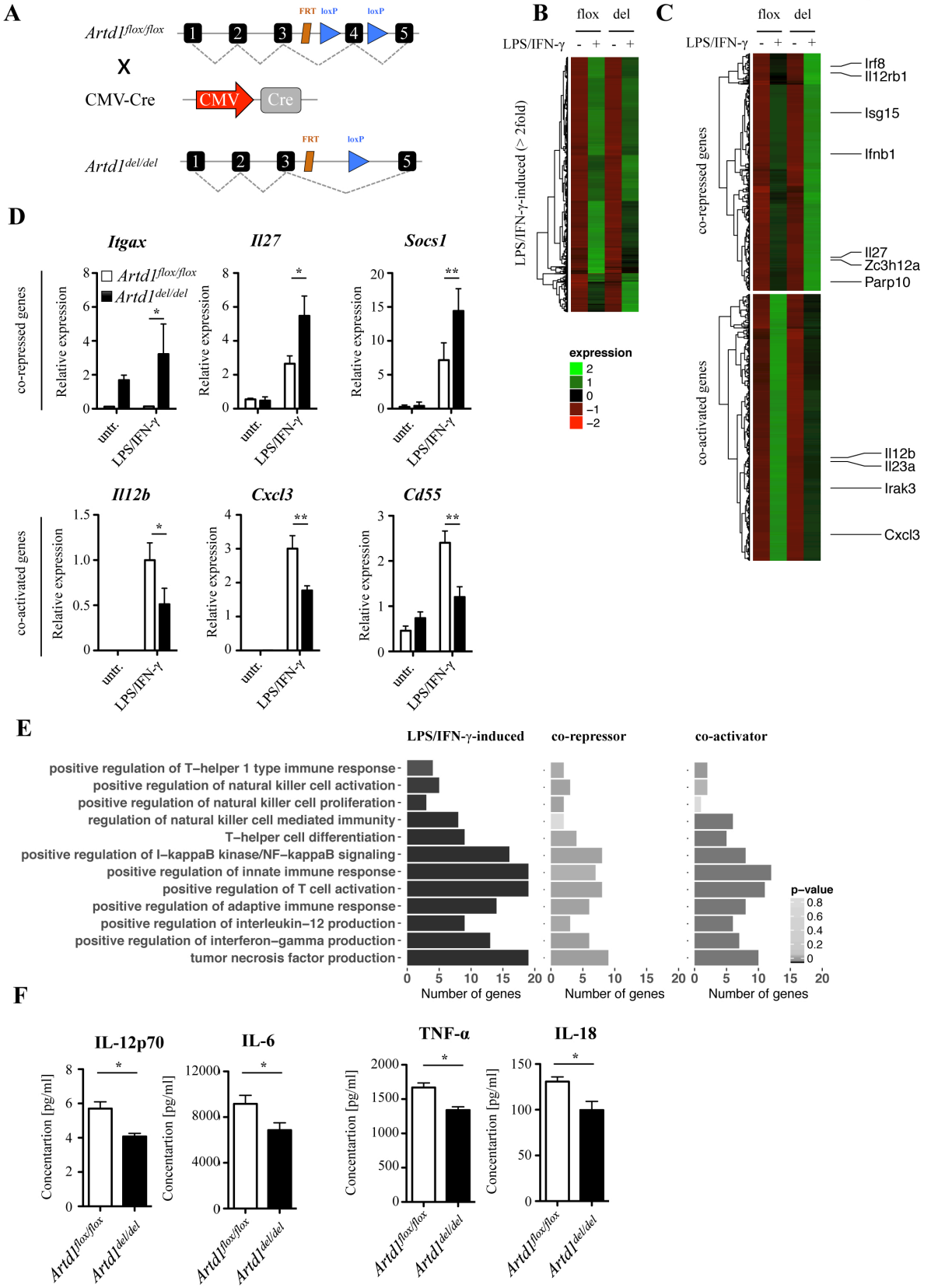
A
Artd1flox/flox
FRT loxP loxP
1 2 3 4 5
X
CMV-Cre
CMV Cre
Artd1del/del
FRT loxP
1 2 3 5
B
flox del
LPS/IFN-γ - + - +
LPS/IFN-γ-induced (> 2fold)
expression
2
1
0
−1
−2
C
flox del
LPS/IFN-γ - + - +
co-repressed genes
co-activated genes
Irf8
Il12rb1
Isg15
Ifnb1
Il27
Zc3h12a
Parp10
Il12b
Il23a
Irak3
Cxcl3
D
Itgax
Il27
Socs1
Il12b
Cxcl3
Cd55
co-repressed genes
co-activated genes
Relative expression
Artd1flox/flox
Artd1del/del
untr.
LPS/IFN-γ
E
LPS/IFN-γ-induced
co-repressor
co-activator
positive regulation of T−helper 1 type immune response
positive regulation of natural killer cell activation
positive regulation of natural killer cell proliferation
regulation of natural killer cell mediated immunity
T−helper cell differentiation
positive regulation of I−kappaB kinase/NF−kappaB signaling
positive regulation of innate immune response
positive regulation of T cell activation
positive regulation of adaptive immune response
positive regulation of interleukin−12 production
positive regulation of interferon−gamma production
tumor necrosis factor production
Number of genes
p−value
0.8
0.6
0.4
0.2
0
F
IL-12p70
IL-6
TNF-α
IL-18
Concentartion [pg/ml]
Artd1flox/flox
Artd1del/del

Figure 2

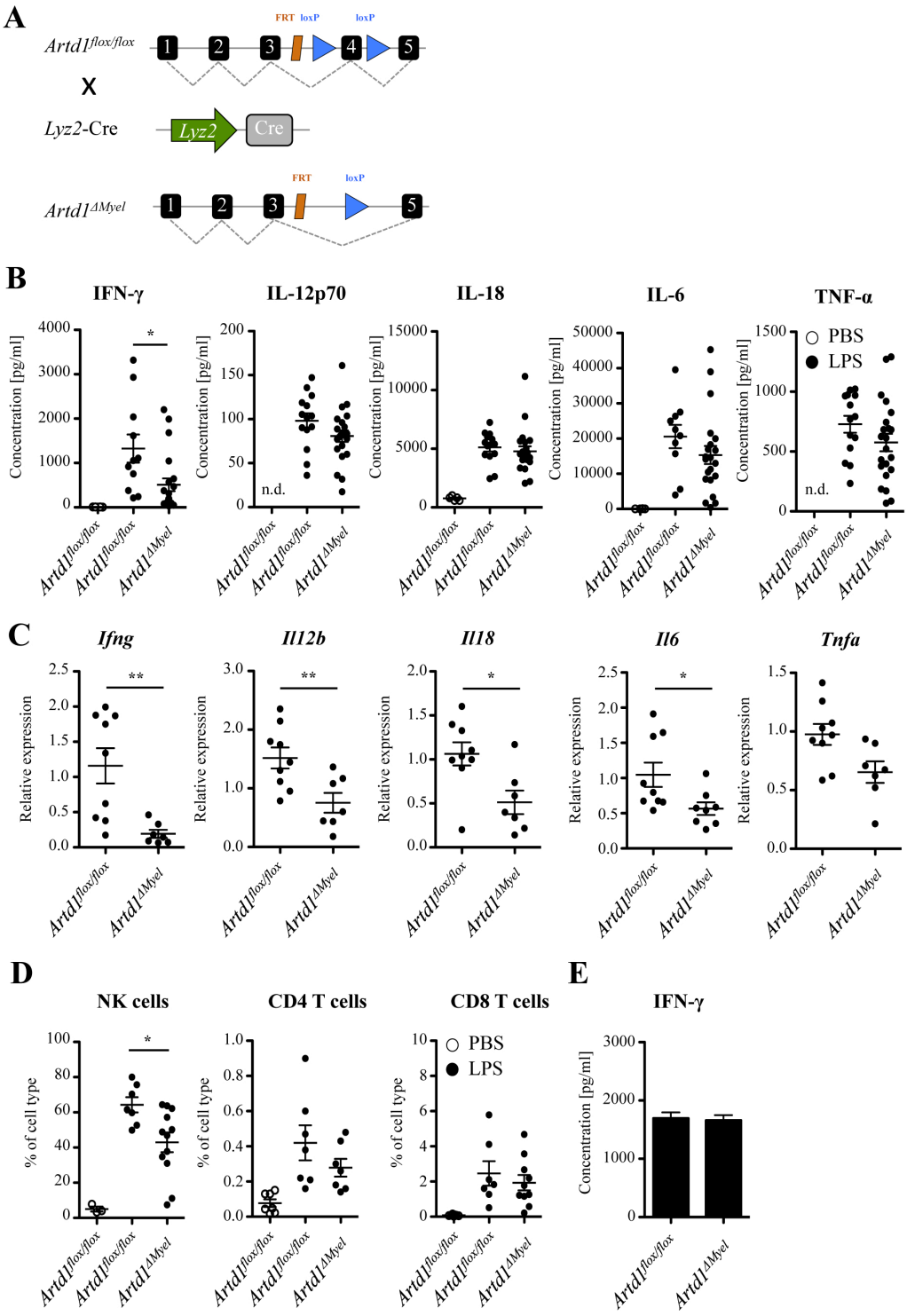
A
Artd1flox/flox
FRT loxP loxP
1 2 3 4 5
X
Lyz2-Cre
Lyz2
Cre
Artd1ΔMyel
FRT loxP
1 2 3 5
B
IFN-γ
IL-12p70
IL-18
IL-6
TNF-α
Concentration [pg/ml]
PBS
LPS
n.d.
Artd1flox/flox
Artd1ΔMyel
C
Ifng
Il12b
Il18
Il6
Tnfa
Relative expression
D
NK cells
CD4 T cells
CD8 T cells
% of cell type
E
IFN-γ
Concentration [pg/ml]

Figure 3

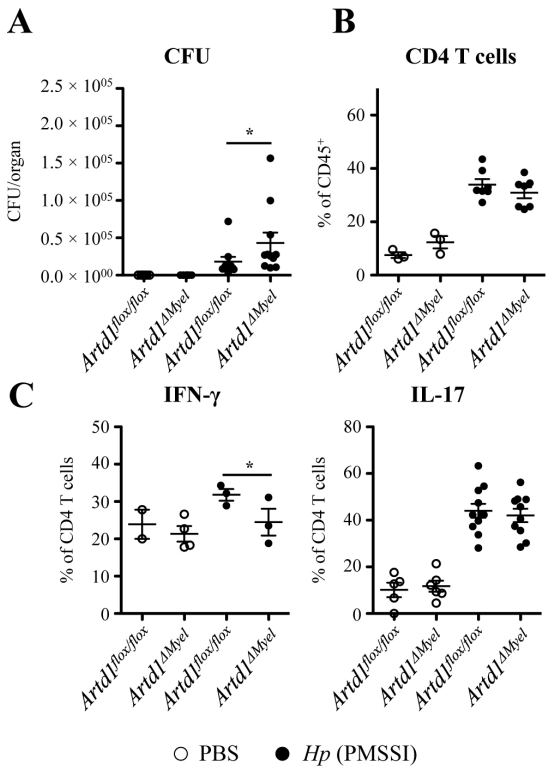
A
CFU
CFU/organ
2.5 × 10^05
2.0 × 10^05
1.5 × 10^05
1.0 × 10^05
0.5 × 10^05
0.0 × 10^00
*
B
CD4 T cells
% of CD45+
60
40
20
0
C
IFN-γ
% of CD4 T cells
50
40
30
20
10
0
*
IL-17
% of CD4 T cells
80
60
40
20
0
Artd1flox/flox
Artd1ΔMyel
Artd1flox/flox
Artd1ΔMyel
○ PBS ● Hp (PMSSI)

Figure 4

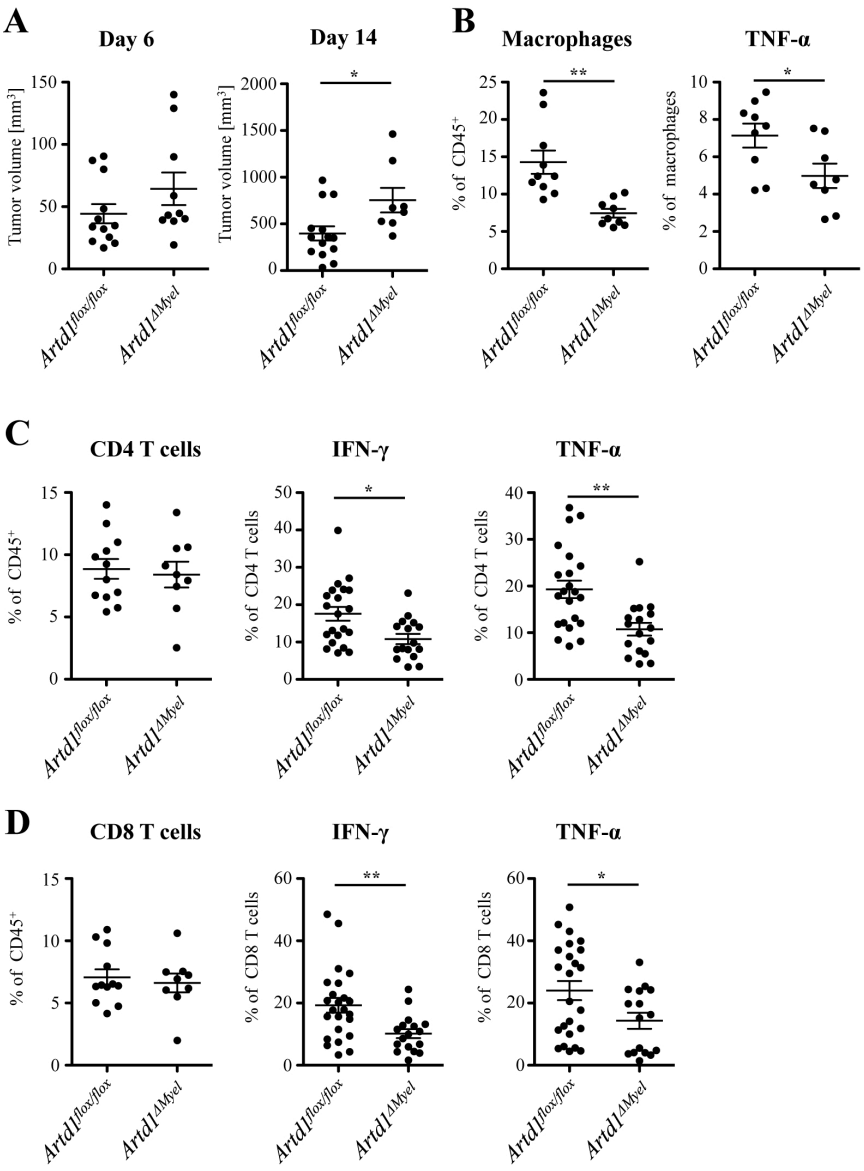
A
Day 6
Day 14
Tumor volume [mm³]
150
100
50
0
2000
1500
1000
500
*
Artd1flox/flox
Artd1ΔMyel
B
Macrophages
TNF-α
% of CD45+
% of macrophages
25
20
15
10
5
2
4
6
8
**
C
CD4 T cells
IFN-γ
TNF-α
% of CD4 T cells
40
30
D
CD8 T cells
% of CD8 T cells
60

Suppl. Figure 1

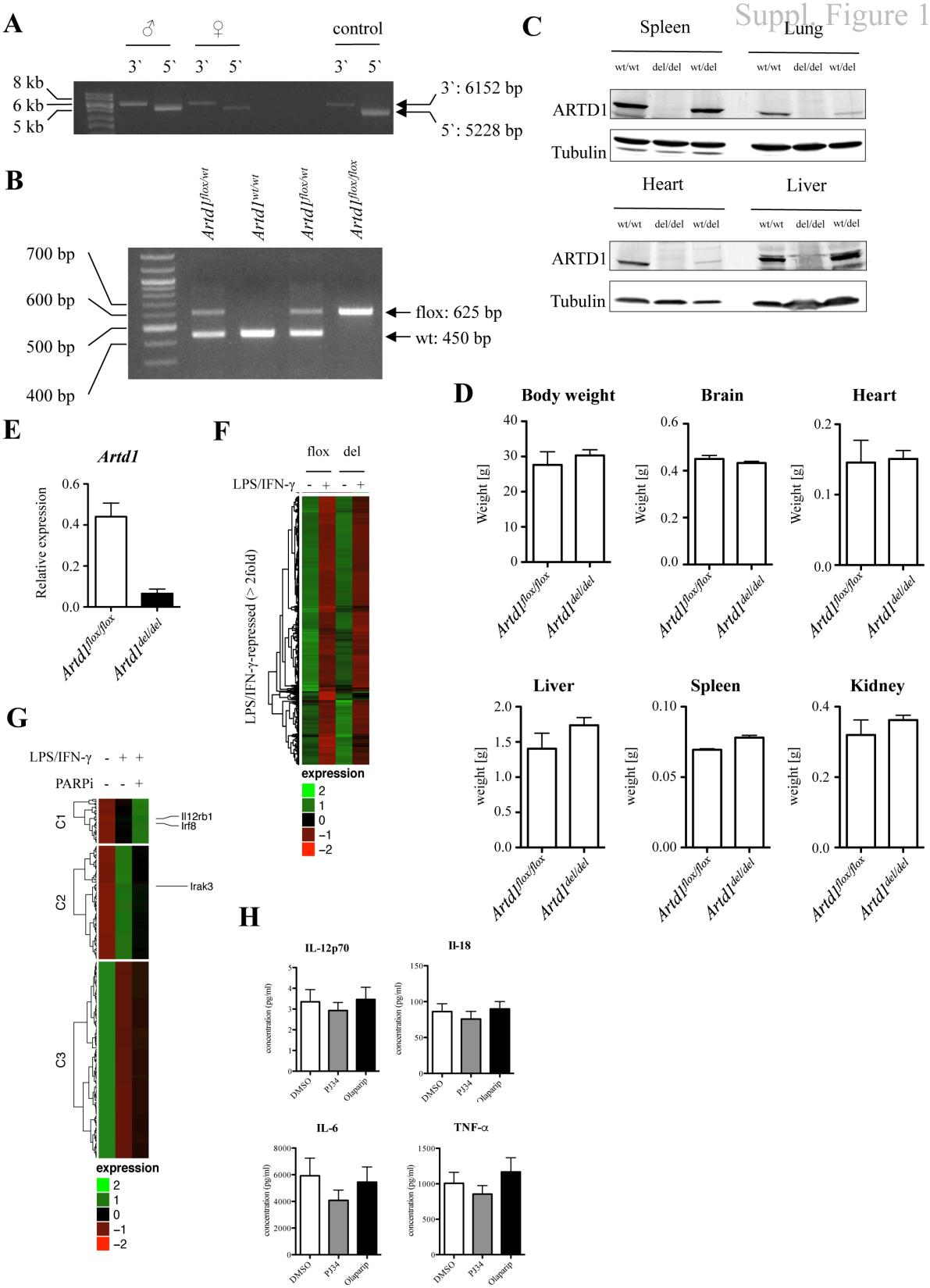

Suppl. Figure 2

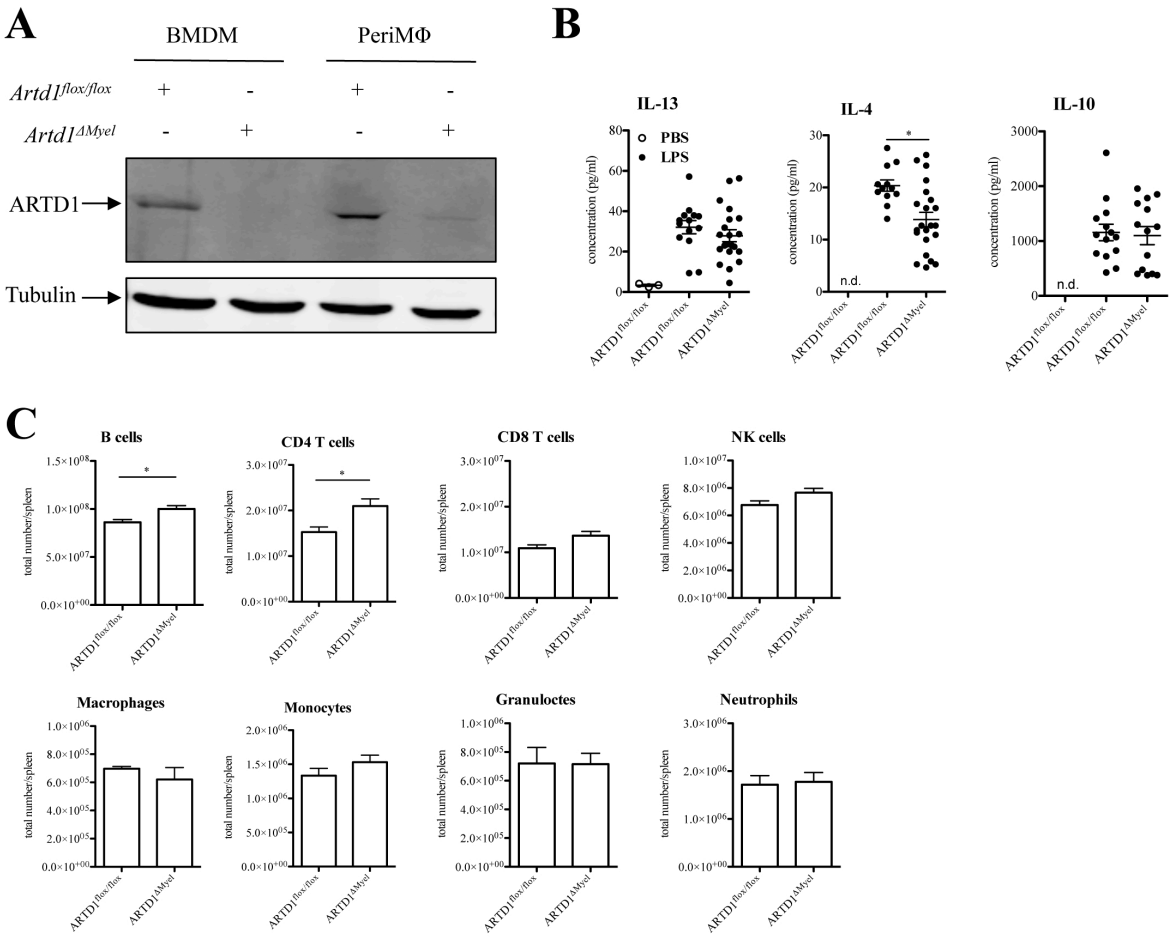

Published online 1 December 2014 *Nucleic Acids Research, 2015, Vol. 43, No. 1* **129–142**
doi: 10.1093/nar/gku1260

ARTD1-induced poly-ADP-ribose formation enhances PPARγ ligand binding and co-factor exchange

Mareike Lehmann[1,2], Eija Pirinen[3,4], Ali Mirsaidi[5,6], Friedrich A. Kunze[1,2], Peter J. Richards[5,6], Johan Auwerx[3] and Michael O. Hottiger[1,5,6,*]

[1]Institute of Veterinary Biochemistry and Molecular Biology, University of Zurich, 8057 Zurich, Switzerland, [2]Life Science Zurich Graduate School, Molecular Life Science Program, University of Zurich, 8057 Zurich, Switzerland, [3]Laboratory of Integrative and Systems Physiology, Ecole Polytechnique Fédérale de Lausanne, 1015 Lausanne, Switzerland, [4]Biotechnology and Molecular Medicine, A.I. Virtanen Institute for Molecular Sciences, Biocenter Kuopio, University of Eastern Finland, Kuopio, Finland, [5]Competence Centre for Applied Biotechnology and Molecular Medicine, University of Zurich, 8057 Zurich, Switzerland and [6]Zurich Centre for Integrative Human Physiology (ZIHP), University of Zurich, 8057 Zurich, Switzerland

Received September 12, 2014; Revised November 11, 2014; Accepted November 15, 2014

ABSTRACT

PPARγ-dependent gene expression during adipogenesis is facilitated by ADP-ribosyltransferase D-type 1 (ARTD1; PARP1)-catalyzed poly-ADP-ribose (PAR) formation. Adipogenesis is accompanied by a dynamic modulation of the chromatin landscape at PPARγ target genes by ligand-dependent co-factor exchange. However, how endogenous PPARγ ligands, which have a low affinity for the receptor and are present at low levels in the cell, can induce sufficient co-factor exchange is unknown. Moreover, the significance of PAR formation in PPARγ-regulated adipose tissue function is also unknown. Here, we show that inhibition of PAR formation in mice on a high-fat diet reduces weight gain and cell size of adipocytes, as well as PPARγ target gene expression in white adipose tissue. Mechanistically, topoisomerase II activity induces ARTD1 recruitment to PPARγ target genes, and ARTD1 automodification enhances ligand binding to PPARγ, thus promoting sufficient transcriptional co-factor exchange in adipocytes. Thus, ARTD1-mediated PAR formation during adipogenesis is necessary to adequately convey the low signal of endogenous PPARγ ligand to effective gene expression. These results uncover a new regulatory mechanism of ARTD1-induced ADP-ribosylation and highlight its importance for nuclear factor-regulated gene expression.

INTRODUCTION

Adipocyte formation relies on the adipogenic differentiation of multipotent mesenchymal stromal cells, resulting in lipid accumulation and which is associated with the capacity to influence numerous biological processes, including signaling and immune functions (1). The underlying mechanism of adipogenesis is a broad reorganization of the transcriptional landscape due to large-scale chromatin changes (2). Instrumental in this step-wise reorganization is the transcription factor peroxisome proliferator-activated receptor gamma (PPARγ) (3,4) and, in particular, the adipocyte-specific isoform PPARγ2 (5,6). PPARγ is a nuclear receptor of the PPAR family that functions as an obligate heterodimer with RXRs (7–10). Like many nuclear receptors, PPARγ contains an N-terminal, non-conserved A/B domain, a DNA-binding domain and a C-terminal ligand binding domain (LBD). Hetero-dimerization with RXRs is governed by the C-terminal domain, and ligand binding is conveyed by the LBD, which harbors multiple hydrophobic residues and is important for ligand-dependent interactions with co-factors (11,12). Binding of ligands to PPARγ triggers a conformational switch that exposes a surface that can interact with LXXLL-containing co-activators. Prior to the activation of PPARγ by its ligands, PPARγ is bound to co-repressors that suppress transcription of target genes and which are dislodged upon ligand binding (13). PPARγ is induced during the differentiation of adipocytes and is highly expressed in white and brown adipose tissue (WAT/BAT) (14). A series of transcription factors, in particular, CCAAT/enhancer-binding proteins (C/EBP) β and δ, bind to promoter regions of adipogenic genes, establishing so-called transcription factor hotspots that are characterized by open chromatin regions and regulate PPARγ2 as well as C/EBP-α expression and DNA binding (2,4). To-

*To whom correspondence should be addressed. Tel: +41 44 635 54 74; Fax: +41 44 635 54 68; Email: hottiger@vetbio.uzh.ch

gether with C/EBP-α, PPARγ2 determines adipocyte function and transcriptionally co-regulates target genes, such as *adipocyte protein 2* (*aP2*), *cluster of differentiation 36* (*CD36*) and *adiponectin* (15–17).

Polymers of ADP-ribose (PAR) are synthesized by enzymes that belong to the family of ADP-ribosyltransferases (ARTs), which transfer the ADP-ribose moiety of nicotinamide dinucleotide (NAD^+) to acceptor proteins. Intracellular ADP-ribosylation is catalyzed by the diphtheria toxin-like ADP-ribosyltransferases (ARTDs), which have previously been referred to as poly (ADP-ribose) polymerases (PARPs). Since not all of them catalyze poly-ADP-ribosylation and polymerases refer to enzymes that synthesize DNA/RNA from a template, the new nomenclature has been adopted (18). In humans, ARTDs are currently comprised of 18 members (ARTD1-18), which function in different cellular compartments (18). Of the 18 enzymes, only four have been reported to synthesize PAR (19). The most abundant and so far best-studied PAR-forming member is the chromatin-associated ARTD1 (formerly PARP1), which has been implicated in a plethora of important cellular and biological processes. Thus, ARTD1-dependent poly-ADP-ribosylation has been implicated in the regulation of chromatin compaction, the recruitment of proteins to chromatin, the regulation of enzymatic activities and was described to be involved in biological processes, such as stress signaling, cell death, inflammation, as well as differentiation (20). Furthermore, defects in ADP-ribosylation or in function of ARTDs have been linked to diseases, such as chronic inflammation, neurodegenerative disorders, cardiovascular diseases and cancer (21). Several inhibitors of ADP-ribosylation have been developed, some of which have entered clinical trial (22), and are for historical reasons widely known under the name of PARP inhibitors. Since these inhibitors are not specific for a single ARTD (23), we will simply refer to them as PARP inhibitors and do not adopt a new nomenclature.

We have previously shown that the regulation of PPARγ2-dependent gene expression and adipocyte function depends on the formation of PAR (24,25). The catalytic activity of ARTD1 is strongly activated during adipogenesis and has been demonstrated to be involved in adipogenesis (24). However, the molecular mechanism that regulates PAR-dependent regulation of PPARγ2 target gene expression and the functional significance of PAR formation in adipogenesis remained elusive. Moreover, most described endogenous PPARγ ligands show a low affinity for the receptor, and how they induce co-factor exchange at low levels in the cell is currently unknown.

The results presented here confirm that PPARγ-dependent gene expression during adipogenesis depends on PAR formation not only *in vitro* but also *in vivo*. According to our findings, this regulatory function of poly-ADP-ribosylation is brought about by the formation of a complex between ARTD1 and PPARγ at the promoter regions of target genes, a process that increases PPARγ ligand binding and causes the exchange of transcriptional co-repressors, such as nuclear receptor co-repressor (NCoR) with transcriptional co-activators, such as p300. Consistent with this notion, the lack of co-factor exchange in the presence of PARP inhibitors was overcome by treating the cells with an excess of the PPARγ ligand rosiglitazone. The present study thus elucidates the molecular mechanism by which ARTD1-induced ADP-ribosylation promotes adipogenesis. In addition, the study identifies a new putative role for ARTD1 in the control of ligand-gated transcription factors.

MATERIALS AND METHODS

Animal experiments

A novel pan-PARP inhibitor MRLB-45696 (IC50 for ARTD1 and -2 <1 nM (26)) was kindly provided by Thomas Vogt from Merck Research Laboratories. Ten-week-old male C57BL/6J mice were fed with pellets made in house containing vehicle or PARP inhibitor (50 mg/kg/day) for 18 weeks. All animal experiments were carried out in accordance with the Swiss and EU ethical guidelines and have been approved by the local animal experimentation committee of the Canton de Vaud under license #2465.

Cell culture

For differentiation, 3T3-L1 cells were plated at 80% confluence, medium was changed after 2 days and induction medium containing 1 μg/ml insulin (I-9278), 0.25 mM 3-isobutyl-1-methylxanthine (I-5879) and 0.5 μM dexamethasone (D-4902) (Sigma Aldrich, St. Louis, MO, USA) was added after 2 days for three additional days. Starting at day 5, medium was changed every second day to Dulbecco's modified Eagle's medium (DMEM) containing insulin (1 μg/ml). Cells were differentiated in the presence or absence of pan-PARP inhibitors PJ34 or ABT888 (both at 1 or 10 μM), PARG inhibitor RBPI-3, TopoII inhibitor merbarone (50 μM), SIRT1 inhibitor EX527 (10 μM) or PPARγ agonist rosiglitazone (1 or 10 μM) added to the cells every 24 h. For differentiation until day 21, ABT888 was added only every second day. H_2O_2 treatment (1 mM, 15 min) was performed in DMEM without fetal calf serum (FCS) (and in the presence of catalase inhibitor 3-AT (30 μM) and in the presence or absence of PJ34 (10 μM)).

GST-pulldown

GST-PPARγ2 was coupled to magnetic GST-Beads (Pierce). Note that 1 μg modified or unmodified ARTD1 (in reaction buffer, 5 pmol 40mer DNA, ±10 μM NAD^+, 30 min at 30°C) and 1 μg His-p300 were added to the GST-PPARγ2. Pulldown was performed for 2 h at 4°C in pulldown buffer (50 mM Tris pH 7.5, 150 mM KCl, 5 mM MgCl2, 0.2 mM ethylenediaminetetraacetic acid (EDTA), 20% glycerol, 0.1% NP40) in the presence of 10 μM PJ34. The beads were washed 3× with wash buffer (20 mM Tris pH 7.5, 150 mM KCl, 5 mM MgCl2, 0.2 mM EDTA, 10% glycerol, 0.1% Tween).

Chromatin immunoprecipitation (ChIP)

ChIP was performed as previously described (27). For Re-ChIP experiments, the first ChIP (anti-ARTD1) was eluted twice in 10 mM DTT (30 min, at 30°C), diluted in ChIP

Nucleic Acids Research, 2015, Vol. 43, No. 1 **131**

buffer and the second ChIP (anti-PPARγ) was performed as previously described (27).

Radioligand binding assay

For saturation binding analysis, baculo purified His-PPARγ2 (1 μg) was incubated at 4°C for 3 h in binding buffer containing 10 mM Tris (pH 8.0), 50 mM KCl, 10 mM DTT with 40 nM ^{3}H-rosiglitazone (specific activity 46 Ci/mmol) in a final volume of 100 μl in the presence or absence of 1000× excess of unlabeled rosiglitazone. Bound ligand was separated from free ligand by filtration over GF/C filter and washing filters twice with ice cold binding buffer. Filters were dried and bound radioactivity quantified by liquid scintillation counting. Unspecific binding was determined by adding 40 μM of unlabeled rosiglitazone to the reaction. Experiments with ARTD1 were performed by incubating ARTD1 wt or ARTD1 Y907A/C908Y mutant (40 nM) with 100 nM NAD^{+}, 2 nM DNA at 30°C for 30 min. The reaction was stopped by the addition of 10 μM PARPi (ABT888), and after addition of His-PPARγ2 and 40 nM ^{3}H-rosiglitazone, binding evaluated as described above. For experiments with free PAR, ARTD1 wt or ARTD1 mutant Y907A/C908Y (40 nM) were incubated with 100 μM NAD^{+}, 2 nM DNA at 30°C for 30 min in binding buffer. ARDT1 was then degraded by Proteinase K over night, followed by inactivation for 10 min at 80°C with PARPi (ABT888 10 μM). After addition of His-PPARγ2 and 40 nM ^{3}H-rosiglitazone, binding was evaluated as described above.

RESULTS

Pan-PARP inhibitor treatment reduces body weight gain, white adipose tissue content and cell size in mice fed with high-fat diet (HFD)

Earlier studies have implicated a function of ADP-ribosylation and, in particular, ARTD1 in adipogenesis and adipocyte function (24,25,28,29). Although the importance of PAR was already described in cells, the physiological relevance of PAR formation *in vivo* has so far not been investigated before. Accordingly, we hypothesized that the inhibition of PAR formation may have beneficial effects on the onset and development of obesity. In order to test this hypothesis, we treated male wild-type (wt) C57BL/6J mice fed with either chow or a HFD for 18 weeks with a recently characterized pan-PARP inhibitor (26). To confirm that PARP inhibitor treatment reduced PAR formation, we measured total ART activity in adipose tissue. As expected, total ART activity was significantly reduced by 35% in both subcutaneous (sc) and epididymal (epi) WAT of PARP inhibitor-treated mice (Supplementary Figure S1A). Overall, vehicle-treated control mice on the HFD presented with a significantly higher body weight gain compared to PARP inhibitor-treated animals (Figure 1A and B), although their food intake was equal (Supplementary Figure S1B). PARP inhibitor-treated animals have been shown to exhibit increased energy expenditure (26). However, body weight of PARP inhibitor-treated mice on HFD was still higher compared to that of those on chow diet, indicating that increased energy expenditure cannot completely compensate for the increased calorie uptake. Previous observations showed that PAR formation is essential for adipocyte differentiation and function in culture (24,25). We thus hypothesized that adipocyte function was impaired in PARP inhibitor-treated animals and that this contributes to the decreased body weight on HFD. HFD caused a marked increase in the amount of scWAT, while only minor increases were observed in epi and perirenal (peri) WAT, as well as in BAT (Figure 1C and D). However, the increase in HFD-mediated scWAT observed in PARP inhibitor-treated mice was found to be significantly lower as compared to vehicle-treated control mice, while no significant differences were observed between epiWAT, periWAT or BAT (Figure 1D). To test if this PARP inhibitor treatment effect manifested itself in the morphology of scWAT adipocytes, scWAT was isolated, fixed, stained and subjected to quantitative microscopic analysis. Adipocytes from PARP inhibitor-treated mice were significantly smaller than corresponding cells from scWAT of vehicle-treated control animals (Figure 1E). To investigate if also the epiWAT was affected by PARP inhibitor treatment, although the fat pad weight was unchanged, we analyzed adipocyte morphology in epiWAT. In agreement with earlier studies, adipocytes in epiWAT from PARP inhibitor-treated animals were significantly smaller than those from chow-fed mice (25) (Supplementary Figure S1C). To test if the smaller adipocyte size correlated with a change in adipogenic gene expression, a quantitative reverse transcriptase-polymerase chain reaction (qRT-PCR) analysis was performed. Consistent with earlier studies (25), the reduced body weight gain, the reduced expansion of the scWAT after HFD and PARP inhibitor treatment (Figure 1A–E), and the expression of PPARγ target genes *adiponectin*, *aP2* and *CD36* was significantly reduced, whereas the expression of the key adipogenic regulator *PPARγ* itself was unaffected (Figure 1F). In contrast, epiWAT showed impaired *PPARγ2* gene expression (Supplementary Figure S1D). Expression of the other adipogenic markers *aP2*, *CD36* and *adiponectin* tended also to be down in epiWAT from PARP inhibitor-treated mice (Supplementary Figure S1D). Small adipocytes have often been shown to be associated with low inflammation (30). To test the inflammatory status of the scWAT of PARP inhibitor-treated animals, we analyzed gene expression of the inflammatory mediators *resistin*, *angiotensinogen*, *interleukin 6 (IL6) and tumor necrosis factor α (TNFα)* (Figure 1G). We found expression of *resistin*, *angiotensinogen* and *IL6* to be downregulated, indicating that the general inflammatory status of PARP inhibitor-treated animals is reduced in comparison to vehicle-treated animals. EpiWAT is known to undergo a substantial degree of inflammation upon feeding with a HFD (31). qRT-PCR analysis of this tissue revealed that PARP inhibitor-treatment also generally reduced HFD-induced inflammatory gene expression in epiWAT (Supplementary Figure S1E).

In summary, these results show that ADP-ribosylation mediates obesity, adipocyte hypertrophy and general adipose tissue inflammation in mice fed with a HFD.

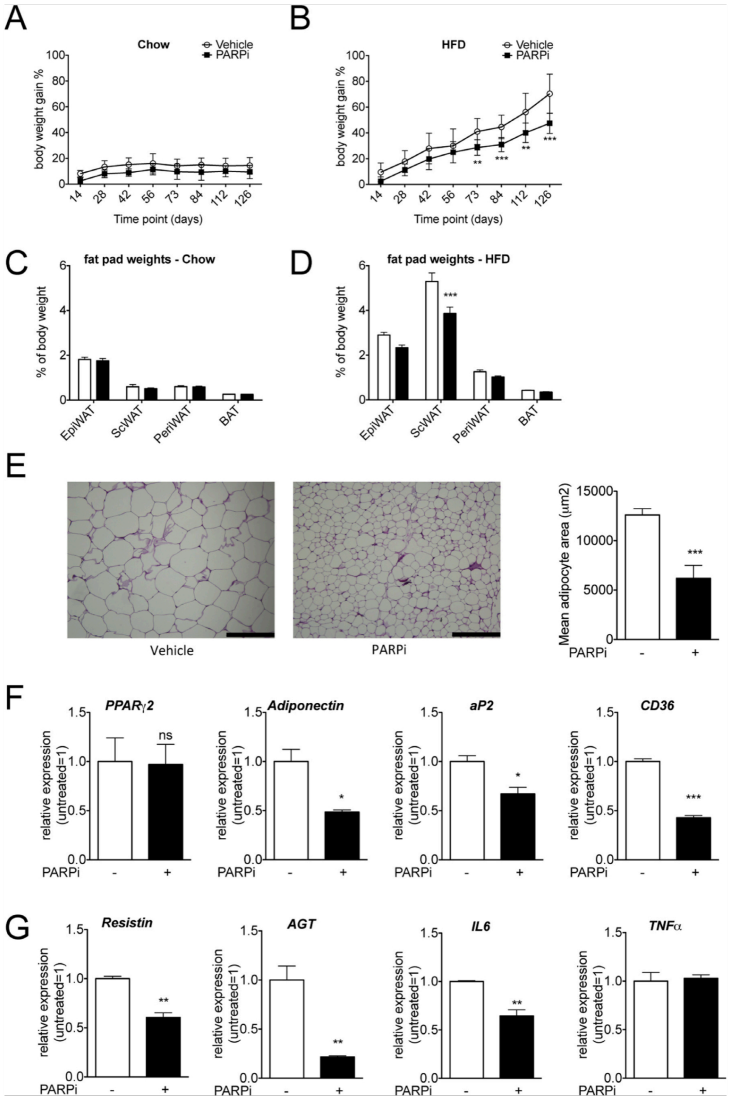

Figure 1. PARP inhibitor treatment reduces body weight and adipose tissue size in mice. (A and B) Weight development during chow and HFD in vehicle- and PARP inhibitor-treated mice. Eight-week-old male C57BL/6J mice were fed with chow or HFD containing vehicle (DMSO) or PARP inhibitor (PARPi, 50 mg/kg/day) for 18 weeks. Body weight gain was monitored at the given time points. Two-way ANOVA analysis revealed $P < 0.001$ for both HFD and chow diet ($n = 10$). (C and D) Fat pad weights on chow and HFD. Animals were sacrificed after overnight fasting using isoflurane inhalation and tissues were collected upon sacrifice and flash-frozen in liquid nitrogen. epiWAT, epididymal white adipose tissue; scWAT, subcutaneous white adipose tissue; periWAT, perirenal white adipose tissue; BAT, brown adipose tissue. Data are mean ± SEM. ANOVA one-way test, $***P < 0.001$ ($n = 10$). (E) Mouse scWAT was fixed, dehydrated and embedded in paraffin wax. Sequential sections (6 µm) were cut and morphological changes visualized using H&E staining (scale bar 200 µm). Blinded analysis of mean adipocyte area in tissue sections from mice ($n = 9$–10 per treatment group) was performed. (F and G) qRT-PCR analysis of PPARγ-dependent and inflammatory genes of scWAT isolated from vehicle- and PARP inhibitor-treated mice. For qRT-PCR analysis of tissue samples, isolated WAT from 8 mice per group was pooled and expression values were normalized against 36BP4. AGT, angiotensinogen. All data are mean ± SEM. *t*-Test: $*P < 0.05$, $**P < 0.01$, $***P < 0.001$.

Nucleic Acids Research, 2015, Vol. 43, No. 1 **133**

PAR formation is required for PPARγ-dependent gene expression

To study the mechanistic details of how PAR formation promotes adipogenesis (24), we characterized adipocyte differentiation in 3T3-L1 pre-adipocyte cultures in the presence or absence of different PARP inhibitors. Adipogenesis was induced in 3T3-L1 cells by the addition of insulin, 3-isobutyl-1-methylxanthine (IBMX) and dexamethasone (32), upon which they consistently formed lipid-laden adipocytes (Figure 2A). In line with our earlier studies (24), in which we used the PARP inhibitor PJ34, the presence of the more potent pan-PARP inhibitor ABT888 (which does not inhibit tankyrases) during the first 7 days of adipogenesis strongly reduced the expression of *PPARγ2* itself and its target genes *aP2*, *CD36* and *adiponectin* (Figure 2B and Supplementary Figure S2A). The inhibitory effect of PARP inhibitors on *PPARγ2* itself can be explained by our previous results, which showed that PARP inhibitor treatment does not inhibit initial *PPARγ2* expression, but rather inhibits the regulatory feedback loop of *C/EBPα* and *PPARγ* expression (16,24). To confirm that PAR formation indeed enhances PPARγ-dependent gene expression and adipogensis, we also performed the reverse experiment and aimed to increase PAR formation by inhibiting PAR degradation with the PARG inhibitor RBPI-3 (Supplementary Figure S2B). In agreement with the hypothesis that PAR formation enhances PPARγ-dependent gene expression, RBPI-3 caused a significant increase in the transcript levels of *PPARγ2*, *aP2*, *CD36* and *adiponectin* (Figure 2C). Similarly, the inhibition of nicotinamide phosphoribosyltransferase (NAMPT) by FK866, which decreases cellular NAD^+ levels and thus interferes with PAR formation, strongly reduced PPARγ-dependent gene expression and PPARγ protein levels (Supplementary Figure S2C and D). Finally, to rule out that an ARTD family member other than ARTD1 was responsible for the effect of PARP inhibitor treatment, we differentiated ARTD1 knockout and wt mouse embryonic fibroblasts (MEFs) to adipocytes. MEFs lacking ARTD1 did not exhibit detectable PAR formation or induction of PPARγ-dependent gene expression (Supplementary Figure S2E and F), indicating that no other ARTD family member can compensate for the lack of ARTD1 and its enzymatic activity. This is in line with our previous findings that *in vitro* knockdown of ARTD1 in 3T3L1 cells inhibits differentiation (24) and that *in vivo* knockout of ARTD1 in mice on HFD reduces adipogenic gene expression (25). To exclude potential effects on early differentiation events in cell culture (e.g. mitotic clonal expansion), we also treated 3T3-L1 cells with PARP inhibitor only during late stages of adipocyte differentiation, from day 7 to day 21. Again, the PARP inhibitor significantly reduced expression of the PPARγ-dependent genes *aP2*, *CD36* and *adiponectin* (Figure 2D). SIRT1 was described to be a repressor of 3T3-L1 differentiation (33). Both ARTD1 and SIRT1 are NAD^+-consuming enzymes that compete for the cellular NAD^+ pool. To exclude the possibility that increased availability of NAD^+ and thus activation of SIRT1 was responsible for the PARP inhibitor effect (which could also lead to repression of PPARγ-dependent genes), we also performed experiments with a SIRT1 inhibitor (Supplementary Figure S2G). As expected, SIRT1 inhibition increased PPARγ-dependent gene expression. However, PARP inhibitor-dependent repression of PPARγ-dependent genes could not be reversed by co-incubation with the SIRT1 inhibitor. We therefore conclude that PAR formation is indeed required for the expression of PPARγ and PPARγ-dependent genes during the differentiation of 3T3-L1 cells to functional, lipid-laden adipocytes.

Topoisomerase II activity is required for ARTD1 recruitment to PPARγ target genes

ARTD1 is the main intracellular ART and generally responsible for about 90% of the nuclear PAR formed under normal conditions (34). The stimulation of PPARγ-dependent gene expression upon PARG inhibitor treatment thus hints at a role for ARTD1 and PAR in regulating the promoter activity of PPARγ target genes. We first assessed the interaction of ARTD1 with PPARγ by immunoprecipitation experiments of PPARγ from nuclear extracts of 3T3-L1 cells on day 7 of differentiation. The results show that automodified ARTD1, which is known to appear at day 7 of differentiation (24), was co-precipitated using an anti-PPARγ antibody (Figure 3A). ChIP experiments with anti-ARTD1 antibodies confirmed the recruitment of ARTD1 at the PPARγ response elements (PPREs) of PPARγ-dependent genes, which was strongly reduced upon PARP inhibitor treatment (Supplementary Figure S3A). To further confirm this interaction and to analyze whether ARTD1 and PPARγ interact at the promoter region of the respective target genes, re-ChIP experiments were performed. Chromatin taken from 3T3-L1 cells 7 days after induction of differentiation was first precipitated with an anti-ARTD1 antibody and then with an anti-PPARγ antibody, and the presence of PPARγ-driven *aP2*, *adiponectin* *CD36* promoters were subsequently analyzed by qRT-PCR. As a negative control, the PPARγ-independent promoter of *keratin 19* (*K19*) was analyzed (29,35), which did not show any PPARγ recruitment at day 7 (Supplementary Figure S3B). The tested PPREs of *adiponectin*, *aP2* and *CD36* were all enriched by the re-ChIP treatment (Figure 3B). In contrast, the negative control gene *K19* was not enriched. These results indicate a direct interaction of ARTD1 with PPARγ at the PPREs of at least a subset of PPARγ target genes.

Since the recruitment of ARTD1 was largely dependent on PAR formation (Supplementary Figure S3A and C) and we have previously shown that topoisomerase II (TopoII) activity is required for PAR formation in adipogenesis (24) we wondered if TopoII activity was also required for ARTD1 recruitment to PPARγ target genes. As expected, ChIP experiments revealed the enrichment of TopoII at the PPREs of the PPARγ-dependent genes *aP2*, *adiponcetin* and *CD36*, while no significant enrichment at the control gene *K19* was observed (Figure 3C). Additionally, ARTD1 recruitment was strongly dependent on TopoII enzymatic activity since merbarone treatment reduced occupancy of ARTD1 at the tested PPREs as measured by ChIP (Figure 3D). Finally, the co-localization of TopoII and ARTD1 in 3T3-L1 cells (day 7 of adipogenesis) was confirmed by immunofluorescence confocal microscopy as well as by re-Chip experiments (Figure 3E and F). In summary, these ex-

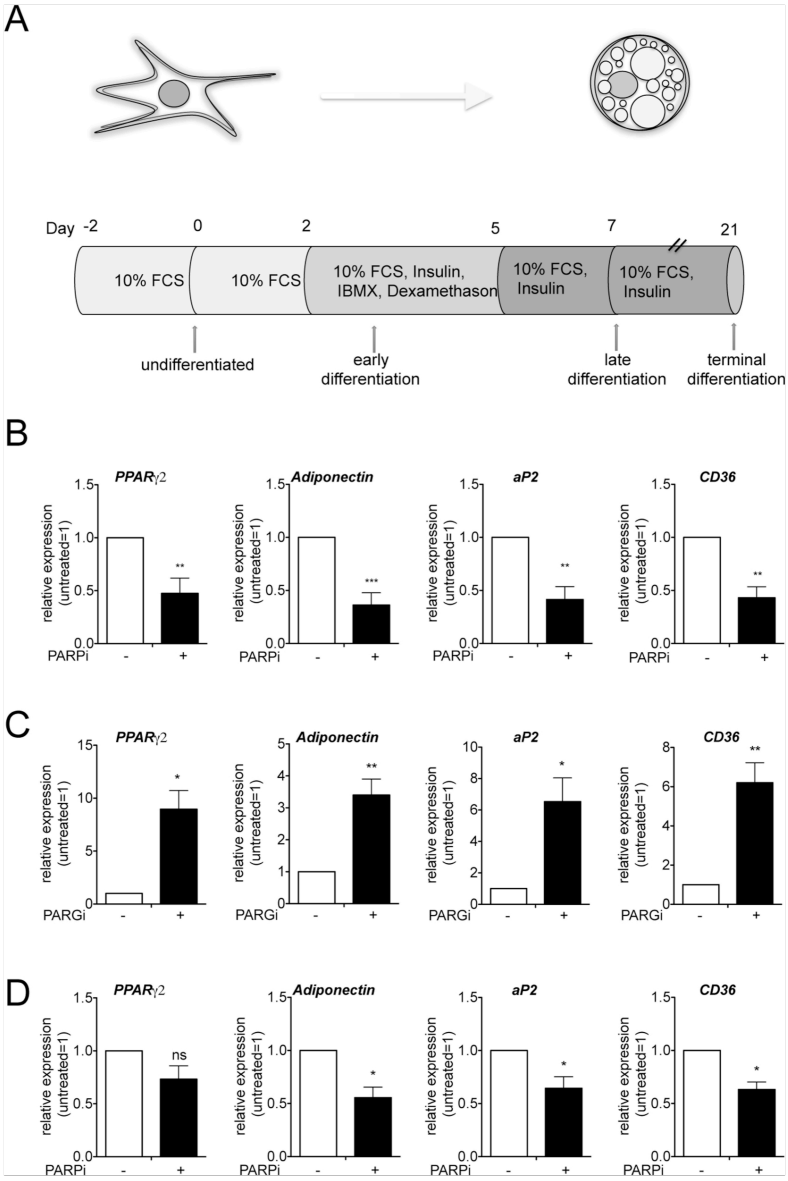

Figure 2. PAR formation is required for PPARγ-dependent gene expression. (A) Scheme of differentiation program: Adipogenesis was induced by adding insulin, 3-isobutyl-1-methylxanthine (IBMX) and dexamethasone for 3 days and maintaining cells in medium containing 10% FCS and insulin. (B) Cells were differentiated in the absence or presence of 10 μM PARP inhibitor (PARPi, ABT888) (daily treatment) until day 7, at which point RNA was isolated ($n = 8$). (C) Differentiating 3T3-L1 cells were left untreated or treated with 10 μM PARG inhibitor (PARGi, RBPI-3) on days 1–5 and RNA was isolated on day 6 of differentiation ($n = 5$). (D) Starting from day 7 of adipogenesis of 3T3-L1 cells, the culture medium containing insulin ± 10 μM PARP inhibitor (PARPi, ABT888) was changed every second day. RNA was isolated at day 21 and gene expression was analyzed by RT-qPCR ($n = 4$). All values represent the mean ± SEM, untreated samples were set as 1. *t*-Test: $^{*}P < 0.05$, $^{**}P < 0.01$, $^{***}P < 0.001$.

Nucleic Acids Research, 2015, Vol. 43, No. 1 **135**

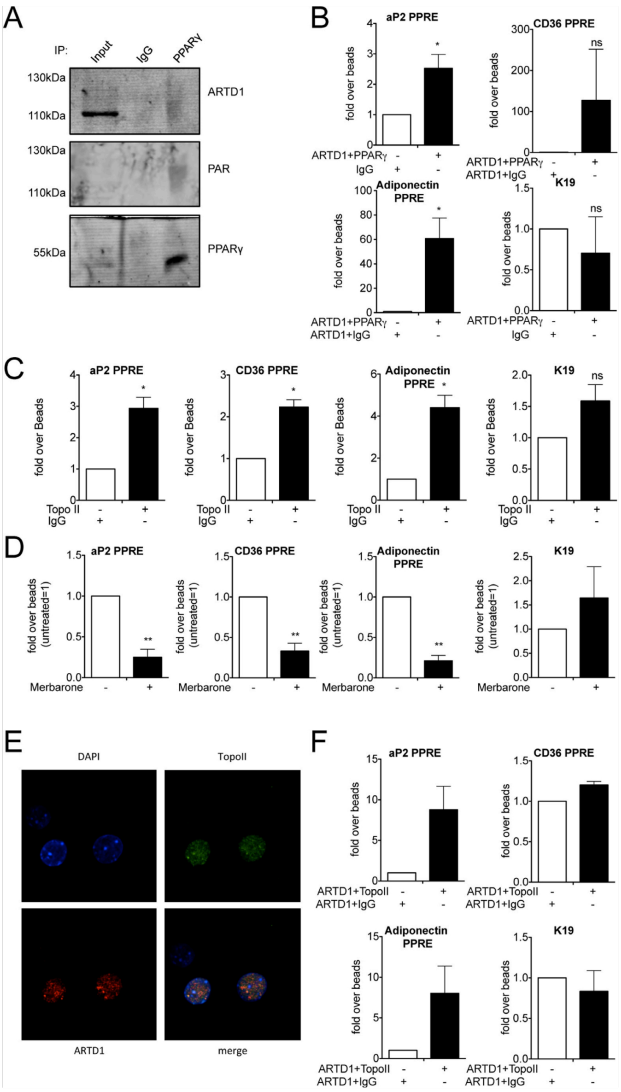

Figure 3. Ligand-dependent interaction of PPARγ and ARTD1 at the PPREs of PPARγ-target genes. (A) 3T3-L1 cells were differentiated until day 7, nuclear protein extracts were prepared and PPARγ was immunoprecipitated. To prevent degradation of PAR, extracts were treated with 10 μM PARG inhibitor (RBPI-3). ChIP values were normalized over immunoglobulin G (IgG) control and over a control region (IL6 promoter). (B) ReChIP of ARTD1 and PPARγ. At day 7 of differentiation, cells were fixed and the chromatin was first precipitated with an ARTD1 antibody and then with a PPARγ antibody ($n = 4$). (C) Cells were fixed at day 7 of differentiation and chromatin was immunoprecipitated with a topoisomerase II (TopoII) antibody ($n = 3$). (D) Cells were treated with 50 μM merbarone at days 5 and 6 and fixed at day 7 of differentiation and chromatin was immunoprecipitated with an ARTD1 antibody ($n = 4$). (E) At day 7 of differentiation, 3T3-L1 cells were fixed with PFA and stained with an antibody against TopoII (green) and ARTD1 (red). DAPI was used to visualize the nuclei (blue). Cells were analyzed by confocal microscopy. (F) ReChIP of ARTD1 and TopoII. At day 7 of differentiation, cells were fixed and the chromatin was first precipitated with an ARTD1 antibody and then with a TopoII antibody ($n = 4$). All values represent the mean ± SEM. ChIP values were normalized over IgG control. *t*-test: $^{*}P < 0.05$, $^{**}P < 0.01$.

136 Nucleic Acids Research, 2015, Vol. 43, No. 1

periments suggest that ARTD1 and PPARγ interact at the PPREs of target genes and that TopoII activity is required for the recruitment of ARTD1 to PPARγ-dependent genes.

ARTD1 induces PAR formation at PPREs of adipogenic genes and increases the transcriptional potential of PPARγ

To investigate if the PAR-polymers induced during differentiation are indeed present at the chromatin of PPREs of PPARγ target genes, an anti-PAR ChIP was performed. PAR was specifically enriched at the promoters of PPARγ-target genes, which increased during differentiation from day 0 to day 7 (Figure 4A), indicating that PAR is specifically formed at PPREs of adipogenic genes during differentiation. To gain further insight into the PAR-regulated transcriptional potential of PPARγ, we performed luciferase assays in the presence and absence of PARP inhibitor. Analysis of transcriptional activity of PPARγ in 3T3-L1 cells revealed that inhibition of PAR formation reduced both basal and rosiglitazone-induced PPARγ transcriptional activity (Figure 4B). In contrast, co-treating the cells with PARG inhibitor increased the response to rosiglitazone as compared to the untreated control (Figure 4C). Since overexpression of wt ARTD1, but not of the enzymatically inactive mutants E988K or Y907A/C908Y, enhanced the RLU Firefly/Renilla signal, PPARγ-dependent gene expression was clearly mediated by ARTD1-dependent PAR formation (Figure 4D). Similar results were obtained by using a different PARP inhibitor and when experiments were carried out in HEK 293T cells (Supplementary Figure S4A–C). To test whether induction of PAR formation by other means also enhances PPARγ activity, we used H_2O_2 to induce PAR formation. Similar to ligand-induced PAR formation, treatment of cells with H_2O_2 also enhanced complex formation between PPARγ2 and ARTD1 in cells (Supplementary Figure S4D and E). H_2O_2 treatment also increased luciferase activity to a level that was comparable to the effect induced by rosiglitazone (Figure 4E). Co-treatment with PARP inhibitor abolished this stimulation, indicating that PAR formation was indeed responsible for the observed effect. Co-treating the cells with PARG inhibitor enhanced the response to H_2O_2 as compared to an inactive control substance (Figure 4F). Since overexpression of wt ARTD1 strongly enhanced the RLU Firefly/Renilla signal, while neither the E988K nor the Y907A/C908Y enzymatically inactive mutant conferred this effect, ARTD1-dependent PAR formation also contributed to the H_2O_2-induced increase in PPARγ-dependent gene expression (Figure 4G). A similar result was observed in HEK 293T cells overexpressing PPARγ and either one of the ARTD1 mutants (Supplementary Figure S4F). To analyze if this ARTD1-dependent increase in PPARγ-dependent gene expression was dependent on TopoII activity, the effect of merbarone on Luciferase activity upon rosiglitazone or H_2O_2 stimulation was analyzed (S4G, S4H). As observed for the differentiating 3T3-L1 cells, TopoII activity was also required for PPARγ-dependent gene expression for this readout. To confirm that H_2O_2-induced PAR formation functionally regulates PPARγ-mediated transcriptional activation with a physiologically more relevant readout, the effect was studied in differentiating 3T3-L1 cells. Cells were treated with H_2O_2 in the presence or absence of PARP inhibitor at day 3 of differentiation. Two hours after treatment with H_2O_2, the expression of *aP2*, *CD36* and *adiponectin* was analyzed by qRT-PCR. H_2O_2 treatment led to significantly increased expression of *adiponectin* in PPARγ-overexpressing 3T3-L1 cells, which was inhibited by PARP inhibitor treatment (Supplementary Figure S4J). Not all PPARγ target genes (e.g. *aP2*) were induced upon H_2O_2 stimulation. These results demonstrate that H_2O_2-induced formation of PAR is sufficient to increase the expression of at least a subset of PPARγ-dependent genes.

PAR formation controls PPARγ-dependent gene expression by enhancing ligand binding and facilitating ligand-induced co-factor exchange

Transcriptional activity of nuclear receptors, such as PPARs, is regulated by the dynamic exchange of co-activator and co-repressor complexes at the promoters of the target genes (11,12,36). Two of the most important regulators of PPARγ functions are the co-activator p300 and the co-repressor NCoR1 (37,38). To elucidate the role of PAR formation in the binding of PPARγ to its co-activator p300, GST pull-down experiments with recombinant ARTD1, p300 and PPARγ were performed. Under the tested conditions, rosiglitazone was poorly able to induce complex formation between PPARγ and p300 (Figure 5A). Addition of unmodified ARTD1 enhanced this formation in a rosiglitazone-dependent manner, which was even further enhanced, when automodified PARylated ARTD1 was added, but using the same concentration of rosiglitazone (Figure 5A), suggesting that ADP-ribosylated ARTD1 enhances PPARγ ligand binding and subsequent complex formation with p300. Indeed, addition of ADP-ribosylated ARTD1 enhanced binding of p300 even at a very low rosiglitazone concentration where no complex formation was observed in samples without ARTD1 or with non-modified ARTD1 (Supplementary Figure S5A). PPARγ/p300 complex formation was also enhanced by inducing ARTD1-dependent PAR formation *in vivo* by H_2O_2 (Supplementary Figure S5B).

To further substantiate that automodified ARTD1 is able to enhance ligand binding to PPARγ2, we took advantage of a ligand-binding assay employing ^{3}H-labeled rosiglitazone (Supplementary Figure S5C). Using recombinant full-length PPARγ2, we detected specific ligand binding to PPARγ2. This ligand binding was significantly enhanced when ADP-ribosylated ARTD1 was added to the binding reaction (Figure 5B). Unmodified ARTD1 (incubated without NAD^+ or using the inactive mutant Y907A/C908Y) did not show this increase, indicating that ADP-ribosylation of ARTD1 was responsible for this phenomenon. To test if also free PAR increases ligand binding, we supplemented the binding reaction with PAR only (Figure 5B). However, no increase in ligand binding was observed upon addition of free PAR, suggesting that it is indeed PAR covalently attached to ARTD1 that changes the ligand binding potential of PPARγ.

Next, we analyzed if recruitment of p300 co-activator to the PPARγ-dependent genes is regulated by PAR formation *in vivo*. In 3T3-L1 cells differentiated for 7 days,

Nucleic Acids Research, 2015, Vol. 43, No. 1 **137**

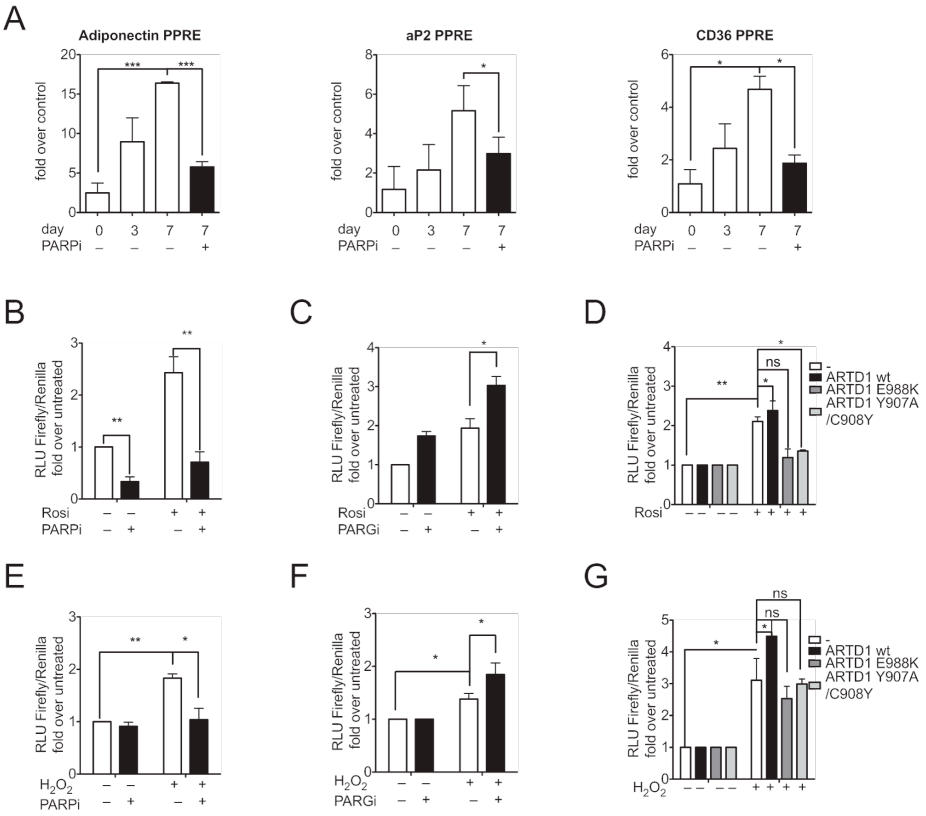

Figure 4. PAR formation enhances ligand binding to PPARγ. (A) 3T3-L1 cells were treated daily with 10 μM PJ34 starting at day 1 or not. At day 0, 3 or 7, cells were fixed with formaldehyde and chromatin was precipitated with an anti-PAR antibody. Values were normalized over IgG and over IL6-100 as control gene. (B) 3T3-L1 cells overexpressing PPARγ2 were treated with 10 μM rosiglitazone in the presence or absence of 10 μM PARP inhibitor (PARPi, PJ34) for 16 h and luciferase activity was subsequently measured ($n = 5$). (C) 3T3-L1 cells overexpressing PPARγ2 were pretreated with 10 μM PARG inhibitor (PARGi, RBPI-3) and treated with 10 μM rosiglitazone for 16 h and luciferase activity was subsequently measured. (D) 3T3-L1 cells co-overexpressing PPARγ2 and ARTD1 (wt, $n = 5$), ARTD1 E988K ($n = 7$), ARTD1 Y907A/C908Y ($n = 3$) or GFP (as a negative control, $n = 7$) were treated with 10 μM rosiglitazone for 16 h in the presence or absence of 10 μM (PARPi, PJ34) and luciferase activity was subsequently measured ($n = 4$). (E) 3T3-L1 cells overexpressing PPARγ2 were treated with 1 mM H_2O_2 for 2 h in the presence of 30 μM catalase inhibitor (3-AT) and in the presence or absence of 10 μM PJ34. Luciferase activity was measured ($n = 4$). (F) 3T3-L1 cells overexpressing PPARγ2 were pretreated with 10 μM PARG inhibitor (RBPI-3) and treated with 1 mM H_2O_2 for 2 h in the presence of 30 μM catalase inhibitor (3-AT) and luciferase activity was subsequently measured. (G) 3T3-L1 cells co-overexpressing PPARγ2 and ARTD1 (wt, $n = 5$), ARTD1 E988K ($n = 4$), ARTD1 Y907A/C908Y ($n = 3$) or GFP (as a negative control, $n = 5$) were treated with 1 mM H_2O_2 for 2 h in the presence of 30 μM catalase inhibitor (3-AT). All values represent the mean ± SEM; *t*-test: $^*P < 0.05$, $^{**}P < 0.01$, $^{***}P < 0.001$.

binding of p300 to the PRRE of *aP2* and *adiponectin* was significantly reduced upon PARP inhibitor treatment (Figure 5C), suggesting that the reduction of p300 at the PPRE translates into reduced expression of the corresponding gene. The PPARγ-dependent gene *CD36* showed the same trend. Importantly, p300 binding was not changed upon PARP inhibitor treatment at the promoter of the PPARγ-independent control gene *K19*. Interestingly, and in agreement with the respective co-activator and co-repressor functions, occupancy of the co-repressor NCoR-1 exhibited the opposite behavior and was increased at the PRREs of PPARγ-dependent genes upon PARP inhibitor treatment (Figure 5D). A similar result was obtained with cells that were treated with PARP inhibitor from day 5 to 8 of differentiation (Supplementary Figure S5D). Additionally, inhibition of TopoII activity, which is needed for PAR for-

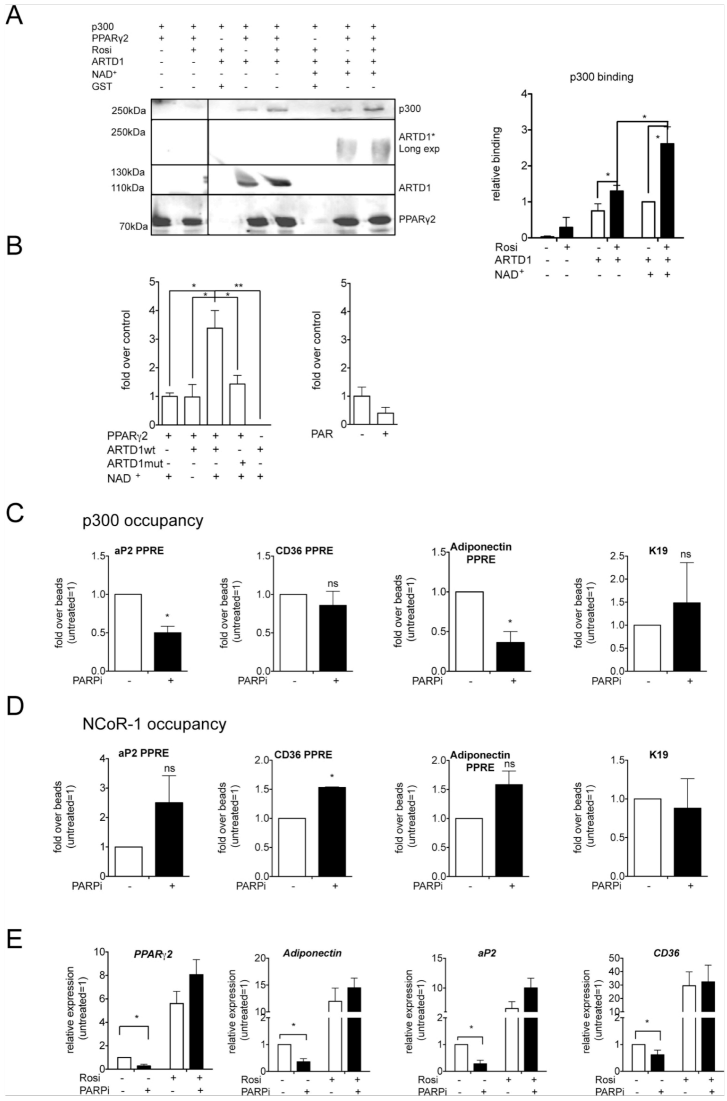

Figure 5. PAR formation controls PPARγ-dependent gene expression by promoting ligand induced cofactor exchange. (A) Left: PPARγ2-GST pull-down of ARTD1 (without NAD^+ = unmodified, with NAD^+ = automodified; please note that modified ARTD1 has a higher molecular weight than unmodified ARTD1) and p300 in the presence or absence of 10 μM rosiglitazone. Black line indicates the removal of lanes on the same blot that are not relevant for the experiment. Right: Quantification of p300 signal. Intensities were normalized against the corresponding PPARγ signal and then normalized against modified ARTD1 in the absence of rosiglitazone (= 1). Statistical analysis represents data from four independent experiments. (B) Radioligand binding assay in the presence of modified or unmodified ARTD1 (wt or mutant (Y907A, C908Y), ±100 nM NAD^+). Values show specific binding normalized to control (PPARγ without ARTD1, column 1) ($n = 3$–5). Radioligand binding assay in the presence or absence of PAR. Values show specific binding normalized to control (PPARγ without ARTD1 ($n = 3$)). (C) Starting from day 2 of adipogenesis, 3T3-L1 cells were treated daily with 10 μM PJ34 or not. At day 7, the cells were fixed with formaldehyde and the chromatin was immunoprecipitated with an anti-p300 antibody ($n = 4$). (D) Same analysis as in C for NCoR-1 ($n = 3$). (E) 3T3-L1 cells were treated with 10 μM rosiglitazone or 10 μM (PARPi, ABT888) or both at days 2–6 of adipogenesis ($n = 4$). All values represent the mean ± SEM; ChIP values were normalized over IgG control. *t*-test: $*P < 0.05$, $**P < 0.01$.

mation, led to reduced p300 levels (Supplementary Figure S5E). If automodified ARTD1 is able to enhance PPARγ ligand binding and subsequently transcriptional co-factor exchange, then treating cells with a high dose of rosiglitazone should functionally compensate the repressory PARP inhibitor effect on PPARγ-dependent gene expression. Differentiating 3T3-L1 cells were therefore treated with PARP inhibitor or not and supplemented with an excess of rosiglitazone. The results of these experiments showed that an excess of rosiglitazone indeed overcomes the PARP inhibitor effect on *aP2*, *CD36*, *adiponectin* and *PPARγ2* gene expression (Figure 5E). This effect was indeed mediated by p300, as treatment with PARP inhibitor in rosiglitazone-treated cells could not reduce p300 levels in contrast to cells that have not been treated with an excess PPARγ ligand and that showed reduced p300 binding upon PARP inhibitor treatment (Supplementary Figure S5F).

In summary, these findings show that ADP-ribosylated ARTD1 interacts with PPARγ, enhances ligand binding to PPARγ and thereby facilitates co-factor exchange, resulting in enhanced gene expression of PPARγ target genes and thus clarifies the mechanism by which ARTD1 promotes adipocyte differentiation and function.

DISCUSSION

Adipogenesis is driven by changes in gene transcription, being reliant on the reprogramming of the cellular transcription profiles through the activation of specific transcription factors (39). Transcription factors that determine the early phase of adipogenesis, such as Stat5a, C/EBP-β and C/EBP-δ, are required for the formation of so-called transcriptional hotspots that prime the chromatin for PPARγ binding (2). PPARγ is a ligand-gated transcription factor and its activity relies on transcriptional co-factors that regulate chromatin compaction and recruit elements of the transcription machinery (2,39). During the course of adipogenesis, co-repressors are replaced by co-activators, which induce a permissive chromatin state, thereby rendering the DNA accessible for the transcription machinery.

We have previously shown that ADP-ribosylation plays an important role in adipogenesis and adipocyte function (24,25). We have shown that ARTD1 activity is important for the late phase of adipogenic differentiation of 3T3-L1 cells and is likely regulated by the formation of transient, site-specific double-strand DNA breaks at promoters of PPARγ-dependent genes (24). This suggested that ARTD1 is not required for the formation of transcription factor hotspots but for sustained PPARγ-dependent gene expression. These initial findings were further corroborated by *in vivo* studies, showing that the presence of ARTD1 is necessary for efficient adipogenesis, whereas lack of ARTD1 limits adipocyte function, adipocyte size and lipid metabolism in the liver (25). Although these studies have established a role for ARTD1 in adipogenesis and adipocyte turnover, the molecular mechanism by which ARTD1, and more specifically its ADP-ribosylation, co-regulate these processes remained to be elucidated.

In the current study, we show that ARTD1-induced poly-ADP-ribosylation is an important mediator of WAT function and PPARγ-dependent gene expression in mice on HFD. Furthermore, our work demonstrates that ARTD1-dependent ADP-ribosylation also influences adipogenic gene expression in cultured cells. Treating cells with an excess of PPARγ ligand overcame the repression of PPARγ-dependent gene expression by PARP inhibitor treatment, indicating that ADP-ribosylated ARTD1 stabilizes PPARγ ligand binding. These results define enhancement of ligand binding as the mechanism by which PAR formation regulates and promotes PPARγ-dependent gene expression in the later phase of adipogenesis and thus uncover a new regulatory mechanism of ARTD1-induced ADP-ribosylation for nuclear factor-regulated gene expression. Together, our results support a model in which TopoII-dependent torsional stress or DNA structures activate ARTD1. Modified ARTD1 interacts with PPARγ and stabilizes PPARγ ligand binding, which allows an exchange of the NCoR1 co-repressor with the p300 co-activator at the promoters of PPARγ target genes (Supplementary Figure S5G).

Interestingly, H_2O_2-induced PAR formation also enhanced PPARγ-dependent gene expression using a luciferase reporter assay or the analysis of endogenous PPARγ target genes. This observation suggests that H_2O_2 signaling enhances gene expression specifically, possibly by inducing ADP-ribosylation to the promoters. Further investigations are required to study how a possible targeting of PAR formation by H_2O_2 is regulated.

We show here that TopoII activity is required for recruitment and activation of ARTD1 at PPARγ-dependent genes. Although ARTD1 activation has been linked to TopoII activity (40), it was not clear yet if the TopoII activity is needed for the recruitment of ARTD1. Here, we show that TopoII activity is indeed required for ARDT1 recruitment and subsequent activation, a finding which supports a model where beginning transcription leads to the requirement of TopoII cleavage, thereby recruiting and activating ARTD1, which leads to increased gene expression. Since TopoII cleavage does not generate free DNA ends and does not activate or require DNA repair mechanisms (41), ADP-ribosylation at TopoII cleavage sites at PPARγ-dependent genes functions differently from the function of this enzyme in DNA repair. In addition, this means that ARTD1 is not activated by free DNA ends, but rather by DNA structures or torsional stress created during TopoII cleavage.

PPARγ is a ligand-dependent transcription factor, but the identity of the physiological ligands remains controversial and is under active investigation. During adipogenesis, 3T3-L1 cells synthesize a PPARγ-activating substance, but its identity remains elusive (42). Polyunsaturated fatty acids and related molecules can activate PPARγ in micromolar concentrations (43–46), but it is not yet known if the concentration inside the cell and in proximity to the receptor is sufficient to activate PPARγ or not (47). We demonstrate here that the increased presence of ARTD1-mediated ADP-ribosylation activates PPARγ-dependent gene expression and show direct binding and interaction of automodified ARTD1 with PPARγ, which increased ligand binding to PPARγ and in this way apparently increases ligand affinity. Interestingly, only ADP-ribosylated ARTD1 but not isolated PAR was able to enhance PPARγ ligand binding, suggesting that the positioning of the polymers in the protein context is impor-

tant. Although PPARγ can be ADP-ribosylated by ARTD1 *in vitro* and modified PPARγ has been described in cells (48), our data clearly show that the automodification of ARTD1 alone is sufficient to strongly enhance ligand binding to PPARγ. It remains to be clarified how automodified ARTD1 enhances binding of PPARγ ligand. One possibility is, that automodified ARTD1 adapts a different confirmation compared to unmodified ARTD1, which subsequently induces a PPARγ confirmation that facilitates ligand binding. Another possibility is that the conformation of PPARγ remains unchanged, but the interaction of modified ARTD1 with PPARγ positions the polymers in a way that they act like a cage, increasing the local ligand concentration and subsequently also PAPRγ/ligand complex formation. The induction of PAR may thus sensitize cells in cases where endogenous PPARγ ligand concentrations are low and thereby facilitate PPARγ-dependent gene expression. Our results define ADP-ribosylated ARTD1 as a new modulator of PPARγ activity and that ARTD1-mediated ADP-ribosylation increases ligand functionality. This is the first study to our knowledge that shows that ADP-ribosylation of ARTD1 changes the properties of an interacting protein.

PPARγ antagonists exhibit gene-silencing activity due to their ability to promote the recruitment of co-repressors and the subsequent formation of a condensed chromatin state (49). Co-repressors, such as NCoR-1, are dislodged from PPARγ upon ligand binding and their inhibition has the potential to increase the expression of PPARγ target genes (13,50). In contrast, agonists favor the formation of co-activator complexes that acetylate histones and thereby induce chromatin de-condensation and transcriptional initiation (49). An important component of such co-activator complexes are the acetyltransferases p300/CBP, which interact with the N-terminus of PPARγ in a ligand-independent manner, whereas binding to the C-terminus is ligand-dependent (36). In the experimental system of adipogenesis studied here, PAR formation favored ligand binding and p300 recruitment to PPREs and thereby ensured continuous expression of PPARγ target genes. In contrast to this, ARTD1 protein, but not its enzymatic activity was required for full transcriptional activation of NF-κB in the presence of p300 (51), indicating that the regulatory mechanism underlying the control of PPARγ-dependent gene expression is different to the one described for NF-κB. Requirement of PAR for p300 recruitment is consistent with the model of PAR as a platform for the recruitment and binding of chromatin remodeling components and elements of the transcription machinery (52). Based on our results, we postulate that ARTD1 represents a new regulator of the PPARγ co-activator complex involved in promoting PPARγ-dependent gene expression during adipogenesis.

Different other nuclear receptors and transcription factors have been linked to TopoII- and ARTD1-dependent activation of gene expression, supporting the idea that this might be a general regulatory mechanism for different nuclear receptors involved in the regulation of various cellular processes (40,53,54). PPARγ is also expressed in cells of the immune system, such as macrophages, where it can act as a repressor for inflammatory gene expression through a process called transrepression (55). It is an intriguing possibility that PAR formation may also be involved in this process. Recently, a role for NCoR1 in systemic insulin resistance upon HFD-induced obesity has been described (56), raising the question as to whether PAR formation might be important for the co-factor recruitment and thus for the development of insulin resistance in this context.

An interesting and unexpected result of this study was the strong effect of PARP inhibitor treatment on WAT formation and the inflammatory status in mice exposed to HFD. Adipocytes are known to secrete inflammatory mediators (30). However, since also macrophages infiltrate adipose tissue under conditions of obesity, the reduced adipose tissue inflammation observed in PARP inhibitor-treated mice could be mediated both by adipocytes and macrophages. Since scWAT is a potential target for therapies aimed at treating metabolic syndrome (57), PARP inhibitors may open up new treatment options for patients suffering from this disorder. Due to their high level of tolerance and anti-inflammatory effects, PARP inhibitors are considered to be promising therapeutic agents.

SUPPLEMENTARY DATA

Supplementary Data are available at NAR Online.

ACKNOWLEDGEMENTS

The RBPI-3 PARG inhibitor was a kind gift of Prof. Dr. Paul J. Hergenrother (University of Illinois, USA). The novel pan-PARP inhibitor MRL-45696 was kindly provided by Thomas Vogt (Merck Research Laboratories). We thank M. Altmeyer (NNF CPR, Copenhagen) for generating the inactive ARTD1 mutant (Y907A/C908Y), Laia Morato (EPFL, Switzerland) for help with ART activity measurements, and C. Wolfrum for the 3T3-L1 cells and for helpful discussions (ETH Zurich, Switzerland). W. Wahli (University of Lausanne) provided the luciferase and PPARγ expression plasmids. We thank Florian Freimoser, Stephan Christen and all other members of the Institute of Veterinary Biochemistry and Molecular Biology (University of Zurich, Switzerland) for help and discussions during the preparation of this manuscript.
Authors Contributions: M.L. planned and performed the experiments, evaluated the data and wrote the manuscript. M.L., A.M. and P.J.R. performed histological and RNA isolation from mouse tissue. M.L. and F.K. analyzed gene expression in adipose tissue. E.P. organized and performed mouse studies and performed measurements of total ART activity in mouse tissue. J.A. supervised experiments and revised the manuscript. M.O.H. supervised the study and wrote the manuscript.
Johan Auwerx is a founder and SAB member of Mitokyne.

FUNDING

Forschungskredit of the University of Zurich [to M.L.]; Academy of Finland, Saastamoinen Foundation, Finnish Cultural Foundation and Finnish Diabetes Foundation [to E.P.]; Ecole Polytechnique Fédérale de Lausanne, the EU Ideas [AdG-23138 'Sirtuins'], Swiss National Science Foundation [31003A-124713 to J.A.]; Kanton of Zurich, Swiss National Science Foundation [310030B_138667 and

310030_157019 to M.O.H.]. Funding for open access charge: Forschungskredit of the University of Zurich [to M.L.]; Swiss National Science Foundation [31003A-124713 to J.A.].
Conflict of interest statement. None declared.

REFERENCES

1. Church,C., Horowitz,M. and Rodeheffer,M. (2012) WAT is a functional adipocyte? *Adipocyte*, **1**, 38–45.
2. Siersbaek,R., Nielsen,R., John,S., Sung,M.H., Baek,S., Loft,A., Hager,G.L. and Mandrup,S. (2011) Extensive chromatin remodelling and establishment of transcription factor 'hotspots' during early adipogenesis. *EMBO J.*, **30**, 1459–1472.
3. Heikkinen,S., Auwerx,J. and Argmann,C.A. (2007) PPARgamma in human and mouse physiology. *Biochim. Biophys. Acta*, **1771**, 999–1013.
4. Tontonoz,P. and Spiegelman,B.M. (2008) Fat and beyond: the diverse biology of PPARγ. *Annu. Rev. Biochem.*, **77**, 289–312.
5. Vidal-Puig,A., Jimenez-Linan,M., Lowell,B.B., Hamann,A., Hu,E., Spiegelman,B., Flier,J.S. and Moller,D.E. (1996) Regulation of PPAR gamma gene expression by nutrition and obesity in rodents. *J. Clin. Invest.*, **97**, 2553–2561.
6. Fajas,L., Auboeuf,D., Raspe,E., Schoonjans,K., Lefebvre,A.M., Saladin,R., Najib,J., Laville,M., Fruchart,J.C., Deeb,S. *et al.* (1997) The organization, promoter analysis, and expression of the human PPARgamma gene. *J. Biol. Chem.*, **272**, 18779–18789.
7. Kliewer,S.A., Umesono,K., Mangelsdorf,D.J. and Evans,R.M. (1992) Retinoid X receptor interacts with nuclear receptors in retinoic acid, thyroid hormone and vitamin D3 signalling. *Nature*, **355**, 446–449.
8. Escher,P., Braissant,O., Basu-Modak,S., Michalik,L., Wahli,W. and Desvergne,B. (2001) Rat PPARs: quantitative analysis in adult rat tissues and regulation in fasting and refeeding. *Endocrinology*, **142**, 4195–4202.
9. Chawla,A., Boisvert,W.A., Lee,C.H., Laffitte,B.A., Barak,Y., Joseph,S.B., Liao,D., Nagy,L., Edwards,P.A., Curtiss,L.K. *et al.* (2001) A PPAR gamma-LXR-ABCA1 pathway in macrophages is involved in cholesterol efflux and atherogenesis. *Mol. Cell*, **7**, 161–171.
10. Siersbaek,R., Nielsen,R. and Mandrup,S. (2010) PPARγ in adipocyte differentiation and metabolism - novel insights from genome-wide studies. *FEBS Lett.*, **584**, 3242–3249.
11. Gampe,R.T. Jr., Montana,V.G., Lambert,M.H., Miller,A.B., Bledsoe,R.K., Milburn,M.V., Kliewer,S.A., Willson,T.M. and Xu,H.E. (2000) Asymmetry in the PPARγ/RXRα crystal structure reveals the molecular basis of heterodimerization among nuclear receptors. *Mol. Cell*, **5**, 545–555.
12. Kallenberger,B.C., Love,J.D., Chatterjee,V.K. and Schwabe,J.W. (2003) A dynamic mechanism of nuclear receptor activation and its perturbation in a human disease. *Nat. Struct. Biol.*, **10**, 136–140.
13. Yu,C., Markan,K., Temple,K.A., Deplewski,D., Brady,M.J. and Cohen,R.N. (2005) The nuclear receptor corepressors NCoR and SMRT decrease peroxisome proliferator-activated receptor gamma transcriptional activity and repress 3T3-L1 adipogenesis. *J. Biol. Chem.*, **280**, 13600–13605.
14. Tontonoz,P., Hu,E., Graves,R.A., Budavari,A.I. and Spiegelman,B.M. (1994) mPPAR gamma 2: tissue-specific regulator of an adipocyte enhancer. *Genes Dev.*, **8**, 1224–1234.
15. Lefterova,M.I., Zhang,Y., Steger,D.J., Schupp,M., Schug,J., Cristancho,A., Feng,D., Zhuo,D., Stoeckert,C.J. Jr., Liu,X.S. *et al.* (2008) PPARγ and C/EBP factors orchestrate adipocyte biology via adjacent binding on a genome-wide scale. *Genes Dev.*, **22**, 2941–2952.
16. Saladin,R., Fajas,L., Dana,S., Halvorsen,Y.D., Auwerx,J. and Briggs,M. (1999) Differential regulation of peroxisome proliferator activated receptor gamma1 (PPARgamma1) and PPARgamma2 messenger RNA expression in the early stages of adipogenesis. *Cell Growth Differ.*, **10**, 43–48.
17. Rosen,E.D., Hsu,C.H., Wang,X., Sakai,S., Freeman,M.W., Gonzalez,F.J. and Spiegelman,B.M. (2002) C/EBPalpha induces adipogenesis through PPARgamma: a unified pathway. *Genes Dev.*, **16**, 22–26.
18. Hottiger,M.O., Hassa,P.O., Luscher,B., Schuler,H. and Koch-Nolte,F. (2010) Toward a unified nomenclature for mammalian ADP-ribosyltransferases. *Trends Biochem. Sci.*, **35**, 208–219.
19. Vyas,S., Matic,I., Uchima,L., Rood,J., Zaja,R., Hay,R.T., Ahel,I. and Chang,P. (2014) Family-wide analysis of poly(ADP-ribose) polymerase activity. *Nat. Commun.*, **5**, 4426.
20. Hassa,P.O. and Hottiger,M.O. (2008) The diverse biological roles of mammalian PARPs, a small but powerful family of poly-ADP-ribose polymerases. *Front. Biosci.*, **13**, 3046–3082.
21. Graziani,G. and Szabo,C. (2005) Clinical perspectives of PARP inhibitors. *Pharmacol. Res.*, **52**, 109–118.
22. Underhill,C., Toulmonde,M. and Bonnefoi,H. (2011) A review of PARP inhibitors: from bench to bedside. *Ann. Oncol.*, **22**, 268–279.
23. Wahlberg,E., Karlberg,T., Kouznetsova,E., Markova,N., Macchiarulo,A., Thorsell,A.G., Pol,E., Frostell,A., Ekblad,T., Oncu,D. *et al.* (2012) Family-wide chemical profiling and structural analysis of PARP and tankyrase inhibitors. *Nat. Biotechnol.*, **30**, 283–288.
24. Erener,S., Hesse,M., Kostadinova,R. and Hottiger,M.O. (2012) Poly(ADP-ribose)polymerase-1 (PARP1) controls adipogenic gene expression and adipocyte function. *Mol. Endocrinol.*, **26**, 79–86.
25. Erener,S., Mirsaidi,A., Hesse,M., Tiaden,A.N., Ellingsgaard,H., Kostadinova,R., Donath,M.Y., Richards,P.J. and Hottiger,M.O. (2012) ARTD1 deletion causes increased hepatic lipid accumulation in mice fed a high-fat diet and impairs adipocyte function and differentiation. *FASEB J.*, **26**, 2631–2638.
26. Pirinen,E., Canto,C., Jo,Y.S., Morato,L., Zhang,H., Menzies,K.J., Williams,E.G., Mouchiroud,L., Moullan,N., Hagberg,C. *et al.* (2014) Pharmacological Inhibition of poly(ADP-ribose) polymerases improves fitness and mitochondrial function in skeletal muscle. *Cell Metab.*, **19**, 1034–1041.
27. Santoro,R., Li,J. and Grummt,I. (2002) The nucleolar remodeling complex NoRC mediates heterochromatin formation and silencing of ribosomal gene transcription. *Nat. Genet.*, **32**, 393–396.
28. Bai,P. and Canto,C. (2012) The role of PARP-1 and PARP-2 enzymes in metabolic regulation and disease. *Cell Metab.*, **16**, 290–295.
29. Bai,P., Houten,S.M., Huber,A., Schreiber,V., Watanabe,M., Kiss,B., de Murcia,G., Auwerx,J. and Menissier-de Murcia,J. (2007) Poly(ADP-ribose) polymerase-2 [corrected] controls adipocyte differentiation and adipose tissue function through the regulation of the activity of the retinoid X receptor/peroxisome proliferator-activated receptor-gamma [corrected] heterodimer. *J. Biol. Chem.*, **282**, 37738–37746.
30. Skurk,T., Alberti-Huber,C., Herder,C. and Hauner,H. (2007) Relationship between adipocyte size and adipokine expression and secretion. *J. Clin. Endocrinol. Metab.*, **92**, 1023–1033.
31. Després,J.-P. and Lemieux,I. (2006) Abdominal obesity and metabolic syndrome. *Nature*, **444**, 881–887.
32. Ntambi,J.M. and Young-Cheul,K. (2000) Adipocyte differentiation and gene expression. *J. Nutr.*, **130**, 3122S–3126S.
33. Picard,F., Kurtev,M., Chung,N., Topark-Ngarm,A., Senawong,T., Machado De Oliveira,R., Leid,M., McBurney,M.W. and Guarente,L. (2004) Sirt1 promotes fat mobilization in white adipocytes by repressing PPAR-gamma. *Nature*, **429**, 771–776.
34. Shieh,W., Amé,J., Wilson,M., Wang,Z., Koh,D., Jacobson,M. and Jacobson,E. (1998) Poly(ADP-ribose) polymerase null mouse cells synthesize ADP-ribose polymers. *J. Biol. Chem.*, **273**, 30069–30072.
35. Tee,M.K., Rogatsky,I., Tzagarakis-Foster,C., Cvoro,A., An,J., Christy,R.J., Yamamoto,K.R. and Leitman,D.C. (2004) Estradiol and selective estrogen receptor modulators differentially regulate target genes with estrogen receptors alpha and beta. *Mol. Biol. Cell*, **15**, 1262–1272.
36. Gelman,L., Zhou,G., Fajas,L., Raspe,E., Fruchart,J.C. and Auwerx,J. (1999) p300 interacts with the N- and C-terminal part of PPARgamma2 in a ligand-independent and -dependent manner, respectively. *J. Biol. Chem.*, **274**, 7681–7688.
37. Lee,J.W., Lee,Y.C., Na,S.Y., Jung,D.J. and Lee,S.K. (2001) Transcriptional coregulators of the nuclear receptor superfamily: coactivators and corepressors. *Cell. Mol. Life Sci.*, **58**, 289–297.
38. Rosenfeld,M., Lunyak,V. and Glass,C. (2006) Sensors and signals: a coactivator/corepressor/epigenetic code for integrating signal-dependent programs of transcriptional response. *Genes Dev.*, **20**, 1405–1428.
39. Rosen,E.D., Walkey,C.J., Puigserver,P. and Spiegelman,B.M. (2000) Transcriptional regulation of adipogenesis. *Genes Dev.*, **14**, 1293–1307.

40. Ju,B.-G., Lunyak,V., Perissi,V., Garcia-Bassets,I., Rose,D., Glass,C. and Rosenfeld,M. (2006) A topoisomerase IIbeta-mediated dsDNA break required for regulated transcription. *Science*, **312**, 1798–1802.
41. Nitiss,J.L. (2009) DNA topoisomerase II and its growing repertoire of biological functions. *Nat. Rev. Cancer*, **9**, 327–337.
42. Tzameli,I., Fang,H., Ollero,M., Shi,H., Hamm,J.K., Kievit,P., Hollenberg,A.N. and Flier,J.S. (2004) Regulated production of a peroxisome proliferator-activated receptor-gamma ligand during an early phase of adipocyte differentiation in 3T3-L1 adipocytes. *J. Biol. Chem.*, **279**, 36093–36102.
43. Forman,B.M., Chen,J. and Evans,R.M. (1997) Hypolipidemic drugs, polyunsaturated fatty acids, and eicosanoids are ligands for peroxisome proliferator-activated receptors alpha and delta. *Proc. Natl. Acad. Sci. U.S.A.*, **94**, 4312–4317.
44. Keller,H., Dreyer,C., Medin,J., Mahfoudi,A., Ozato,K. and Wahli,W. (1993) Fatty acids and retinoids control lipid metabolism through activation of peroxisome proliferator-activated receptor-retinoid X receptor heterodimers. *Proc. Natl. Acad. Sci. U.S.A.*, **90**, 2160–2164.
45. Kliewer,S.A., Sundseth,S.S., Jones,S.A., Brown,P.J., Wisely,G.B., Koble,C.S., Devchand,P., Wahli,W., Willson,T.M., Lenhard,J.M. *et al.* (1997) Fatty acids and eicosanoids regulate gene expression through direct interactions with peroxisome proliferator-activated receptors alpha and gamma. *Proc. Natl. Acad. Sci. U.S.A.*, **94**, 4318–4323.
46. Krey,G., Braissant,O., L'Horset,F., Kalkhoven,E., Perroud,M., Parker,M.G. and Wahli,W. (1997) Fatty acids, eicosanoids, and hypolipidemic agents identified as ligands of peroxisome proliferator-activated receptors by coactivator-dependent receptor ligand assay. *Mol. Endocrinol.*, **11**, 779–791.
47. Houseknecht,K.L., Cole,B.M. and Steele,P.J. (2002) Peroxisome proliferator-activated receptor gamma (PPARγ) and its ligands: a review. *Domest. Anim. Endocrinol.*, **22**, 1–23.
48. Huang,D., Yang,C., Wang,Y., Liao,Y. and Huang,K. (2009) PARP-1 suppresses adiponectin expression through poly(ADP-ribosyl)ation of PPAR gamma in cardiac fibroblasts. *Cardiovasc. Res.*, **81**, 98–107.
49. Bourguet,W., Germain,P. and Gronemeyer,H. (2000) Nuclear receptor ligand-binding domains: three-dimensional structures, molecular interactions and pharmacological implications. *Trends Pharmacol. Sci.*, **21**, 381–388.
50. Li,P., Fan,W., Xu,J., Lu,M., Yamamoto,H., Auwerx,J., Sears,D.D., Talukdar,S., Oh,D., Chen,A. *et al.* (2011) Adipocyte NCoR knockout decreases PPARgamma phosphorylation and enhances PPARgamma activity and insulin sensitivity. *Cell*, **147**, 815–826.
51. Hassa,P.O., Buerki,C., Lombardi,C., Imhof,R. and Hottiger,M.O. (2003) Transcriptional coactivation of nuclear factor-κB-dependent gene expression by p300 is regulated by poly(ADP)-ribose polymerase-1. *J. Biol. Chem.*, **278**, 45145–45153.
52. Tulin,A. and Spradling,A. (2003) Chromatin loosening by poly(ADP)-ribose polymerase (PARP) at Drosophila puff loci. *Science*, **299**, 560–562.
53. Ju,B.-G., Solum,D., Song,E., Lee,K.-J., Rose,D., Glass,C. and Rosenfeld,M. (2004) Activating the PARP-1 sensor component of the groucho/ TLE1 corepressor complex mediates a CaMKinase IIdelta-dependent neurogenic gene activation pathway. *Cell*, **119**, 815–829.
54. Ju,B.-G. and Rosenfeld,M. (2006) A breaking strategy for topoisomerase IIbeta/PARP-1-dependent regulated transcription. *Cell Cycle*, **5**, 2557–2560.
55. Straus,D.S. and Glass,C.K. (2007) Anti-inflammatory actions of PPAR ligands: new insights on cellular and molecular mechanisms. *Trends Immunol.*, **28**, 551–558.
56. Li,P., Spann,N.J., Kaikkonen,M.U., Lu,M., Oh da,Y., Fox,J.N., Bandyopadhyay,G., Talukdar,S., Xu,J., Lagakos,W.S. *et al.* (2013) NCoR repression of LXRs restricts macrophage biosynthesis of insulin-sensitizing omega 3 fatty acids. *Cell*, **155**, 200–214.
57. Rodriguez,A., Catalan,V., Gomez-Ambrosi,J. and Fruhbeck,G. (2007) Visceral and subcutaneous adiposity: are both potential therapeutic targets for tackling the metabolic syndrome? *Curr. Pharm. Des.*, **13**, 2169–2175.

www.nature.com/scientificreports

SCIENTIFIC REPORTS

OPEN

ARTD1 regulates osteoclastogenesis and bone homeostasis by dampening NF-κB-dependent transcription of *IL-1β*

Received: 06 October 2015
Accepted: 18 January 2016
Published: 17 February 2016

Agnieszka Robaszkiewicz[1,2], Chao Qu[3], Ewelina Wisnik[2], Tomasz Ploszaj[4], Ali Mirsaidi[5], Friedrich A. Kunze[1,6], Peter J. Richards[5], Paolo Cinelli[7], Gabriel Mbalaviele[3] & Michael O. Hottiger[1,5]

While ADP-ribosyltransferase diphtheria toxin-like 1 (ARTD1, formerly PARP1) and its enzymatic activity have been shown to be important for reprogramming and differentiation of cells, such as during adipogenesis, their role and mechanism in regulating osteoclastogenesis and bone homeostasis are largely unknown. Here, in cell culture-based RANKL-induced osteoclastogenesis models, we show that silencing of ARTD1 or inhibition of its enzymatic activity enhances osteoclast differentiation and function. As a consequence of ARTD1 silencing or inhibition, the recruitment of p65/RelA to the *IL-1β* promoter, which is associated with transcriptionally active histone marks, *IL-1β* expression and inflammasome-dependent secretion of IL-1β are enhanced. This subsequently promotes sustained induction of the transcription factor *Nfatc1*/A and osteoclastogenesis in an autocrine manner via the IL-1 receptor. *In vivo*, *Artd1*-deficient mice display significantly decreased bone mass as a consequence of increased osteoclast differentiation. Accordingly, the expression of osteoclast markers is enhanced in mutant compared to wild-type mice. Together, these results indicate that ARTD1 controls osteoclast development and bone remodelling via its enzymatic activity by modulating the epigenetic marks surrounding the *IL-1β* promoter and expression of *IL-1β* and subsequently also *Nfatc1*/A.

ADP-ribosyltransferase diphtheria toxin-like 1 (ARTD1, formerly called PARP1) belongs to the family of ADP-ribosyltransferases (ARTs) and utilizes NAD^+ for the synthesis of ADP-ribose polymers on acceptor proteins. The human ARTD family consists of 18 proteins with either mono- or poly-ADP-ribosyltransferase activity that all share the same ARTD signature motif in their homologous catalytic domain. Several inhibitors have been developed that inhibit ARTD1 activity, but also other ARTD family members, because of their similarity and because they mostly mimic β-NAD^+ [1]. Since the discovery of ARTD1, most studies have focused on its role in DNA damage detection and repair responses[2]. However, over the past decade, ARTD1 has gained increasing attention for its role in gene regulation[3–7]. Previous studies have shown that ARTD1 is the now long forgotten RNA polymerase II basal transcription factor TFIIC, which represses nick-dependent transcription in biochemical assays[8]. The positive or negative impact of ARTD1 on gene expression results primarily from its cooperation with transcription factors such as NF-κB, and chromatin remodelling and modification[9].

Accumulating data are now linking ARTD1 activity with cell differentiation and cell fate commitment. The change from preadipocytes to adipocytes triggered by the nuclear receptor PPARγ is a prime example of the role of nuclear ADP-ribosylation reactions in cellular differentiation. ARTD1-dependent PAR formation increases

[1]Department of Molecular Mechanisms of Disease, University of Zurich, 8057 Zurich, Switzerland. [2]Department of Environmental Pollution Biophysics, University of Lodz, Pomorska 141/143, 90-236 Lodz, Poland. [3]Division of Bone and Mineral Diseases, Washington University School of Medicine, 660 South Euclid Avenue, Campus Box 8301, St. Louis, MO 63110. [4]Department of Molecular Biology, Medical University of Lodz, Narutowicza 60, 90-136 Lodz, Poland. [5]Competence Centre for Applied Biotechnology and Molecular Medicine, University of Zurich, 8057 Zurich, Switzerland. [6]Life Science Zurich Graduate School, Molecular Life Science Program, University of Zurich, 8057 Zurich, Switzerland. [7]Division of Trauma Surgery, Center for Clinical Research, University Hospital Zurich, 8091 Zurich, Switzerland. Correspondence and requests for materials should be addressed to M.O.H. (email: michael.hottiger@dmmd.uzh.ch)

during differentiation of 3T3L1 preadipocytes and is required for sustained expression of PPARγ target genes[10]. Similarly, adipogenic differentiation is reduced in adipose-derived stromal cells isolated from *Artd1* knockout mice[11]. This function of ARTD1 is specific for adipogenesis, as osteogenic differentiation of adipose-derived stromal cells is not affected by *Artd1* deletion[10,11]. A recent study has shown that the methylcytosine dioxygenase ten-eleven translocation 1 (TET1) interacts with PPARγ in an ADP-ribosylation-dependent manner during adipogenesis[12], suggesting a model of active, PAR-dependent DNA demethylation of key adipocyte-specific genes by TET1[12]. Moreover, ADP-ribosylation positively regulates TET1 expression by maintaining a permissive chromatin state at the gene locus.

Bone is a highly dynamic tissue that undergoes continuous remodelling, being dependent on an intricate array of factors, including cytokines/chemokines, hormones, and mechanical stimuli[13,14]. Normal bone turnover is maintained through the coordinated actions of osteoblasts and osteoclasts on bone formation and resorption respectively[15]. While osteoblasts develop from mesenchymal stem cells, osteoclasts are of myeloid origin[16]. The differentiation of osteoclast precursors (monocytes/macrophages) into fully functional osteoclasts depends on the stimulation of the receptor activator of nuclear factor kappa-B (NF-κB) (RANK) by its ligand (RANKL) and comprises of several steps: fate commitment, early phase multinucleation and late phase fusion with other committed cells, which finally gives rise to the large and functionally active bone-resorbing cells[17].

At the molecular level, RANKL stimulation triggers the induction of the NF-κB heterodimer p65 (RelA)/p50 (NF-κB1), which induces the expression of nuclear factor of activated T-cells (*NFATc1*), a transcription factor that regulates the terminal RANKL-induced differentiation of osteoclasts[18]. NFATc1 drives the formation of bone-resorbing cells and regulates expression of osteoclast-specific genes such as that of cathepsin K (*Ctsk*) and tartrate-resistant acid phosphatase (*Tracp*)[18]. In addition, the RANKL-induced NF-κB pathway controls the transcription of a wide range of pro-inflammatory cytokines, chemokines and growth factors[19]. Some of these cytokines such as TNFα, IL-1, IL-17, IL-4, and IFNs have been well documented to modulate the maturation of functionally active osteoclasts in an autocrine feedback loop[20,21].

Two recent papers have shown that ARTD1 promotes osteoblast differentiation of mesenchymal stem cells *in vitro*, suggesting a possible involvement of ARTD1 in bone remodelling[22,23]. Furthermore, ARTD1 has also been reported to repress the gene expression of bone-resorbing factors such as *Tracp* and the a3 isoform of V-ATPase subunit (*Tcirg1*) during RANKL-induced osteoclastogenesis[24,25], suggesting that ARTD1 might also regulate osteoclastogenesis and thereby bone remodelling, although the detailed molecular mechanism by which ARTD1 is thought to regulate osteoclastogenesis and bone formation is unknown.

These findings and our observation that ARTD1 is a co-factor of NF-κB-dependent gene expression prompted us to elucidate the molecular mechanisms responsible for the involvement of ARTD1 in osteoclastogenesis and bone homeostasis. Here, we report that silencing or inhibition of *Artd1* epigenetically enhances RANKL-induced and NF-κB-dependent expression of *IL-1β* that subsequently drives *NFATc1*-dependent osteoclastogenesis. The epigenetic regulation of *IL-1β* expression strongly depends on the enzymatic activity of ARTD1. Furthermore, *Artd1*-deficiency impairs bone mass, which is likely due to alterations in osteoclastogenesis.

Results

ARTD1 activity represses RANKL-induced osteoclast differentiation. To study the role of ARTD1 in osteoclastogenesis, RAW 264.7 macrophage-derived cells that overexpress an shRNA by retroviral transduction against a control sequence (shMock) or against *Artd1* (shARTD1) (Suppl. Fig. 1A,B) were stimulated with RANKL and allowed to differentiate into osteoclasts (see Suppl. Fig. 1C for overall experimental design). As expected, early multinucleation was observed in RAW 264.7 cells expressing shMock on day 2 (D2) after RANKL administration, and osteoclast expansion on day 3 (D3) (Suppl. Fig. 1C). Remarkably, silencing of *Artd1* in RAW 264.7 cells strongly enhanced the RANKL-induced number of multinucleated cells when compared to RANKL-stimulated shMOCK-expressing RAW 264.7 cells (Fig. 1A), indicating that ARTD1 represses osteoclastogenesis. The same experiment with stable knockdown of *p65* expression in RAW 264.7 cells caused reduced matrix dissolution and multinucleation (Suppl. Fig. 1 A,B,D), confirming the NF-κB-dependency of the system. An even more prominent effect of ARTD1 was found between RANKL-stimulated bone marrow-derived macrophages (BMDM) isolated from WT mice compared to *Artd1*-deficient (−/−) mice (Fig. 1B), confirming the results obtained with the engineered RAW 264.7 cells. RANKL treatment of shMock RAW 264.7 macrophages was associated with an induction of PAR formation on day 2 and 3 of differentiation (early development), which was inhibited by co-treatment of the cells with the ADP-ribosylation inhibitor olaparib (Fig. 1C). The presence of olaparib for the entire duration of osteoclast differentiation using shMOCK RAW 264.7 cells or WT BMDM phenocopied the enhanced multinucleation observed in RANKL-stimulated shARTD1-treated or *Artd1* (−/−) macrophages (*cf.* Fig. 1A,B), indicating that ADP-ribosylation is important for repressing osteoclastogenesis. Since inhibition with olaparib did not further increase multinucleation in ARTD1-depleted or -deficient cells (Fig. 1A,B), the effect of olaparib on ARTD1-proficient cells was likely primarily due to inhibition of ARTD1. Multinucleated osteoclasts derived from *Artd1*-silenced or olaparib-treated RAW 264.7 macrophages were fully functional, as demonstrated by the dissolution of a mineral-coated surface (Fig. 1D, Suppl. Fig. 1E). At the molecular level, *Artd1* silencing or inhibition led to increased expression of the osteoclast marker gene *Nfatc1/A* (but not *Nfatc1/B* or *C*) (Fig. 1E), as well as increased TRAP enzymatic activity (Fig. 1F) 72 h after RANKL stimulation of RAW 264.7 macrophages, while transcription of *Ctsk* and *Tracp* was only affected by ARTD1 silencing and not inhibition.

To test at which time point during RANKL-induced multinucleation ARTD1 and its enzymatic activity are important, multinucleation was induced with RANKL for 48 (Fig. 1G) or 72 h (Suppl. Fig. 2A) and olaparib added at different time points following RANKL-treatment. A significant increase in multinucleation could be observed when olaparib was added in both settings from the beginning (48 h and 72 h, respectively) or for at least 24 h after RANKL treatment (24 h and 48 h respectively), while supplementation for a shorter time did not enhance

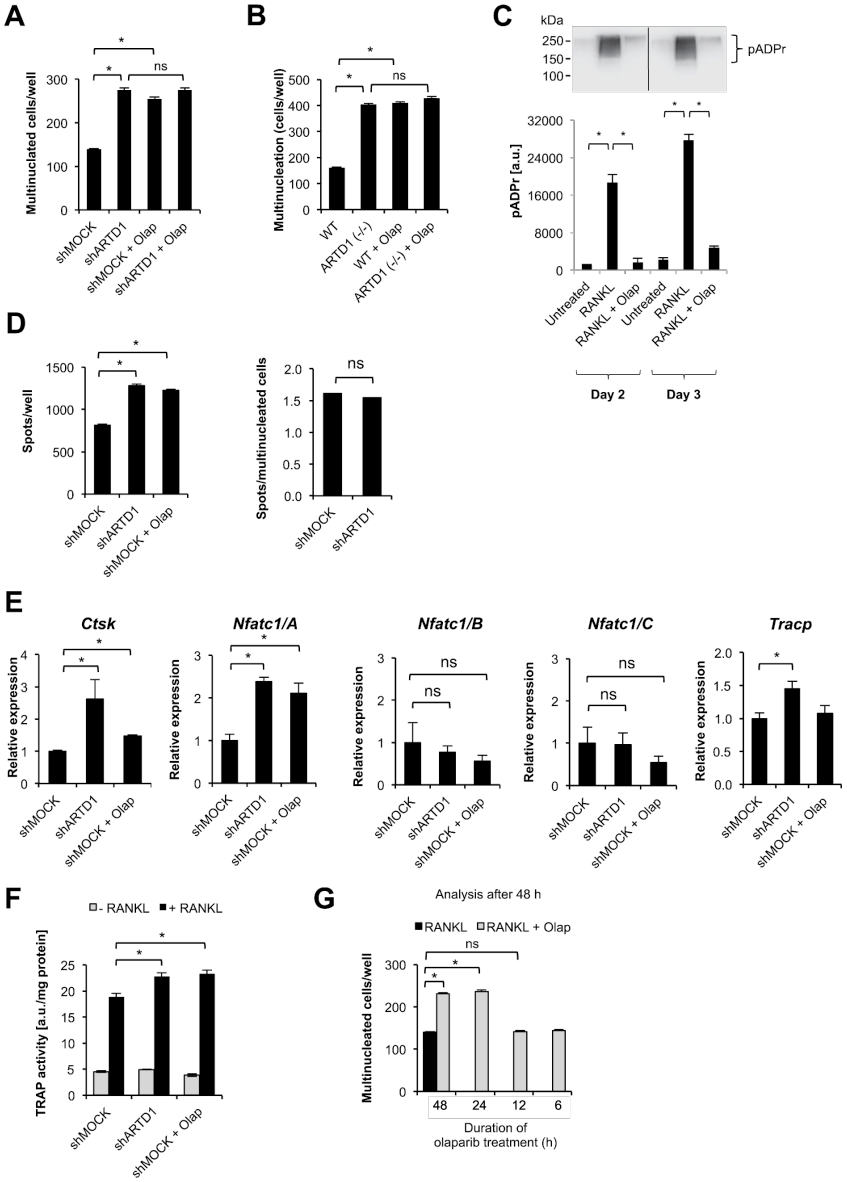

Figure 1. ARTD1 silencing or inhibition enhances osteoclast differentiation. The multinucleation capacity of (**A**) RAW264.7 macrophages expressing basal levels of *Artd1* (shMOCK) and *Artd1* knock-down (shARTD1), as well as of (**B**) bone marrow-derived macrophages (BMDM) isolated from wild-type (WT) and *Artd1*-deficient mice was quantified 48 h after RANKL (50 ng/ml) administration. The ADP-ribosylation inhibitor olaparib (1 μM) was added to shMOCK and WT BMDM cell cultures simultaneously with RANKL

and was present throughout the course of differentiation. (**C**) The accumulation of ADP-ribosylated proteins in untreated BMDM (osteoclast precursors) and in 2 and 3 day old osteoclasts differentiated in the presence and absence of olaparib was studied with western blot. Densitometry was employed for quantification of ADP-ribosylation. (**D**) The resorbing activity of osteoclasts differentiated for 72 h in the presence of RANKL from RAW 264.7 cells with silenced and inhibited ARTD1 were determined based on matrix dissolution (left panel). The number of matrix dissolution spots was normalized to the number of multinucleated cells (right panel). (**E**) The gene expression of osteoclast markers was analysed in purified RAW 264.7-derived 3-day-old osteoclasts. (**F**) TRAP activity was quantified in RAW264.7 cells differentiated in the presence of RANKL for 48 h. (**G**) Olaparib was administered at selected time points after induction of osteoclastogenesis, and multinucleated cells were counted after 48 h.

multinucleation, suggesting that ARTD1 and its enzymatic activity enhance osteoclastogenesis during the time period between 24 and 48 h of differentiation, and not during the initial RANKL signalling (i.e. the first 24 h after RANKL treatment).

Together, these results demonstrate that ARTD1 and its enzymatic activity regulate RANKL-induced multinucleation and expression of the osteoclast differentiation driver NFATc1/A after initiation of the differentiation process and that the enhanced differentiated osteoclasts are fully functional.

ARTD1 activity is induced during osteoclast differentiation in a topoisomerase II-dependent manner. Since our data indicated that the enzymatic activity of ARTD1 regulates osteoclastogenesis, we next investigated the mechanism by which the enzymatic activity of ARTD1 is induced. Since ROS have been described to strongly activate ARTD1[26], we investigated whether the presence of the potent ROS scavenger N-acetylcysteine affect the differentiation potential of differentiating osteoclasts. However, no significant effects of N-acetylcysteine on cell multinucleation were observed at the concentration tested (Suppl. Fig. 3A). We have recently provided evidence that activation of ARTD1 and PAR formation during adipogenesis is dependent on topoisomerase II (topo II) activity[27]. Interestingly, treatment of RAW 264.7 cells during osteoclastogenesis with the topo II inhibitor merbarone enhanced multinucleation to the same level as observed with *Artd1* silencing (Suppl. Fig. 3B), suggesting that the observed ARTD1-mediated repression of cell multinucleation is regulated by topo II. The same observation was made with osteoclast progenitors from WT and *Artd1* (−/−) mice. Treatment of progenitors with merbarone enhanced osteoclastogenesis in WT but not *Artd1* (−/−) cells, suggesting that indeed topoisomerase activity induces ARTD1 activity, which subsequently represses osteoclastogenesis (Suppl. Fig. 3C).

ARTD1 silencing or inhibition enhances osteoclastogenesis by stimulating IL-1β secretion and autocrine cell stimulation. As autocrine or paracrine acting cytokines are known to regulate the differentiation of osteoclasts, we investigated whether ARTD1 controls osteoclastogensis via a secreted cytokine. Cultivation of RANKL-treated RAW264.7 macrophages with conditioned medium of either shARTD1 or olaparib-treated shMOCK, but not shMOCK osteoclasts, increased the multinucleation of RAW 264.7 macrophages through a secreted factor (Fig. 2A). Since IL-1β plays a major role in bone metabolism under physiological conditions[28,29], we tested whether IL-1β could be involved in the enhanced multinucleation induced by ARTD1 depletion, inhibition or deficiency. Repeated addition of IL-1β neutralizing antibody to medium (every 8 h) from RANKL-induced *Artd1*-silenced or inhibited RAW 264.7 macrophages, as well as *Artd1* (−/−) BMDM substantially reduced the ability of the medium to enhance multinucleation of RANKL-treated RAW264.7 macrophages (Fig. 2B), indicating that IL-1β is indeed the secreted factor responsible for the observed enhanced multinucleation of *Artd1* (−/−), knock-downs or olaparib-treated cells. The transient silencing of *IL-1 receptor 1* (*IL-1r1*) in shMOCK or shARTD1 macrophages phenocopied the effect of IL-1β neutralizing antibody on the differentiation potential of macrophages (Fig. 2C, Suppl. Fig. 3D), further supporting the idea that the observed effect is mediated by IL-1β. Differentiation of RAW 264.7 and BMDM with a mixture of RANKL and recombinant IL-1β (10 ng/ml every 8 h[30]) led to an increase in the number of osteoclasts formed comparable to the level of RANKL-stimulated shARTD1-treated and *Artd1*-deficient macrophages, respectively (Fig. 2D). To further strengthen the importance of IL-1β in RANKL-induced osteoclastogenesis during the initial/sustained phase of osteoclastogenesis, shMOCK RAW264.7 macrophages were treated with either RANKL alone or RANKL together with IL-1β for different periods of times. RANKL alone was able to induce multinucleation only when added for at least 48 h, but not for a shorter time period (Fig. 2E). Addition of IL-1β at different time points to 48 h RANKL-treated macrophages significantly enhanced multinucleation for all tested time points, but 6 h of IL-1β (Fig. 2E), although analysis of the multinucleation for this sample after an additional 24 h (72 h after RANKL) also revealed significantly enhanced multinucleation (Suppl. Fig. 2B), suggesting that IL-1β is able to enhance RANKL-induced multinucleation throughout the analysed osteoclastogenesis, but required at least 12 h of incubation. Interestingly, the contribution of IL-1β to osteoclast formation was not limited to enhancement of multinucleation, since after a certain stage of osteoclast commitment (between 6 and 12 h after RANKL stimulation) and subsequent removal of RANKL, IL-1β drove osteoclast differentiation even in the absence of RANKL (Fig. 2F), indicating that IL-1β is important for sustaining osteoclastogenesis, once RANKL has initiated the differentiation process.

Inflammasome activity is required for IL-1β secretion, and subsequent expression of the osteoclastogenic transcription factor NFATc1/A. Caspase-1 is a subunit of the inflammasome complex, which cleaves pro-IL-1β, thereby causing the release of the active cytokine. We thus tested whether the pan-caspase inhibitor Z-VAD-fmk prevents the enhanced osteoclast formation observed in *Artd1*-silenced RAW 264.7 and

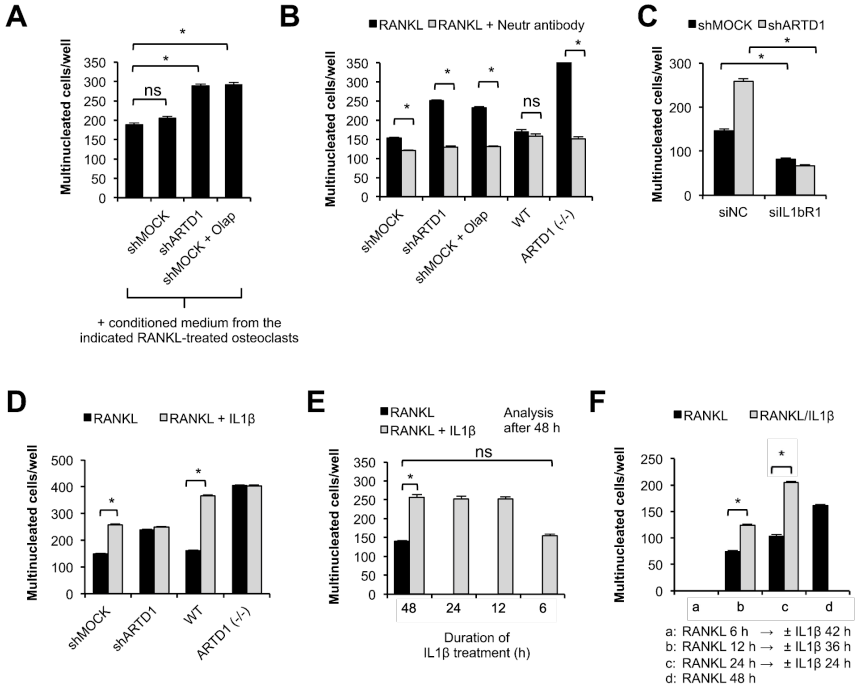

Figure 2. Inhibition of ADP-ribosylation as well as *Artd1* knock-out and knock-down are responsible for *IL-1β* overexpression-induced increase in osteoclast differentiation. (**A**) The pro-osteoclastogenic potential of media conditioned for 24 h by 3-day-old osteoclasts derived from RAW264.7 macrophages with normal ARTD1 levels as well as ARTD1 silenced and inhibited cells was compared. RANKL was added to the cell culture in combination with 30% conditioned medium and multinucleation was quantified after 48 h. (**B**) IL-1β neutralizing antibody (100 ng) was added every 8 h to RAW 264.7 and BMDM induced with RANKL for differentiation. (**C**) 24 h after transfection of shMOCK and shARTD1 RAW 264.7 macrophages with siRNA targeting IL-1β receptor 1 (*IL-1r1*) expression, cells were supplemented with RANKL and the role of IL-1R1 in the differentiation process was determined based on multinucleation. (**D**) To test the impact of IL-1β on osteoclastogenesis, RANKL was added to RAW 264.7 and BMDM cultured in the presence or absence of IL-1β (10 ng/ml) and the number of osteoclasts was counted on day 2. (**E**) IL-1β (2 ng/ml) was added at the indicated time points to shMOCK RAW 264.7 macrophages cultured in the presence of RANKL, and multinucleated cells were quantified 48 h after RANKL administration. (**F**) shMOCK RAW 264.7 macrophages were stimulated with RANKL for the indicated periods of time. RANKL was then washed away and the differentiation was allowed to continue for a total time of 48 h in the presence (grey bars) or absence (black bars) of IL-1β (10 ng/ml).

Artd1-deficient BMDM (Fig. 3A). Indeed, Z-VAD-fmk added to the cell culture together with RANKL reduced the number of shARTD1-treated or *Artd1*-deficient osteoclasts to the level of shMOCK-treated and WT BMDM treated with caspase inhibitor, similar to the effect of IL-1β neutralizing antibody, indicating that caspase activity was required for osteoclast differentiation. IL-1β repeatedly added to the culture of differentiating cells was able to overcome the Z-VAD-fmk-induced repression of osteoclast formation (Fig. 3B), suggesting that caspase inhibition prevented processing of IL-1β. BMDM derived from *Casp-1*-deficient mice showed a reduced differentiation potential upon stimulation with RANKL when compared to WT BMDM, and very interestingly, olaparib failed to enhance osteoclast formation from *Casp-1*-deficient BMDM, further confirming that caspase-1 is indispensible for mediating the effect of ARTD1 silencing or inhibition on osteoclastogenesis (Fig. 3C). RANKL-stimulated *Casp-1*-deficient BMDM also expressed *Nfatc1/A, Tracp* and *Ctsk* mRNA to a significantly reduced level, which were not affected by treatment with olaparib (Fig. 3D), further supporting that the inflammasome-induced activation of caspase-1 and subsequent processing of IL-1β is required to enhance osteoclast differentiation due to ARTD1 deficiency or inhibition and stimulate the expression of *Nfatc1/A*.

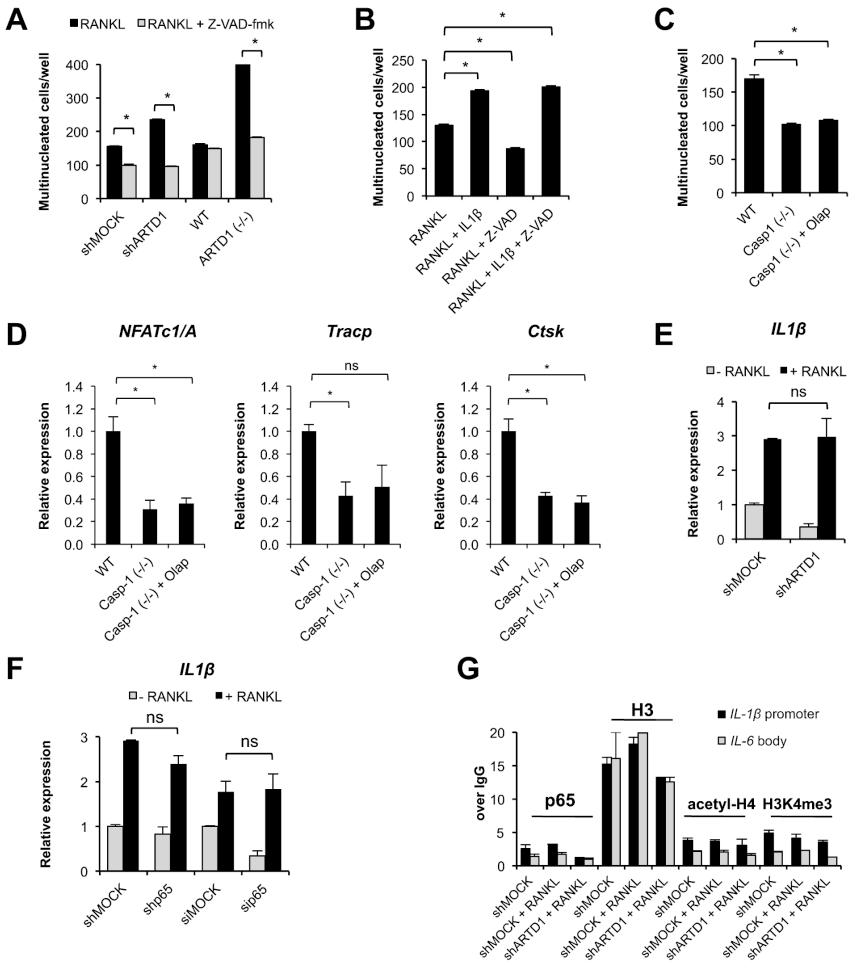

Figure 3. Inhibition of ADP-ribosylation as well as *Artd1* knock-out and knock-down are responsible for enhanced IL-1β expression during osteoclast differentiation. (**A**) The contribution of the inflammasome to osteoclast differentiation was studied by comparing cell multinucleation in RANKL-induced RAW 264.7 macrophage cultures supplemented or not with pan-caspase inhibitor Z-VAD-fmk (10 μM). (**B**) IL-1β (2 ng/ml) was added every 8 h to RANKL-induced RAW 264.7 macrophages (shMOCK) cultured in the presence or absence of Z-VAD-fmk. (**C**) The multinucleation of BMDM isolated from WT or *Casp-1*-deficient mice differentiated in the presence of RANKL and co-treated with olaparib or not for 2 d. (**D**) The expression of osteoclast markers in 3-day-old osteoclasts isolated from the RANKL-induced culture of WT, *Casp-1*-deficient BMDM and *Casp-1*-deficient BMDM incubated with olaparib was compared using real-time PCR. (**E**) *IL-1β* expression was compared between shMOCK and shARTD1 RAW264.7 macrophages stimulated with RANKL for 3 h. (**F**) The expression of *IL-1β* was compared between shMOCK or siMOCK RAW 264.7 macrophages and cells treated with shRNA or siRNA against *p65* after 3 h cell stimulation with RANKL. (**G**) The association of p65 with the promoter of *IL-1β* as well as H3 occupancy, H3K4 trimethylation and H4 acetylation was determined by ChIP in RAW 264.7 macrophages (shMOCK, shARTD1) incubated with RANKL for 1 h.

ARTD1 does not control expression of IL-1β upon initial RANKL signalling. To further elucidate the mechanism underlying the ARTD1 involvement in the regulation of *IL-1β* transcription during the differentiation of osteoclasts, we analysed the expression of *IL-1β* in RAW 264.7 macrophages after initial (3 h) RANKL stimulation (Fig. 3E). Although the level of *IL-1β* mRNA was increased 3 h after RANKL treatment, *Artd1* silencing had no effect on the expression of *IL-1β* in these cells. As the canonical NF-κB pathway is known to promote IL-1β production, we tested whether *IL-1β* expression is regulated by p65 during the initial RANKL-stimulation of RAW 264.7 macrophages. While RANKL stimulation for 3 h triggered *IL-1β* transcription, the level of *IL-1β* mRNA remained the same in shp65/sip65-silenced cells compared to the corresponding shMOCK/siMOCK-treated cells, suggesting that the initial RANKL-induced expression of *IL-1β* in macrophages is independent of the canonical NF-κB pathway (Fig. 3F). ChIP experiments confirmed a lack of p65 recruitment to the *IL-1β* promoter and a lack of chromatin remodelling within this sequence after short-term RANKL treatment (Fig. 3G). Furthermore, silencing of *Artd1* did not influence p65 binding, which agrees with our previous finding that ARTD1 does not regulate *IL-1β* transcription induced by short-term RANKL treatment (Fig. 3E).

ARTD1 limits expression of IL-1β during sustained osteoclastogenesis by reducing NF-κB recruitment to the IL-1β promoter and maintaining a transcriptionally silent chromatin state around the p65-binding site. In contrast to the above described short-term experiments (i.e., the initial RANKL-induced phase), ARTD1 silencing or inhibition significantly augmented *IL-1β* expression after 3 d of RANKL-induced osteoclastogenesis (Fig. 4A), suggesting that RANKL-induced osteoclast differentiation paves the way for ARTD1 to control the regulation of *IL-1β* expression. We also analysed the expression of *IL-1β* in differentiating osteoclast precursors isolated from *Artd1* (−/−) mice, confirming that *IL-1β* expression is indeed significantly upregulated in the absence of ARTD1 (Fig. 4B, left panel). This effect was independent of whether M-CSF was present during the RANKL-induced differentiation or not (Fig. 4B, right panel). To see whether the canonical NF-κB pathway is activated in 3 d differentiated osteoclasts that lack ARTD1, we analysed nuclear translocation of p65 by Western blot analysis. Indeed, p65 was increased in the nuclear extract of day 3 differentiated pre-osteoclasts derived from *Artd1* (−/−) mice compared to their WT counterparts (Fig. 4C). Furthermore, p65 phosphorylation at Ser536 was also enhanced in day 3 differentiated pre-osteoclasts derived from *Artd1* (−/−) mice compared to their WT counterparts (Fig. 4D). Addition of neutralizing IL-1β antibody reversed both the enhanced nuclear translocation of RelA and its phosphorylation at Ser536 in the cells from *Artd1* (−/−) mice (Fig. 4C,D). These results provide strong evidence that the observed enhanced RelA activation is driven by an autocrine (i.e. local) IL-1β loop.

Furthermore, ChIP experiments with ARTD1-silenced or inhibited cells revealed facilitated p65 recruitment to the *IL-1β* promoter in multinucleated cells (Fig. 4E), the eviction of histone H3 (Fig. 4F), as well as trimethylation of histone H3 and acetylation of H4 (Fig. 4G), histone marks of transcriptionally active chromatin. Stable silencing of *p65* resulted in decreased *IL-1β* expression in 3 d differentiated osteoclasts even in the presence of olaparib, indicating that during the sustained phase of differentiation, ARTD1-mediated ADP-ribosylation represses *IL-1β* transcription in osteoclasts in a p65-dependent manner (Fig. 4H). Furthermore, enhanced recruitment of p65 to the *IL-1β* promoter by olaparib treatment was inhibited in cells with stably knocked-down p65 (Fig. 4I). Interestingly, ARTD1 activity, but not the protein itself was required to control expression of *IL-1β*, because olaparib phenocopied the effect of ARTD1 without leading to dissociation of the enzyme from the chromatin (Suppl. Fig. 3F).

To confirm the contribution of canonical NF-κB signalling in the enhanced IL-1β-mediated osteoclast formation after 3 d by *Artd1*-silencing or inhibition, we compared the differentiation capacity between *Artd1* and *p65* single and double knock-downs (Fig. 4J, Suppl. Fig. 3G). The targeting of *Artd1* in shp65 RAW 264.7 macrophages with siRNA did not intensify the differentiation process, whereas silencing of *p65* dramatically reduced the osteoclastogenic potential of shARTD1 RAW 264 macrophages, suggesting that when p65 is knocked-down, ARTD1 does not repress osteoclastogenesis. Moreover, the presence of olaparib in differentiating shp65 osteoclasts had no influence on the differentiation process (Suppl. Fig. 2C). The change in osteoclast differentiation was also not observed in differentiating cells supplemented with conditioned medium from 3-d-old shp65 osteoclasts cultured in the presence or absence of olaparib (Suppl. Fig. 2D), providing further evidence that IL-1β is not released from *p65*-silenced osteoclasts even upon inhibition of ARTD1. Importantly, expression levels of the osteoclast markers *Nfatc1/A* (but not of *Nfatc1/B* and *Nfatc1/C*), *Ctsk* and *Tracp* were all dependent on p65, but remained unchanged after additional olaparib treatment of differentiating *p65*-silenced cells, further supporting that the presence of p65 is also required downstream of ARTD1-regulated *IL-1β* expression (Fig. 4K, Suppl. Fig. 3E).

***Artd1*-deficient mice display a low bone mass phenotype owing to increased osteoclast differentiation.** Our cell culture experiments provided strong evidence that ARTD1 represses the sustained phase of osteoclastogenesis. Mice lacking ARTD1 are thus to be expected to have altered bone structure due to enhanced osteoclast activity. To investigate whether ARTD1 indeed regulates bone homeostasis *in vivo*, long bones of age- and sex-matched wild-type (WT) and *Artd1*-deficient (−/−) mice were collected and analysed by micro-CT and histology. At 8 weeks of age, male *Artd1* (−/−) mice exhibited a significant decrease in bone mass (BV/TV, Fig. 5A,B), along with decreases in bone mineral density (BMD, Fig. 5B), trabecular number (Tb.N) and a significant increase in trabecular spacing (Tb.Sp) (Suppl. Fig. 4A). Also the cortical envelope is osteopenic in *Artd1* (−/−) mice compared to WT littermates (Suppl. Fig. 4B). The abnormal bone phenotype in *Artd1* (−/−) mice is likely due to alterations in osteoclastogenesis, since the number of osteoclasts is significantly increased in mutant mice (Fig. 5C,D) while the number of osteoblasts was comparable between both mouse strains (Suppl. Fig. 4C). To strengthen the notion that the altered trabecular structure is the result of increased osteoclast differentiation, we analysed the expression levels of osteoclast specific gene markers in femurs (Fig. 5E). Indeed, the expression levels of *Tracp, Ctsk*, and *Rank* were all significantly upregulated in the bones of *Artd1* (−/−) mice.

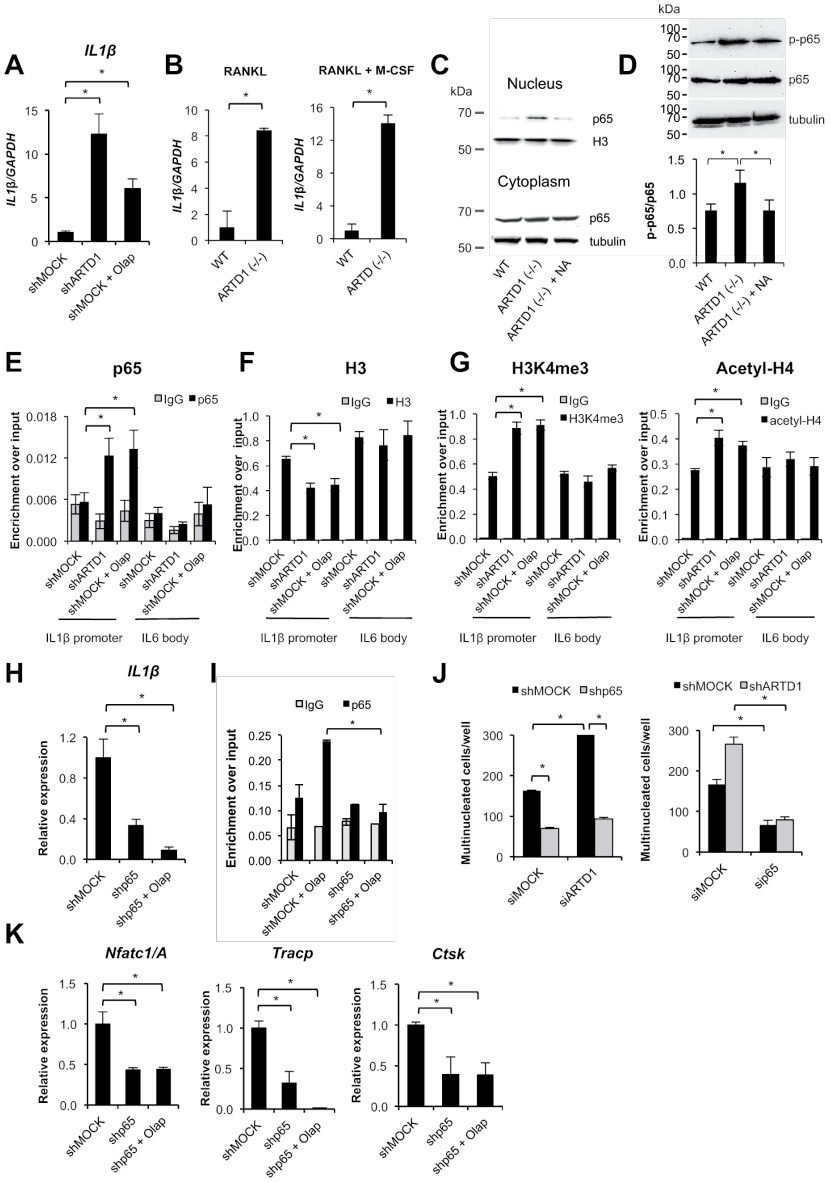

Figure 4. ARTD1 silencing or inhibition of ADP-ribosylation facilitates p65 recruitment to the promoter of *IL-1β* and chromatin remodelling at this site. (**A**) *IL-1β* expression was compared between 3-day-old osteoclasts derived from shMOCK and shARTD1 RAW264.7 macrophages. (**B**) The expression of IL-1β was quantified in 3-day-old osteoclasts derived from WT and *Artd1* (−/−) BMDM by real-time PCR. (**C,D**) The

activation of NF-κB was analysed by measuring nuclear translocation (**C**) and Ser536 phosphorylation (**D**) of p65/RelA in 3-day-old osteoclasts derived from BMDM isolated from WT and *Artd1* (−/−) by western blotting. IL-1β neutralizing antibody (NA) was added to the medium of differentiating *Artd1* (−/−) every 8 h. (**E–G**) The association of p65 with the promoter of *IL-1β* as well as H3 occupancy, H3K4 trimethylation and H4 acetylation was determined by ChIP in RAW 264.7 macrophages-derived osteoclasts differentiated in the presence of RANKL for 72 h. As a negative control, the body of IL6 was used. (**H**) The expression of *IL-1β* was compared between 3-day-old osteoclasts derived from shMOCK and shp65 RAW 264.7 macrophages treated or not with olaparib. (**I**) Recruitment of p65 to the *IL-1β* promoter was assessed in 3-day-old osteoclasts derived from shMOCK and shp65 RAW 264.7 macrophages treated or not with olaparib. (**J**) The multinucleation of double-silenced RAW 264.7 macrophages (left panel: siARTD1/shp65, right panel: sip65/shARTD1) was quantified 48 h after induction of the differentiation with RANKL (72 h after cell transfection with siRNA). (**K**) The expression of osteoclast markers in 3-day-old shMOCK and shp65 (± olaparib) osteoclasts was quantified using real-time PCR.

The expression of the dentin sialophosphoprotein gene *Dspp*, the osteopontin gene *Opn*, and *Nfatc1/A* was also upregulated in *Artd1* (−/−) mice (Fig. 1E), strongly supporting that the observed bone phenotype in *Artd1* (−/−) mice is due to enhanced osteoclast formation.

Discussion

Osteoclast deregulation is associated with several diseases, either through deficient osteoclast function, resulting in osteopetrosis[31], or aberrant hyperactivation, giving rise to generalized bone loss as observed in osteoporosis[32] and rheumatoid arthritis[33]. Moreover, osteoclasts cause bone complications in cancers, including multiple myeloma[34], prostate and breast cancers[35]. Thus, understanding the molecular mechanisms that govern osteoclast differentiation and function is of major importance in the development of more effective therapeutic strategies to combat these diseases. The differentiation of osteoclasts from peripheral blood macrophages in cell culture allows studying osteoclastogenesis in great detail[36]. Our results show that ARTD1 regulates NF-κB-induced *IL-1β* expression in osteoclasts, leading to autocrine regulation of the expression of osteoclast markers (e.g. NFATc1/A). This is achieved through ARTD1's ability to enzymatically alter the epigenetic status of the *IL-1β* promoter during sustained osteoclastogenesis. Thus, ARTD1 through the regulation of *IL-1β* expression has the ability to affect bone homeostasis (Fig. 6).

IL-1β is a multifunctional cytokine that regulates various cellular tissue functions including osteoclastogenesis[37,38]. In our analysis, *IL-1β* was initially induced in a RANKL-dependent but NF-κB-independent manner when tested after 3 h after RANKL treatment. It remains to be investigated, through which signalling cascade and transcription factor the (short term) expression of *IL-1β* is initiated. Besides canonical NF-κB, RANKL binding to its surface receptor also activates non-canonical NF-κB, AP1 and NFATc1[39]. All these factors possess the consensus sequence for the interaction with the *IL-1β* promoter, and may therefore be responsible for the observed expression of this cytokine. Moreover, the lack of promoter responsiveness to RANKL stimulation may be a result of the type of osteoclast precursors employed in this study. Bone marrow-derived macrophages require alternative cell polarization with M-CSF, which directs them toward anti-inflammatory responses, while RAW 234.7 macrophages express surface markers of type 2 macrophages (M2)[39]. Therefore, the differentiation process associated with extensive chromatin dynamics may prime *IL-1β* regulatory elements to effective *IL-1β* transcription, as well as place the ADP-ribosylation process in the centre of *IL-1β* expression regulatory events. In contrast, RANKL treatment for 3 days revealed that ARTD1 fully regulates *IL-1β* expression at this later time point in a NF-κB-independent manner, suggesting that RANKL induces IL-1β, which subsequently, in an autocrine loop (local manner), sustains its expression in an NF-κB- and ARTD1-dependent manner. IL-1β was able to enhance RANKL-induced multinucleation, but its action required at least 12 h of incubation. Interestingly, the contribution of IL-1β to osteoclast formation was not limited to enhancement of multinucleation, since after a certain stage of osteoclast commitment (between 6 and 12 h after RANKL stimulation) and subsequent removal of RANKL, IL-1β drove osteoclast differentiation even in the absence of RANKL.

Under physiological conditions, osteoclastogenesis is thought to be dependent on M-CSF and RANKL. However, IL-1β has been reported to induce osteoclast formation directly from M-CSF-induced osteoclast precursors overexpressing *c-Fos* or *Nfatc1*[40], thus supporting the important function of IL-1β during osteoclastogenesis. Similarly, overexpression of *type 1 IL-1R* in BMDM is sufficient to drive osteoclastogenesis when RANKL is neutralized with a RANK–Fc fusion protein, suggesting that IL-1β can also act independently of RANKL[30,41]. Indeed, our studies indicate that IL-1β is important for sustaining osteoclastogenesis in an autocrine manner by inducing the sustained expression levels of important osteoclast markers such as NFATc1/A. The ARTD inhibitor olaparib did not completely phenocopy the effect of ARTD1 silencing on *Ctsk* and *Tracp,* as it did in the case of *Nfatc1/A*, but rather corresponded to *IL1β* expression, which is more strongly increased in shARTD1 than in shMOCK + Olap. Moreover, expression of these genes in differentiating osteoclasts is controlled by the RANKL–IL1β–p65 axis, as shown in Figs 3D and 4K. Therefore, their transcription is affected indirectly by ARTD1 and the p65–IL1β–p65 autocrine feedback loop. The olaparib-induced increase in *IL1β* expression is sufficient to achieve maximum osteoclast differentiation, although concomitant *Nfatc1/A* transcription might not be sufficient to augment *Tracp* and *Ctsk* expression.

The importance of IL-1β is further underlined by the observation that *IL-1β*-deficient mononuclear cells have a decreased RANKL responsiveness, although the response to TNF-α is maintained[42,43]. Molecular characterization of osteoclast precursors revealed a decreased expression of RANK as the underlying cause for a blunted

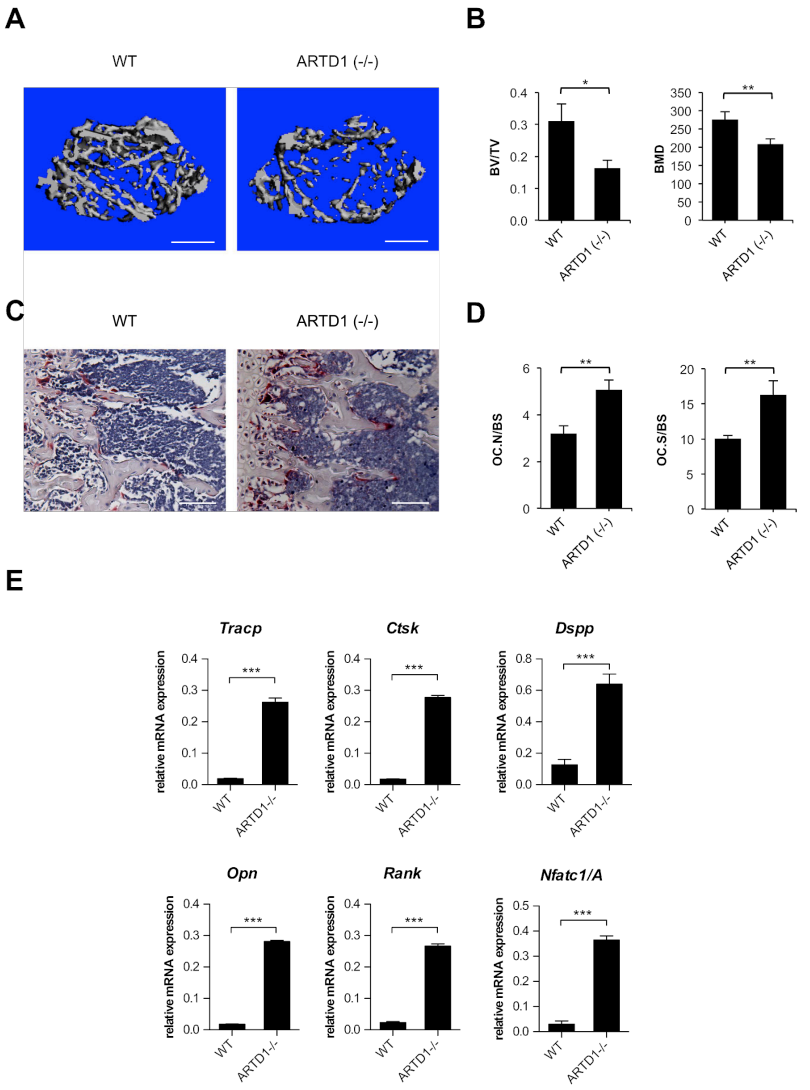

Figure 5. ARTD1 deficiency results in osteopenia and increased osteoclastogenesis. Femurs of 8-week-old *Artd1*-deficient (−/−) mice (n = 4) and their wild-type littermates (n = 4) were analysed by μCT. (**A**) Representative 3D reconstruction. Size bars = 500 μm. (**B**) Bone volume density (BV/TV) and bone mineral density (BMD) were quantified. (**C**) TRAP staining of tibial sections. Size bars = 100 μm. (**D**) Number of osteoclast (stained in red)/bone surface (Oc.N/BS) and osteoclast surface/bone surface (Oc.S/BS) were quantified. Values are mean ± SD. $^{**}p < 0.01$. (**E**) Expression profiles of osteoclastogenic markers were analysed by qRT-PCR of RNA isolated from the proximal tibial epiphysis and part of the diaphysis of wt (n = 4) and *Artd1* (−/−) (n = 5).

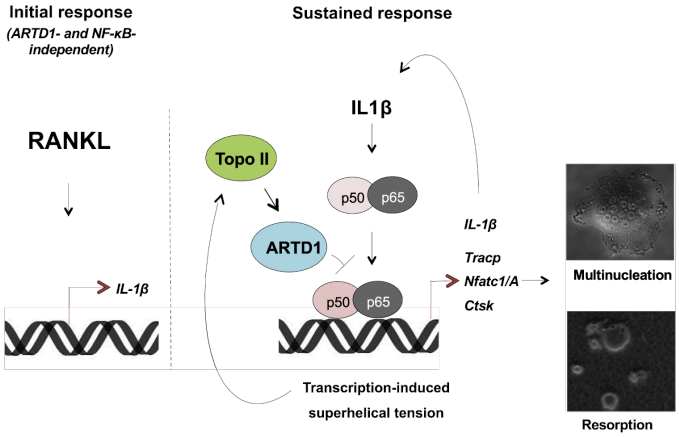

Figure 6. Graphical representation of the functional role of ARTD1 in RANKL-induced osteoclastogenesis.

response of *IL-1β*-deficient cells to RANKL, whereas other surface and functional markers such as c-fms, cathepsin K, TRAP, and MMP9 were similarly expressed.

Since olaparib also inhibits other ARTD family members, we cannot per se exclude that other ARTDs also contribute to osteoclastogensis. However, co-treatment of shARTD1-treated or *Artd1*-deficient cells with RANKL and olaparib did not cause a further increase in the number of osteoclasts developed, strongly suggesting that the inhibitory effect is primarily due to inhibition of the enzymatic activity of ARTD1. Our experiments using the topo II inhibitor merbarone suggest that topo II is responsible for the activation of ARTD1 during IL-1β-induced/sustained osteoclastogenesis, leading to the repression of fully functional osteoclast formation. The differentiation process is accompanied by extensive transcription of genes contributing to conditioning of osteoclast function and phenotype. The transcription machinery requires topo II activity, which may activate ARTD1, placing topo II upstream of ARTD1. A comparable mode of action has already been described for adipogenesis[27], although the actual molecular mechanism remains to be elucidated. However, it is most likely that the enzymatic activity of topo II and the subsequent structural changes of the chromatin contribute to this process. In our *in vitro* model of osteoclast differentiation, topo II serves as a major component of the transcription–differentiation–transcription feedback loop, as transcription-induced DNA gyrase activity represses transcription of osteoclastogenic genes by activating ARTD1. Although investigating topo II recruitment to the *IL-1β* promoters in osteoclasts would be interesting, the lack of suitable antibodies currently prevents this type of analysis.

The impact of ARTD1 on gene expression remains mostly undefined, as its function is cell type-specific and depends e.g. on the local histone variants, interacting partner and ADP-ribosylation acceptor protein, and may therefore differ after differentiation. Moreover, ARTD1 has recently been shown to function in various aspects of the transcription process through a variety of mechanisms, including roles as a modulator of chromatin and a regulator of DNA methylation[4,5]. PARylation of KDM5B, a histone lysine demethylase that acts on H3 lysine 4 trimethyl (H3K4me3), has been shown to block the binding of KDM5B to chromatin and inhibit its demethylase activity[44]. Our results are thus in line with recent data showing that inhibition of the enzymatic activity of ARTD1 regulates the activity of KDM5[44]. It remains to be elucidated whether ARTD1 auto-modification is sufficient to promote these changes, or whether other proteins (histone modifiers or histone themselves) are also modified.

Of note, we cannot preclude that ARTD1 itself acts as a cofactor in the transcription machinery assembled with other transcription factors activated upon RANK stimulation, such as NFATc1 or AP1 independent of its enzymatic activity; however, this requires further analysis. Moreover, our results provide evidence that the inflammasome NOD-like receptor (NLR) family, pyrin domain-containing 3 (NLRP3) is activated upon RANKL stimulation to process pre-IL-1β, which is followed by subsequent secretion of IL-1β, although an inflammasome-independent source of IL-1β has already been described to also provoke inflammation and osteolytic bone disease[45]. Based on our results, inflammasome-dependent IL-1β would signal to the osteoclast in an autocrine manner, which is consistent with previous findings that osteoclasts express IL-1β receptor[46]. Restriction of an activating D301N mutation in Nlrp3 in myeloid cells of mice, induced systemic inflammation and severe osteopenia similar to mice globally expressing the knock-in mutation[47,48]. Mice expressing D301N only in osteoclasts show the same phenotype, due to increased osteolysis, without changing the number of osteoclasts or inducing systemic inflammation. Aside from its role in IL-1β maturation, $Nlrp3^{D301N}$ expression enhances osteoclast bone resorbing ability through reorganization of the actin cytoskeleton, while promoting the degradation

of ARTD1 at the same time. Thus, NLRP3 inflammasome activation is not restricted to the production of pro-inflammatory mediators only, but also leads to intracellular autonomous responses.

Interestingly, analysis of the bones from *Artd1* (−/−) mice showed a severely decreased BV/TV as a result of a decreased bone mineral density (BMD), number of trabeculae (Tb.N) and increased trabecular space (Tb.Sp). The cortical envelope in *Artd1* (−/−) mice was also osteopenic compared to wild-type littermates. Histological analysis of the bone samples by histology revealed the low bone mass phenotype is likely caused by deregulated osteoclastogenesis, since the number of osteoclasts is increased in mutant mice, while that of osteoblasts is unaffected, strongly supporting that the observed bone phenotype in *Artd1* (−/−) mice is due to enhanced osteoclast formation and activity.

Taken together, our results provide important novel insights into the mechanisms underlying the fine-tuning of the transcriptional processes involved in macrophage-to-osteoclast differentiation. Most importantly, ARTD1 and its enzymatic activity repress the expression of osteoclastogenesis-driving genes, including several osteoclast-specific genes through controlling the expression of *IL-1β*. Secondly, our results reinforce the essential function of ARTD1's enzymatic activity for the role of NF-κB as a direct regulator of osteoclast formation. ARTD1 and its enzymatic activity thus keep the detrimental expression of *IL-1β* in osteoclasts in check by altering the chromatin structure and subsequently the accessibility of transcription factors such as NF-κB.

Materials and Methods

Antibodies and reagents. p65/RelA antibody (sc-372), α-tubulin antibody (H-300, sc-5546), and IgG (sc-2027) was from Santa Cruz Biotechnology, PARP1 antibody, histone H3 antibody (D1H2, #4499), and Cell Fractionation Kit (#9038) from Cell Signaling Technology, growth media, FBS, antibiotics, and Lipofectamine RNAiMAX from Life Technologies, IL-1β, IL6, TNFα and Z-VAD-fmk from Sigma Aldrich, H3K4me3 and acetyl-H4 antibody from Millipore, H3 antibody from Abcam, RANKL from Peprotech, siRNA from Qiagen. Corning Osteo Assay plates were from Corning. IL-1β neutralizing antibody was from R&D.

Animals. Male *Artd1*-deficient C57BL/6J mice and aged-matched wild-type littermates were sacrificed at 6 and 8 weeks of age for retrieving bones for BMDM isolation and bone structure analysis, respectively. The *Artd1*-deficient mice were originally kindly provided by Zhao-Qi Wang[49], and all mice were bred at the animal facility of the University of Zurich. We have focused on male C57BL/6J mice, because they exhibit higher bone mass (BV/TV) at baseline than female mice. All animal experiments were carried out in accordance with the Swiss and EU ethical guidelines and have been approved by the local animal experimentation committee of the Canton of Zurich under license #2012207 and following the 3R guidelines.

Isolation of bone marrow-derived macrophages (BMDM). Bone marrow was isolated from femurs and tibiae of 6-week-old male mice and after lysis of erythrocytes, cells were cultivated for one week in RPMI supplemented with 10% heat inactivated FBS, antibiotics (50 U/ml penicillin, 50 μg/ml streptomycin) and 20% M-CSF-containing medium conditioned by L929 fibroblasts. Over the following two weeks conditioned medium free RPMI was gradually replaced by DMEM.

Cell culture condition. Both RAW 264.7 and BMDM were cultured in DMEM supplemented with 10% FBS, 50 U/ml penicillin, 50 μg/ml streptomycin, and 1% L-glutamine (growth medium) at 37°C in a humidified atmosphere of 5% CO_2.

Osteoclast differentiation. The differentiation of BMDM and RAW 264.7 macrophages was initiated by the addition of 50 ng/ml RANKL one day after cell seeding. For osteoclast quantification and determination of TRAP activity at the earliest possible time point, cells were plated at the density of 8,100 per cm^2 and analysed 48 h after supplementation of the cell culture with RANKL (D2). For all other experiments, which required more osteoclasts, cells were seeded at the density of 32,400 per cm^2 and analysed 72 h after RANKL administration (D3). The undifferentiated cells were removed from strongly attached osteoclasts by successive washing with DMEM (1x) and PBS (3x).

Osteoclast formation and determination of their activity. Two-day-old cultures of differentiating cells were stained for TRAP activity using Acid Phosphatase, Leukocyte (TRAP) Kit (Sigma Aldrich) according to the manufacturer's instructions. TRAP-positive, multinucleated cells (carrying 3 ≥ nuclei) were counted as osteoclasts and data shown represent the number of multinucleated cells derived from initially 2,500 bone marrow or RAW 264.7-derived macrophages stimulated with RANKL.

For quantification of TRAP activity, stained cells were dissolved in DMSO, solution was acidified with 3% HCl, absorbance was measured at 540 nm and normalized to the protein content, which was quantified with Lowry assay. Osteoclast resorbing activity was evaluated in the culture of cells differentiated for 3 days by counting matrix dissolution spots on the Corning® Osteo Assay plates (Corning Life Sciences). Undifferentiated cells were removed by washing and remaining osteoclasts were trypsinised for 15 min and washed off. After drying, images of plate surface were acquired on an Olympus inverted microscope.

Generation of stable ARTD1 and p65 knock-downs and siRNA transfection. shRNA constructs specific for *ARTD1* and for *p65/RelA* (see Suppl. Table 1) in pSUPER retroviral vector were packed in HEK-293cell line into invasive viruses. RAW 264.7 macrophages were infected with generated retroviruses for 8 h. After another 48 h, puromycin (5 μg/ml) was added to select the transduced cells. For transient silencing *Artd1* and *p65* were targeted with siRNA using Lipofectamine RNAiMAX as a carrier. Efficiency of the silencing was monitored by Western blot analysis and real-time PCR. In order to analyse the impact of ARTD1 and p65 in

osteoclast development, RANKL was added to cells 24 h after their transfection with siRNA and multinucleation was quantified on day 2 (D2).

Gene expression. RNA was extracted with TRI Reagent, reversed transcribed (High Capacity cDNA Reverse Transcription Kit, Life Technologies) and cDNA was quantified by real-time PCR (Rotor-Gene 3000, Qiagen) using primers listed in Suppl. Table 1 and SYBR Green (Kapa Biosystems). *Gapdh* was used as a housekeeping control gene.

Chromatin immunoprecipitation. Recruitment of p65 to promoter sequences, H3 and ARTD1 occupation as well as H3K4 trimethylation and H4 acetylation was studied with ChIP according to[50]. In brief, cells were cross-linked with 1% formaldehyde solution, isolated chromatin was sheared with the Bioruptor (Diagenode) and after incubation with antibody-conjugated protein G magnetic Dynabeads (Life Technologies), chromatin was isolated with phenol:chlorophorm:isoamyl alcohol. Extracted DNA was further analysed with real-time PCR. The list of primers used for IL-1β promoter and IL6 body are listed in Suppl. Table 1.

Isolation of RNA from mouse bone. Total RNA was isolated from a region encompassing the proximal tibial epiphysis and part of the diaphysis of WT (n = 4) and *Artd1*$^{-/-}$ (n = 5) mice using TRIzol reagent, and treated with TURBO DNase (Life Technologies) as previously described[51].

Bone mass and microstructure. Femurs from 8-week-old male mice were stabilized in 2% agarose gel, and analysed by micro-computed tomography (μCT) system (μCT 40; Scanco Medical AG, Zurich, Switzerland) as described previously[48]. The volume of interest analysed was located just proximal to the growth plate, spanning a height of 350 μm each for the metaphyseal region.

Histology and histomorphometry. Tibiae were fixed in 10% formalin, decalcified in 14% (w/v) EDTA pH 7.2 for 10–14 days at room temperature, embedded in paraffin, sectioned at 5 μm thickness and mounted on glass slides. Sections stained with haematoxylin and eosin or for TRAP were used for the analysis of osteoblasts and osteoclasts, respectively, as described previously[48]. Photographs were taken and cell number counted using nanozoomer (Hamamatsu).

Statistical analysis. Bars in the figures represent mean ± standard error of the mean (SEM). Student's t-test was used to compare the difference between two means. $^{*}P < 0.05$, $^{**}P < 0.01$, $^{***}P < 0.001$. Results of the *in vitro* model of differentiation represent data from three independent biological replicates (with three technical replicates each).

References

1. Hottiger, M. O. Nuclear ADP-Ribosylation and Its Role in Chromatin Plasticity, Cell Differentiation, and Epigenetics. *Annu. Rev. Biochem.* **84,** 227–263 (2015).
2. D'Amours, D., Desnoyers, S., D'Silva, I. & Poirier, G. G. Poly(ADP-ribosyl)ation reactions in the regulation of nuclear functions. *Biochem. J.* **342,** 249–268 (1999).
3. Ji, Y. & Tulin, A. V. The roles of PARP1 in gene control and cell differentiation. *Curr. Opin. Genet. Dev.* **20,** 512–518 (2010).
4. Kraus, W. L. Transcriptional control by PARP-1: chromatin modulation, enhancer-binding, coregulation, and insulation. *Curr. Opin. Cell Biol.* **20,** 294–302 (2008).
5. Krishnakumar, R. & Kraus, W. L. The PARP side of the nucleus: molecular actions, physiological outcomes, and clinical targets. *Mol. Cell* **39,** 8–24 (2010).
6. Frizzell, K. M. *et al.* Global analysis of transcriptional regulation by poly(ADP-ribose) polymerase-1 and poly(ADP-ribose) glycohydrolase in MCF-7 human breast cancer cells. *J. Biol. Chem.* **284,** 33926–33938 (2009).
7. Luo, X. & Kraus, W. L. On PAR with PARP: cellular stress signaling through poly(ADP-ribose) and PARP-1. *Genes Dev.* **26,** 417–432 (2012).
8. Slattery, E., Dignam, J. D., Matsui, T. & Roeder, R. G. Purification and analysis of a factor which suppresses nick-induced transcription by RNA polymerase II and its identity with poly(ADP-ribose) polymerase. *J. Biol. Chem.* **258,** 5955–5959 (1983).
9. Kraus, W. L. & Hottiger, M. O. PARP-1 and gene regulation: progress and puzzles. *Mol. Aspects Med.* **34,** 1109–1123 (2013).
10. Erener, S., Hesse, M., Kostadinova, R. & Hottiger, M. O. Poly(ADP-ribose)polymerase-1 (PARP1) controls adipogenic gene expression and adipocyte function. *Mol. Endocrinol.* **26,** 79–86 (2012).
11. Erener, S. *et al.* ARTD1 deletion causes increased hepatic lipid accumulation in mice fed a high-fat diet and impairs adipocyte function and differentiation. *FASEB J.* **26,** 2631–2638 (2012).
12. Fujiki, K. *et al.* PPARgamma-induced PARylation promotes local DNA demethylation by production of 5-hydroxymethylcytosine. *Nat. Commun.* **4,** 2262 (2013).
13. Suda, T. *et al.* Modulation of osteoclast differentiation and function by the new members of the tumor necrosis factor receptor and ligand families. *Endocr. Rev.* **20,** 345–357 (1999).
14. Teitelbaum, S. L. Bone resorption by osteoclasts. *Science* **289,** 1504–1508 (2000).
15. Walsh, M. C. *et al.* Osteoimmunology: interplay between the immune system and bone metabolism. *Annu. Rev. Immunol.* **24,** 33–63 (2006).
16. Long, F. Building strong bones: molecular regulation of the osteoblast lineage. *Nat. Rev. Mol. Cell Biol.* **13,** 27–38 (2012).
17. Boyle, W. J., Simonet, W. S. & Lacey, D. L. Osteoclast differentiation and activation. *Nature* **423,** 337–342 (2003).
18. Takayanagi, H. *et al.* Induction and activation of the transcription factor NFATc1 (NFAT2) integrate RANKL signaling in terminal differentiation of osteoclasts. *Dev. Cell* **3,** 889–901 (2002).
19. Hayden, M. S., West, A. P. & Ghosh, S. NF-kappaB and the immune response. *Oncogene* **25,** 6758–6780 (2006).
20. Boyce, B. F., Schwarz, E. M. & Xing, L. Osteoclast precursors: cytokine-stimulated immunomodulators of inflammatory bone disease. *Curr. Opin. Rheumatol.* **18,** 427–432 (2006).
21. Lee, S. K. & Lorenzo, J. Cytokines regulating osteoclast formation and function. *Curr. Opin. Rheumatol.* **18,** 411–418 (2006).
22. Robaszkiewicz, A. *et al.* Hydrogen peroxide-induced poly(ADP-ribosyl)ation regulates osteogenic differentiation-associated cell death. *Free Radic. Biol. Med.* **53,** 1552–1564 (2012).
23. Robaszkiewicz, A. *et al.* The role of p38 signaling and poly(ADP-ribosyl)ation-induced metabolic collapse in the osteogenic differentiation-coupled cell death pathway. *Free Radic. Biol. Med.* **76,** 69–79 (2014).

24. Beranger, G. E., Momier, D., Rochet, N., Carle, G. F. & Scimeca, J. C. Poly(adp-ribose) polymerase-1 regulates Tracp gene promoter activity during RANKL-induced osteoclastogenesis. *J. Bone Miner. Res.* **23,** 564–571 (2008).
25. Beranger, G. E. *et al.* RANKL treatment releases the negative regulation of the poly(ADP-ribose) polymerase-1 on Tcirg1 gene expression during osteoclastogenesis. *J. Bone Miner. Res.* **21,** 1757–1769 (2006).
26. Rodriguez-Vargas, J. M. *et al.* ROS-induced DNA damage and PARP-1 are required for optimal induction of starvation-induced autophagy. *Cell Res.* **22,** 1181–1198 (2012).
27. Lehmann, M. *et al.* ARTD1-induced poly-ADP-ribose formation enhances PPARgamma ligand binding and co-factor exchange. *Nucleic Acids Res.* **43,** 129–142 (2015).
28. Lee, Y. M., Fujikado, N., Manaka, H., Yasuda, H. & Iwakura, Y. IL-1 plays an important role in the bone metabolism under physiological conditions. *Int. Immunol.* **22,** 805–816 (2010).
29. Scianaro, R. *et al.* Deregulation of the IL-1beta axis in chronic recurrent multifocal osteomyelitis. *Pediatr Rheumatol Online J* **12,** 30 (2014).
30. Kim, J. H. *et al.* The mechanism of osteoclast differentiation induced by IL-1. *J. Immunol.* **183,** 1862–1870 (2009).
31. Tolar, J., Teitelbaum, S. L. & Orchard, P. J. Osteopetrosis. *N. Engl. J. Med.* **351,** 2839–2849 (2004).
32. Rachner, T. D., Khosla, S. & Hofbauer, L. C. Osteoporosis: now and the future. *Lancet* **377,** 1276–1287 (2011).
33. Scott, D. L., Wolfe, F. & Huizinga, T. W. Rheumatoid arthritis. *Lancet* **376,** 1094–1108 (2010).
34. Mundy, G. R., Raisz, L. G., Cooper, R. A., Schechter, G. P. & Salmon, S. E. Evidence for the secretion of an osteoclast stimulating factor in myeloma. *N. Engl. J. Med.* **291,** 1041–1046 (1974).
35. Yoneda, T. Cellular and molecular mechanisms of breast and prostate cancer metastasis to bone. *Eur. J. Cancer* **34,** 240–245 (1998).
36. Nicholson, G. C. *et al.* Induction of osteoclasts from CD14-positive human peripheral blood mononuclear cells by receptor activator of nuclear factor kappaB ligand (RANKL). *Clin. Sci.* **99,** 133–140 (2000).
37. Garlanda, C., Dinarello, C. A. & Mantovani, A. The interleukin-1 family: back to the future. *Immunity* **39,** 1003–1018 (2013).
38. Dewhirst, F. E., Stashenko, P. P., Mole, J. E. & Tsurumachi, T. Purification and partial sequence of human osteoclast-activating factor: identity with interleukin 1 beta. *J. Immunol.* **135,** 2562–2568 (1985).
39. Souza, P. P. & Lerner, U. H. The role of cytokines in inflammatory bone loss. *Immunol. Invest.* **42,** 555–622 (2013).
40. Yao, Z., Xing, L., Qin, C., Schwarz, E. M. & Boyce, B. F. Osteoclast precursor interaction with bone matrix induces osteoclast formation directly by an interleukin-1-mediated autocrine mechanism. *J. Biol. Chem.* **283,** 9917–9924 (2008).
41. Wei, S., Kitaura, H., Zhou, P., Ross, F. P. & Teitelbaum, S. L. IL-1 mediates TNF-induced osteoclastogenesis. *J. Clin. Invest.* **115,** 282–290 (2005).
42. Polzer, K. *et al.* Interleukin-1 is essential for systemic inflammatory bone loss. *Ann. Rheum. Dis.* **69,** 284–290 (2010).
43. Zwerina, J. *et al.* TNF-induced structural joint damage is mediated by IL-1. *Proc. Natl. Acad. Sci. USA* **104,** 11742–11747 (2007).
44. Krishnakumar, R. & Kraus, W. L. PARP-1 regulates chromatin structure and transcription through a KDM5B-dependent pathway. *Mol. Cell* **39,** 736–749 (2010).
45. Lukens, J. R. *et al.* Critical role for inflammasome-independent IL-1beta production in osteomyelitis. *Proc. Natl. Acad. Sci. USA* **111,** 1066–1071 (2014).
46. Jimi, E. *et al.* Activation of NF-kappaB is involved in the survival of osteoclasts promoted by interleukin-1. *J. Biol. Chem.* **273,** 8799–8805 (1998).
47. Bonar, S. L. *et al.* Constitutively activated NLRP3 inflammasome causes inflammation and abnormal skeletal development in mice. *PLoS ONE* **7,** e35979 (2012).
48. Qu, C. *et al.* NLRP3 mediates osteolysis through inflammation-dependent and -independent mechanisms. *FASEB J.* **29,** 1269–1279 (2015).
49. Wang, Z. Q. *et al.* Mice lacking ADPRT and poly(ADP-ribosyl)ation develop normally but are susceptible to skin disease. *Genes Dev.* **9,** 509–520 (1995).
50. Saccani, S., Pantano, S. & Natoli, G. p38-Dependent marking of inflammatory genes for increased NF-kappa B recruitment. *Nat. Immunol.* **3,** 69–75 (2002).
51. Mirsaidi, A. *et al.* Therapeutic potential of adipose-derived stromal cells in age-related osteoporosis. *Biomaterials* **35,** 7326–7335 (2014).

Acknowledgements

We thank Alan Valaperti for help with bone isolation. We thank Stephan Christen and the other members of the Department of Molecular Mechanisms of Disease (University of Zurich, Switzerland) for help and discussions during the preparation of this manuscript. This work was financed by the Science Exchange Program [12.193 to A.R.], the Kanton of Zurich, Swiss National Science Foundation [310030B_138667 and 310030_157019 to M.O.H.] and by the Mäxi Foundation (for consumables). The research in the laboratory of A.R. is funded by Polish National Science Centre grant UMO-2013/11/D/NZ2/00033, and that in the laboratory of G.M. by NIH/NIAMS R01-AR064755.

Author Contributions

A.R. planned and performed the experiments, evaluated the data and wrote the manuscript. P.J.R. and A.M. isolated RNA from bones. F.K. analysed gene expression in bone. E.W. and T.P. analysed gene expression in BMDM. A.R., P.C., C.Q. and G.M performed the μCT experiments, and C.Q. and G.M additionally performed histological analyses of the bones. MOH supervised experiments and wrote the manuscript. All authors have read and approved the manuscript.

Additional Information

Supplementary information accompanies this paper at http://www.nature.com/srep

Competing financial interests: The authors declare no competing financial interests.

How to cite this article: Robaszkiewicz, A. *et al.* ARTD1 regulates osteoclastogenesis and bone homeostasis by dampening NF-κB-dependent transcription of *IL-1β*. *Sci. Rep.* **6**, 21131; doi: 10.1038/srep21131 (2016).

UNPUBLISHED RESULTS

1. Obtained data related to aim 2:

To investigate whether and in which cell type ADP-ribosylation inhibitors (i.e. Talazoparib or Olaparib) affect proinflammatory signaling.

1.1. Co-treatment of wild type animals with LPS and PARP inhibitors reduce different cytokines in the serum

ADP-ribosylation regulates different DAMP-mediated inflammatory conditions such as ischemia-reperfusion-induced necrosis, but also PAMP-mediated inflammations such as bacterial infections[180]. First-generation PARPi reduce the burden in LPS-induced inflammatory models[166,213]. Although these unspecific first generation PARPi lack enzyme specificity, LPS-induced endotoxic shock resistant ARTD1 knock-out mice[77] emphasize that ARTD1 is the major ADP-ribosylating enzyme contributing to systemic bacterial infections. The expression of soluble mediators during infections activates and primes host cells to orchestrate pathogen elimination[163]. To gain insights about ADP-ribosylation, particularly ARTD1-dependent cytokine expression, during LPS-induced sepsis *in vivo,* we treated wild-type mice with Dimethylsulfoxide (DMSO) or the most specific ARTD1 inhibitor available (Olaparib, 5 mg/kg) for 1 h. Subsequently, the animals received 4 mg/kg LPS and proinflammatory mediators were enzyme-linked immunosorbent assay (ELISA)-quantified in blood serum after additional 4 hrs (Figure 7). Animal conditions (lethargy, mobility) strongly suggested the induction of a severe inflammation. In addition, we could determine significantly reduced IFN-γ, IL-18, IL-6 and TNF-α, but not IL-12p70 levels in Olaparib treated mice compared to the DMSO treated mice.

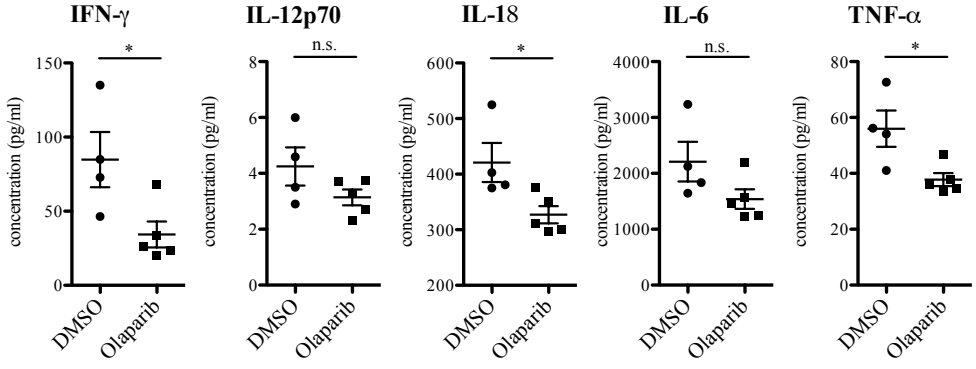

Figure 7. PARPi inhibit proinflammatory cytokine expression during LPS-induced sepsis. ELISA quantified IFN-γ, IL-12p70 IL-18, IL6 and TNF-α in blood serum. Wild-type mice were i.p. injected with either DMSO or 5 mg/kg Olaparib. After 1 h, mice received i.p. 4 mg/kg LPS. After 4 h, the mice were sacrificed, whole blood was obtained by cardiac puncture and serum was isolated. Levels of selected cytokines were quantified by luminex ELISA. Data shown as mean ± SEM. *t*-Test: $*P < 0.05$

The data suggests anti-inflammatory actions of PARPi during LPS-induced sepsis. However, the responsible cell type for the observed effect remains elusive. In addition, Olaparib also inhibits other ARTD1 family members (i.e. ARTD2), thus determining the responsible ARTD family member to inhibit inflammatory cytokine expression needs further investigations.

1.2. NK cells are PARPi sensitive

NK cells are lymphocyte cells that belong to the innate immunity and were initially described for their ability to kill leukemic cells without prior sensitization[214]. Circulating NK cells make up approximately 4-15% of blood lymphocytes and are in a resting phase. Upon activation by cytokines such as IL-12, IL-18 or IL-15, NK cells infiltrate pathogen infected or malignant tissue and carry out cytotoxic functions[215]. In contrast, NK cells in peripheral tissues such as tonsils lymph nodes and spleen are activated by dendritic cells via cell-to-cell contact and via the abovementioned cytokines. Activated NK cell secrete high levels of IFN-γ, TNF-α or GM-CSF to amplify the inflammatory response and particularly activate T cells[215]. The fact that pharmacologic inhibition of ADP-ribosylation protects against different diseases, in particular against septic shock, motivated us to identify the cell type that would account for the observed protection. During sepsis, NK cells are the very early and main producers of IFN-γ, thereby priming and amplifying the hosts inflammatory response[216].

To identify the main PARPi sensitive cell type that was responsible for the observed differences in the serum cytokine levels (Figure 7), isolated splenocytes of wild-type mice were treated for 1 h with control buffer, 5 µM Olaparib or 25 nM Talazoparib prior the stimulation with 0.1 µg/ml LPS for 18 hrs. Quantification of secreted IFN-γ levels by ELISA revealed a significant LPS-induced IFN-γ induction, which was significantly reduced by both Olaparib and Talazoparib (Figure 8A).

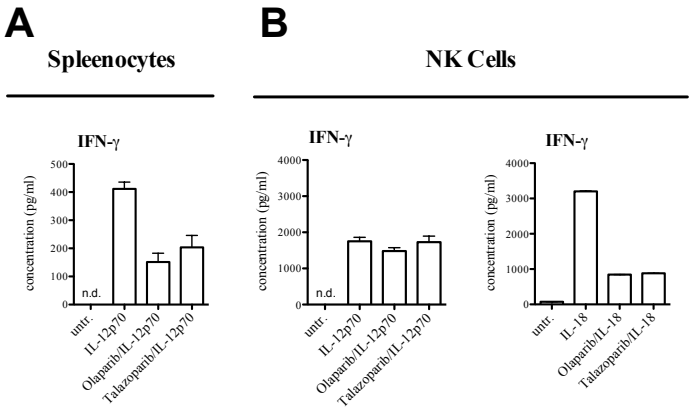

Figure 8. The IL-18 signaling pathway in NK cells is PARPi sensitive. ELISA quantification of cell culture supernatant for IFN-γ. (A) Splenocyte suspensions of wild type mice were either left untreated or incubated with 5 µM Olaparib or 25 nM Talazoparib for 1 h and subsequently stimulated with 0.1 µg/ml LPS for 18 h. (B) MACS sorted NK cells of wild type mice were either left untreated or incubated with 5 µM Olaparib or 25 nM Talazoparib for 1 h and subsequently stimulated with 10 ng/ml IL-12p70 or 10 ng/ml IL-18 for 18 h.

NK cell mediated IFN-γ expression relies on innate immune cell secretion of IL-12 and/or IL-18. Earlier studies provided evidence that proinflammatory cytokine expression of e.g. macrophages do not depend on ARTD1 catalytic activity, but on the protein itself[72] (and the prepared manuscript in section 3). Hence, the provided data suggested that the differential IFN-γ expression levels are indeed regulated by ADP-ribosylation and that NK cells might be mainly sensitive to PARPi treatment.

To directly address the question whether NK cell-mediated IFN-γ expression is enzymatically dependent on ADP-ribosylation, we sorted NK cells of wild type mice by magnetic-activated cell sorting (MACS) and confirmed NK cell purity being between 80-90 % (data not shown). Enriched NK cells were subsequently either left untreated or incubated with 5 μM Olaparib or 25 nM Talazoparib for 1 h prior the stimulation with either 10 ng/ml IL-12p70 or 10 ng/ml IL-18 for 18 h (Figure 2B). ELISA Quantification of the IFN-γ levels for both treatments (i.e. IL-12p70 and IL-18 treated NK cells) revealed a significant increase of IFN-γ by both cytokines, however to a different extent: IL-18 was about twice as potent to induce IFN-γ in NK cells *in vitro* as compared to IL-12p70. Very interestingly, PARPi reduced only IL-18, but not IL-12p70-induced IFN-γ in NK cells, suggesting that the IL-18 signaling pathway in NK cells is sensitive to PARPi and that this is the case for both tested inhibitors (i.e. Olaparib and Talazoparib). It is currently not known which ARTD family member might contribute to the PARPi sensitivity in NK cells. Mechanistically, IL-18 signaling involves, comparable to LPS stimulation, the transcription factor NF-κB for the transcriptional regulation of IL-18-induced target genes (i.e. IFN-γ). Given that ARTD1 is a known co-factor of NF-κB, these findings might suggest that ARTD1 functions in a cell type dependent manner; either via its scaffolding ability (i.e. only dependent on the protein) in macrophages and fibroblasts[72], or via its enzymatic activity in NK cells. Further *in vivo* experiments are planned to investigate the PARP inhibitor sensitivity in NK cells, for example by the generation of ARTD1-specific NK cell knock-out mouse.

2. Obtained data related to aim 3:

To identify additional ARTD family members involved in the LPS-induced inflammatory signaling response in fibroblasts.

2.1. Several ARTD family members control LPS-induced proinflammatory gene expression in fibroblasts

Since the discovery of low potency PARPi like 3-AB, their development greatly enhanced the inhibitor's specificity towards the ARTD family. Nevertheless, PARPi profiling revealed that the currently available PARPi lack specificity towards a distinct ARTD family member[148]. Besides inhibiting the growth of *BRCA* deficient tumor cells, PARPi have also been described to exert anti-inflammatory effects, which could additionally account for their anti-tumorigenic

effects[81,135,149]. This raised the question whether other ARTD family members could contribute to the anti-inflammatory effects of PARPi as well. Along this line our lab provided strong evidence for the transcriptional cofunction of ARTD1 in NF-κB-dependent gene expression[72].

To identify ARTD family members possibly regulating NF-κB mediated proinflammatory signaling, a siRNA screen was performed. Mouse lung fibroblast (MLF) cells were transfected with siRNAs against all 17 murine ARTDs and stimulated with 0.1 µg/ml LPS for 4 hrs. Total RNA was extracted and reverse transcribed into cDNA to quantify by quantitative real-time PCR (qRT-PCR) the expression of *Cxcl10*, a primary NF-κB target gene[217] (Figure 9).

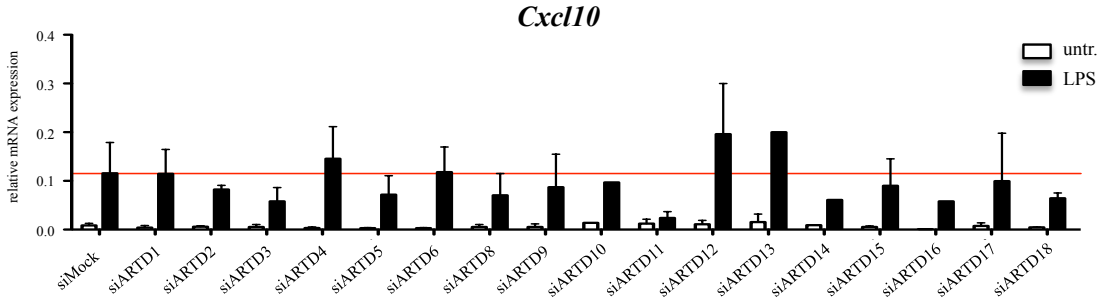

Figure 9. ARTD family members differentially regulate NF-κB dependent gene expression in fibroblast cells. Quantitative RT-PCR analysis of mouse lung fibroblast transfected with siMock and siRNAs against all 17 murine ARTD family members. After 48 hrs, the cells were stimulated with 0.1 µg/ml LPS for 4 hrs, total RNA was extracted, reverse transcribed and *Cxcl10* expression was determined by qRT-PCR. The red line indicates the expression level in LPS-treated siMock fibroblasts.

The extensive LPS-induced up-regulation of *Cxcl10* in siMock transfected MLFs confirmed the successful stimulation of the cells. While knock-down of ARTD4, ARTD12 and ARTD13 lead to enhanced *Cxcl10* expression compared to siMock, knock-down of ARTD2, ARTD3, ARTD11, ARTD14, ARTD15 in contrast reduced the *Cxcl10* expression, although to different extents. These experiments revealed that loss of these latter ARTD family members reduce LPS-induced *Cxcl10* expression in fibroblast, suggesting that they might function as NF-κB co-factors. Surprisingly knockdown of ARTD1 did not affect *Cxcl10* gene expression under the tested conditions. This could be due to compensatory mechanisms in the used mouse lung fibroblast cell line or that *Cxcl10* is not regulated by ARTD1.

2.2. ARTD11 selectively enhances proinflammatory cytokine expression of *Cxcl2* and *Cxcl10* but not *Il6* in fibroblasts

Since siARTD11 attenuated *Cxcl10* expression to the strongest extent, its involvement in NF-κB-dependent gene expression was further investigated. To this end, the expression of additional NF-κB target genes was analyzed in an ARTD11-dependent manner at two

different time points after stimulation. siMock and siARTD11 transfected MLFs were stimulated with 0.1 µg/ml LPS for 1 hr or 4 hrs. Subsequently, the expression of the classical primary NF-κB response genes *Cxcl10, Cxcl2* and the secondary NF-κB response gene *Il6* were quantified by qPCR (Figure 10)[218]. Successful siRNA mediated knock-down of ARTD11 selectively reduced the LPS-induced expression of the proinflammatory mediators *Cxcl10* and *Cxcl2* (for the latter however not to a statistically significant extent due to high variation), while the expression of *Il6* was not affected.

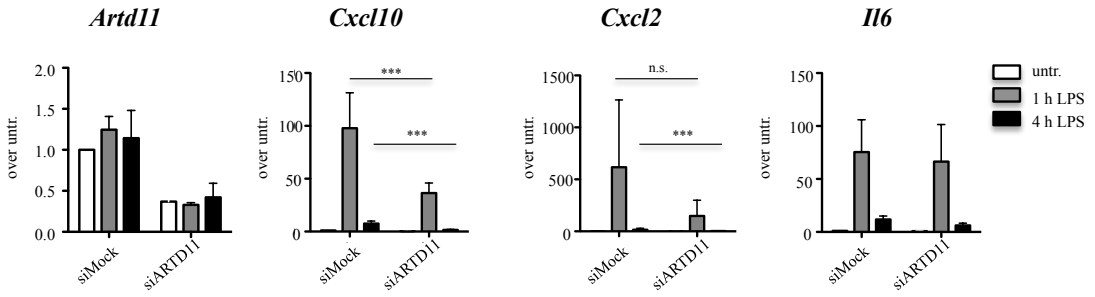

Figure 10. ARTD11 enhances *Cxcl10* and *Cxcl2*, but not *Il6* expression in fibroblast cells. Quantitative RT-PCR analysis of mouse lung fibroblast transfected with siMock and ARTD11. After 48 hrs, the cells were stimulated with 0.1 µg/ml LPS for 1 hr and 4 hrs, total RNA was extracted, reverse transcribed and *Artd11*, *Il6*, *Cxcl10 and Cxcl2* expression was determined by qRT-PCR. Data is normalized over untreated and presented as mean + SD of three biological replicates. *t*-Test: ***$P <$ 0.001.

The expression inhibition (%) of *Cxcl2* and *Cxcl10* was comparable, although *Cxcl2* was induced ten times stronger by LPS compared to *Cxcl10*. These data indicated that ARTD11 specifically regulates the expression of only a subset of proinflammatory cytokines (i.e. the primary target genes) rather than functioning as a general NF-κB co-regulator.

2.3. ARTD11 does not enhance proinflammatory cytokine expression in macrophages.

Although different cell types express the same proinflammatory cytokines, their underlying molecular expression mechanisms might differ, depending on the cell type[219]. To test whether ARTD11 regulates proinflammatory gene expression also in a different cell type, we repeated the above-described experiments with primary macrophages. Since primary macrophages are difficult to transfect and in the meantime ARTD11 deficient ($^{-/-}$) mice were available, bone marrow derived macrophages (BMDM) from *Artd11*$^{+/+}$ and *Artd11*$^{-/-}$ mice (see below) were generated, stimulated with 10 ng/ml LPS for 1 hr or 4 hrs and gene expression of *Cxcl10*, *Cxcl2* and *Il6* analyzed by qRT-PCR. Although LPS treatment induced all defined NF-κB target genes, the knock-out of ARTD11 in macrophages did not alter their gene expression (Figure 11).

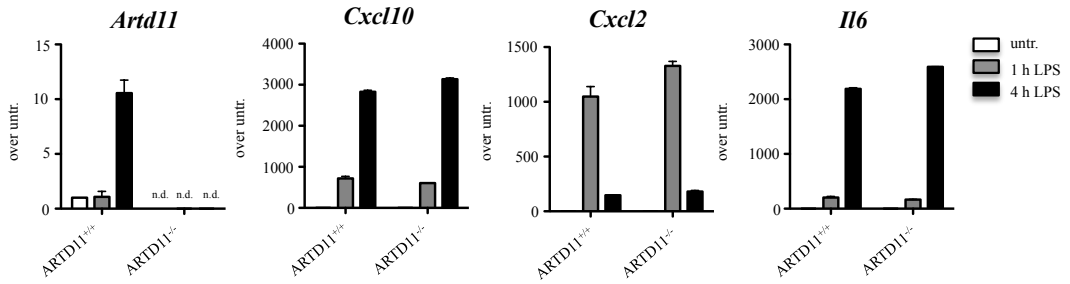

Figure 11. ARTD11 does not regulate *Il6*, *Cxcl10* or *Cxcl2* in macrophages. Quantitative RT-PCR analysis of primary bone marrow derived macrophages from ARTD11$^{+/+}$ and ARTD11$^{-/-}$ mice. After 5 days of differentiation, the cells were stimulated with 1 ng/ml LPS for 1 hr and 4 hrs, total RNA was extracted, reverse transcribed and *Artd11*, *Il6*, *Cxcl10 and Cxcl2* expression was determined by qRT-PCR. Data is normalized over untreated ARTD11$^{+/+}$.

The data thus suggests, that ARTD11 enhances *Cxcl10* and *Cxcl2* proinflammatory gene-expression in a cell type specific manner (i.e. in fibroblast cells but not in macrophages). The *Artd11*$^{-/-}$ BMDM thus likely evolved compensatory mechanisms during their development to overcome the lack of ARTD11 for LPS induced gene expression, although additional genes should be analyzed to strengthen this conclusion.

2.4. ARTD11 acts downstream of NF-κB nuclear translocation

ARTD11 could affect NF-κB function at different levels. To assess whether ARTD11 alters the NF-κB nuclear translocation, NF-κB was monitored by immunofluorescence in siARTD11 or siMock treated MLFs stimulated for 30 min with LPS. After 30 min LPS, the large subunit of NF-κB translocated to the nucleus, independently of whether ARTD11 was expressed or knocked down. This indicates that ARTD11 itself does not regulate cytoplasmatic LPS signaling events, but rather regulates NF-κB target gene expression at the chromatin or at the post-transcriptional level (Figure 12).

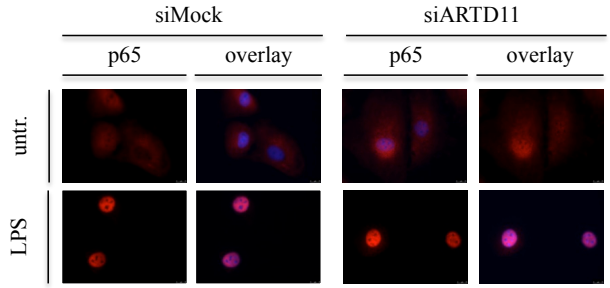

Figure 12. ARTD11 does not regulate LPS-induced NF-κB nuclear translocation. Immunofluorescent analysis of mouse lung fibroblast cells transfected with siMock and ARTD11. After 48 hrs, the cells were stimulated with 0.1 µg/ml LPS for 30 mins and formaldehyde fixed. The localization of p65 (red) was determined by staining with a respective antibody. The nucleus was counterstained with DAPI (blue).

2.5. ARTD11 localizes to the nuclear envelope.

The functional analysis of proinflammatory gene expression and the unchanged p65 translocation in ARTD11 deficient cells strongly indicated, that ARTD11 regulates NF-κB after its nuclear translocation (see 2.2 and 2.4). Previous reports described a nuclear envelope localization for ARTD11[220]. To gain additional mechanistic insights about the molecular function of ARTD11 during its transcriptional regulation of *Cxcl2* and *Cxcl10*, the localization of ARTD11 was further investigated. Due to the lack of suitable antibodies, ARTD11 was overexpressed as a green fluorescent protein (GFP)-tagged fusion protein in HEK293T cells. Immunofluorescent analyses confirmed the previous report and the localization of ARTD11 at the nuclear envelope (Figure 13A/13B). Further investigations are necessary to specify ARTD11 localization at the inner or outer nuclear membrane.

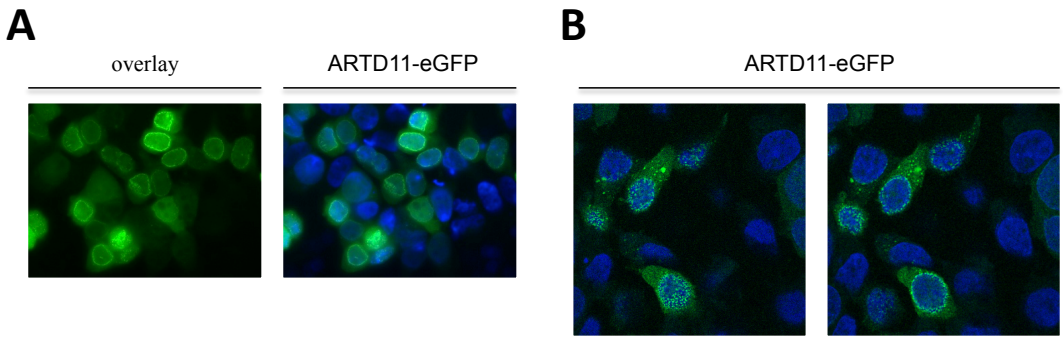

Figure 13. ARTD11 localizes to the nuclear envelope. Immunofluorescent analysis of HEK293T cells transfected with murine ARTD11-eGFP constructs**.** After 48 hrs, the cells were formaldehyde fixed and the localization of ARTD11 (green) was determined by fluorescent microscopy (A). Z-stack images were acquired by confocal microscopy (B). The nucleus was counterstained with DAPI (blue).

2.6. *Artd11*$^{-/-}$ mice develop normally

To learn more about the role of ARTD11 in a whole organism in steady state, we performed phenotyping of *Artd11*$^{-/-}$ mice. Previous publications reported a role of ARTD11 during spermatogenesis resulting in infertility of *Artd11*$^{-/-}$ male mice[220]. After successful generation of male and female *Artd11*$^{-/-}$ mice, their breeding resulted in no offspring. In contrast, female *Artd11*$^{-/-}$ and male *Artd11*$^{+/-}$ mice breed normally with regular litter sizes. Having confirmed the infertility phenotype, *Artd11*$^{-/-}$ mouse development was analyzed by necropsy in collaboration with Dr. Giovanni Pellegrini (Pathology, Vetsuisse Faculty, UZH). The whole body weights of two *Artd11*$^{+/+}$ and three *Artd11*$^{-/-}$ male mice of 8 weeks as well as the weights of some selected organs (brain, heart, kidney, liver, spleen and testis) were measured and the tissue composition assessed by immunohistochemical analyses. The analysis revealed neither macroscopic nor microscopic differences between the analyzed genotypes (Figure 14; data not shown).

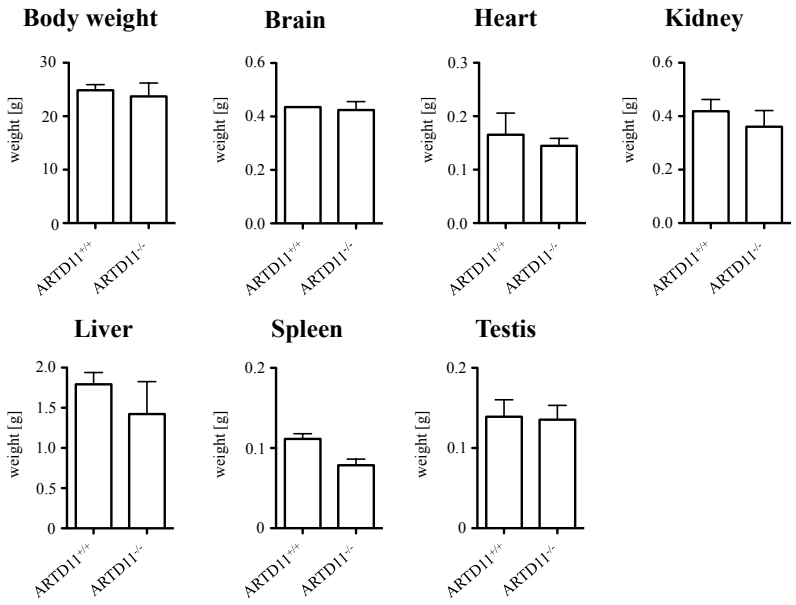

Figure 14. ARTD11 knock-out mice develop normal and do not show phenotypic differences to wild-type littermates. Necropsy analysis of three *Artd11*$^{-/-}$ and two *Artd1*$^{+/+}$ male mice of 8 weeks. Body weights as well as indicated organ weights were determined.

To investigate whether the development of immune cells was affected by ARTD11 knock-out, a immunophenotyping of the splenic immune compartment in four *Artd11*$^{+/+}$ and five *Artd11*$^{-/-}$ was performed (collaboration with Juliana Komuczki, Institute of Experimental Immunology, UZH). Single cell suspensions of the spleen were stained with specific antibodies and the cell populations quantified by flow cytometry (Figure 15).

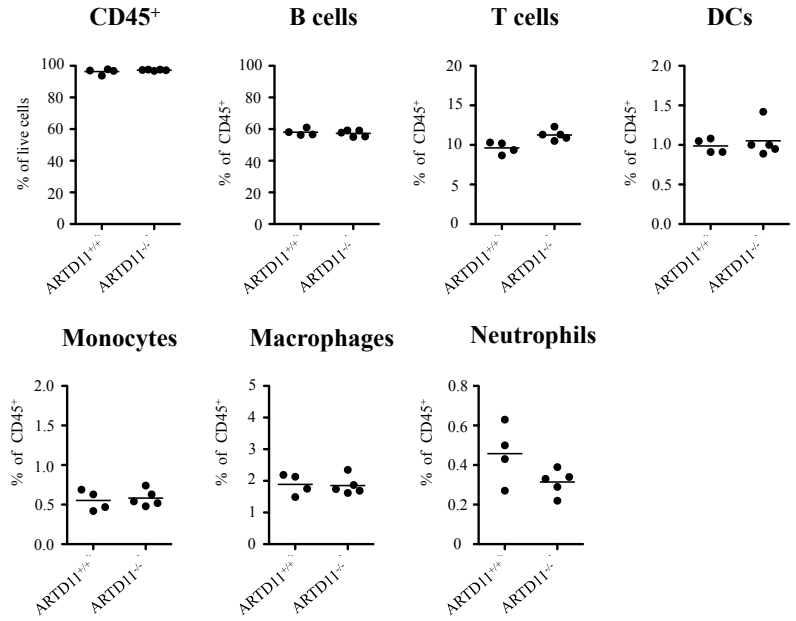

Figure 15. ARTD11 knock-out mice do not have significant differences in the cellular composition of the spleen. Immunophenotyping of four ARTD11$^{+/+}$ and five ARTD11$^{-/-}$ male mice. Single cell suspensions of the spleen were stained with the respective antibodies and cell numbers were acquired by flow cytometry. Data presented as % of CD45^{+} cells.

No significant differences between *Artd11*$^{+/+}$ and *Artd11*$^{-/-}$ mice were identified, suggesting that under basal conditions, apart from the published infertility, *Artd11*$^{+/+}$ and *Artd11*$^{-/-}$ mice do not show any other phenotypic difference. We are currently performing inflammation models that are mainly based on the fibroblast reaction (PMA into ear) to further validate the functional role of ARTD11 in inflammation.

3. Other data (not related to aims)

3.1. The generation of a tamoxifen-inducible ARTD1 deficient mouse

The options for studying ARTD1 gene function *in vivo* are currently limited when using the classical *Artd1*$^{-/-}$ mouse generated by Zhao-Qi Wang[221]. Although ARTD1 plays important functions during DNA repair it is not essential for murine development[222]. Interestingly, the *Artd1/2* double knock-out is embryonically lethal[13], suggesting a compensatory mechanism(s) and partially overlapping function of ARTD1 and ARTD2. To further investigate this hypothesis and specifically to investigate whether double deficiency of *Artd1/2* is only important during development or also during adulthood we generated first an tamoxifen-inducible *Artd1*$^{-/-}$ strain with the plan to cross this strain later into the *Artd2*$^{-/-}$ strain, allowing us to delete ARTD1 in these mice (but also in isolated cells) at any desired time-point.

To generate the tamoxifen-inducible *Artd1*$^{-/-}$ strain we crossed *Artd1*$^{flox/flox}$ mice with B6.129-Gt(ROSA)26Sor$^{tm1(cre/ERT2)Tyj}$ from the Jackson Laboratory (Strain ID #008463). Having generated the strain (genotyping results not shown) we next assessed the recombination efficiency *in vivo*. Three mice received 1 mg tamoxifen by i.p. injection for five consecutive days. Similarly, two control animals were vehicle-treated (PBS). Ten days after the last tamoxifen administration, the mice were euthanized and lung, liver, spleen and testis were isolated. Whole cell protein extracts were generated and 150 µg of protein loaded on a SDS-PAGE gel. ARTD1 levels were quantified by Western Blot using tubulin as a loading control (Figure 16).

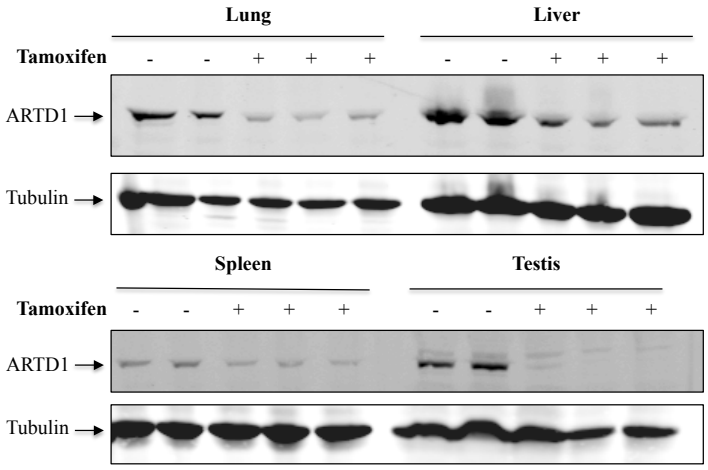

Figure 16. Tamoxifen administration to *Rosa26*-Cre^{ERT2+} *Artd1*$^{flox/flox}$ mice efficiently deletes *Artd1*. One milligram Tamoxifen or PBS (vehicle) was administrated i.p. into *Rosa26*-Cre^{ERT2+} *Artd1*$^{flox/flox}$ mice for five consecutive days. Whole cell lysates (150 µg protein) of the indicated organs were subjected to Western Blot analysis and stained with antibodies against ARTD1 or tubulin.

In all analyzed tissues, ARTD1 levels markedly decreased upon tamoxifen administration, although tissue specific differences in ARTD1 reduction were observed. The strongest tamoxifen-induced ARTD1 reduction was observed in testis, moderately in lung, liver and spleen. Notably, the absolute expression of ARTD1 was the highest in liver, moderately in testis and lung and the lowest in the spleen. Together these data indicate that a tamoxifen-inducible *Artd1*$^{-/-}$ mouse strain was successfully generated. Different layers of complexity can account for the observed tissue-specific differences. First, the injected tamoxifen might not reach any given target cell in the mouse. Second, translocation of the ERT2 protein into the nucleus of the target cell affects the expression of the Cre-recombinase. Lastly, the expressed Cre has to assess and recombine the floxed locus on the DNA. Depending on the tissue, the chromatin environment of specific loci might vary and influencing Cre recombination efficiency. Whether the observed reduction in the individual organs is sufficient to investigate phenotypical changes *in vivo* remains to be investigated. For example, ischemia-reperfusion injuries may be a first disease model to determine the functional impact on ARTD1 reduction.
Next, we assessed Cre-mediated ARTD1 recombination efficiency not only *in vivo*, but also *in vitro.* To do so, BMDM of either *Artd1*$^{flox/flox}$ or *Rosa26*-Cre^{ERT2+} *Artd1*$^{flox/flox}$ mice were differentiated for 10 days. On day 5, the culture medium was supplemented with either 20 µM 4-Hydroxytamoxifen (4-OHT), or vehicle (PBS). Whole cell extracts were generated and ARTD1 levels quantified by Western Blot (Figure 17). The quantification of the ARTD1 levels revealed a successful reduction of ARTD1 in 4-OHT treated *Rosa26*-Cre^{ERT2+} *Artd1*$^{flox/flox}$ BMDM. The ARTD1 levels were below the detection limit, suggesting that the recombination of the ARTD1 locus is very efficient if tamoxifen is readily available as is the case *in vitro*.

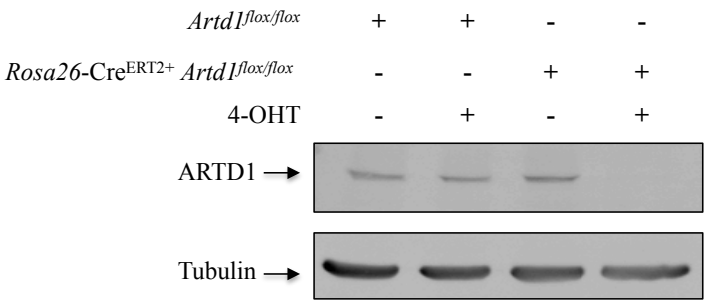

Figure 17. Tamoxifen efficiently deletes *Artd1* in *Rosa26*-Cre^{ERT2+} *Artd1*$^{flox/flox}$ BMDM. BMDM were differentiated for 10 days. On day 5, the medium was supplemented with 20 µM Hydroxytamoxifen (4-OHT) or PBS. Whole cell lysates (150 µg protein) were subjected to Western Blot analysis and stained with antibodies against ARTD1 or tubulin.

3.2. Towards the generation of an ARTD1/2 double knock-out mouse

As already indicated above *Artd1*$^{-/-}$/*Artd2*$^{-/-}$ double mutant mice are not viable and die at the onset of gastrulation, thus demonstrating the crucial role of PARylation during embryonic development[222]. To study the involvement of PARylation during development and adulthood, we generated a tamoxifen-inducible *Artd1*$^{-/-}$ mouse in an *Artd2*$^{-/-}$ background. Hence, tamoxifen administration would induce a partial (see 3.1 and Figure 16) double knock-out *in vivo*. After having successfully combined all three alleles (*Rosa26*-Cre^{ERT2}, *Artd1*$^{flox/flox}$ and *Artd2*$^{-/-}$) in mice, the animals were administrated 1 mg tamoxifen or vehicle (PBS) for 5 consecutive days. After another 10 days to allow for recombination and residual ARTD1 to be degraded, the mice were viable and did not show any phenotypic abnormalities. Thus, new breeding pairs of tamoxifen-treated and vehicle-treated mice were generated. A significantly lower reproduction, if any at all, was observed over at least 3 generations in tamoxifen-treated mice, compared to normal litter sizes of vehicle treated animals. Additionally, we noticed no macroscopic differences of tamoxifen- and vehicle treated animals during aging up to 8 months.

The data suggests, that indeed ARTD1 and ARTD2 are only necessary during embryonic development, but dispensable during adulthood under basal conditions. It remains very interesting to learn how these animals would behave during different disease models or under (genotoxic) stress conditions.

4. Material and methods to unpublished data

Mice. *Artd11*$^{-/-}$ mice were generated with support of the Laboratory Animal Service Center (LASC) at the University Zürich. Cryopreserved oocytes from *Parp11*$^{tm1(KOMP)Vlcg}$ mice were purchased from the KOMP repository (ID VG12032, www.komp.org, University of California Davis). The mice were generated by embryotransfer into a C57BL/6 foster mother by the LASC.

Tamoxifen-inducible ARTD1 knock-out mice were generated by crossing *Artd1*$^{flox/flox}$ mice with B6.129-Gt(ROSA)26Sor$^{tm1(cre/ERT2)Tyj}$ from Jackson Laboratory (Bar Harbor, USA) and kindly provided by Rafaela Santoro (University Zürich). Cre recombination was performed as described[223]. Briefly, 1 mg of tamoxifen (Sigma Aldrich) (dissolved in 90% cornoil 10% ethanol) or vehicle was administrated intra peritoneal for 5 consecutive days.

Artd1/Artd2 double knock out mice were generated by crossing the previously generated tamoxifen-inducible *Artd1*$^{-/-}$ strain to the constitutive *Artd2-/-* knock-out strain. Again, Cre recombination was performed as described above.

All animals were housed in pathogen free conditions at the University Zürich. All animal experiments were carried out in accordance with the Swiss and EU ethical guidelines and have been approved by the local animal experimentation committee of the Canton Zurich under licenses 207/2015 and 266/2014.

Cell Culture and reagents. NIH 3T3 and HEK293T cells were cultivated in Dulbecco modified Eagle medium (Gibco) supplemented with 10 % fetal calf serum, 5 % penicillin/streptamycin. Murine bone marrow derived macrophages (BMDM) were generated as previously described[224] and maintained in RPMI1640 (Gibco) supplemented with 10 % fetal calf serum, 5 % penicillin/streptamycin and 20 ng/ml recombinant murine M-CSF or (Preprotech)[225]. The supplementation 20 µM hydroxytamoxifen (4-OHT) was performed on day 5 to induce Cre mediated ARTD1 recombination. Cells were harvested after another 5 days and ARTD1 expression quantified by Westernblot.

Cell culture grade LPS (*Escherichia coli* O111:B4) was purchased from Sigma-Aldrich and recombinant murine interferon gamma from Preprotech.

siRNA transfection. siRNA transfection was performed as described earlier[78]. Briefly, Negative-control AllStars (siMOCK) and siRNAs targeting all mouse ARTD family members were purchased from Qiagen (Hilden). Cells were seeded and transfected with 20 nmol of small interfering RNA (siRNA) per well (in six-well plate) with RNAiMAX Lipofectamine (Invitrogen). The experiment was performed 3 days after transfection.

Plasmid transfection. Plasmid transfection in HEK293T cells was performed by calcium phosphate as described earlier[226].The pEGFP-ARTD11 plasmid was provided by P. Chang[14].

MACS based NK cell isolation. Splenic NK cells were isolated by using the NK Cell Isolation Kit (#130-096-892, Milteneyi Biotech) according to the manufacturer's protocols. Isolated NK cells were maintained in RPMI supplemented with 10 % fetal calf serum, 5 % penicillin/streptomycin, 10 ng/ml recombinant murine IL-15 (Preprotech) and 10 mM mercaptoethanol (Gibco). The PARP inhibitors Olaparib and Talazoparib were purchased from Selleckchem. Recombinant murine IL-12-p70 and IL-18 were purchased from Preprotech.

ELISA. IFN-γ cell culture supernatant levels were quantified by Mouse IFN-gamma DuoSet ELISA (R&D) according to the manufacturer's protocols.

Immunofluorescence. Immunofluorescence was performed as described[227]. The α-p65 antibody (C-20, Santa Cruz) was diluted 1:250, and DNA was stained in a separate step using Hoechst 33258 (Sigma) before mounting.

RNA extraction and quantitative real time PCR (qPCR) analysis. RNA isolation and qPCR were performed as described earlier[78]. Briefly, RNA extraction was performed with the NucleoSpin RNA II kit (Macherey-Nagel,). RNA was quantified with a NanoDrop reverse transcribed according to the supplier's protocol (Applied Biosystems). qPCRs were performed with the SYBR green KAPA SYBR® FAST (Sigma-Aldrich) and a Rotor-Gene Q 2plex HRM system (Qiagen). The relative amounts of each mRNA were normalized to the *Rps12*.

Westernblot. Western Blotting was performed as described[227]. For Western Blot analysis, proteins were separated by SDS- PAGE, and bands were visualized using the Odyssey infrared imaging system (LI- COR). Antibodies used for western blotting were anti-ARTD1/PARP-1 (1:1000, Santa Cruz sc-7150) and anti-Tubulin (1:10,000, Sigma, #T6199).

DISCUSSION AND PERSPECTIVES

1. Summary

The objective of this thesis was to study ADP-ribosylation during inflammation. The first aim addressed ARTD1 function of macrophages in innate immune cells and its contributions during inflammation. To identify ARTD1 dependent target genes in macrophages during proinflammatory signaling, we performed RNA-sequencing of LPS/IFN-γ stimulated *Artd1*$^{flox/flox}$ and *Artd1*$^{del/del}$ BMDM. Among others, we identified LPS/IFN-γ-induced *Il12b* to be significantly lower expressed in *Artd1*$^{del/del}$ BMDMs. We showed that ARTD1 protein but not its enzymatic activity contributes to the observed gene expression changes. *Il12b* encodes the p40 subunit of the IL-12p70 cytokine, which is a crucial mediator of lymphocyte activation. To study the effect of reduced *Il12b* expression *in vivo* we generated a myeloid cell specific *Artd1*$^{-/-}$ strain (*Artd1*$^{\Delta Myel}$) and tested the stain in three inflammatory models: a) acute systemic LPS-induced inflammation, b) local gastric *Helicobacter pylori* (*H.pylori*) infection and c) a subcutaneous MC-38 tumor model. In all tested models we observed reduced lymphocyte activation by decreased IFN-γ expression in *Artd1*$^{\Delta Myel}$ mice compared to *Artd1*$^{flox/flox}$ control animals. In particular we determined decreased NK cell activation during sepsis and decreased CD4 and CD8 T cell activation during *H.pylori* infection as well as the MC-38 tumor model.

The second aim of this thesis addresses the effect of ADP-ribosylation inhibitors (i.e. PARPi). Co-treatment of wild-type mice with LPS and PARPi revealed that even at the tested low LPS dose (i.e. 4 mg/kg) the serum levels of different cytokines were reduced (unpublished results Figure 2). Moreover, pretreatment of isolated splenocytes from wild-type mice phenocopied the reduced expression levels of different cytokines (unpublished results Figure 2). Finally, experiments with isolated NK cells in culture, revealed that IL-18-induced IFN-γ levels are sensitive to PARPi treatment while IL-12 induced IFN-γ levels were not.

The third aim of the thesis addressed the identification of novel ARTD family members involved in inflammatory signaling. During a siRNA screen in mouse fibroblasts we identified ARTD11 to selectively enhance *Cxcl2*, *Cxcl10* but not *Il6* expression. Additionally, we observed an ARTD11 nuclear envelope localization, which did not influence nuclear translocation of NF-κB. Beside the infertility of homozygous male mice, we did not identify macroscopic or histological differences in *Artd11*$^{-/-}$ mice compared to *Artd11*$^{+/+}$ mice.

2. To be active, or not to be active, that is the question - reoccurring discrepancies regarding the involvement of ADP-ribosylation

How ADP-ribosylation and ARTD1 controls inflammatory gene expression, in particular NF-κB-induced transcriptional activation is still under debate. Detailed analyses of our lab in

macrophages and fibroblasts revealed that ARTD1 regulates NF-κB dependent gene expression in an enzymatically independent manner[72]. ARTD1 serves as a scaffold protein to allow physical interaction of p300, the mediator complex and p65/p50 promoting gene expression[72]. In contrast, Martinez-Zamudio et al suggest that LPS-induced ARTD1 histone PARylation causes nucleosome remodeling to facilitate NF-κB binding at proinflammatory gene promoters[75]. Recently, a publication confirmed the involvement of ARTD1 for the LPS-induced *Il12b* expression in macrophages[228]. Both, ARTD1 deficient or pharmacologically inhibited BMDMs expressed *Il12b* significantly lower as wild-type control BMDMs. In contrast, we identified ARTD1 protein but not its enzymatic activity to regulate *Il12b* expression. While we used the clinically approved PARPi Olaparib which is among the most specific ARTD1 inhibitors available, Zhao and colleagues treated BMDMs with the first-generation PARPi 3-AB[228]. Studies with 3-AB, the first known PARPi generation, clearly provided evidence that this compound has unspecific functions (towards also other enzymes) and inhibits multiple ARTD family members[148]. Hence, other (non)-ADP-ribosylation dependent signaling cascades affected by 3-AB might contribute to *Il12b* repression observed by Zhao et al. In fact, STAT-mediated signaling also regulates *Il12b* expression[229]. Interestingly ARTD8 was shown to MARylate STAT1 antagonizing its phosphorylation and decreasing proinflammatory gene expression[121]. To test whether 3-AB inhibits ARTD8-mediated STAT1 ADP-ribosylation, *in vitro* trans-ADP-riboylation assays of ARTD8 and STAT1 should be performed. Moreover, to test the functional consequence of 3-AB-dependent ARTD8 inhibition on LPS-induced *Il12b* gene expression, siRNA depletion of ARTD8 in 3-AB treated BMDM would reveal the contribution of ARTD8.

The *Il12b* gene is a well-studied example that requires chromatin remodeling during inflammation-induced gene expression. Studies of the *Il12b* promoter identified binding sites for various transcription factors including NF-κB, C/EBP, AP-1 and NFAT[230-232]. However their binding sites, -30 to -175 bp upstream the transcription start site, are blocked by nucleosomes and require nucleosome remodeling prior transcription[233]. Indeed the SWItch/Sucrose Non-Fermentable (SWI-SNF) complex, which is responsible for nucleosome positioning[234] is recruited to target genes in LPS-stimulated macrophages[235]. Different models describe the targeting of chromatin remodeling machines to their site of action, i.e. acetylated histones that target and stabilize the SWI-SNF complex at target loci[236]. Since ARTD1 localizes to the *Il12b* promoter[228] and serves as a scaffold protein to facilitate the interaction of NF-κB and p300[72], it is intriguing to speculate that ARTD1 enhances SWI-SNF binding via p300-mediated histone acetylation at distinct gene loci such as *Il12b.* Chromatin immunoprecipitation (ChIP) experiments for SWI-SNF with p300 inhibitor treated ARTD1 knock-out and wild-type cells during inflammatory signaling could elucidate the proposed

model. Ideally, re-ChIP experiments for histone acetylation and SWI-SNF would indicate their presence at the same nucleosome.

Another approach to discriminate ARTD1 adaptor functions from its enzymatically dependent functions is the generation of a catalytically dead *Artd1* knock-in mouse model. Similarly, Schuhwerk et al mutated the amino acid at position 993 from an aspartic acid to an alanaine to generate a hypo-PARyating ARTD1 mutant mouse[237]. CRISPR-Cas9-mediated engineering of mouse ES cells and substitution of tyrosine to alanine at position 906 would allow the generation of a catalytically deficient *Artd1*$^{Y906A/Y906A}$ mouse strain. The tyrosine residue 906 is located in ARTD1s catalytic domain and essential for NAD^+ binding. Successful generation of the described strain and testing their phenotype in different inflammation models *in vivo* as well as primary cells *in vitro* is an exciting approach to dissect the different ways ARTD1 is thought to function during inflammatory gene expression.

3. Primary and secondary inflammatory gene expression – Does ARTD1 play a key function?

SWI-SNF-mediated chromatin remodeling helps to differentiate primary and secondary inflammatory response genes. Whereas early primary response genes are expressed independently of SWI-SNF, late primary and particularly secondary response genes require SWI-SNF mediated chromatin remodeling[217,238]. Potentially, ARTD1 serves as a crucial determinant for the expression of secondary response genes, as it was identified to regulate *Nos2*, *Il6* and *Il1b*[73,88]. Both PARylation and SWI-SNF-dependent chromatin remodeling are active processes consuming NAD^+ or ATP respectively. Possibly, cells evolved different energy-consuming ways of chromatin remodeling to regulate primary and secondary response genes. Mechanistically, ARTD1 could render the promoter more accessible by either functioning in a SWI-SNF dependent manner as described above, in a PARylation dependent mode independently of SWI-SNF or requiring both PARylation and SWI-SNF activity.

ARTD1's function during chromatin remodeling is worthwhile to be addressed further. For mechanistic insights it would be essential to determine the genome wide occupancy (ChIP-Sequencing) of ARTD1 in macrophages before and after proinflammatory stimulation. Furthermore, to gain a global picture on ARTD1 function during inflammation-induced chromatin remodeling, macrophages could be analyzed by assay for transposase-accessible chromatin (ATAC)-sequencing[239]. Comparison of LPS and/or IFN-γ treated *Artd1*$^{wt/wt}$, *Artd1*$^{wt/wt}$ + PARPi, *Artd1*$^{Y906A/Y906A}$ and *Artd1*$^{del/del}$ macrophages would identify distinct loci whose chromatin remodeling are dependent on ARTD1 and PARylation. I propose that ARTD1 regulates gene expression in a highly chromatin environment dependent manner. The fact that ARTD1 is preferentially localized to nucleosome dense regions[18] and

that PARylation is a very fast and dynamic process could indicate that cells rely indeed on the fast activation of ADP-ribosylation for the remodeling of more heterochromatic regions to allow gene expression to take place, particularly during differentiation. In contrast, more euchromatic regions such as *Il12b* would rely on a much slower SWI-SNF dependent chromatin remodeling process thus requiring ARTD1 as an adaptor molecule for histone acetylation.

4. ARTD1 in NK cells – an opportunity for PARPi for medication use?

The synthetically lethal interaction between ARTD1 and BRCA1/2 proteins and the development of PARPi is an important therapeutic opportunity for breast and ovarian cancers[135]. Emerging evidences suggest that not only malignancies but also inflammation related diseases could benefit from the application of PARPi[135]. Lately, mainly opinion leaders of the field published an appeal for the investigation of PARPi in non-oncological diseases[150]. Sepsis, clinically also known as "systemic inflammatory response syndrome", is a severe infection of mostly bacterial origin[240]. Sepsis causes a major health-care problem, i.e. accounting for 200,000 deaths per year in the United States[216]. Although significant advances in the early implementation of symptomatic care through fluid resuscitation, antibiotic therapies and specific organ support techniques have been established, these strategies unfortunately did not reduce mortality in severe septic patients[216]. In addition, increasing microbial resistances and the slow development of new antimicrobial agents require new therapeutic approaches to treat this deadly disease[216]. Both PARPi administration or genetic deficiency of ARTD1 rendered mice significantly more resistant towards sepsis induced by intraperitoneal LPS injection[89,166] or cecal ligation puncture (CLP)[165]. The protective PARPi effect has not been linked to a particular cell type and it is currently not known whether the observed effects are directly mediated by ARTD1 or indirectly (e.g. by transcriptional activation of another ARTD family member).

In this thesis we discovered, that not macrophages, but NK cell are sensitive to PARPi during their IL-18 mediated activation (unpublished data Figure 8). PARPi treated MACS isolated murine NK cells expressed significantly lower levels of IFN-γ than their untreated control counterparts. NK-cell type regulated processes might thus be a promising cell type to be treated with PARPi. These include non-oncological disease models such as sepsis, arteriosclerosis, graft versus host disease and diabetes where NK cell activation is augmenting disease progression[215].

While research has extensively focused on the roles of macrophages, neutrophils and conventional T lymphocytes during sepsis, only lately the roles of natural killer cells have been increasingly appreciated[216]. Systemic administration of monoclonal anti-NK1.1 or polyclonal antiasialo GM1 antibodies in mice significantly reduce NK cell numbers *in vivo*[241].

In a CLP model, mice treated with anti-asialo-GM1 were protected against CLP-induced mortality compared to IgG-treated controls[242]. Moreover these animals are significantly protected against LPS-induced shock characterized by significantly reduced cytokine levels (i.e. IFN-γ and TNF-α). It is well appreciated that during CLP-induced shock, NK cells migrate from blood and spleen to the inflamed peritoneal cavity where they amplify the proinflammatory activities of the myeloid cell population. It is thus intriguing to speculate that the known anti-inflammatory PARPi effect during sepsis would (a) dampen NK-cell mediated IFN-γ expression, (b) interfere with their amplification role and (c) reduce the inflammatory burden of the host. NK cell specific *Artd1*$^{-/-}$ mice are proposed to be protected against sepsis by reduced IFN-γ levels. Thus, their investigation in the above-mentioned disease models would be interesting.

5. Cellular high-resolution analysis of ARTD1 *in vivo*- A new era to study ADP-ribosylation?

Since the discovery of ARTD1 in 1963[243], the field went through different phases and fascinating contributions to our understanding of ADP-ribosylation[43]. The phase involved biochemical characterization of the purified writers (i.e. ARTD1) and the erasers (i.e. PARG) as well as dynamics of PAR levels in living cells. The second phase comprised the development of the first generation of PARP inhibitors and their contribution to DNA damage induced cytotoxicity in tumor cells[23]. The establishment of todays routine molecular methodologies allowed the cloning of ARTD1 cDNA during the third phase, which revolutionized the field for the first time. From here on the field of ADP-ribosylation evolved and expanded during a fourth phase by many exciting advances such as the crystallographic structure analyses of ARTD proteins and domains, a comprehensive coverage of all ART family members and the identification of PAR-binding motifs. Any of the described evolutions in ADP-ribosylation biology started with ARTD1 and ADP-ribosylation remains mainly associated with various kinds of cellular stress and pathological conditions. Although we learned a lot from cell based systems, they are very limited in their utility to study complex cellular interactions that regulated all diseases. Functional studies of ARTD1 *in vivo* has so far only been possible by the whole body knock-out mouse models[221,244,245]. I thus propose a new -fifth- phase of ADP-ribosylation biology by generating and studying tissue specific knock-out animals which allow high resolution *in vivo* studies of writers, readers or erasers of ADP-ribosylation. In this thesis we present the pioneering work of a conditional and myeloid cell type specific *Artd1*$^{-/-}$ mouse and its utility to confirm and extent the complex aspects of ARTD1 during immunity in a particular cell type. Especially for immunological aspects *in vivo* mouse models are essential to understand the complex cellular interactions. The ability to apply the generated "floxed" *Artd1* mouse strain is only limited by the

availability of suitable Cre-expressing mouse lines and the disease models[246]. The immune system is very powerful as it can very efficiently eliminate foreign material, but also host cells. CD4 T cells are important cells to balance pro- and anti-inflammatory actions, as they differentiate into T helper cells or Treg cells. Treg cells suppress proinflammatory Th1 and Th17 immune reponses[107]. Studies of the classical whole body ARTD1 knock-out animals revealed increased numbers of Treg cells as compared to wild type littermates[111]. To date we cannot address whether increased Treg cell number in *Artd1*$^{-/-}$ mice is a direct intrinsic or an indirect extrinsic driven process, but it would be very interesting to address these questions and their physiological relevance in more detail by generating a CD4 T cell specific ARTD1 knock-out mouse.

Additionally, since our knowledge about other ART superfamily members[247] significantly increased over the past years it is very exciting to expand the collection of tissue specific knock-out models beyond ARTD1 to learn and prepare the field for the next phase of ADP-ribosylation biology.

6. ARTD11 – The nuclear bouncer: You`re in or out!

The knowledge about ARTD11 is very limited: It plays at the animal level an essential role during spermatogenesis and its absence renders *Artd11*$^{-/-}$ mice infertile[220]. At the cellular level, ARTD11 localizes to the nuclear envelope[220]. Another study overexpressed a genetically manipulated ARTD11 in cells and discovered potential ARTD11 MARylated target proteins mainly involved in RNA transport[248]. In our study we identified ARTD11 to selectively enhance *Cxcl2* and *Cxcl10* expression but not *Il6* (unpublished data Figure 5). The formation of messenger ribonucleoprotein particels (mRNPs) is an essential step for mRNA export through the nuclear pore complex into the cytoplasm. Based on our studies and the published data, it is tempting to propose that ARTD11 selectively regulates nuclear RNA exports in a MARylation dependent manner of only a subset of inflammatory cytokine mRNAs. Mechanistically, ARTD11 could modify either nuclear pore complex molecules or mRNPs to promote mRNP transport. Retained mRNAs are directly degraded and thus not detectable by qPCR. To further investigate ARTD11 function, nuclear-cytolosic fractionation and subsequent proinflammatory cytokine mRNA quantification in both compartments would identify faulty nuclear mRNA export. Alternatively, RNA fluorescence in situ hybridization (RNA FISH) mediated quantification and localization analyses could also strengthen the proposed model. Additionally, specific ARTD11 inhibitor development would allow the dissection of an enzymatically dependent and an enzymatically independent phenotype.

ABBREVIATIONS

3-AB	3-aminobenzamide
4-OHT	4-Hydroxytamoxifen
AA	Aminoacids
AIF	Apoptosis-inducing factor
Arg	Argine
ARTC	ADP-ribosyltransferase C2/C3 cholera toxin-like
ARTD	ADP-ribosyltransferase diphtheria toxin like
ARTs	ADP-ribosyltransferase
ATP	Adnosine triphosphate
BER	Base excision repair
BMDM	Bone marrow derived macrophages
CBP	CREB-binding protein
ChIP	Chromatin immunoprecipitation
CLP	Cecal ligation uncture
CSF2	Colony stimmulating factor
DAMPs	Danger associated molecular pattern
DDR	DNA damage response
DMSO	Dimethyl sulfoxide
DNA	Deoxyribonucleic acid¨
DNBS	Dinitrobenzene sulfonic acid
DP	Double posistive
DSB	Double strand break
DSS	Dextran sulfate sodium
DTX3L	Deltex E3 ubiquitin ligase 3L
ELISA	Enzyme-linked immunosorbent assay
FoxP3	Forkhead box P3
GFP	Green fluorescent protein
GM-CSF	Granulocyte-macrophage colony-stimulating factor
HDAC2	Histone Deacetylase
HEK293T	Human embryonic kidney cells
HIV-1	Human immunodeficiency virus
HMGB1	High mobility group box 1 protein
HNP	Human neutrophil peptide
HR	Homologous recombination
hr	Hour
HuR	Human antigen R
IBD	Inflammatory bowel disease
IFN-γ	Interferon gamma
Ig	Immunoglobulin
IL-12,	Interlekin 12
IL-18	Interlekin 18
IL-1β	Interlekin 1 beta
Il-23	Interlekin 23
IL-6	Interleukin 6

ILC	Innate lymphoid cell
ISG	Interferon-stimulated gene
kDa	Kilo dalton
LIF	Leukemia inhibitory factor
Lys	Lysine
MACS	Magnetic-activated cell sorting
MARylation	Mono-ADP-ribosylation
MCAO	Middle cerebral artery occlusion
MEF	Mouse embryonic fibrobasts
Mins	Minutes
miRNA	Micro RNA
ml	Milliliter
MLF	Mouse lung fibroblast
mRNPs	Messenger ribonucleoprotein particels
NAD	Nicotinamide adenine dinucleotide
NEMO	NF-kB essential modulator
NF-κB	Nuclear factor kappa-light-chain-enhancer of activated B cells
NFAT	Nuclear factor of activated T-cells
NK cells	Natural killer cells
nNOS	Neuronal nitric oxide synthase
NOS	Nitric oxide
p300	E1A binding protein p300
$p38^{MAPK}$	Mitogen-activated protein kinase 3
PAAN	Parthanatos AIF-associated nuclease
PARG	Poly-ADP-ribose glycohydrolase
PARPi	PARP inhibitors
PARylation	Poly-ADP-ribosylation
PBS	Phosphate buffered saline
PD	Parkinson`s disease
PLC-γ	Phospholipase C-γ
PTM	Posttranslational modification
qRT-PCR	Quantitative real-time PCR
RA	Rheumatoid Arthritis
RAGE	Receptor for advanced glycation endproducts
RISC	RNA-induced silencing complex
RNA FISH	RNA fluorescence in situ hybridization
RNS	Reactive nitrogen species
ROS	Reactive oxygen species
rRNA	Ribosomal RNA
STAT	Signal transducer and activator of transcription
SWI-SNF	SWItch/Sucrose Non-Fermentable
TCR	T cell receptor
TF	Transcription factor
TGF	Tranforming groth factor
TGFbR	Tranforming groth factor receptor

TNF-α	Tumor necrosis factor alpha
TRAF	Tumour-necrosis factor receptor-associated factor
µg	Microgramm
VEEV	Venezuelan equine encephalitis virus

REFERENCES

1. Abplanalp, J. & Hottiger, M. O. Cell fate regulation by chromatin ADP-ribosylation. *Semin. Cell Dev. Biol.* **63,** 114–122 (2017).
2. Sandvig, K. & Olsnes, S. Diphtheria toxin entry into cells is facilitated by low pH. *J Cell Biol* **87,** 828–832 (1980).
3. Chen, Y., Johnson, J. A., Pusch, G. D., Morris, J. G. & Stine, O. C. The genome of non-O1 Vibrio cholerae NRT36S demonstrates the presence of pathogenic mechanisms that are distinct from those of O1 Vibrio cholerae. *Infect. Immun.* **75,** 2645–2647 (2007).
4. Antoine, R. & Locht, C. Roles of the disulfide bond and the carboxy-terminal region of the S1 subunit in the assembly and biosynthesis of pertussis toxin. *Infect. Immun.* **58,** 1518–1526 (1990).
5. Aktories, K. *et al.* Botulinum C2 toxin ADP-ribosylates actin. *Nature* **322,** 390–392 (1986).
6. Simon, N. C., Aktories, K. & Barbieri, J. T. Novel bacterial ADP-ribosylating toxins: structure and function. *Nat. Rev. Microbiol.* **12,** 599–611 (2014).
7. Hottiger, M. O. SnapShot: ADP-Ribosylation Signaling. *Molecular Cell* **58,** –1134.e1 (2015).
8. Hottiger, M. O., Hassa, P. O., Lüscher, B., Schüler, H. & Koch-Nolte, F. Toward a unified nomenclature for mammalian ADP-ribosyltransferases. *Trends in Biochemical Sciences* **35,** 208–219 (2010).
9. Seman, M., Adriouch, S., Haag, F. & Koch-Nolte, F. Ecto-ADP-ribosyltransferases (ARTs): emerging actors in cell communication and signaling. *Curr. Med. Chem.* **11,** 857–872 (2004).
10. Haigis, M. C. *et al.* SIRT4 inhibits glutamate dehydrogenase and opposes the effects of calorie restriction in pancreatic beta cells. *Cell* **126,** 941–954 (2006).
11. Mao, Z. *et al.* SIRT6 promotes DNA repair under stress by activating PARP1. *Science* **332,** 1443–1446 (2011).
12. Gupte, R., Liu, Z. & Kraus, W. L. PARPs and ADP-ribosylation: recent advances linking molecular functions to biological outcomes. *Genes Dev.* **31,** 101–126 (2017).
13. Hassa, P. O., Haenni, S. S., Elser, M. & Hottiger, M. O. Nuclear ADP-Ribosylation Reactions in Mammalian Cells: Where Are We Today and Where Are We Going? *Microbiology and Molecular Biology Reviews* **70,** 789–829 (2006).
14. Vyas, S., Chesarone-Cataldo, M., Todorova, T., Huang, Y.-H. & Chang, P. A systematic analysis of the PARP protein family identifies new functions critical for cell physiology. *Nature Communications* **4,** (2013).
15. Vyas, S., Matic, I., Uchima, L., Rood, J. & Zaja, R. Family-wide analysis of poly (ADP-ribose) polymerase activity. *Nature* (2014).
16. Teloni, F. & Altmeyer, M. Readers of poly(ADP-ribose): designed to be fit for purpose. *Nucleic Acids Research* **44,** 993–1006 (2016).
17. Altmeyer, M. & Hottiger, M. O. Poly (ADP-ribose) polymerase 1 at the crossroad of metabolic stress and inflammation in aging. *Aging (Albany NY)* (2009).
18. Hottiger, M. O. Nuclear ADP-Ribosylation and Its Role in Chromatin Plasticity, Cell Differentiation, and Epigenetics. *Annu. Rev. Biochem.* **84,** 227–263 (2015).
19. Kraus, W. L. & Lis, J. T. PARP goes transcription. *Cell* **113,** 677–683 (2003).
20. Kraus, W. L. PARPs and ADP-Ribosylation: 50 Years … and Counting. *Molecular Cell* **58,** 902–910 (2015).
21. Barton, G. M. A calculated response: control of inflammation by the innate immune system. *J. Clin. Invest.* **118,** 413–420 (2008).
22. Medzhitov, R. Origin and physiological roles of inflammation. *Nature* **454,** 428–435 (2008).
23. Bürkle, A. & Virág, L. Poly (ADP-ribose): PARadigms and PARadoxes. *Molecular Aspects of Medicine* (2013).
24. Bianchi, M. E. DAMPs, PAMPs and alarmins: all we need to know about danger. *J Leukoc Biol* **81,** 1–5 (2007).
25. De Vos, M., Schreiber, V. & Dantzer, F. The diverse roles and clinical relevance of PARPs in DNA damage repair: current state of the art. *Biochemical Pharmacology* **84,** 137–146 (2012).
26. Ray Chaudhuri, A. & Nussenzweig, A. The multifaceted roles of PARP1 in DNA repair and chromatin remodelling. *Nat Rev Mol Cell Biol* **18,** 610–621 (2017).
27. Hassa, P. O. & Hottiger, M. O. The diverse biological roles of mammalian PARPS, a small but powerful family of poly-ADP-ribose polymerases. *Front Biosci* (2008).
28. Potaman, V. N., Shlyakhtenko, L. S., Oussatcheva, E. A., Lyubchenko, Y. L. & Soldatenkov, V. A. Specific binding of poly(ADP-ribose) polymerase-1 to cruciform hairpins. *Journal of*

Molecular Biology **348,** 609–615 (2005).
29. Lonskaya, I. *et al.* Regulation of poly(ADP-ribose) polymerase-1 by DNA structure-specific binding. *J. Biol. Chem.* **280,** 17076–17083 (2005).
30. Soldatenkov, V. A., Vetcher, A. A., Duka, T. & Ladame, S. First evidence of a functional interaction between DNA quadruplexes and poly(ADP-ribose) polymerase-1. *ACS Chem. Biol.* **3,** 214–219 (2008).
31. Ali, A. A. E. *et al.* The zinc-finger domains of PARP1 cooperate to recognize DNA strand breaks. *Nature Structural & Molecular Biology* **19,** 685–692 (2012).
32. Robert, I., Karicheva, O., Reina San Martin, B., Schreiber, V. & Dantzer, F. Functional aspects of PARylation in induced and programmed DNA repair processes: preserving genome integrity and modulating physiological events. *Molecular Aspects of Medicine* **34,** 1138–1152 (2013).
33. Curtin, N. J. & Szabó, C. Therapeutic applications of PARP inhibitors: Anticancer therapy and beyond. *Molecular Aspects of Medicine* **34,** 1217–1256 (2013).
34. Luo, X. & Kraus, W. L. On PAR with PARP: cellular stress signaling through poly(ADP-ribose) and PARP-1. *Genes Dev.* **26,** 417–432 (2012).
35. Lazebnik, Y. A., Kaufmann, S. H., Desnoyers, S., Poirier, G. G. & Earnshaw, W. C. Cleavage of poly(ADP-ribose) polymerase by a proteinase with properties like ICE. *Nature* **371,** 346–347 (1994).
36. Virág, L. & Szabó, C. The therapeutic potential of poly(ADP-ribose) polymerase inhibitors. *Pharmacol. Rev.* **54,** 375–429 (2002).
37. Pétrilli, V. *et al.* Noncleavable poly(ADP-ribose) polymerase-1 regulates the inflammation response in mice. *J. Clin. Invest.* **114,** 1072–1081 (2004).
38. Simbulan-Rosenthal, C. M., Rosenthal, D. S., Ding, R., Bhatia, K. & Smulson, M. E. Prolongation of the p53 response to DNA strand breaks in cells depleted of PARP by antisense RNA expression. *Biochem. Biophys. Res. Commun.* **253,** 864–868 (1998).
39. Houtkooper, R. H., Cantó, C., Wanders, R. J. & Auwerx, J. The secret life of NAD+: an old metabolite controlling new metabolic signaling pathways. *Endocr. Rev.* **31,** 194–223 (2010).
40. Skidmore, C. J. *et al.* The involvement of poly(ADP-ribose) polymerase in the degradation of NAD caused by gamma-radiation and N-methyl-N-nitrosourea. *Eur. J. Biochem.* **101,** 135–142 (1979).
41. Goodwin, P. M., Lewis, P. J., Davies, M. I., Skidmore, C. J. & Shall, S. The effect of gamma radiation and neocarzinostatin on NAD and ATP levels in mouse leukaemia cells. *Biochim. Biophys. Acta* **543,** 576–582 (1978).
42. Bai, P. *et al.* PARP-1 Inhibition Increases Mitochondrial Metabolism through SIRT1 Activation. *Cell Metabolism* **13,** 461–468 (2011).
43. Bürkle, A. & Virág, L. Poly(ADP-ribose): PARadigms and PARadoxes. *Molecular Aspects of Medicine* **34,** 1046–1065 (2013).
44. Ha, H. C. & Snyder, S. H. Poly(ADP-ribose) polymerase is a mediator of necrotic cell death by ATP depletion. *Proc Natl Acad Sci USA* **96,** 13978–13982 (1999).
45. Berger, N. A., Sims, J. L., Catino, D. M. & Berger, S. J. Poly(ADP-ribose) polymerase mediates the suicide response to massive DNA damage: studies in normal and DNA-repair defective cells. *Int. Symp. Princess Takamatsu Cancer Res. Fund* **13,** 219–226 (1983).
46. Virág, L., Robaszkiewicz, A., Rodríguez-Vargas, J. M. & Oliver, F. J. Poly(ADP-ribose) signaling in cell death. *Molecular Aspects of Medicine* **34,** 1153–1167 (2013).
47. Goto, S. *et al.* Poly(ADP-ribose) polymerase impairs early and long-term experimental stroke recovery. *Stroke* **33,** 1101–1106 (2002).
48. Paschen, W., Oláh, L. & Mies, G. Effect of transient focal ischemia of mouse brain on energy state and NAD levels: no evidence that NAD depletion plays a major role in secondary disturbances of energy metabolism. *J. Neurochem.* **75,** 1675–1680 (2000).
49. Zhou, Y., Feng, X. & Koh, D. W. Activation of cell death mediated by apoptosis-inducing factor due to the absence of poly(ADP-ribose) glycohydrolase. *Biochemistry* **50,** 2850–2859 (2011).
50. David, K. K., Andrabi, S. A., Dawson, T. M. & Dawson, V. L. Parthanatos, a messenger of death. *Frontiers in bioscience (Landmark edition)* **14,** 1116–1128 (2009).
51. Yu, S.-W. *et al.* Mediation of poly(ADP-ribose) polymerase-1-dependent cell death by apoptosis-inducing factor. *Science* **297,** 259–263 (2002).
52. Galluzzi, L. *et al.* Molecular definitions of cell death subroutines: recommendations of the Nomenclature Committee on Cell Death 2012. *Cell Death Differ.* **19,** 107–120 (2012).
53. Fatokun, A. A., Dawson, V. L. & Dawson, T. M. Parthanatos: mitochondrial-linked

mechanisms and therapeutic opportunities. *Br. J. Pharmacol.* **171,** 2000–2016 (2014).
54. Hangen, E., Blomgren, K., Bénit, P., Kroemer, G. & Modjtahedi, N. Life with or without AIF. *Trends in Biochemical Sciences* **35,** 278–287 (2010).
55. Yu, S.-W. *et al.* Outer mitochondrial membrane localization of apoptosis-inducing factor: mechanistic implications for release. *ASN Neuro* **1,** AN20090046 (2009).
56. Zhu, C. *et al.* Apoptosis-inducing factor is a major contributor to neuronal loss induced by neonatal cerebral hypoxia-ischemia. *Cell Death Differ.* **14,** 775–784 (2007).
57. Klein, J. A. *et al.* The harlequin mouse mutation downregulates apoptosis-inducing factor. *Nature* **419,** 367–374 (2002).
58. Vahsen, N. *et al.* AIF deficiency compromises oxidative phosphorylation. *The EMBO Journal* **23,** 4679–4689 (2004).
59. Andrabi, S. A. *et al.* Poly(ADP-ribose) (PAR) polymer is a death signal. *Proc Natl Acad Sci USA* **103,** 18308–18313 (2006).
60. Yu, S.-W. *et al.* Apoptosis-inducing factor mediates poly(ADP-ribose) (PAR) polymer-induced cell death. *Proc Natl Acad Sci USA* **103,** 18314–18319 (2006).
61. Gagné, J.-P. *et al.* Proteome-wide identification of poly(ADP-ribose) binding proteins and poly(ADP-ribose)-associated protein complexes. *Nucleic Acids Research* **36,** 6959–6976 (2008).
62. Wang, Y. *et al.* Poly(ADP-ribose) (PAR) binding to apoptosis-inducing factor is critical for PAR polymerase-1-dependent cell death (parthanatos). *Sci Signal* **4,** ra20–ra20 (2011).
63. Koh, D. W., Dawson, T. M. & Dawson, V. L. Mediation of cell death by poly(ADP-ribose) polymerase-1. *Pharmacol. Res.* **52,** 5–14 (2005).
64. Maté, M. J. *et al.* The crystal structure of the mouse apoptosis-inducing factor AIF. *Nat. Struct. Biol.* **9,** 442–446 (2002).
65. Ye, H. *et al.* DNA binding is required for the apoptogenic action of apoptosis inducing factor. *Nat. Struct. Biol.* **9,** 680–684 (2002).
66. Kono, H. & Rock, K. L. How dying cells alert the immune system to danger. *Nat. Rev. Immunol.* **8,** 279–289 (2008).
67. Yang, M. *et al.* Poly-ADP-ribosylation of HMGB1 regulates TNFSF10/TRAIL resistance through autophagy. *Autophagy* **11,** 214–224 (2015).
68. Ditsworth, D., Zong, W.-X. & Thompson, C. B. Activation of poly(ADP)-ribose polymerase (PARP-1) induces release of the pro-inflammatory mediator HMGB1 from the nucleus. *J. Biol. Chem.* **282,** 17845–17854 (2007).
69. Yang, Z. *et al.* PARP-1 mediates LPS-induced HMGB1 release by macrophages through regulation of HMGB1 acetylation. *J Immunol* **193,** 6114–6123 (2014).
70. Iwasaki, A. & Medzhitov, R. Control of adaptive immunity by the innate immune system. *Nat. Immunol.* **16,** 343–353 (2015).
71. Hassa, P. O., Buerki, C., Lombardi, C., Imhof, R. & Hottiger, M. O. Transcriptional coactivation of nuclear factor-kappaB-dependent gene expression by p300 is regulated by poly(ADP)-ribose polymerase-1. *J. Biol. Chem.* **278,** 45145–45153 (2003).
72. Hassa, P. O. *et al.* Acetylation of poly(ADP-ribose) polymerase-1 by p300/CREB-binding protein regulates coactivation of NF-kappaB-dependent transcription. *J. Biol. Chem.* **280,** 40450–40464 (2005).
73. Hassa, P. O., Covic, M., Hasan, S., Imhof, R. & Hottiger, M. O. The enzymatic and DNA binding activity of PARP-1 are not required for NF-kappa B coactivator function. *J. Biol. Chem.* **276,** 45588–45597 (2001).
74. Hassa, P. O. & Hottiger, M. O. A role of poly (ADP-ribose) polymerase in NF-kappaB transcriptional activation. *Biol. Chem.* **380,** 953–959 (1999).
75. Martinez-Zamudio, R. & Ha, H. C. Histone ADP-ribosylation facilitates gene transcription by directly remodeling nucleosomes. *Mol. Cell. Biol.* **32,** 2490–2502 (2012).
76. Martínez-Zamudio, R. I. & Ha, H. C. PARP1 enhances inflammatory cytokine expression by alteration of promoter chromatin structure in microglia. *Brain Behav* **4,** 552–565 (2014).
77. Oliver, F. J. *et al.* Resistance to endotoxic shock as a consequence of defective NF-kappaB activation in poly (ADP-ribose) polymerase-1 deficient mice. *The EMBO Journal* **18,** 4446–4454 (1999).
78. Minotti, R., Andersson, A. & Hottiger, M. O. ARTD1 Suppresses Interleukin 6 Expression by Repressing MLL1-Dependent Histone H3 Trimethylation. *Mol. Cell. Biol.* **35,** 3189–3199 (2015).
79. Hayden, M. S. & Ghosh, S. NF-κB, the first quarter-century: remarkable progress and outstanding questions. *Genes Dev.* **26,** 203–234 (2012).

80. Oeckinghaus, A. & Ghosh, S. The NF-kappaB family of transcription factors and its regulation. *Cold Spring Harb Perspect Biol* **1,** a000034–a000034 (2009).
81. Krishnakumar, R. & Kraus, W. L. The PARP Side of the Nucleus: Molecular Actions, Physiological Outcomes, and Clinical Targets. *Molecular Cell* **39,** 8–24 (2010).
82. Rouleau, M., Aubin, R. A. & Poirier, G. G. Poly(ADP-ribosyl)ated chromatin domains: access granted. *Journal of Cell Science* **117,** 815–825 (2004).
83. Althaus, F. R. *et al.* Histone shuttling by poly ADP-ribosylation. *Mol Cell Biochem* **138,** 53–59 (1994).
84. Erener, S. *et al.* Inflammasome-Activated Caspase 7 Cleaves PARP1 to Enhance the Expression of a Subset of NF-kB Target Genes. *Molecular Cell* 1–12 (2012). doi:10.1016/j.molcel.2012.02.016
85. Hassa, P. O. & Hottiger, M. O. The functional role of poly(ADP-ribose)polymerase 1 as novel coactivator of NF-kappaB in inflammatory disorders. *Cell. Mol. Life Sci.* **59,** 1534–1553 (2002).
86. Carrillo, A. *et al.* Transcription regulation of TNF-α-early response genes by poly(ADP-ribose) polymerase-1 in murine heart endothelial cells. *Nucleic Acids Research* **32,** 757–766 (2004).
87. Zerfaoui, M. *et al.* Nuclear translocation of p65 NF-kappaB is sufficient for VCAM-1, but not ICAM-1, expression in TNF-stimulated smooth muscle cells: Differential requirement for PARP-1 expression and interaction. *Cell. Signal.* **20,** 186–194 (2008).
88. Ha, H. C., Hester, L. D. & Snyder, S. H. Poly(ADP-ribose) polymerase-1 dependence of stress-induced transcription factors and associated gene expression in glia. *PNAS* **99,** 3270–3275 (2002).
89. Oliver, F. J. Resistance to endotoxic shock as a consequence of defective NF-kappa B activation in poly (ADP-ribose) polymerase-1 deficient mice. *The EMBO Journal* **18,** 4446–4454 (1999).
90. Akira, S., Uematsu, S. & Takeuchi, O. Pathogen Recognition and Innate Immunity. *Cell* **124,** 783–801 (2006).
91. Gibson, B. A. & Kraus, W. L. New insights into the molecular and cellular functions of poly(ADP-ribose) and PARPs. *Nat Rev Mol Cell Biol* **13,** 411–424 (2012).
92. Kassner, I. *et al.* SET7/9-dependent methylation of ARTD1 at K508 stimulates poly-ADP-ribose formation after oxidative stress. *Open Biol* **3,** 120173–120173 (2013).
93. Ke, Y. *et al.* PARP1 promotes gene expression at the post-transcriptiona level by modulating the RNA-binding protein HuR. *Nature Communications* **8,** 14632 (2017).
94. Ivanov, P. & Anderson, P. Post-transcriptional regulatory networks in immunity. *Immunological Reviews* **253,** 253–272 (2013).
95. Ji, Y. & Tulin, A. V. Post-transcriptional regulation by poly(ADP-ribosyl)ation of the RNA-binding proteins. *Int J Mol Sci* **14,** 16168–16183 (2013).
96. Galbis-Martínez, M., Saenz, L., Ramírez, P., Parrilla, P. & Yélamos, J. Poly(ADP-ribose) polymerase-1 modulates interferon-gamma-inducible protein (IP)-10 expression in murine embryonic fibroblasts by stabilizing IP-10 mRNA. *Mol. Immunol.* **47,** 1492–1499 (2010).
97. Rothenberg, E. V. & Taghon, T. Molecular genetics of T cell development. *Annu. Rev. Immunol.* **23,** 601–649 (2005).
98. Grossman, Z. & Paul, W. E. Dynamic tuning of lymphocytes: physiological basis, mechanisms, and function. *Annu. Rev. Immunol.* **33,** 677–713 (2015).
99. Yélamos, J. *et al.* PARP-2 deficiency affects the survival of CD4 CD8+ double-positive thymocytes. *The EMBO Journal* **25,** 4350–4360 (2006).
100. Navarro, J. *et al.* PARP-1/PARP-2 double deficiency in mouse T cells results in faulty immune responses and T lymphomas. *Nature Publishing Group* **7,** 41962 (2017).
101. Huang, J., Meyer, C. & Zhu, C. T cell antigen recognition at the cell membrane. *Mol. Immunol.* **52,** 155–164 (2012).
102. Adriouch, S. *et al.* ADP-ribosylation at R125 gates the P2X7 ion channel by presenting a covalent ligand to its nucleotide binding site. *FASEB J.* **22,** 861–869 (2008).
103. Adriouch, S., Ohlrogge, W., Haag, F., Koch-Nolte, F. & Seman, M. Rapid induction of naive T cell apoptosis by ecto-nicotinamide adenine dinucleotide: requirement for mono(ADP-ribosyl)transferase 2 and a downstream effector. *J. Immunol.* **167,** 196–203 (2001).
104. Liu, Z. X., Azhipa, O., Okamoto, S., Govindarajan, S. & Dennert, G. Extracellular nicotinamide adenine dinucleotide induces t cell apoptosis in vivo and in vitro. *J. Immunol.* **167,** 4942–4947 (2001).
105. Okamoto, S., Azhipa, O., Yu, Y., Russo, E. & Dennert, G. Expression of ADP-

ribosyltransferase on normal T lymphocytes and effects of nicotinamide adenine dinucleotide on their function. *J. Immunol.* **160,** 4190–4198 (1998).
106. Rissiek, B., Haag, F., Boyer, O., Koch-Nolte, F. & Adriouch, S. P2X7 on Mouse T Cells: One Channel, Many Functions. *Frontiers in Immunology* **6,** 204 (2015).
107. Bluestone, J. A., Mackay, C. R., O'Shea, J. J. & Stockinger, B. The functional plasticity of T cell subsets. *Nat. Rev. Immunol.* **9,** 811–816 (2009).
108. Shevach, E. M. Certified professionals: CD4(+)CD25(+) suppressor T cells. *The Journal of experimental medicine* **193,** F41–6 (2001).
109. Fontenot, J. D. & Rudensky, A. Y. A well adapted regulatory contrivance: regulatory T cell development and the forkhead family transcription factor Foxp3. *Nat. Immunol.* **6,** 331–337 (2005).
110. Zhang, P. *et al.* PARP-1 regulates expression of TGF-β receptors in T cells. *Blood* **122,** 2224–2232 (2013).
111. Nasta, F., Laudisi, F., Sambucci, M., Rosado, M. M. & Pioli, C. Increased Foxp3+ regulatory T cells in poly(ADP-Ribose) polymerase-1 deficiency. *J Immunol* **184,** 3470–3477 (2010).
112. Zhang, P. *et al.* PARP-1 controls immunosuppressive function of regulatory T cells by destabilizing Foxp3. *PLoS ONE* **8,** e71590 (2013).
113. Macian, F. NFAT proteins: key regulators of T-cell development and function. *Nat. Rev. Immunol.* **5,** 472–484 (2005).
114. Olabisi, O. A. *et al.* Regulation of transcription factor NFAT by ADP-ribosylation. *Mol. Cell. Biol.* **28,** 2860–2871 (2008).
115. Valdor, R. *et al.* Regulation of NFAT by poly(ADP-ribose) polymerase activity in T cells. *Mol. Immunol.* **45,** 1863–1871 (2008).
116. Saenz, L. *et al.* Transcriptional regulation by poly(ADP-ribose) polymerase-1 during T cell activation. *BMC Genomics* **9,** 171 (2008).
117. Jagtap, P. & Szabó, C. Poly(ADP-ribose) polymerase and the therapeutic effects of its inhibitors. *Nature Reviews Drug Discovery* **4,** 421–440 (2005).
118. Barry, M. & Bleackley, R. C. Cytotoxic T lymphocytes: all roads lead to death. *Nat. Rev. Immunol.* **2,** 401–409 (2002).
119. Nathan, C. Points of control in inflammation. *Nature* **420,** 846–852 (2002).
120. Murray, P. J. *et al.* Macrophage activation and polarization: nomenclature and experimental guidelines. *Immunity* **41,** 14–20 (2014).
121. Iwata, H. *et al.* PARP9 and PARP14 cross-regulate macrophage activation via STAT1 ADP-ribosylation. *Nature Communications* **7,** 12849 (2016).
122. Verheugd, P., Forst, A. H., Milke, L. & Herzog, N. Regulation of NF-κB signalling by the mono-ADP-ribosyltransferase ARTD10. *Nature* (2013).
123. Kolaczkowska, E. & Kubes, P. Neutrophil recruitment and function in health and inflammation. *Nat. Rev. Immunol.* **13,** 159–175 (2013).
124. Kefalas, P., Saxty, B., Yadollahi-Farsani, M. & MacDermot, J. Chemotaxin-dependent translocation of immunoreactive ADP-ribosyltransferase-1 to the surface of human neutrophil polymorphs. *Eur. J. Biochem.* **259,** 866–871 (1999).
125. Grahnert, A. *et al.* Review: NAD +: a modulator of immune functions. *Innate Immun* **17,** 212–233 (2011).
126. Paone, G. *et al.* ADP ribosylation of human neutrophil peptide-1 regulates its biological properties. *Proc Natl Acad Sci USA* **99,** 8231–8235 (2002).
127. Paone, G. *et al.* ADP-ribosyltransferase-specific modification of human neutrophil peptide-1. *J. Biol. Chem.* **281,** 17054–17060 (2006).
128. Moser, M. & Leo, O. Key concepts in immunology. *Vaccine* **28 Suppl 3,** C2–13 (2010).
129. Xu, Z., Zan, H., Pone, E. J., Mai, T. & Casali, P. Immunoglobulin class-switch DNA recombination: induction, targeting and beyond. *Nat. Rev. Immunol.* **12,** 517–531 (2012).
130. Ambrose, H. E. *et al.* Poly(ADP-ribose) polymerase-1 (Parp-1)-deficient mice demonstrate abnormal antibody responses. *Immunology* **127,** 178–186 (2009).
131. Shockett, P. & Stavnezer, J. Inhibitors of poly(ADP-ribose) polymerase increase antibody class switching. *J. Immunol.* **151,** 6962–6976 (1993).
132. Mehrotra, P. *et al.* PARP-14 Functions as a Transcriptional Switch for Stat6-dependent Gene Activation. *J. Biol. Chem.* **286,** 1767–1776 (2011).
133. Chen, J.-K., Lin, W.-L., Chen, Z. & Liu, H.-W. PARP-1-dependent recruitment of cold-inducible RNA-binding protein promotes double-strand break repair and genome stability. *PNAS* **115,** E1759–E1768 (2018).
134. McLornan, D. P., List, A. & Mufti, G. J. Applying synthetic lethality for the selective

targeting of cancer. *N. Engl. J. Med.* **371,** 1725–1735 (2014).
135. Lord, C. J. & Ashworth, A. PARP inhibitors: Synthetic lethality in the clinic. *Science* **355,** 1152–1158 (2017).
136. Terada, M., Fujiki, H., Marks, P. A. & Sugimura, T. Induction of erythroid differentiation of murine erythroleukemia cells by nicotinamide and related compounds. *Proc Natl Acad Sci USA* **76,** 6411–6414 (1979).
137. Purnell, M. R. & Whish, W. J. Novel inhibitors of poly(ADP-ribose) synthetase. *Biochem. J.* **185,** 775–777 (1980).
138. Brightwell, M. D., Leech, C. E., O'Farrell, M. K., Whish, W. J. & Shall, S. Poly(adenosine diphosphate ribose) polymerase in Physarum polycephalum. *Biochem. J.* **147,** 119–129 (1975).
139. Peralta-Leal, A. *et al.* PARP inhibitors: New partners in the therapy of cancer and inflammatory diseases. *Free Radical Biology and Medicine* **47,** 13–26 (2009).
140. Shen, Y. *et al.* BMN673, a Novel and Highly Potent PARP1/2 Inhibitor for the Treatment of Human Cancers with DNA Repair Deficiency. *Clin Cancer Res* **19,** 5003–5015 (2013).
141. Benafif, S. & Hall, M. An update on PARP inhibitors for the treatment of cancer. *Onco Targets Ther* **8,** 519–528 (2015).
142. Lord, C. J. & Ashworth, A. Mechanisms of resistance to therapies targeting BRCA-mutant cancers. *Nat. Med.* **19,** 1381–1388 (2013).
143. Farmer, H. *et al.* Targeting the DNA repair defect in BRCA mutant cells as a therapeutic strategy. *Nature* **434,** 917–921 (2005).
144. Bryant, H. E. *et al.* Specific killing of BRCA2-deficient tumours with inhibitors of poly(ADP-ribose) polymerase. *Nature* **434,** 913–917 (2005).
145. Murai, J. *et al.* Stereospecific PARP trapping by BMN 673 and comparison with olaparib and rucaparib. *Mol. Cancer Ther.* **13,** 433–443 (2014).
146. Murai, J. *et al.* Trapping of PARP1 and PARP2 by Clinical PARP Inhibitors. *Cancer Res* **72,** 5588–5599 (2012).
147. Pommier, Y., O'Connor, M. J. & de Bono, J. Laying a trap to kill cancer cells: PARP inhibitors and their mechanisms of action. *Sci Transl Med* **8,** 362ps17–362ps17 (2016).
148. Wahlberg, E. *et al.* Family-wide chemical profiling and structural analysis of PARP and tankyrase inhibitors. *Nature Biotechnology* **30,** 283–288 (2012).
149. Hottiger, M. O. Poly (ADP-ribose) polymerase inhibitor therapeutic effect: are we just scratching the surface? *Expert opinion on therapeutic targets* (2015).
150. Berger, N. A. *et al.* Opportunities for the repurposing of PARP inhibitors for the therapy of non-oncological diseases. *Br. J. Pharmacol.* **175,** 192–222 (2018).
151. Giansanti, V., Donà, F., Tillhon, M. & Scovassi, A. I. PARP inhibitors: New tools to protect from inflammation. *Biochemical Pharmacology* **80,** 1869–1877 (2010).
152. Manev, H., Favaron, M., Guidotti, A. & Costa, E. Delayed increase of Ca2+ influx elicited by glutamate: role in neuronal death. *Mol. Pharmacol.* **36,** 106–112 (1989).
153. Lai, T. W., Zhang, S. & Wang, Y. T. Excitotoxicity and stroke: identifying novel targets for neuroprotection. *Prog. Neurobiol.* **115,** 157–188 (2014).
154. Szabó, C. & Dawson, V. L. Role of poly(ADP-ribose) synthetase in inflammation and ischaemia-reperfusion. *Trends Pharmacol. Sci.* **19,** 287–298 (1998).
155. Alano, C. C., Ying, W. & Swanson, R. A. Poly(ADP-ribose) polymerase-1-mediated cell death in astrocytes requires NAD+ depletion and mitochondrial permeability transition. *J. Biol. Chem.* **279,** 18895–18902 (2004).
156. Chiu, L.-Y., Ho, F.-M., Shiah, S.-G., Chang, Y. & Lin, W.-W. Oxidative stress initiates DNA damager MNNG-induced poly(ADP-ribose)polymerase-1-dependent parthanatos cell death. *Biochemical Pharmacology* **81,** 459–470 (2011).
157. Mandir, A. S. *et al.* NMDA but not non-NMDA excitotoxicity is mediated by Poly(ADP-ribose) polymerase. *J. Neurosci.* **20,** 8005–8011 (2000).
158. Culmsee, C. *et al.* Apoptosis-inducing factor triggered by poly(ADP-ribose) polymerase and Bid mediates neuronal cell death after oxygen-glucose deprivation and focal cerebral ischemia. *J. Neurosci.* **25,** 10262–10272 (2005).
159. Li, X. *et al.* Contributions of poly(ADP-ribose) polymerase-1 and -2 to nuclear translocation of apoptosis-inducing factor and injury from focal cerebral ischemia. *J. Neurochem.* **113,** 1012–1022 (2010).
160. Wang, H., Shimoji, M., Yu, S.-W., Dawson, T. M. & Dawson, V. L. Apoptosis inducing factor and PARP-mediated injury in the MPTP mouse model of Parkinson's disease. *Ann. N. Y. Acad. Sci.* **991,** 132–139 (2003).

161. van der Poll, T., van de Veerdonk, F. L., Scicluna, B. P. & Netea, M. G. The immunopathology of sepsis and potential therapeutic targets. *Nat. Rev. Immunol.* **17,** 407–420 (2017).
162. van der Poll, T. & Opal, S. M. Host-pathogen interactions in sepsis. *Lancet Infect Dis* **8,** 32–43 (2008).
163. Schulte, W., Bernhagen, J. & Bucala, R. Cytokines in sepsis: potent immunoregulators and potential therapeutic targets--an updated view. *Mediators Inflamm.* **2013,** 165974–16 (2013).
164. Liaudet, L. *et al.* Protection against hemorrhagic shock in mice genetically deficient in poly(ADP-ribose)polymerase. *Proc Natl Acad Sci USA* **97,** 10203–10208 (2000).
165. Soriano, F. G. *et al.* Resistance to acute septic peritonitis in poly(ADP-ribose) polymerase-1-deficient mice. *Shock* **17,** 286–292 (2002).
166. Jagtap, P., Soriano, F. G., Virág, L. & Liaudet, L. Novel phenanthridinone inhibitors of poly (adenosine 5'-diphosphate-ribose) synthetase: potent cytoprotective and antishock agents. *Crit Care* (2002).
167. García, S. & Conde, C. The Role of Poly(ADP-ribose) Polymerase-1 in Rheumatoid Arthritis. *Mediators Inflamm.* **2015,** (2015).
168. Mabley, J. G. *et al.* Anti-inflammatory effects of a novel, potent inhibitor of poly (ADP-ribose) polymerase. *Inflamm. Res.* **50,** 561–569 (2001).
169. Szabó, C. *et al.* Protection against peroxynitrite-induced fibroblast injury and arthritis development by inhibition of poly(ADP-ribose) synthase. *Proc Natl Acad Sci USA* **95,** 3867–3872 (1998).
170. Gonzalez-Rey, E. *et al.* Therapeutic Effect of a Poly(ADP-Ribose) Polymerase-1 Inhibitor on Experimental Arthritis by Downregulating Inflammation and Th1 Response. *PLoS ONE* **2,** e1071 (2007).
171. García, S., Bodaño, A., Pablos, J. L., Gómez-Reino, J. J. & Conde, C. Poly(ADP-ribose) polymerase inhibition reduces tumor necrosis factor-induced inflammatory response in rheumatoid synovial fibroblasts. *Ann. Rheum. Dis.* **67,** 631–637 (2008).
172. Szabó, C. Roles of poly(ADP-ribose) polymerase activation in the pathogenesis of diabetes mellitus and its complications. *Pharmacol. Res.* **52,** 60–71 (2005).
173. Xie, Z., Chang, C. & Zhou, Z. Molecular mechanisms in autoimmune type 1 diabetes: a critical review. *Clin Rev Allergy Immunol* **47,** 174–192 (2014).
174. Rerup, C. C. Drugs producing diabetes through damage of the insulin secreting cells. *Pharmacol. Rev.* **22,** 485–518 (1970).
175. Rossini, A. A., Like, A. A., Chick, W. L., Appel, M. C. & Cahill, G. F. Studies of streptozotocin-induced insulitis and diabetes. *Proc Natl Acad Sci USA* **74,** 2485–2489 (1977).
176. Kolb, H. Mouse models of insulin dependent diabetes: low-dose streptozocin-induced diabetes and nonobese diabetic (NOD) mice. *Diabetes Metab Rev* **3,** 751–778 (1987).
177. Uchigata, Y., Yamamoto, H., Kawamura, A. & Okamoto, H. Protection by superoxide dismutase, catalase, and poly(ADP-ribose) synthetase inhibitors against alloxan- and streptozotocin-induced islet DNA strand breaks and against the inhibition of proinsulin synthesis. *J. Biol. Chem.* **257,** 6084–6088 (1982).
178. Yellon, D. M. & Hausenloy, D. J. Myocardial reperfusion injury. *N. Engl. J. Med.* **357,** 1121–1135 (2007).
179. Pillai, J. B., Isbatan, A., Imai, S.-I. & Gupta, M. P. Poly(ADP-ribose) polymerase-1-dependent cardiac myocyte cell death during heart failure is mediated by NAD+ depletion and reduced Sir2alpha deacetylase activity. *J. Biol. Chem.* **280,** 43121–43130 (2005).
180. Rosado, M. M., Bennici, E., Novelli, F. & Pioli, C. Beyond DNA repair, the immunological role of PARP-1 and its siblings. *Immunology* **139,** 428–437 (2013).
181. Liaudet, L. *et al.* Suppression of poly (ADP-ribose) polymerase activation by 3-aminobenzamide in a rat model of myocardial infarction: long-term morphological and functional consequences. *Br. J. Pharmacol.* **133,** 1424–1430 (2001).
182. Xavier, R. J. & Podolsky, D. K. Unravelling the pathogenesis of inflammatory bowel disease. *Nature* **448,** 427–434 (2007).
183. Perše, M. & Cerar, A. Dextran sodium sulphate colitis mouse model: traps and tricks. *J. Biomed. Biotechnol.* **2012,** 718617–13 (2012).
184. Mazzon, E. *et al.* GPI 6150, a PARP inhibitor, reduces the colon injury caused by dinitrobenzene sulfonic acid in the rat. *Biochemical Pharmacology* **64,** 327–337 (2002).
185. Sánchez-Fidalgo, S., Villegas, I., Martín, A., Sánchez-Hidalgo, M. & Alarcón de la Lastra, C. PARP inhibition reduces acute colonic inflammation in rats. *Eur. J. Pharmacol.* **563,** 216–223 (2007).

186. Di Paola, R. *et al.* Treatment with PARP-1 inhibitors, GPI 15427 or GPI 16539, ameliorates intestinal damage in rat models of colitis and shock. *Eur. J. Pharmacol.* **527,** 163–171 (2005).
187. Zingarelli, B., O'connor, M. & Hake, P. W. Inhibitors of poly (ADP-ribose) polymerase modulate signal transduction pathways in colitis. *Eur. J. Pharmacol.* **469,** 183–194 (2003).
188. Zingarelli, B. *et al.* Activator protein-1 signalling pathway and apoptosis are modulated by poly(ADP-ribose) polymerase-1 in experimental colitis. *Immunology* **113,** 509–517 (2004).
189. Jijon, H. B. *et al.* Inhibition of poly(ADP-ribose) polymerase attenuates inflammation in a model of chronic colitis. *Am. J. Physiol. Gastrointest. Liver Physiol.* **279,** G641–51 (2000).
190. Larmonier, C. B. *et al.* Transcriptional Reprogramming and Resistance to Colonic Mucosal Injury in Poly(ADP-ribose) Polymerase 1 (PARP1)-deficient Mice. *J. Biol. Chem.* **291,** 8918–8930 (2016).
191. Verheugd, P., Bütepage, M., Eckei, L. & Lüscher, B. Players in ADP-ribosylation: Readers and Erasers. *Curr. Protein Pept. Sci.* **17,** 654–667 (2016).
192. Min, W. & Wang, Z.-Q. Poly (ADP-ribose) glycohydrolase (PARG) and its therapeutic potential. *Frontiers in bioscience (Landmark edition)* **14,** 1619–1626 (2009).
193. Meyer-Ficca, M. L., Meyer, R. G., Coyle, D. L., Jacobson, E. L. & Jacobson, M. K. Human poly(ADP-ribose) glycohydrolase is expressed in alternative splice variants yielding isoforms that localize to different cell compartments. *Exp. Cell Res.* **297,** 521–532 (2004).
194. Brochu, G. *et al.* Mode of action of poly(ADP-ribose) glycohydrolase. *Biochim. Biophys. Acta* **1219,** 342–350 (1994).
195. Di Meglio, S. *et al.* Poly(ADPR) polymerase-1 and poly(ADPR) glycohydrolase level and distribution in differentiating rat germinal cells. *Mol Cell Biochem* **248,** 85–91 (2003).
196. Gao, H. *et al.* Altered poly(ADP-ribose) metabolism impairs cellular responses to genotoxic stress in a hypomorphic mutant of poly(ADP-ribose) glycohydrolase. *Exp. Cell Res.* **313,** 984–996 (2007).
197. Brochu, G., Shah, G. M. & Poirier, G. G. Purification of poly(ADP-ribose) glycohydrolase and detection of its isoforms by a zymogram following one- or two-dimensional electrophoresis. *Anal. Biochem.* **218,** 265–272 (1994).
198. Cortes, U. *et al.* Depletion of the 110-kilodalton isoform of poly(ADP-ribose) glycohydrolase increases sensitivity to genotoxic and endotoxic stress in mice. *Mol. Cell. Biol.* **24,** 7163–7178 (2004).
199. Meyer, R. G., Meyer-Ficca, M. L., Whatcott, C. J., Jacobson, E. L. & Jacobson, M. K. Two small enzyme isoforms mediate mammalian mitochondrial poly(ADP-ribose) glycohydrolase (PARG) activity. *Exp. Cell Res.* **313,** 2920–2936 (2007).
200. Genovese, T. *et al.* Treatment with a novel poly(ADP-ribose) glycohydrolase inhibitor reduces development of septic shock-like syndrome induced by zymosan in mice. *Crit. Care Med.* **32,** 1365–1374 (2004).
201. Cuzzocrea, S. *et al.* PARG activity mediates intestinal injury induced by splanchnic artery occlusion and reperfusion. *FASEB J.* **19,** 558–566 (2005).
202. Lu, X.-C. M. *et al.* Post-treatment with a novel PARG inhibitor reduces infarct in cerebral ischemia in the rat. *Brain Res.* **978,** 99–103 (2003).
203. Patel, N. S. A. *et al.* Mice lacking the 110-kD isoform of poly(ADP-ribose) glycohydrolase are protected against renal ischemia/reperfusion injury. *J. Am. Soc. Nephrol.* **16,** 712–719 (2005).
204. Cuzzocrea, S. *et al.* Role of poly(ADP-ribose) glycohydrolase in the development of inflammatory bowel disease in mice. *Free Radical Biology and Medicine* **42,** 90–105 (2007).
205. Atasheva, S., Frolova, E. I. & Frolov, I. Interferon-Stimulated Poly(ADP-Ribose) Polymerases Are Potent Inhibitors of Cellular Translation and Virus Replication. *J. Virol.* **88,** 2116–2130 (2014).
206. Zhang, Y. *et al.* PARP9-DTX3L ubiquitin ligase targets host histone H2BJ and viral 3C protease to enhance interferon signaling and control viral infection. *Nat. Immunol.* (2015). doi:10.1038/ni.3279
207. Seo, G. J. *et al.* Reciprocal inhibition between intracellular antiviral signaling and the RNAi machinery in mammalian cells. *Cell Host Microbe* **14,** 435–445 (2013).
208. Gao, G., Guo, X. & Goff, S. P. Inhibition of retroviral RNA production by ZAP, a CCCH-type zinc finger protein. *Science* **297,** 1703–1706 (2002).
209. Leung, A., Todorova, T., Ando, Y. & Chang, P. Poly(ADP-ribose) regulates post-transcriptional gene regulation in the cytoplasm. *RNA Biology* **9,** 542–548 (2012).
210. Kozaki, T. *et al.* Mitochondrial damage elicits a TCDD-inducible poly(ADP-ribose)

polymerase-mediated antiviral response. *PNAS* **114,** 2681–2686 (2017).
211. Riffell, J. L., Lord, C. J. & Ashworth, A. Tankyrase-targeted therapeutics: expanding opportunities in the PARP family. *Nature Reviews Drug Discovery* **11,** 923–936 (2012).
212. Li, Z. *et al.* Herpes simplex virus requires poly(ADP-ribose) polymerase activity for efficient replication and induces extracellular signal-related kinase-dependent phosphorylation and ICP0-dependent nuclear localization of tankyrase 1. *J. Virol.* **86,** 492–503 (2012).
213. Wang, G. *et al.* PARP-1 Inhibitor, DPQ, Attenuates LPS-Induced Acute Lung Injury through Inhibiting NF-kappa B-Mediated Inflammatory Response. *PLoS ONE* **8,** (2013).
214. Herberman, R. B., Nunn, M. E. & Lavrin, D. H. Natural cytotoxic reactivity of mouse lymphoid cells against syngeneic acid allogeneic tumors. I. Distribution of reactivity and specificity. *Int. J. Cancer* **16,** 216–229 (1975).
215. Mandal, A. & Viswanathan, C. Natural killer cells: In health and disease. *Hematol Oncol Stem Cell Ther* **8,** 47–55 (2015).
216. Chiche, L. *et al.* The role of natural killer cells in sepsis. *J. Biomed. Biotechnol.* **2011,** 986491–8 (2011).
217. Ramirez-Carrozzi, V. R. *et al.* Selective and antagonistic functions of SWI/SNF and Mi-2beta nucleosome remodeling complexes during an inflammatory response. *Genes Dev.* **20,** 282–296 (2006).
218. Liu, M. *et al.* CXCL10/IP-10 in infectious diseases pathogenesis and potential therapeutic implications. *Cytokine Growth Factor Rev.* **22,** 121–130 (2011).
219. Dabitao, D., Hedrich, C. M., Wang, F., Vacharathit, V. & Bream, J. H. Cell-Specific Requirements for STAT Proteins and Type I IFN Receptor Signaling Discretely Regulate IL-24 and IL-10 Expression in NK Cells and Macrophages. *J Immunol* **200,** 2154–2164 (2018).
220. Meyer-Ficca, M. L. *et al.* Spermatid head elongation with normal nuclear shaping requires ADP-ribosyltransferase PARP11 (ARTD11) in mice. *Biol Reprod* **92,** 80–80 (2015).
221. Wang, Z. Q. *et al.* Mice lacking ADPRT and poly(ADP-ribosyl)ation develop normally but are susceptible to skin disease. *Genes Dev.* **9,** 509–520 (1995).
222. Boehler, C. *et al.* Phenotypic characterization of Parp-1 and Parp-2 deficient mice and cells. *Methods Mol. Biol.* **780,** 313–336 (2011).
223. Feil, S., Valtcheva, N. & Feil, R. Inducible Cre mice. *Methods Mol. Biol.* **530,** 343–363 (2009).
224. Zhang, X., Goncalves, R. & Mosser, D. M. The isolation and characterization of murine macrophages. *Curr Protoc Immunol* **Chapter 14,** Unit 14.1 (2008).
225. Fortier, A. H. & Falk, L. A. Isolation of murine macrophages. *Curr Protoc Immunol* **Chapter 14,** Unit 14.1–14.1.9 (2001).
226. Kingston, R. E., Chen, C. A. & Rose, J. K. Calcium phosphate transfection. *Curr Protoc Mol Biol* **Chapter 9,** Unit 9.1 (2003).
227. Abplanalp, J. *et al.* Proteomic analyses identify ARH3 as a serine mono-ADP-ribosylhydrolase. *Nature Communications* **8,** 2055 (2017).
228. Zhao, Q., Du, Q., Wei, F., Xie, J. & Ma, X. An Infectious Disease-Associated Il12b Polymorphism Regulates IL-12/23 p40 Transcription Involving Poly(ADP-Ribose) Polymerase 1. *J Immunol* **198,** 2935–2942 (2017).
229. Trinchieri, G. Interleukin-12 and the regulation of innate resistance and adaptive immunity. *Nat. Rev. Immunol.* **3,** 133–146 (2003).
230. Plevy, S. E., Gemberling, J. H., Hsu, S., Dorner, A. J. & Smale, S. T. Multiple control elements mediate activation of the murine and human interleukin 12 p40 promoters: evidence of functional synergy between C/EBP and Rel proteins. *Mol. Cell. Biol.* **17,** 4572–4588 (1997).
231. Zhu, C., Gagnidze, K., Gemberling, J. H. & Plevy, S. E. Characterization of an activation protein-1-binding site in the murine interleukin-12 p40 promoter. Demonstration of novel functional elements by a reductionist approach. *J. Biol. Chem.* **276,** 18519–18528 (2001).
232. Murphy, T. L., Cleveland, M. G., Kulesza, P., Magram, J. & Murphy, K. M. Regulation of interleukin 12 p40 expression through an NF-kappa B half-site. *Mol. Cell. Biol.* **15,** 5258–5267 (1995).
233. Weinmann, A. S. *et al.* Nucleosome remodeling at the IL-12 p40 promoter is a TLR-dependent, Rel-independent event. *Nat. Immunol.* **2,** 51–57 (2001).
234. Whitehouse, I. *et al.* Nucleosome mobilization catalysed by the yeast SWI/SNF complex. *Nature* **400,** 784–787 (1999).
235. Lai, D. *et al.* Induction of TLR4-target genes entails calcium/calmodulin-dependent regulation of chromatin remodeling. *PNAS* **106,** 1169–1174 (2009).

236. Becker, P. B. & Hörz, W. ATP-dependent nucleosome remodeling. *Annu. Rev. Biochem.* **71,** 247–273 (2002).
237. Schuhwerk, H. *et al.* Kinetics of poly(ADP-ribosyl)ation, but not PARP1 itself, determines the cell fate in response to DNA damage in vitro and in vivo. *Nucleic Acids Research* **45,** 11174–11192 (2017).
238. Fowler, T., Sen, R. & Roy, A. L. Regulation of primary response genes. *Molecular Cell* **44,** 348–360 (2011).
239. Buenrostro, J. D., Wu, B., Chang, H. Y. & Greenleaf, W. J. ATAC-seq: A Method for Assaying Chromatin Accessibility Genome-Wide. *Curr Protoc Mol Biol* **109,** 21.29.1–9 (2015).
240. Deutschman, C. S. & Tracey, K. J. Sepsis: current dogma and new perspectives. *Immunity* **40,** 463–475 (2014).
241. Heremans, H., Dillen, C., van Damme, J. & Billiau, A. Essential role for natural killer cells in the lethal lipopolysaccharide-induced Shwartzman-like reaction in mice. *European Journal of Immunology* **24,** 1155–1160 (1994).
242. Sherwood, E. R., Enoh, V. T., Murphey, E. D. & Lin, C. Y. Mice depleted of CD8+ T and NK cells are resistant to injury caused by cecal ligation and puncture. *Lab. Invest.* **84,** 1655–1665 (2004).
243. CHAMBON, P., WEILL, J. D. & Mandel, P. Nicotinamide mononucleotide activation of new DNA-dependent polyadenylic acid synthesizing nuclear enzyme. *Biochem. Biophys. Res. Commun.* **11,** 39–43 (1963).
244. Masutani, M. *et al.* Function of poly(ADP-ribose) polymerase in response to DNA damage: gene-disruption study in mice. *Mol Cell Biochem* **193,** 149–152 (1999).
245. de Murcia, J. M. *et al.* Requirement of poly(ADP-ribose) polymerase in recovery from DNA damage in mice and in cells. *Proc Natl Acad Sci USA* **94,** 7303–7307 (1997).
246. Abram, C. L., Roberge, G. L., Hu, Y. & Lowell, C. A. Comparative analysis of the efficiency and specificity of myeloid-Cre deleting strains using ROSA-EYFP reporter mice. *J. Immunol. Methods* **408,** 89–100 (2014).
247. Cohen, M. S. & Chang, P. Insights into the biogenesis, function, and regulation of ADP-ribosylation. *Nature Chemical Biology* **14,** 236–243 (2018).
248. Carter-O'Connell, I. *et al.* Identifying Family-Member-Specific Targets of Mono-ARTDs by Using a Chemical Genetics Approach. *Cell Rep* (2016). doi:10.1016/j.celrep.2015.12.045

ACKNOWLDEGEMENTS

First of all, I am very grateful to my scientific mentor Prof. Dr. Hottiger who believed in me long time before I did it myself. His everlasting support, motivation, advice and patience shaped me to the scientist I am today. Thank you so much!

Additionally, I would like to thank my thesis committee Prof. Sabine Werner, Prof. Jean Pieters and Prof. Burkhard Becher for critical discussions, valuable scientific recommendations and technical assistance during the committee meetings and beyond. I also want to thank my collaborators Juliana Komuczki and Margit Lanzinger from the Becherlab for teaching me everything I know about mice work; and Michael Bauer and Anne Müller for their experimental help and critical discussions. Acknowledgements go also to Prof. Dr. José Yelamos who kindly agreed to be external reviewer for this thesis. Not to forget Tobias Suter for his work during the writing of the thesis and the paper.

A big thanks goes to the institute for help and an enjoyable working atmosphere. The Hottigerlab was a great place to work and laugh: Thanks to Jeannatte for teaching me Swiss German, thanks to Anka for teaching me creativity, thanks to Kathi for being Kathi, thanks to Lavi for memorable small group meetings, thanks to Alessandra for counting down the days and thanks to Yessika for pulling irony up on the next level. All your support meant a lot for me.

I am humble and thankful for all the people I met during my journey in Zürich, many of which became friends: The social geniuses Flo&Schelli, time-optimizing gsprütze wisse drinking Eva, sports-addicted Anneli&Matthias and the true scientific geniuses Mario and Damian from the Bierhalle Wouf.

I would not be standing here today without the lifelong support from my parents. I am thankful for what you have made possible for me. Kira, words cannot express my love for you. I am deeply grateful of you being a part of my life. Thank you for everything!

CURRICULUM VITAE

Personal information

Name	Kunze
First Name	Friedrich Alexander
Date of Birth	12. May 1987
Place of Birth	Bonn, Germany
Address	Loeschckestr. 25, 53129 Bonn, Germany
Email	FriedrichKunze@gmx.de

Education

PhD candidate in Molecular Life Sciences 10/2013 -

University of Zurich (UZH), Switzerland present
Dept. of Molecular Mechanisms of Disease
PhD Program in Molecular Life Sciences, LSZGS

Thesis title:
"Elucidating the Function of ARTD1 in Macrophages *In Vivo*"
Supervisor: Prof. Michael Hottiger

Master of Science in Molecular Biotechnology 10/2011 –

Rheinische-Friedrich-Wilhelms Universität Bonn, Germany 03/2013
Center of Molecular Biotechnology

Master Thesis, University Hospital Bonn, Institute of Pathology
"The role of the potential tumor suppressor gene *FOXF1* in prostate cancer"
Supervisors: Prof. Sven Perner, Prof. Reiner Probstmeier

Bachelor of Science (double degree) 10/2007 –

University of Applied Science Bonn-Rhein-Sieg, Germany 09/2010
HAN University of Applied Science Nijmegen, Netherlands

German Abitur 08/1997 –

Friedrich-Ebert-Gymnasium, Bonn, Germany 07/2006

Publications

1. M. Lehmann, E. Pirinen, A. Mirsaidi, **F. A. Kunze**, P. J. Richards, J. Auwerx, and M. O. Hottiger, "ARTD1-induced poly-ADP-ribose formation enhances PPARγ ligand binding and co-factor exchange.," Nucleic Acids Research, vol. 43, no. 1, pp. 129–142, Jan. 2015.

2. A. Robaszkiewicz, C. Qu, E. Wisnik, T. Ploszaj, A. Mirsaidi, **F. A. Kunze**, P. J. Richards, P. Cinelli, G. Mbalaviele, and M. O. Hottiger, "ARTD1 regulates osteoclastogenesis and bone homeostasis by dampening NF-κB-dependent transcription of IL-1β.," Nature Publishing Group, vol. 6, no. 1, p. 21131, Feb. 2016.